ISSN 0021-9673

VOL. 543 NO. 2 MAY 10, 1991

THIS ISSUE COMPLETES VOL. 543

JOURNAL OF CHROMATOGRAPHY

INCLUDING ELECTROPHORESIS AND OTHER SEPARATION METHODS

ELSEVIER

JOURNAL OF CHROMATOGRAPHY

Scope. The *Journal of Chromatography* publishes papers on all aspects of chromatography, electrophoresis and related methods. Contributions consist mainly of research papers dealing with chromatographic theory, instrumental development and their applications. The section *Biomedical Applications*, which is under separate editorship, deals with the following aspects: developments in and applications of chromatographic and electrophoretic techniques related to clinical diagnosis or alterations during medical treatment; screening and profiling of body fluids or tissues with special reference to metabolic disorders; results from basic medical research with direct consequences in clinical practice; drug level monitoring and pharmacokinetic studies; clinical toxicology; analytical studies in occupational medicine.

Submission of Papers. Manuscripts (in English; *four* copies are required) should be submitted to: Editorial Office of *Journal of Chromatography*, P.O. Box 681, 1000 AR Amsterdam, The Netherlands, Telefax (+31-20) 5862 304, or to: The Editor of *Journal of Chromatography, Biomedical Applications*, P.O. Box 681, 1000 AR Amsterdam, The Netherlands. Review articles are invited or proposed by letter to the Editors. An outline of the proposed review should first be forwarded to the Editors for preliminary discussion prior to preparation. Submission of an article is understood to imply that the article is original and unpublished and is not being considered for publication elsewhere. For copyright regulations, see below.

Publication. The *Journal of Chromatography* (incl. *Biomedical Applications*) has 38 volumes in 1991. The subscription prices for 1991 are:

J. Chromatogr. (incl. *Cum. Indexes, Vols. 501–550*) + *Biomed. Appl.* (Vols. 535–572):
Dfl. 7220.00 plus Dfl. 1140.00 (p.p.h.) (total *ca.* US$ 4519.00)

J. Chromatogr. (incl. *Cum. Indexes, Vols. 501–550*) only (Vols. 535–561):
Dfl. 5859.00 plus Dfl. 810.00 (p.p.h.) (total *ca.* US$ 3604.75)

Biomed. Appl. only (Vols. 562–572):
Dfl. 2387.00 plus Dfl. 330.00 (p.p.h.) (total *ca.* US$ 1468.75).

Subscription Orders. The Dutch guilder price is definitive. The US$ price is subject to exchange-rate fluctuations and is given as a guide. Subscriptions are accepted on a prepaid basis only, unless different terms have been previously agreed upon. Subscription orders can be entered only by calendar year (Jan.–Dec.) and should be sent to Elsevier Science Publishers, Journal Department, P.O. Box 211, 1000 AE Amsterdam, The Netherlands, Tel. (+31-20)5803642, Telefax (+31-20) 5803598, or to your usual subscription agent. Postage and handling charges include surface delivery except to the following countries where air delivery via SAL (Surface Air Lift) mail is ensured: Argentina, Australia, Brazil, Canada, Hong Kong, India, Israel, Japan*, Malaysia, Mexico, New Zealand, Pakistan, PR China, Singapore, South Africa, South Korea, Taiwan, Thailand, USA. * For Japan air delivery (SAL) requires 50% additional charge of the normal postage and handling charge. For all other countries airmail rates are available upon request. Claims for missing issues must be made within three months of our publication (mailing) date, otherwise such claims cannot be honoured free of charge. Back volumes of the *Journal of Chromatography* (Vols. 1–534) are available at Dfl. 208.00 (plus postage). Customers in the USA and Canada wishing information on this and other Elsevier journals, please contact Journal Information Center, Elsevier Science Publishing Co. Inc., 655 Avenue of the Americas, New York, NY 10010, USA, Tel. (+1-212) 633 3750, Telefax (+1-212) 633 3990.

Abstracts/Contents Lists published in Analytical Abstracts, Biochemical Abstracts, Biological Abstracts, Chemical Abstracts, Chemical Titles, Chromatography Abstracts, Clinical Chemistry Lookout, Current Contents/Life Sciences, Current Contents/Physical, Chemical & Earth Sciences, Deep-Sea Research/Part B: Oceanographic Literature Review, Excerpta Medica, Index Medicus, Mass Spectrometry Bulletin, PASCAL-CNRS, Pharmaceutical Abstracts, Referativnyi Zhurnal, Research Alert, Science Citation Index and Trends in Biotechnology.

See inside back cover for Publication Schedule, Information for Authors and information on Advertisements.

0021-9673/91/$03.50

Printed in The Netherlands

CONTENTS

(Abstracts/Contents Lists published in Analytical Abstracts, Biochemical Abstracts, Biological Abstracts, Chemical Abstracts, Chemical Titles, Chromatography Abstracts, Current Contents/Life Sciences, Current Contents/Physical, Chemical & Earth Sciences, Deep-Sea Research/Part B: Oceanographic Literature Review, Excerpta Medica, Index Medicus, Mass Spectrometry Bulletin, PASCAL-CNRS, Referativnyi Zhurnal, Research Alert and Science Citation Index)

REGULAR PAPERS

Column Liquid Chromatography

(Continued overleaf)

Contents (continued)

In articles with more than one author, the name of the author to whom correspondence should be addressed is indicated in the article heading by a 6-pointed asterisk (*)

Journal of Chromatography, 543 (1991) 267–275
Elsevier Science Publishers B.V., Amsterdam

CHROM. 23 123

Application of the UNIFAC method for assessment of retention in reversed-phase liquid chromatography

ĽUBOMÍR DAŠKO[a]
Polymer Institute SAS, Dúbravská 10, Bratislava (Czechoslovakia)
(First received October 29th, 1990; revised manuscript received January 14th, 1991)

ABSTRACT

A method for the qualitative assessment of the retention of analytes in reversed-phase liquid chromatography is suggested. The separation is based on the partitioning of analyte molecules between the stationary and mobile phases. The stationary phase is represented by hexane, cumene and 1-octanol and the mobile phase is composed of mixtures of acetonitrile and water or methanol and water. With the help of the UNIFAC group contribution method, the activity coefficients of analytes in both phases were determined. Subsequently the partition coefficients were calculated and used for the assessment of retention. The theoretical results were compared with experimental data and reasonable agreement was achieved.

INTRODUCTION

The development of a reversed-phase liquid chromatographic (RPLC) separation method for a new analyte is usually a time-consuming process. It is preferable to choose one of the many procedures available in the literature for retention prediction. A review devoted to theory and methodology of LC was published recently by Dorsey *et al.* [1].

The mechanism of separation in RPLC is often considered to be based on the partitioning of molecules of analytes between the stationary and mobile phases. The value of the partition coefficient can be used for the assessment of retention because the logarithm of the capacity factor is closely related to the logarithm of the partition coefficient [2].

In the case of pure liquid–liquid (L–L) partitioning, the exact compositons of the stationary and mobile phases must be defined for the calculation of partition coefficients. The composition of the mobile phase is well known, but that of the stationary phase is more problematic.

A pure L–L partition mechanism for the separation of analytes in RPLC is unlikely. Horváth *et al.* [2] took into account hydrophobic interactions of the hydrophobic part of an analyte molecule with a bonded alkyl ligand. Martire and

[a] Address for correspondence: Kovpakova 12, 851 01 Bratislava, Czechoslovakia.

0021-9673/91/$03.50

Boehm [3] applied statistical thermodynamics for the calculation of chemical potentials of analytes in both phases with respect to the density of coverage of the silica gel surface with alkyl ligands and conformational changes in bonded ligands depending on the composition of the eluent (breathing of bonded phases).

These two models are an excellent introduction to the understanding of the mechanism of separation in RPLC. Their practical utilization is complicated because of problems with the determination of parameters for calculation.

A pure L–L partition model has also been developed. Grünbauer and Tomlinson [4] modelled the stationary phase with cyclohexane. For the calculation of the logarithm of the partition coefficient they applied Wilson's concept of local composition. The binary interaction parameters were calculated by a curve-fitting procedure from experimental information.

The partition coefficient can be calculated from known values of the activity coefficients of the substance of interest in both phases. An interesting and simple means for the assessment of activity coefficients is the UNIFAC group contribution method [5], where the parameters for calculation are tabulated for immediate reference. This method has been utilized for retention prediction in gas–liquid chromatography [6,7]. Petrovic *et al.* [8] have used the UNIFAC method in RPLC, but they did not calculate directly the activity coefficients of analytes in the stationary phase.

In this paper a method is described for the assessment of the retention of analytes by applying the UNIFAC group contribution method. A pure L–L partition model is adopted. Direct calculation of activity coefficients of analytes in model stationary and mobile phases was performed. By comparing calculated and experimental results and taking into account the effort required to obtain theoretical results according to this model, the acceptability of this strong approximation is confirmed.

DESCRIPTION OF THE MODEL

This model is similar to that of Grünbauer and Tomlinson [4]. In this case stationary phase is represented by a liquid (hexane, cumene and 1-octanol). It is assumed that molecules of the stationary phase cannot diffuse into the mobile phase. The mobile phase is composed of mixtures of methanol and water or acetonitrile and water. The same precondition as for stationary phase is valid for the mobile phase, *i.e.*, molecules of the mobile phase cannot penetrate into the stationary phase. Molecules of analytes are partitioned between the stationary and mobile phase. Model analytes used were 1-alcohols, alkylbenzenes, phenol, benzene and chlorobenzene.

The partition process is assumed to be an equilibrium process and the following equation is valid [9]:

$$\mu_a^0 + RT \ln x_a^s \gamma_a^s = \mu_a^0 + RT \ln x_a^m \gamma_a^m \quad (1)$$

where μ_a^0 denotes to the chemical potential of the analyte in the standard state, x_a^s, γ_a^s, x_a^m and γ_a^m are the mole fraction and and activity coefficients of the analyte in the stationary and mobile phase, respectively, T is absolute temperature and R is the gas constant.

In the case of the same standard state for both phases, it follows for the partition coefficient [9]:

$$\ln K = \ln \left(\frac{x_a^s}{x_a^m} \right) = \ln \left(\frac{\gamma_a^m}{\gamma_a^s} \right) \tag{2}$$

According to eqn. 2 one can calculate the logarithm of the partition coefficient of an analyte on a mole fraction basis.

The UNIFAC group contribution method was applied for the calculation of the activity coefficients of analytes of interest. The group contribution method transforms a solution of molecules into a solution of groups. In the original paper [5] it is stated that "The number of distinct groups must remain small, but not so small as to neglect significant effects of molecular structure on physical properties".

The UNIFAC method is closely related to UNIQUAC [10]. The logarithm of the activity coefficient of component a (γ_a) is the sum of combinatorial (γ_a^C) and residual (γ_a^R) parts [5]:

$$\ln \gamma_a = \ln \gamma_a^C + \ln \gamma_a^R \tag{3}$$

In the UNIFAC method the definition equation for the combinatorial part is the same as in UNIQUAC:

$$\ln \gamma_a^C = \ln \left(\frac{\phi_a}{x_a} \right) + \frac{z}{2} \cdot q_a \ln \left(\frac{\theta_a}{\phi_a} \right) + l_a - \left(\frac{\phi_a}{x_a} \right) \sum_p x_p l_p \tag{4}$$

where x_a is the mole fraction of component (analyte) a, the summation is over all components, θ_a is the area fraction and ϕ_a is the segment fraction. The definition equations are

$$\theta_a = \frac{q_a \, x_a}{\sum_p \phi_p \, x_p} \tag{5}$$

$$\phi_a = \frac{r_a \, x_a}{\sum_p r_p \, x_p} \tag{6}$$

The parameters r_a and q_a are defined by

$$r_a = \sum_k \nu_k^{(a)} \, R_k \tag{7}$$

$$q_a = \sum_k \nu_k^{(a)} \, Q_k \tag{8}$$

where $\nu_k^{(a)}$ is the number of groups of type k in molecule a. The parameters R_k and Q_k represent the Van der Waals group volume and surface area, respectively.

The last parameter for calculation of the combinatorial part is l_a, for which the following equation is valid:

$$l_a = \frac{z}{2}(r_a - q_a) - (r_a - 1) \tag{9}$$

$$z = 10 \tag{10}$$

The difference between the UNIFAC and UNIQUAC methods is in the expressions for calculation of the residual part. The residual part in UNIFAC can be calculated according to the following equation [5]:

$$\ln \gamma_a^R = \sum_k \nu_k^{(a)} [\ln \Gamma_k - \ln \Gamma_k^{(a)}] \tag{11}$$

where Γ_k is the group residual activity coefficient and $\Gamma_k^{(a)}$ is the residual activity coefficient of group k in a reference solution of molecules a only. Γ_k and $\Gamma_k^{(a)}$ can be calculated by the same equation [5]:

$$\ln \Gamma_k = Q_k \left[1 - \ln \left(\sum_m \Xi_m \psi_{mk} \right) - \sum_m \left(\frac{\Xi_m \psi_{km}}{\sum_n \Xi_n \psi_{nm}} \right) \right] \tag{12}$$

where Ξ_m is the area fraction of group m:

$$\Xi_m = \frac{Q_m X_m}{\sum_n Q_n X_n} \tag{13}$$

and X_m is the mole fraction of group m in the mixture. Sums are over all different groups. ψ_{mn} is the group interaction parameter, given by

$$\psi_{mn} = \exp - \left[\frac{U_{mn} - U_{nn}}{RT} \right] = \exp - \left[\frac{A_{mn}}{T} \right] \tag{14}$$

where U_{mn} is the measure of the interaction energy between groups m and n. Parameters A_{mn} must be evaluated from exprimental phase equilibrium data.

$$A_{mn} \neq A_{nm} \tag{15}$$

All known group interaction parameters are tabulated together with other parameters which are necessary for calculation [11]. Of course, the table of interaction parameters is not completely comprehensive [11]. Some parameter are missing because of deviations from experimental results after calculations [5]. On the other hand, very good correlations were obtained in various mixtures [5,12].

Calculated results were transformed to a volume fraction scale.

The concentration of analyte is usually very low in both phases, which is why the concept of infinitesimal dissolution was applied.

EXPERIMENTAL

Chromatographic measurements were made using a VCM-300 membrane pump, a six-port injection valve, and a UVM-4 UV–VIS detector (all from Development Works CSAS, Prague, Czechoslovakia). An RIDK 101 refracive index detector (Laboratory Works, Prague, Czechoslovakia) was used for detection of alcohols. For both detectors aTZ-4200 chart recorder was used (Laboratory Works).

Eluents were prepared from acetonitrile (UCB, Brussels, Belgium), methanol (Lachema, Brno, Czechoslovakia) and doubly distilled water. The analytes were 1-alcohols, alkylbenzenes, benzene, chlorobenzene and phenol from Fluka (Buchs, Switzerland) and were used as received.

The separation column (150 × 3.3 mm I.D.) was filled with Separon Six C_{18} (Tessek, Prague, Czechoslovakia). The dead volume was determined using sodium nitrate.

Calculations were performed on a TI-56 calculator (Texas Instruments, Dallas, TX, U.S.A.). All parameters necessary for calculation are available in the literature [11].

RESULTS AND DISCUSSION

Activity coefficients were calculated using the UNIFAC group contribution method [5]. Subsequently partition coefficients (K) were calculated according to eqn. 2. Plots of ln K *versus* volume fraction of water (φ_w) in the mobile phase were constructed. In fig. 1a, b and c the stationary phase is represented by hexane, cumene and 1-octanol, respectively. A homologous series of 1-alcohols were used as analytes. The mobile phase was acetonitrile–water. Experimental results are represented by a plot of logarithm of capacity factor (k') *versus* volume fraction of water in Fig. 1d.

Fig. 1a–d show a fairly good agreement from the qualitative point of view regardless of the stationary phase selected. Plots of both ln k' and ln K *versus* volume fraction of water are markedly curved within the composition range 0–0.4, probably owing to interactions of free silanols groups with the hydroxyl group of the alcohol. The changes in the composition of the mobile phase could induce conformational changes in the alcohol molecules too. Conformational changes are closely related to the hydrophobic surface of the molecules of alcohols. These effects together can contribute to the total behaviour of alcohols in RPLC.

Using the same procedure as for alcohols, the values of ln K were calculated for alkylbenzenes and the results are shown in Fig. 2a, b and c, where stationary phases are represented by hexane, cumene and 1-octanol, respectively. The experimental results are shown in Fig. 2d. In contrast to the plots for alcohols, plots of ln k' and ln K versus volume fraction of water are represented by straight lines for alkylbenzenes. In this instance there is no chance of silanophilic interactions. Conformational changes in short alkyl chains are improbable; if they do occur the changes in the surface are not significant.

From Figs. 1 and 2, one cannot draw any conclusion about the best choice for the stationary phase from the suggested liquids. This is why one had to take into account another analytes, *i.e.*, chlorobenzene and phenol. The mobile phase had to be changed to methanol–water, because not all the necessary parameters for the

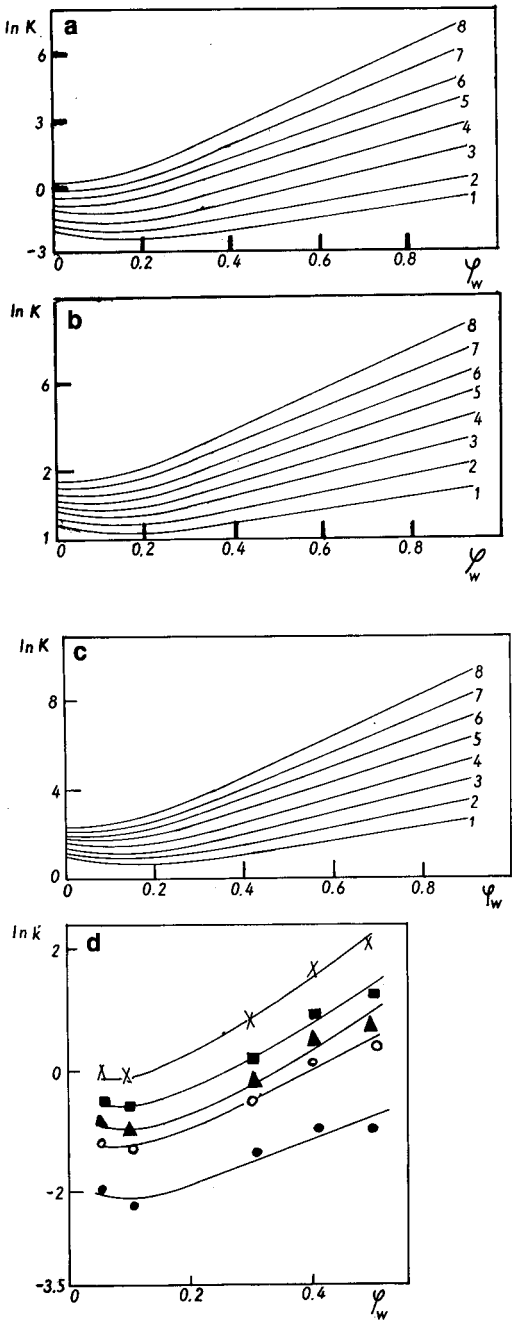

Fig. 1. (a–c) Calculated plots of ln *K versus* volume fraction of water in acetonitrile–water mobile phase. Stationary phase: (a) hexane; (b) cumene; (c) 1-octanol. 1 = 1-Propanol; 2 = 1-butanol; 3 = 1-pentanol; 4 = 1-hexanol; 5 = 1-heptanol; 6 = 1-octanol; 7 = 1-nonanol; 8 = 1-decanol. (d) Experimental results for selected 1-alcohols: plots of ln *k' versus* volume fraction of water in acetonitrile–water mobile phase. ● = 1-Propanol; ○ = 1-hexanol; ▲ = 1-heptanol; ■ = 1-octanol; × = 1-decanol.

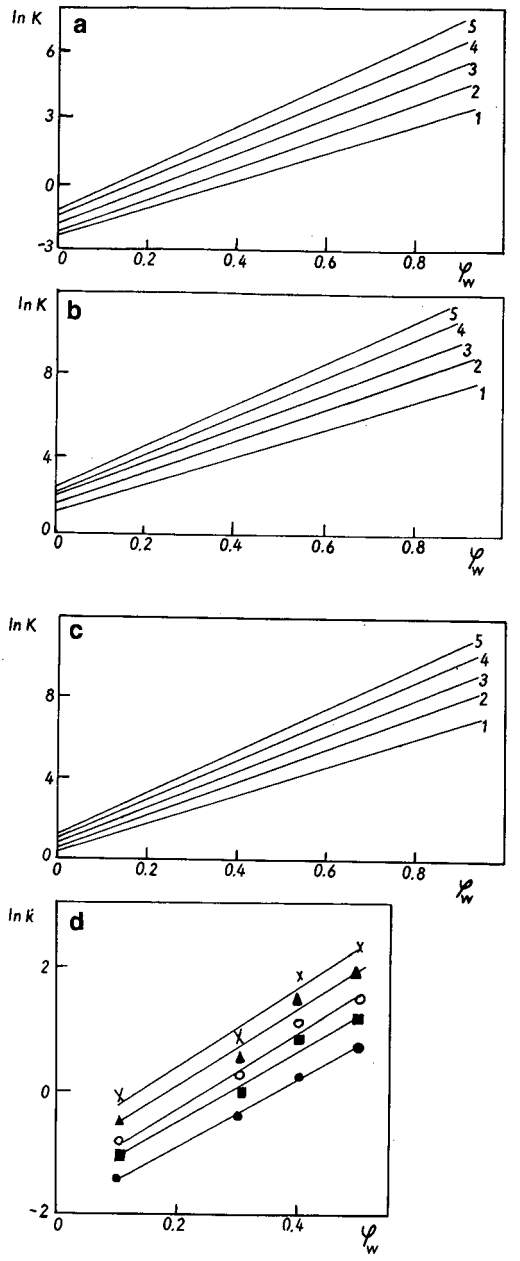

Fig. 2. (a–c) Calculated plots of ln *K versus* volume fraction of water in acetonitrile–water mobile phase. Stationary phase: (a) hexane; (b) cumene; (c) 1-octanol. 1 = Benzene; 2 = toluene; 3 = ethylbenzene; 4 = propylbenzene; 5 = butylbenzene. (d) Experimental plots of ln *k' versus* volume fraction of water in acetonitrile–water mobile phase. ● = Benzene; ■ = toluene; ○ = ethylbenzene; ▲ = propylbenzene; × = butylbenzene.

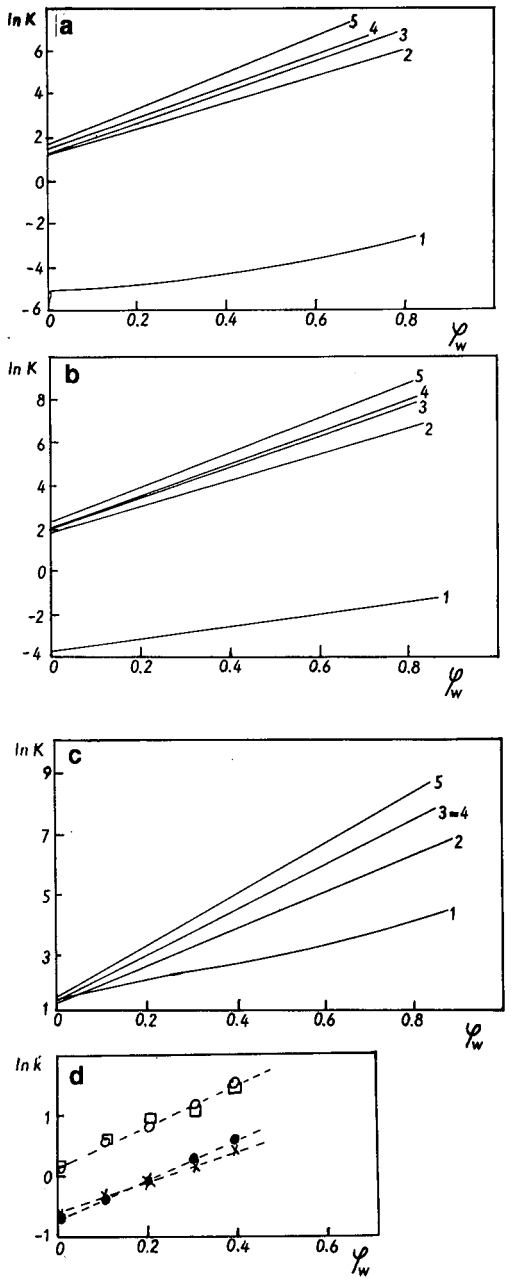

Fig. 3. (a–c) Calculated plots of ln *K versus* volume fraction of water for methanol–water mobile phase. Stationary phase: (a) hexane; (b) cumene; (c) 1-octanol. 1 = Phenol; 2 = benzene; 3 = toluene; 4 = chlorobenzene; 5 = ethylbenzene. (d) Experimental plots of ln *k' versus* volume fraction of water in methanol–water mobile phase. × = Phenol; ● = benzene; ○ = toluene; □ = chlorobenzene.

acetonitrile–phenol and acetonitrile–chlorobenzene pairs in the UNIFAC group contribution method are known [11].

Calculated plots of ln *K versus* volume fraction of water are shown in Fig. 3a, b and c, where the stationary phase is represented by hexane, cumene and 1-octanol, respectively. Comparing the calculated results with the experimental results (see Fig. 3D), one can see that the best choice for the stationary phase is 1-octanol.

CONCLUSIONS

A simple method for the qualitative prediction of the retention of analytes in RPLC has been presented. It has been shown that the UNIFAC group contribution method is suitable for calculating activity coefficients and consequently partition coefficients of small molecules between model stationary and mobile phases. The best choice for the stationary phase is 1-octanol. Fairly good assessments of the retention of analytes in RPLC can be obtained in a reasonable time.

REFERENCES

1 J. G. Dorsey, J. P. Foley, W. T. Cooper and R. A. Barford, *Anal. Chem.*, 62 (1990) 324R.
2 Cs. Horváth, W. R. Melander and I. Molnár, *J. Chromatogr.*, 268 (1976) 129,
3 D. E. Martire and R. F. Boehm, *J. Phys. Chem.*, 87 (1983) 1045.
4 H. J. M. Grünbauer and E. Tomlinson, *J. Chromatogr.*, 268 (1983) 277.
5 A. Fredenslund, R. L. Jones and J. M. Prausnitz, *AIChE J.*, 21 (1975) 1086.
6 M. Roth and J. Novak, *J. Chromatogr.*, 258 (1983) 23.
7 G. J. Price and M. R. Dent, *J. Chromatogr.*, 483 (1989) 1.
8 J. Petrovic, S. Lomic and I. Sefer, *J. Chromatogr.*, 348 (1985) 49.
9 H. J. M. Grünbauer, T. Bultsma and R. R. Rekker, *Eur. J. Med. Chem.*, 17 (1982) 411.
10 D. S. Abrams and J. M. Prausnitz, *AIChE J.*, 21 (1975) 116.
11 J. Gmehling, P. Rasmussen and A. Fredenslund, *Ind. Eng. Chem., Process Des. Dev.*, 21 (1982) 118.
12 A. Fredenslund, *Fluid Phase Equilib.*, 52 (1989) 135.

Journal of Chromatography, 543 (1991) 277–286
Elsevier Science Publishers B.V., Amsterdam

CHROM. 23 134

Preparation and evaluation of chiral high-performance liquid chromatographic stationary phases of mixed character (π-donor and π-acceptor) for the resolution of racemic compounds

LAUREANO OLIVEROS* and CRISTINA MINGUILLÓN[a]

Conservatoire National des Arts et Métiers, Laboratoire de Chimie Générale (CNRS URA 1103), 292 rue Saint-Martin, 75141 Paris Cédex 03 (France)

and

BERNARD DESMAZIÈRES and PAUL-LOUIS DESBÈNE

URA 455, Université P. et M. Curie, Laboratoire de Chimie Organique Structurale, 4 Place Jussieu 75230 Paris Cédex 05 (France) and Université de Rouen, L.A.S.O.C., 43 rue Saint Germain, 27000 Evreux (France)

(First received October 23rd, 1990; revised manuscript received January 28th, 1991)

ABSTRACT

Up to now, most stationary phases have had either π-acceptor or π-donor characteristics. In this study, the behaviour of stationary phases having mixed characteristics (π-donor and π-acceptor) was investigated and compared with that of silicas bonded either with the same π-acceptor group or with the same π-donor group. The chiral selectors, (*S*)-1-(α-naphthyl)ethylamine associated with (*S*)-phenylalanine and (*S*)-N-(3,5-dinitrobenzoyl)phenylalanine, were bound to a γ-aminopropylsilanized silica gel. Stationary phases possessing mixed character were obtained either by bonding the two chiral selectors on the same silica or by mixing two chiral silicas bonded with only one of two chiral selectors. The selectivity of these chiral stationary phases possessing π-donor and π-acceptor characters are similar; the α values are intermediate between those shown by the two chiral stationary phases with only π-donor or π-acceptor character. The results obtained in the resolution of a series of racemic compounds with either π-donor or π-acceptor character show that the chiral recognition mechanism is probably more complex than the conventional face-to-face π-interactions usually described.

INTRODUCTION

The resolution of racemic compounds by liquid chromatography using chiral stationary phases, consisting of silica gel bonded to small optically active compounds, has made notable advances in the last decade [1–4]. In addition to these stationary phases, the chiral identity of which is, in general, a molecule with a π-acceptor or a π-donor radical, more recently new stationary phases based on asymmetric natural (albumin, glycoproteins, cellulose derivatives, etc.) [5] or synthetic [6–8] macromole-

[a] Present address: Laboratorio de Química Farmacéutica, Facultad de Farmacia, Universidad de Barcelona, Avd. Diagonal s/n, 08028-Barcelona, Spain.

0021-9673/91/$03.50

cules have appeared. Even the noteworthy return of old asymmetric supports such as cellulose [9,10] and cellulose triacetate [11] cannot be forgotten.

Classical silica-bonded chiral stationary phases are easy to prepare and to use. Nevertheless, their scope of application is relatively limited when compared with that of stationary phases based on natural or synthetic macromolecules [12].

In order to obtain a wider range of application for these kinds of stationary phases we synthesized silicas carrying both a π-donor and a π-acceptor group. They were obtained in two different ways. First, we successively bonded the two chiral moieties carrying a π-donor group and a π-acceptor group on the same silica. Second, we explored the possibility of mechanically mixing a silica carrying a π-donor group with a silica carrying a π-acceptor group. We used (*S*)-N-(3,5-dinitrobenzoyl)phenylalanine as a π-acceptor group and (*S*)-1-(α-naphthyl)ethylamine associated with (*S*)-phenylalanine as a π-donor group. We then compared the chiral stationary phase CSP-AD1 (Fig. 1), made by successively bonding the two different groups, with the

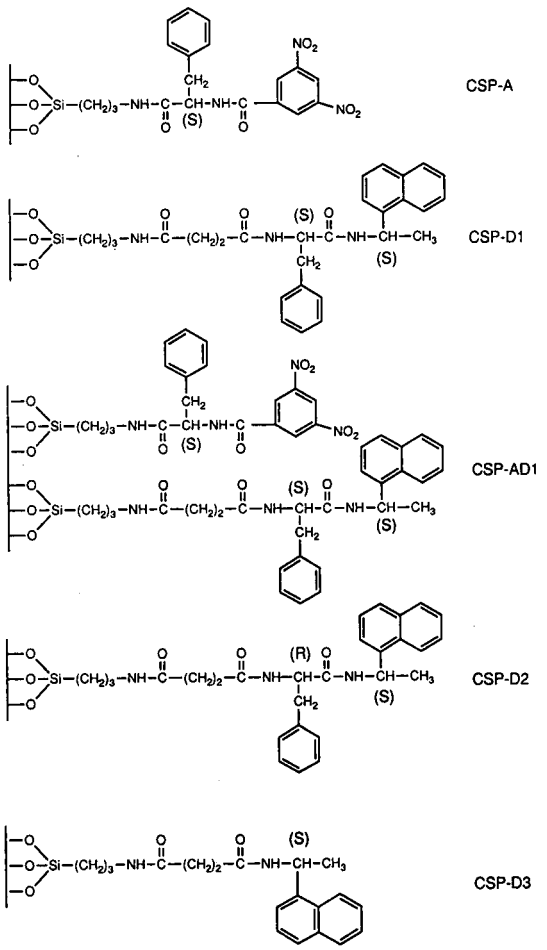

Fig. 1. Structures of chiral stationary phases.

stationary phase obtained by packing the column with a mixture (1:1) of CSP-A [13] and CSP-D1 (Fig. 1) (hereafter referred to as CSP-A + D1) and with the simple stationary phases CSP-A and CSP-D1. In order to test all the chiral stationary phases we used racemic compounds with either π-donor or π-acceptor character.

Silicas bonded to one chiral molecule with radicals possessing different character have already been described [14,15], but these are silicas bonded to a chiral molecule with both π-donor and π-acceptor radicals and, to our knowledge, no comparative study of the properties of a mixed stationary phase with those of two simple stationary phases with only one kind of radical has been undertaken. However, one example has been described [16] of γ-aminopropylsilanized silica on which a mixture of two chiral compounds was fixed by ionic bonding, but the two chiral compounds both had π-acceptor character.

We have studied the influence of the chiral centre of the phenylalanine moiety in CSP-D1 in which the naphthylethylamine group already has a chiral centre. Therefore, we prepared and tested two new chiral stationary phases, one of them by replacing (*S*)-phenylalanine with (*R*)-phenylalanine in CSP-D1 and the other by suppressing the amino acid (CSP-D2 and CSP-D3 [17], respectively, Fig. 1). We also tested a mixture (1:1) of CSP-A and CSP-D3 (hereafter referred to as CSP-A + D3).

EXPERIMENTAL

NMR spectra were measured at 200 MHz using a Bruker AC200 spectrometer. Tetramethylsilane (TMS) was used as the internal standard. Rotatory power was measured with a Perkin-Elmer Model 241 polarimeter. Elemental analyses were performed by the Service Central de Microanalyse du CNRS (Vernaison, France). The chromatographic experiments were carried out on an HP 1090 liquid chromatograph (Hewlett-Packard, Palo Alto, CA, U.S.A.) equipped with a PU4020 UV detector (Philips, Cambridge, U.K.) (254 nm). The chiral stationary phases were packed into stainless-steel tubes (100 mm × 4.6 mm I.D.) by the slurry method according to Coq *et al.* [18]. The volume of sample injected was of 5 μl. The flow-rate of the pump was 1 ml/min. The mobile phases consisted of various mixtures of *n*-heptane, chloroform and methanol.

Chemicals and reagents

Compounds **1–3** (Fig. 2) were obtained by treating the methyl ester of each amino acid with 3,5-dinitrobenzoyl chloride. Compound **6** was prepared by the method described previously [19]. All were identified by their ^{1}H NMR spectra and elemental analysis. Compounds **4**, **5** and **7–9** were purchased from Aldrich.

(S)-tert.-Butoxycarbonylphenylalanyl-(S)-1-(α-naphthyl)ethylamine (**10**) (Fig. 3). L-N-Boc-phenylalanine-N′-hydroxysuccinimide ester (Sigma) (5 g, 13.8 mmol) was dissolved in dichloromethane (120 ml) and cooled in an ice-bath. (*S*)-1-(α-naphthyl)ethylamine (2.4 g, 14.0 mmol) in dichloromethane (50 ml) was added over 10 min with magnetic stirring. The solution was stirred at 0°C for 1.5 h and left to stand at room temperature for 10 h. The solution was diluted with dichloromethane (200 ml) and washed with 1% orthophosphoric acid, 0.2 *M* potassium hydroxide and distilled water. After drying over magnesium sulphate, the solution was evaporated to dryness and the residue collected. Recrystallization from toluene gave 4.5 g (78%) of a white

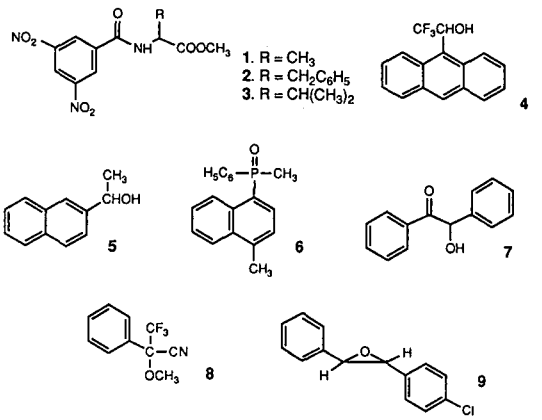

Fig. 2. Structures of test compounds.

solid, m.p. 145°C. ^{1}H NMR (200 MHz): δ ($CDCl_3$) 1.36 (s, 9H, *t*-Bu), 1.58 (d, 3H, CH_3), 3.01 (m, 2H, CH_2Ar), 4.38 (m, 1H, CH_3CH), 5.95 (m, 1H, NCHCO), 7.0–8.2 ppm (m, 12H, ArH). ^{13}C NMR (50.3 MHz): δ ($CDCl_3$) 20.9 (CH_3), 28.1 [$(CH_3)_3$], 38.4 (CH_2), 44.6 (CH_3CH), 56.0 (NCHCO), 80.1 (C_q), 130.9, 133.8, 136.4 and 137.9 (C_q aromatic), 155.2 (O–CO–N), 170.0 ppm (CO–N). $[\alpha]_D^{23} = -3.6°$ (*c* = 1, dichloromethane). Analysis: calculated for $C_{26}H_{30}N_2O_3$, C 74.61, H 7.22, N 6.69; found, C 74.08, H 7.16, N 6.66%.

(R)-tert.-Butoxycarbonylphenylalanyl-(S)-1-(α-naphthyl)ethylamine (**11**). Analogously to **10**, compound **11** was obtained from D-N-Boc-phenylalanine-N′-hydroxysuccinimide ester. Recrystallization from toluene gave 5 g (86%) of a white solid, m.p. 154°C. ^{1}H NMR (200 MHz): δ ($CDCl_3$) 1.36 (s, 9H, *t*-Bu), 1.47 (d, 3H, CH_3), 3.06 (m, 2H, CH_2Ar), 4.38 (m, 1H, NCHCO), 5.90 (m, 1H, CHN), 7.2–8.1 ppm (m, 12H, ArH). ^{13}C NMR (50.3 MHz): δ ($CDCl_3$) 20.8 (CH_3), 28.2 [$(CH_3)_3$], 38.5 (CH_2), 44.8 (CH_3CH), 56.1 (NCHCO), 79.9 (C_q), 130.8, 133.8, 136.7 and 138.0 (C_q aromatic), 154.5 (O–CO–N), 169.9 ppm (CO–N). $[\alpha]_D^{23} = +33.0°$ (*c* = 1.4, dichloromethane). Analysis: calculated for $C_{26}H_{30}N_2O_3$, C 74.61, H 7.22, N 6.69; found, C 74.83, H 7.28, N 6.73%.

Succinyl-(S)-phenylalanyl-(S)-1-(α-naphthyl)ethylamine (**12**). A 4.2-g (10-mmol) amount of **10** was dissolved in glacial acetic acid (45 ml) and cooled in an ice-bath. Hydrogen chloride was passed through for 40 min and the solution was left to stand at room temperature for 3 h. The solvent was removed *in vacuo* and the residual solid washed with diethyl ether. The solid was then dissolved in pyridine (12 ml) and succinic anhydride (1.1 g, 11 mmol) was added. After stirring for 24 h at room temperature, the mixture was evaporated to dryness and the residue treated with 5% orthophosphoric acid (120 ml) and distilled water. Recrystallization from ethanol–water gave 3.5 g (83%) of a white solid, m.p. 155°C ^{1}H NMR (200 MHz): δ (acetone-d_6) 1.54 (d, 3H, CH_3), 2.45–2.58 (m, 4H, CH_2CH_2), 2.68 and 3.10 (m, 2H, CH_2Ar), 4.73 (dq, 1H, CH_3CH), 5.85 (m, 1H, NCHCO), 7.1–8.3 ppm (m, 12H, ArH). ^{13}C NMR (50.3 MHz): δ (acetone-d_6) 22.0 (CH_3), 29.7 and 31.1 (CH_2CH_2), 38.7 (CH_2Ar), 45.6 (CH_3CH), 55.5 (NCHCO), 131.7, 134.8, 138.6 and 140.8 (C_q

aromatic), 170.9, 172.4 and 174.5 ppm (CO). $[\alpha]_D^{23} = -20.5°$ ($c = 2$, pyridine). Analysis: calculated for $C_{25}H_{26}N_2O_4$, C 71.75, H 6.26, N 6.69; found C 71.41, H 6.11, N 6.68%.

Succinyl-(R)-phenylalanyl-(S)-1-(α-naphthyl)ethylamine (**13**). Analogously to **12**, compound **13** was obtained from **11**. Recrystallization from ethanol–water gave 3.8 g (90.5%) of a white solid, m.p. 156°C. ^{1}H NMR (200 MHz): δ ($CDCl_3$–DMSO-d_6) 1.36 (d, 3H, CH_3), 2.20–2.50 (m, 4H, CH_2CH_2), 2.93 (m, 2H, CH_2Ar), 4.60 (q, 1H, CH_3CH), 5.70 (m, 1H, NCHCO), 7.0–8.1 ppm (m, 12H, ArH). ^{13}C NMR (50.3 MHz): δ ($CDCl_3$–DMSO-d_6) 20.8 (CH_3), 29.2 and 30.5 (CH_2CH_2), 37.6 (CH_2), 44.4 (CH_3CH), 54.1 (NCHCO), 130.5, 133.4, 136.8 and 138.6 (C_q aromatic), 169.7, 171.7 and 174.5 ppm (CO). $[\alpha]_D^{23} = +52.5°$ ($c = 2$, pyridine). Analysis: calculated for $C_{25}H_{26}N_2O_4$, C 71.75, H 6.26, N 6.69; found, C 71.56, H 6.26, N 6.66%.

Chiral stationary phases

General procedure. To a solution of 3.1 mmol of the appropriate chiral acidic moiety in 60 ml of tetrahydrofuran (THF), 3.5 g of γ-aminopropylsilanized silica, obtained from a spherical silica (5 μm, 100 Å, Nucleosil 100-5; Macherey, Nagel & Co.) according to the method of Pirkle *et al.* [1] (analysis: C 3.10, H 1.05, N 0.90%) and a solution of 0.93 g (3.7 mmol) of 2-ethoxy-1-ethoxycarbonyl-1,2-dihydroquinoline (EEDQ) in 15 ml of THF were added successively while stirring at room temperature. The mixture was allowed to react overnight. The resulting bonded silica was collected by filtration and washed exhaustively with THF, ethanol, water, acetone and diethyl ether and dried *in vacuo* at room temperature. All elemental analyses are given in Table I.

Phase CSP-AD1. This CSP was prepared in two steps according to the above-described general procedure. First, 3 g of γ-aminopropylsilanized silica were treated with a solution of 150 mg of **12** in 150 ml of THF and 120 mg of EEDQ in 10 ml of THF. In the second step, 2.5 g of the previously obtained silica (analysis: C 5.18, H 1.43, N 1.33%) was treated with a solution of 1 g of (*S*)-N-(3,5-dinitrobenzoyl)phenylalanine in 40 ml of THF. CSP-AD1 was collected by filtration and washed as usual.

TABLE I

ELEMENTARY ANALYSES OF CHIRAL STATIONARY PHASES

Chiral stationary phase	Elemental analysis (%)			Ratio of carbon atoms per nitrogen atom		Bonded chiral moieties per gram of stationary phase (mmol)[a]	
	C	H	N	Analytical	Theoretical[a]	From %C	From %N
CSP-A	10.93	1.76	2.69	4.74	4.75	0.48	0.48
CSP-D1	15.53	2.02	2.01	9.01	9.33	0.46	0.48
CSP-AD1	11.80	1.80	2.40	5.74	6.71	0.42	0.49
CSP-D2	10.65	1.79	1.77	7.02	9.33	0.32	0.42
CSP-D3	9.41	1.65	1.54	7.13	9.50	0.41	0.55

[a] Calculations made with regard to organic moiety structures in each stationary phase. The remaining free NH_2 groups were not considered. In CSP-AD1 a ratio of 1:1 between both kinds of chiral moieties was considered.

TABLE II

CAPACITY FACTORS, k'_p, OF FIRST-ELUTED ENANTIOMER AND SELECTIVITY FACTORS, α, IN THE COLUMNS TESTED

Chiral stationary phase	Compound 1		2		3		4		5		6		7		8		9	
	k'_1	α	k'_1	α	k'_1	α	k'_1	α	k'_1	α	k'_1	α	k'_1	α	k'_1	α	k'_1	α
CSP-A	1.84(*R*)[a]	1.19	0.74(*R*)	1.24	1.03(*R*)	1.22	2.18(*S*)	1.19	8.10	1.06	19.17	1.13	6.59	1.04	0.35	1.27	0.52	1.60
CSP-D1	1.73(*R*	1.42	0.38(*R*)	1.39	0.71(*R*)	1.51	2.72	1.00	3.88	1.00	3.73	1.00	2.73	1.00	0.19	7.93	0.21	1.53
CSP-AD1	2.97(*R*)	1.23	1.11(*R*)	1.29	1.47(*R*)	1.35	3.59(*S*)	1.13	8.51	1.00	19.06	1.04	7.14	1.00	0.33	1.00	0.50	1.66
CSP-A + D1	2.43(*R*)	1.21	1.00(*R*)	1.27	0.89(*R*)	1.32	2.39(*R*)	1.13	7.73	1.00	7.87	1.00	5.14	1.09	0.29	2.23	0.34	1.68
CSP-D2	4.37(*R*)	1.07	1.87(*S*)	1.02	1.78(*R*)	1.06	3.49	1.00	4.55	1.00	2.29	1.00	3.14	1.00	0.25	10.00	0.18	1.04
CSP-D3	3.40(*R*)	1.46	1.11(*R*)	1.30	0.59[b](*R*)	1.76	3.00	1.09	4.50	1.00	2.34	1.00	2.43	1.00	0.23	9.24	0.21	1.44
CSP-A + D3	2.02(*R*)	1.34	0.78(*R*)	1.23	0.59[b](*R*)	1.33	2.74(*S*)	1.14	6.71	1.02	10.52	1.00	4.04	1.00	0.30	2.46	0.37	1.55
Mobile phase, chloroform + 0.5% methanol–heptane	70:30		80:20		70:30		70:30		25:75		50:50		25:75		10:90		25:75	

[a] Absolute configuration of first-eluted enantiomer.
[b] Composition of mobile phase 80:20.

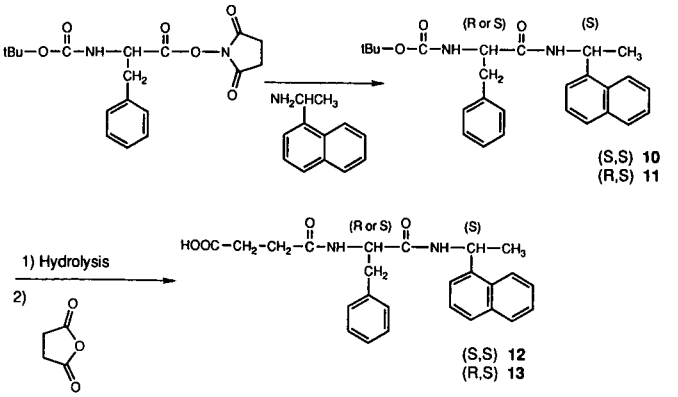

Fig. 3. Synthetic scheme for the preparation of **12** and **13**.

Phase CSP-D3. This has already been described by Ôi *et al.* [17] and was prepared by our general procedure.

Phases CSP-A + D1 and CSP-A + D3. These were prepared by mechanically mixing either CSP-A and CSP-D1 or CSP-A and CSP-D3 phases (50:50, w/w).

RESULTS AND DISCUSSION

The chemical structures of the racemic compounds used as test compounds are shown in Fig. 2. The results obtained after testing the chiral stationary phases are given in Table II.

It appears clearly that racemic products **1**, **2** and **3**, N-(3,5-dinitro)benzoyl derivatives of amino acids, therefore having a π-acceptor character, can be separated by all the stationary phases tested, even CSP-A, a chiral stationary phase with the same π-character. The racemic compound **4**, usually used as a test compound for testing the chromatographic behaviour of chiral stationary phases and itself having a π-donor character, is only resolved by chiral stationary phases having a π-acceptor or a mixed character. On the other hand, **5**, **6** and **7** are not resolved by most of the chiral stationary phases tested. Compounds **8** and **9** are weakly retained by our chiral phases but, in general, they are well resolved. However, **8** shows an unexpected behaviour. It is not resolved by CSP-AD1. Moreover, one of the enantiomers of **8** interacts very weakly with the other chiral phases while the second enantiomer is strongly retained. Therefore compound **8** seems appropriate for the study of chiral recognition mechanisms.

As several racemic products (**1**, **2** and **3**) are resolved in the same way by silicas with either a π-acceptor or a π-donor group, the need for these groups may be questioned. We synthesized and tested a chiral stationary phase in which the nitrobenzoyl radical in CSP-A has been replaced with an acetyl radical (CSP-0, Fig. 4). The selectivity values in this case, for the same elution strength, are 1.02 (k' = 1.13) for **1**, 1.00 (k' = 0.35) for **2** and 1.00 (k' = 0.42) for **3**. According to these clearly low values, it can be deduced that an electronic interaction between CSP-A and compounds **1–3** is

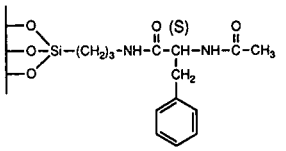

Fig. 4. Structure of CSP-0.

established by dinitrobenzoyl groups. Therefore, in certain instances, a non-classical electronic interaction between π-acceptor groups [20,21] instead of the classical charge-transfer interaction between a π-acceptor and a π-donor group exists. This could be the origin of the known easy separation of compounds with a dinitrobenzoyl group [4] and that of the wide field of application of chiral stationary phases bearing that group, even showing a good resolving power for compounds containing the same group [22]. We can draw the same conclusion when we consider that a number of racemic compounds containing a 3,5-dinitrobenzoyl radical are separated by chiral stationary phases bearing a π-donor group as weak as a C–C double bond [23]. These results suggest that solute–chiral entities in the stationary phase interactions, which take part in the chiral recognition mechanism, are probably more complex than the standard face-to-face π-system interactions considered by most workers.

Comparison between CSP-A and CSP-D1

CSP-A itself has a large separation capacity. It separates compounds that can be considered to be π-donors in addition to π-acceptors.

We tried to improve its selectivity further by blocking the remaining NH_2 groups with 3,5-dinitrobenzoyl chloride, thus increasing the number of π-acceptor interaction sites. In fact, we established that the retention values increase but the selectivity is slightly lower (**1**, $k' = 4.59$, $\alpha = 1.14$; **4**, $k' = 2.38$, $\alpha = 1.10$). Therefore, the resulting bonded silica does not show any improvement over CSP-A for the same elution strength.

On the other hand, as would be expected, CSP-D1 acts by separating almost exclusively compounds with a manifest π-acceptor character. Nevertheless, the very good separation of **8** and **9**, compounds possessing neither pronounced π-donor nor π-acceptor character, can be noted.

Comparison between CSP-AD1 and CSP-A + D1

In CSP-AD1 we find, except for **8** (loss of separation), a small decrease when we compare it to the individual performances of CSP-A and CSP-D1. This decrease in α can result from the dilution of each chiral moiety in the other.

A π-character interaction between the 3,5-dinitrobenzoyl group in one of the chiral moieties and the naphthylethylamine group in the other can be postulated in CSP-AD1. The absence of resolution for **8** may be produced by the mutual inhibition that these π-characters interactions can produce between the chiral moieties as they can block the interaction of this racemic compound with the chiral stationary phase. As **8** is the least retained of all the tested compounds, it is the most affected by this phenomenon. Moreover, it can be said that this interference can only be established at short distances, as it does not exist with CSP-A + D1.

CSP-A + D1, prepared by mechanically mixing CSP-A and CSP-D1 (1:1, w/w), shows a chromatographic behaviour similar to that of CSP-AD1: the α values are intermediate between those for CSP-A and CSP-D1 before mixing. This mixed stationary phase is constituted of silica particles with only one of two different chiral entities. Thus, the foregoing hypothesis of interaction between chiral moieties having different character cannot be applied. In this instance, the reduction in α comes from a decrease in the mixed stationary phase of the amount of chiral silica suitable for each racemic compound. Although CSP-A + D1 and CSP-AD1 show similar performances, one of the main advantages of the chiral stationary phase over CSP-AD1 is the ease of preparation. Moreover, the mixing of different kinds of bonded silica particles avoids interferences due to the proximity of chiral moieties.

Effect of chiral centres on CSP-D selectivity

In CSP-D1 there are two asymmetric centres because the choosen π-donor group itself is a chiral entity. Previous papers [23–27] have shown that the performances of chiral stationary phases remain the same or are slightly improved on going from one to two asymmetric centres in the chiral moiety. However, we have seen that interferences could exist between two chiral entities in the same bonded silica. It can be considered that the same phenomenon can exist in a chiral moiety possessing two different chiral centres. To study the existence of this effect, we synthesized and tested CSP-D2 and CSP-D3.

CSP-D2 differs from CSP-D1 in the absolute configuration of the phenylalanine moiety. Surprisingly, the α values decrease considerably in all instances (except for **8**, which is very well resolved). Thus, CSP-D2 gives α values near unity even with π-acceptor compounds that are well separated by CSP-D1. These results seem to show the importance of the absolute configuration in the phenylalanine asymmetric center. However, when it is eliminated (CSP-D3), the α values recover their previous magnitude. Hence, a competition between the stereoisomers of racemic compounds and the two asymmetric centres, located here in the sole chiral entity (CSP-D1 or CSP-D2), must exist. Therefore, in general, the existence of two or more chiral centres in a chiral stationary phase does not improve the separation but, depending on the configuration of these centres and the relative affinity of the two enantiomers for them, it can seriously interfere with the selectivity.

As a consequence of data obtained from CSP-D3, we also tested its mixture with CSP-A (1:1, w/w) (CSP-A + D3). As with CSP-A + D1, we obtained α values intermediate between those of CSP-A and CSP-D3 and an overall chromatographic behaviour resulting from the addition of their individual behaviours. Hence, it can be considered that mixtures of bonded silicas with different chromatographic behaviours can be useful for increasing the performances of the individual components.

CONCLUSION

The performances of two different stationary phases can be combined by packing the same column with a mixture of the two components. This stationary phase preparation method is better than bonding successively the different chiral entities whose characteristics we wish to combine.

Two different chiral asymmetric centres in the same stationary phase can, depending on their configuration, lead to bad selectivity.

According to our results, the validity of the recognition models proposed previously and based in π-acceptor–π-donor interactions may be questioned.

ACKNOWLEDGEMENT

C. M. thanks the Ministerio de Educación y Ciencia of Spain for a postdoctoral fellowship.

REFERENCES

1 W. H. Pirkle, D. W. House and J. M. Finn, *J. Chromatogr.*, 192 (1980) 143.
2 J. M. Finn, in M. Zief and L. J. Crane (Editors), *Chromatographic Chiral Separations* (*Chromatographic Science Series*, Vol. 40), Marcel Dekker, New York, 1988, Ch. 3, pp. 53–90.
3 W. H. Pirkle and T. C. Pochapsky, *Chem. Rev.*, 89 (1989) 347.
4 W. J. Lough (Editor), *Chiral Liquid Chromatography*, Blackie, London, 1989.
5 A. Ichida, T. Shibata, I. Okamoto, Y. Yuki, H. Namikoshi and Y. Toga, *Chromatographia*, 19 (1984) 280.
6 Y. Okamoto, R. Aburatani and K. Hatada, *Bull. Chem. Soc. Jpn.*, 63 (1990) 955.
7 Y. Okamoto, R. Aburatani, K. Hatano and K. Hatada, *J. Liq. Chromatogr.*, 11 (1988) 2147.
8 Y. Okamoto, R. Aburatani and K. Hatada, *J. Chromatogr.*, 389 (1987) 95.
9 T. Fukuhara, M. Itoh, M. Isoyama, A. Shimada and S. Yuasa, *J. Chromatogr.*, 354 (1986) 325.
10 A. O. Kuhn, M. Lederer and M. Sinibaldi, *J. Chromatogr.*, 469 (1989) 253.
11 R. Isaksson, P. Erlandsson, L. Hansson, A. Holmberg and S. Benner, *J. Chromatogr.*, 498 (1990) 257.
12 S. G. Allenmark, *Chromatographic Enantioseparation: Methods and Applications*, Ellis Horwood, Chichester, 1988, Ch. 7, pp. 90–141.
13 L. Oliveros and M. Cazau, *J. Chromatogr.*, 409 (1987) 183.
14 M. Ho Hyun and W. H. Pirkle, *J. Chromatogr.*, 393 (1987) 357.
15 N. Ôi, H. Kitahara, Y. Matsumoto, H. Nakajima and Y. Horikawa, *J. Chromatogr.*, 462 (1989) 382.
16 J. Kip, P. van Haperen and J. C. Kraak, *J. Chromatogr.*, 356 (1986) 423.
17 N. Ôi, M. Nagase and T. Doi, *J. Chromatogr.*, 257 (1983) 111.
18 B. Coq, C. Gonnet and J. L. Rocca, *J. Chromatogr.*, 106 (1975) 249.
19 P. Pescher, M. Caude, R. Rosset, A. Tambuté and L. Oliveros, *Nouv. J. Chim.*, 9 (1985) 621.
20 W. L. Jorgensen and D. L. Severance, *J. Am. Chem. Soc.*, 112 (1990) 4768.
21 C. A. Hunter and J. K. M. Sanders, *J. Am. Chem. Soc.* 112 (1990) 5525.
22 P. Macaudière, M. Lienne, M. Caude, R. Rosset and A. Tambuté, *J. Chromatogr.*, 467 (1989) 357.
23 N. Ôi, M. Nagase, Y. Inda and T. Doi, *J. Chromatogr.*, 259 (1983) 487.
24 N. Ôi, M. Nagase, Y. Inda and T. Doi, *J. Chromatogr.*, 265 (1983) 111.
25 N. Ôi and H. Kitahara, *J. Chromatogr.*, 265 (1983) 117.
26 N. Ôi, M. Nagase and Y. Sawade, *J. Chromatogr.*, 292 (1984) 427.
27 M. J. B. Lloyd, *J. Chromatogr.*, 351 (1986) 219.

Journal of Chromatography, 543 (1991) 287–297
Elsevier Science Publishers B.V., Amsterdam

CHROM. 23 095

Enantiomeric separation of amines using N-benzoxycarbonylglycyl-L-proline as chiral additive and porous graphitic carbon as solid phase[a]

A. KARLSSON and C. PETTERSSON*

Department of Analytical Pharmaceutical Chemistry, Biomedical Centre, Uppsala University, Box 574, S-751 23 Uppsala (Sweden)

(First received December 27th, 1989; revised manuscript received January 9th, 1991)

ABSTRACT

A study of the separation of enantiomeric amines as diastereometric complexes (ion pairs) with N-benzoxycarbonylglycyl-L-proline (L-ZGP) as chiral additive is presented. The chromatographic performances of two solid stationary phases, porous graphitic carbon (PGC) and LiChrosorb DIOL, were compared and the carbon-based phase was found to have advantages with regard to column efficiency and short equilibration times. Less than 15 column volumes of the mobile phase (L-ZGP in dichloromethane) were sufficient to obtain constant chromatographic conditions with porous graphitic carbon. The water content of the organic mobile phase had no significant effect on the equilibration time of the PGC phase. The chiral counter ion (N-benzoxycarbonylglycyl-L-proline) could be used with aqueous mobile phase on PGC for chiral separations of enantiomeric polyaromatic amines.

INTRODUCTION

Several enantiomeric amino alcohols, *e.g.*, propranolol, metoprolol and alprenolol, have been resolved in the direct separation mode using ion-pair chromatography with N-benzoxycarbonylglycyl-L-proline (L-ZGP) as the chiral counter ion [1,2]. The L-ZGP was dissolved in dichloromethane (containing 30–500 ppm of water) in order to promote a high degree of ion-pair formation. A non-chiral solid phase, *e.g.*, LiChrosorb DIOL, was used to separate the diastereomeric complexes (ion pairs) of enantiomeric amines with L-ZGP. The chromatographic system showed good stability and has recently been applied to the determination of propranolol enantiomer in plasma [3]. However, a relatively large volume of mobile phase (300–400 ml) was needed before constant retention times were obtained. The gradual decrease in retention during the equilibration was probably due to the deactivation of strong adsorption sites on the solid phase. Water dissolved in organic solvents of low polarity

[a] Presented at the *13th International Symposium on Column Liquid Chromatography, Stockholm, July 1989*. The majority of the papers presented at this symposium have been published in *J. Chromatogr.*, Vols. 506 + 507 (1990).

0021-9673/91/$03.50

adsorbs and changes the properties of polar solid phases, *e.g.*, silica or surface-modified silica [4].

Recently, a new high-performance liquid chromatographic (HPLC) support, porous graphitic carbon (PGC), developed by Gilbert *et al.* [5], was made commercially available (Hypercarb; Shandon, Runcorn, U.K.). The PGC phase is a strongly hydrophobic adsorbent with a flat surface consisting of layers of hexagonally arranged carbon atoms [6]. PGC has mainly been used as an alternative to reversed-phase bonded silica gels, but the planar and rigid surface structure also gives new and interesting separation capabilities for normal-phase chromatography. One advantage of the PGC phase is the homogeneous surface of the carbon molecule layers as they only possess a minimum of polar groups at their edges [6]. Further, as PGC has low contents of polar functionalities, the retention and selectivity of solutes might be less susceptible to small changes in the concentration of water and polar modifiers when applying organic mobile phases of low polarity.

The aim of this investigation was to compare a silica-based support, LiChrosorb DIOL, and PGC as adsorbing phases in chiral ion-pair chromatography. The possible effects of the stationary phase on the stereoselectivity in separations with a chiral counter ion are discussed.

In the comparison of the phases, particular emphasis was placed on the volume of mobile phase necessary to obtain constant retention times and stereoselectivity and also the chromatographic performance (efficiency and peak symmetry). The mobile phases were L-ZGP in dichloromethane with different contents of water. The effect of adding triethylamine (TEA) to the mobile phase as a "tailing reducer" was also studied.

Enantioselective separations for various classes of amines are given in order to illustrate the potential of porous graphitic carbon as adsorbing phase in chiral ion-pair chromatography. The separation of racemic 1-phenyl-2-aminopropane was of special interest as it has no polar functions apart from the amino group.

The successful application of PGC for the separation of enantiomeric amines using L-ZGP in aqueous mobile phases is also demonstrated.

EXPERIMENTAL

Apparatus

The liquid chromatographic system consisted of a Constametric III (LDC, Riviera Beach, FL, U.S.A.) pump, a 7125 injecor (Rheodyne, Cotati, CA, U.S.A.) with a 20-μl loop and a Spectromonitor III UV detector (LDC) with a 12-μl cell.

The LiChrosorb DIOL column (150 × 3.0 mm I.D.) was packed by a slurry technique using chloroform as suspending medium [1]. The PGC columns (100 × 4.7 mm I.D.) were packed with 7-μm particles. The PGC 134 column (Batch PGC 93) was a gift from Professor J. H. Knox (Department of Chemistry, University of Edinburgh). The Hypercarb column was supplied by Shandon. Columns and solvent reservoir were thermostated at 25.0 ± 0.1°C with a HETO type 2 pt 293 TC water-bath (Birkerød, Denmark).

Chromatographic technique

The columns were pre-equilibrated with 250–300 ml of dry dichloromethane (containing <30 ppm of water) before the mobile phase was introduced.

The chromatographic performance was characterized by reduced plate height (h), enantioselectiviy (α) and the peak asymmetry factor (Asf) obtained at a reduced velocity of 1.9 mm/s. Measurements were made using standard equations [7], but as the peak frequently showed severe tailing the data were used only as a qualitative measure of the peak performance. The void volume was determined by injection of chloroform, which was assumed to be unretained.

Chemicals

LiChrosorb DIOL (5 μm), dichloromethane (LiChrosolv), chloroform (analytical-reagent grade), methanol (analytical-reagent grade) and molecular sieves 4Å were obtained from E. Merck (Darmstadt, Germany).

Dichloromethane dried with molecular sieves had a water content of less than 30 ppm. The water contents of the eluents were adjusted by mixing dry and water-saturated (2100 ppm of water [8]) dichloromethane.

N-Benzoxycarbonylglycyl-L-proline was obtained from Nova Biochem (Switzerland). (*R*)- and (*S*)-propranolol · HCl was supplied by ICI (Macclesfield, U.K.), (*R,S*)-atenolol · HCl, (*R,S*)-2′-methylpropanolol · HCl and (*R,S*)-tocainide · HCl were gifts from Hässle (Mölndal, Sweden), (*R*)- and (*S*)-prilocaine · HCl was obtained from Astra (Södertälje, Sweden), (*R,S*)-mexiletine · HCl from Boehringer (Ingelheim, Germany), racemic and (*S*)-1-phenyl-2-aminopropane sulphate were gifts from the Department of Organic Pharmaceutical Chemistry (Uppsala, Sweden) and (*R.S*)-promethazine · HCl was provided by Kabi-Pharma (Stockholm, Sweden).

RESULTS AND DISCUSSION

Solid phase

LiChrosorb DIOL had a very strong affinity for amines and thus high counter-ion concentrations (L-ZGP) were required in order to elute the amines from the column, (Table I). The chromatographic performance was unsatisfactory with poorly shaped peaks and low efficiency that impaired the chiral resolution. A previous study [2] had shown that the addition of an amine, *e.g.*, triethylamine, to the mobile phase could enhance the resolution by increasing the efficiency and improving the peak shape. In this study acceptable peak symmetries ($Asf = 1.2$) and complete resolution ($R_S = 2.0$) of propranolol and metoprolol enantiomers could be obtained by using 10 m*M* L-ZGP and 0.20 m*M* TEA in dichloromethane as the eluent (Table I). The modified silica surface is energetically heterogeneous [9] and the observed improvement in the chromatographic performance was probably due to deactivation of strong adsorption sites by the TEA. The presence of the amine in the mobile phase also reduced the retention times, but had only a negligible effect on the enantioselectivity.

At low counter ion concentration, asymmetric peaks were obtained with porous graphitic carbon as the adsorbing phase. The bad peak shape might be due to retention of the free amine on strong adsorption sites with limited capacities as addition of competing amine, triehylamine, improved the peak performance (Table II). Further, high L-ZGP concentrations, *i.e.*, a high degree of ion-pair formation and retention as ion pairs, improved the peak symmetry and efficiency.

TABLE I

INFLUENCE OF TRIETHYLAMINE AND L-ZGP CONCENTRATIONS ON CHROMATOGRAPHIC PERFORMANCE WITH LICHROSORB DIOL AS STATIONARY PHASE

Mobile phase: L-ZGP and TEA in dichloromethane (containing 80 ppm of water).

Mobile phase	Parameter[a]	Solute	
		Metoprolol	Propranolol
[L-ZGP] = 10 m*M*, [TEA] = 0 m*M*	k'_R	5.1	5.8
	h	56	61
	Asf	2.5	2.3
	α	1.40	1.36
[L-ZGP] = 2.5 m*M*, [TEA] = 0.25 m*M*	k'_R	5.2	7.4
	h	32	32
	Asf	1.4	1.4
	α	1.40	1.37
[L-ZGP] = 10 m*M*, [TEA] = 0.20 m*M*	k'_R	3.0	3.5
	h	26	22
	Asf	1.2	1.2
	α	1.43	1.36

[a] k'_R = capacity factor for *R* enantiomer; *h* = observed reduced plate height; *Asf* = asymmetry factor; $\alpha = k'_S/k'_R$.

TABLE II

INFLUENCE OF TRIETHYLAMINE AND L-ZGP CONCENTRATIONS ON CHROMATOGRAPHIC PERFORMANCE WITH HYPERCARB AS STATIONARY PHASE

Mobile phase: L-ZGP and TEA in dichloromethane (containing 80 ppm of water).

Mobile phase	Parameter[a]	Solute	
		Metoprolol	Propranolol
[L-ZGP] = 2.5 m*M*, [TEA] = 0 m*M*	k'_R	2.7	20
	h	20	–[b]
	Asf	2.6	–[b]
	α	1.24	1.58
[L-ZGP] = 10 m*M*, [TEA] = 0 m*M*	k'_R	2.4	13
	h	8	11
	Asf	1.4	2.0
	α	1.25	1.48
[L-ZGP] = 2.5 m*M*, [TEA] = 0.25 m*M*	k'_R	2.2	13
	h	8	–[b]
	Asf	1.7	–[b]
	α	1.24	1.47
[L-ZGP] = 10 m*M*, [TEA] = 0.25 m*M*	k'_R	2.3	11
	h	7	8
	Asf	1.0	1.7
	α	1.26	1.48

[a] See Table I.
[b] Severe tailing.

Addition of triethylamine had no significant effect on the enantioselectivity except for a minor decrease in the separation factor of propranolol.

Regarding column efficiency, the PGC phase was found to be superior to the LiChrosorb DIOL phase. However, it was not possible to eliminate completely the bad peak shape for the propranolol enantiomers obtained on PGC with 0.25 m*M* TEA added to the mobile phase, whereas the metoprolol enantiomers eluted as symmetrical peaks (Table II).

The reason for the change in stereoselectivity on replacing LiChrosorb DIOL with PGC (*cf.*, Tables I and II) has not yet been elucidated, but it may be due to differences in the adsorption of the two diastereomeric ion pairs [(*R*)-A–(*S*)-HX and (*S*)-A–(*S*)-HX] to the solid phases. The apolar PGC phase will interact with the ion pair and its components by dispersion forces and π–π interactions, whereas LiChrosorb DIOL gives mainly polar interactions (*e.g.*, hydrogen bonding). Previously it has been demonstrated, by using L-ZGP [2] and 10-camphorsulphonic acid [10] as chiral counter ions, that the hydrogen-bonding properties of different modified silica phases affected the enantioselectivity and resolution of enantiomeric amines.

As discussed by, *e.g.*, Davankov [11], in systems having a chiral additive several different chiral mechanisms responsible for the stereoselectivity are possible. A chiral acid might promote stereoselective ion-pair formation in the mobile phase and a selective distribution of the two diastereomeric ion pairs. The enantioselective separation may also be due to stereoselective interaction of the enantiomeric amines with the chiral acid adsorbed on the solid phase.

The retention of the enantiomeric amine, (*R*)-A, as an ion pair [(*R*)-A–(*S*)-HX] with the chiral acid, (*S*)-HX, can be expressed by the equilibria

$$(R)\text{-A}_m + (S)\text{-HX}_m \overset{K_{RS}}{\rightleftharpoons} (R)\text{-A–(}S\text{)-HX}_m \overset{K^*_{RS}}{\rightleftharpoons} (R)\text{-A–(}S\text{)-HX}_s \qquad (1)$$

where m and s refers to the solid and mobile phase, respectively, and K_{RS} and K^*_{RS} are constants for the ion-pair formation and distribution of the ion pair between the mobile and stationary phase, respectively. The free amine might also be retained by adsorption on the solid phase:

$$(R)\text{-A}_m \overset{K_1}{\rightleftharpoons} (R)\text{-A}_s \qquad (2)$$

The adsorption constant K_1 is the same for the (*R*)- and (*S*)-amines as the binding to the solid phase of the free amine is non-stereoselective.

So far it has not been possible to predict the change in the separation factor, $\alpha_{S/R}$, on replacing, *e.g.*, LiChrosorb DIOL with PGC. This would require a knowledge of the adsorption constants for the free amine (K_1) and the ion-pairs (K^*_{RS}, K^*_{SS}) and also the ion-pair formation constants (K_{RS}, K_{SS}) in the mobile phase. The stationary phase with the highest selectivity for diastereomeric ion-pair adsorption ($\alpha = K^*_{SS}/K^*_{RS}$) also gives the highest enantioselectivity provided that the enantioselective ion-pair formation is not dominating and counteracting (*i.e.*, $K_{RS} > K_{SS}$) the selective ion-pair adsorption.

Influence of water content on the equilibration of the chromatographic system

Fig. 1 shows the number of column volumes (V_m) that had to pass the PGC column in order to obtain stable chromatographic conditions. The breakthrough volumes of L-ZGP were only slightly higher than the void volume, demonstrating a low

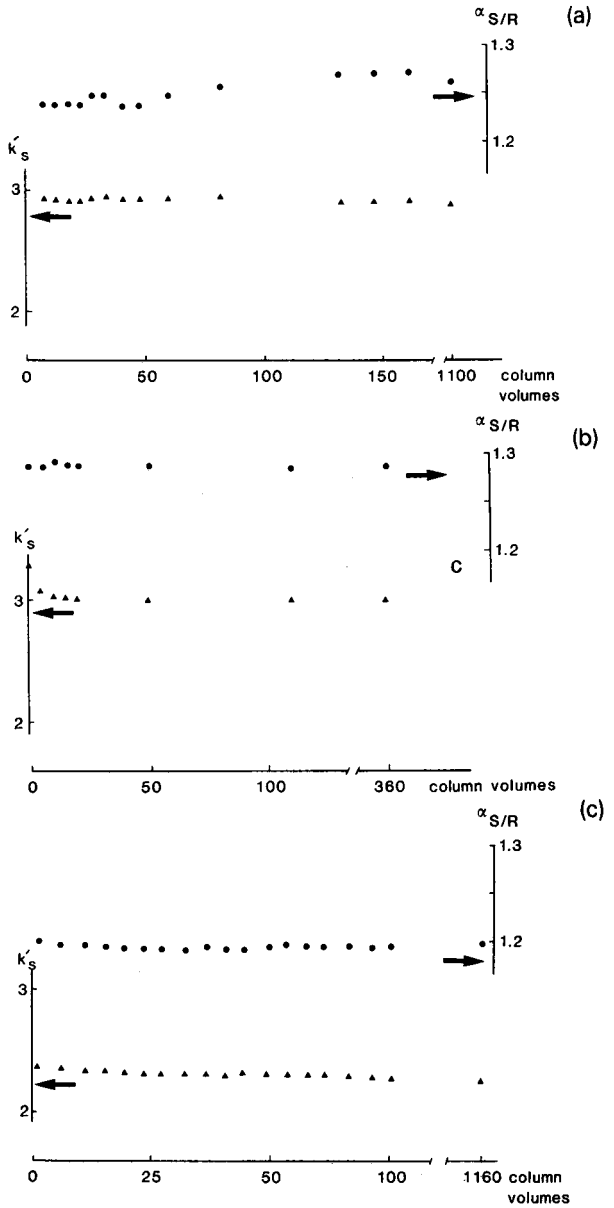

Fig. 1. Equilibration of chromatographic system. Stationary phase, Hypercarb; mobile phase, 10 m*M* L-ZGP in dichloromethane (containing *X* ppm water); solute, (*R,S*)-metoprolol. (a) $X = 80$; (b) $X = 500$; (c) $X = 2100$. (▲) Capacity factors; (●) separation factors.

adsorption constant of L-ZGP with respect to the PGC phase. Furthermore, thermodynamic equilibrium in the column, *i.e.*, constant retention times and separation factors, were obtained within less than fifteen column volumes, (Fig. 1). The water content of the mobile phase had no significant effect on the equilibration time. This indicates a low adsorption of water on PGC.

A decrease in the capacity and separation factors was observed when the mobile phase was saturated with water (2100 ppm of water) (Fig. 1). High concentrations of water gave more effective solvation of the diastereomeric ion pairs and their components which probably affected their stabilities and their distribution properties. Thus, a water content of about 500 ppm was preferable as it gave negligible differences in retention and stereoselectivity compared with mobile phases containing 80 ppm of water (Fig. 1b and a). However, it is more convenient to prepare and easier to control a mobile phase with a higher water content (*e.g.*, 500 ppm).

In comparison, 300 column volumes of mobile phase were required in order to obtain constant chromatographic conditions with LiChrosorb DIOL as stationary phase (Fig. 2). Interestingly, the separation factor becomes constant after 50 column volumes, whereas more than 300 column volumes had to pass the column before constant retention times were obtained. This indicated that the retentions of the enantiomers were affected to the same extent during the equilibration of the column. As discussed above, with silica-based phases it was necessary to include an amine in the mobile phase in order to obtain a good chromatographic performance. The deactivation of the LiChrosorb DIOL was dependent on the concentrations of amine, counter ion and water. It was extremely time consuming to condition LiChrosorb DIOL when the triethyamine ws omitted from the mobile phase. More than 500 ml of

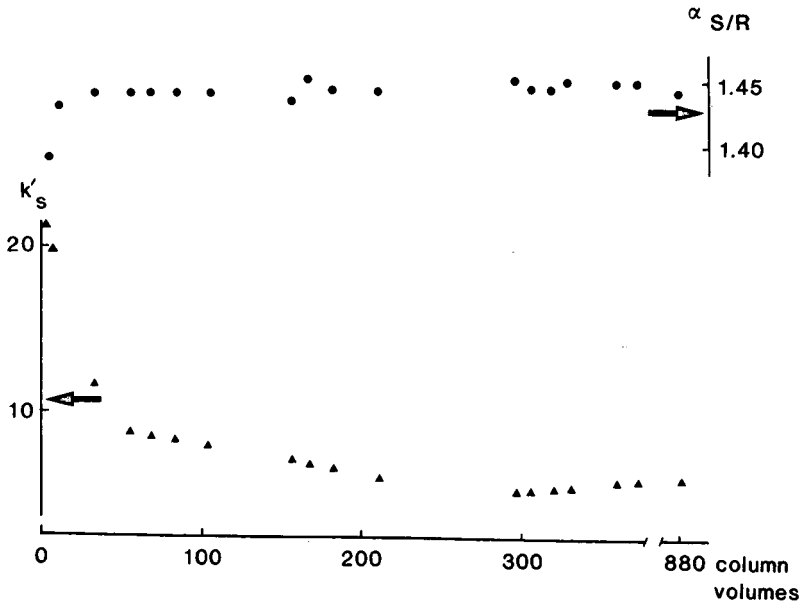

Fig. 2. Equilibration of chromatographic system. Stationary phase, LiChrosorb DIOL; mobile phase, 10 m*M* L-ZGP and 0.20 m*M* TEA in dichloromethane (containing 500 ppm of water). Symbols as in Fig. 1.

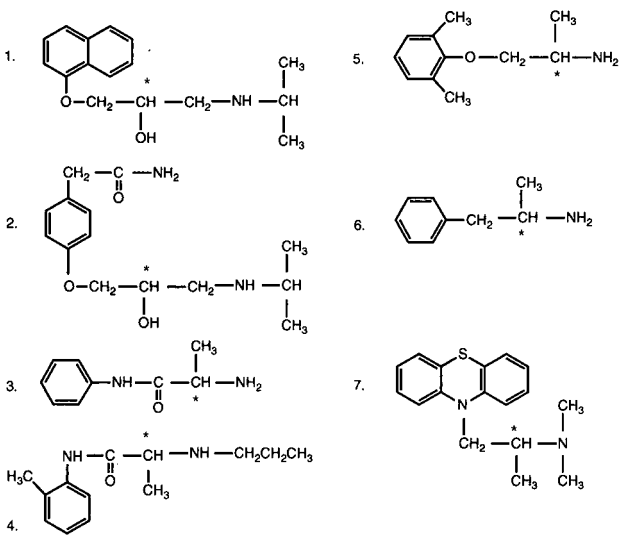

Fig. 3. Structures of solutes (see Table III). ★, Asymmetric centre.

dichloromethane containing 500 ppm of water and 10 m*M* L-ZGP were required to obtain a constant retention and selectivity. Close control of the water content and the presence of an amine in the mobile phase were essential in order to obtain rapid equilibration and reproducible systems when applying silica-based phases.

Solute structure and enantioselectivity

Chiral separations of some pharmaceutical compounds (Fig. 3) with L-ZGP as the counter ion and porous graphitic carbon as the adsorbing phase are shown in Table III. The highest separation factors were observed for the amino alcohols (propranolol and atenolol) which can give multi-point interactions (electrostatic attraction and hydrogen bonding) with the counter ion. This is in accordance with previous findings using modified silica supports (LiChrosorb DIOL and Nucleosil CN) [2]. The surface-modified silica phases gave more or less the same stereoselectivity (α = 1.2–

TABLE III

INFLUENCE OF SOLUTE STRUCTURE ON RETENTION AND STEREOSELECTIVITY

Stationary phase, PGC 134; mobile phase, 10 m*M* L-ZGP in dichloromethane (containing 80 ppm of water).

No.[a]	Solute	k'_1	α^b
1	Propranolol	11	1.47
2	Atenolol	4.1	1.35
3	Tocainide	3.4	1.20
4	Prilocaine	0.91	1.12
5	Mexiletine	3.9	1.21
6	1-Phenyl-2-aminopropane	3.8	1.15
7	Promethazine	1.0	1.15

[a] For structures see Fig. 3.

[b] k' (second-eluted enantiomer)/k' (first-eluted enantiomer).

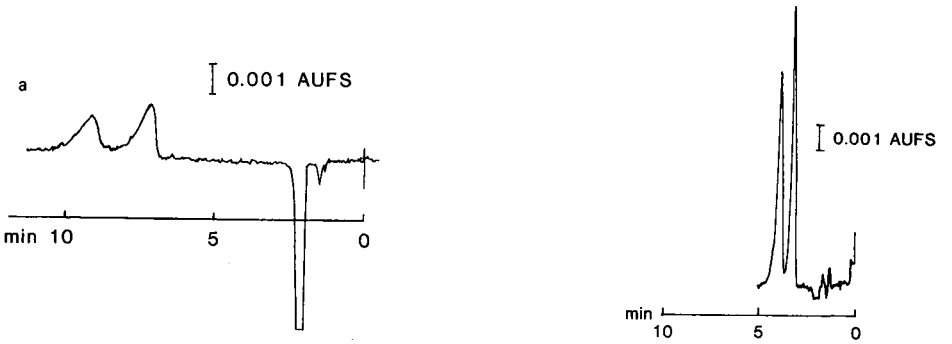

Fig. 4. Resolution of (*R,S*)-atenolol. Stationary phase, PGC 134; mobile phase, 10 m*M* L-ZGP and *X* m*M* TEA in dichloromethane (containing 80 ppm of water). (a) $X = 0$ m*M*; (b) $X = 1.0$ m*M*.

1.8) as PGC but they retained the hydrophilic amino alcohols (*e.g.*, atenolol) more strongly than propranolol. As discussed above, high concentrations of L-ZGP and addition of TEA to the mobile phase were necessary in order to obtain a reasonable retention time with the modified silica phases. Thus, hydrophilic chiral amines and amino alcohols are preferably separated using PGC, as demonstrated by the separation of (*R,S*)-atenolol in Fig. 4a. A complete resolution of the enatiomers was obtained within less than 10 min using 10 m*M* L-ZGP in dichloromethane as the eluent. As indicated in Table II, the bad peak shape could be improved by an addition of triethylamine (Fig. 4b).

The combination of L-ZGP as the chiral additive and a modified silica as the adsorbing phase generally separated enantiomeric β-amino alcohols but not amines lacking a strong hydrogen bonding group in the vicinity of the asymmetric carbon atom [1,2]. With PGC, on the other hand, separations of several different classes of enantiomeric amines (Table III) were possible. Interestingly, chiral recognition was observed for 1-phenyl-2-aminoproprane, an amine with no polar function attached to the chiral centre apart from the amino group. The separation (Fig. 5) indicated that

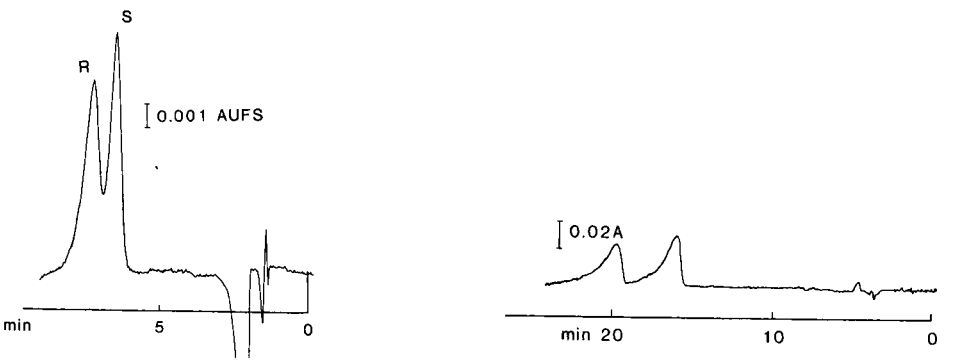

Fig. 5. Separation of racemic 1-phenyl-2-aminopropane. Conditions as in Fig. 4a.

Fig. 6. Reversed-phase separation of (*R,S*)-promethazine. Stationary phase, PGC 134; mobile phase: 5.2 m*M* L-ZGP in methanol–water (95:5).

ion-pair formation and the possibility of additional weaker hydrophobic or steric interaction between the L-ZGP and enantiomeric amines were sufficient for chiral resolution. However, introducing a polar group, *e.g.*, –O– (mexiletine, Table III) or –CONH– (tocainide and prilocaine, Table III) in the vicinity of the chiral centre improved the stereoselectivity. It is possible that two or more strong interactions (electrostatic attraction, hydrogen bonding, dipole–dipole) between the ions enhanced the differences in stability or distribution properties of the diastereomeric ion pairs.

Chiral separations were also carried out for tertiary amines, *e.g.*, promethazine (Table III).

Chiral separations in reversed-phase systems

The enantioselectivity obtained using L-ZGP in water-saturated dichloromethane suggested the possibility of chiral recognition in mobile phases of high polarity. Indeed, L-ZGP dissolved in methanol–water (95:5) promoted the separation of enantiomeric amines with a polyaromatic structure structure (Fig. 6). The column efficiency was moderate but a complete resolution of racemic promethazine was possible owing to the high stereoselectivity ($\alpha = 1.25$).

Based on the limited data available, it was not possible to elucidate if the decrease in capacity factors at the higher L-ZGP concentration (Table IV) was due to an increased formation of less retained ion pairs or to a more effective competition by the counter ion for the limited adsorption capacity of the stationary phase. Further, the mixed effects on the separation factors by the 3-fold increase in the counter ion concentration indicated complex retention mechanism(s).

CONCLUSION

The study of PGC has revealed some advantageous properties as an HPLC stationary phase. Chiral separations of amines with different hydrogen-bonding capabilities were possible using N-benzoxycarbonylglycyl-L-proline dissolved in organic mobile phases with high water contents. Fast equilibration (less than fifteen column volumes) were obtained without the addition of an amine to the mobile phases, whereas LiChrosorb DIOL as adsorbing phase gave long equilibration times despite the use of triethylamine in the mobile phase. The bad peak shape obtained on the

TABLE IV

CHIRAL SEPARATION USING AQUEOUS MOBILE PHASES

Stationary phase, PGC 134; mobile phase, L-ZGP in methanol–water (95:5).

Solute	L-ZGP concentration (m*M*)			
	5.22		19.0	
	k'_1	α	k'_1	α
Propranolol	32	1.08	5.4	1.12
Promethazine	17	1.25	3.9	1.20
2′-Methylpropranolol	57	1.06	5.5	1.0

DIOL and PGC phases was improved by the addition of triethylamine to the mobile phase.

Enantiomeric amines having a polyaromatic ring were resolved with L-ZGP dissolved in an aqueous mobile phase.

ACKNOWLEDGEMENTS

We are grateful to Professor D. Westerlund for valuable comments on the manuscript. This project was supported by the Swedish Natural Science Research Council. Research grants from the Swedish Academy of Pharmaceutical Science and the I. F. Foundation for Pharmaceutical Research are gratefully acknowledged.

REFERENCES

1 C. Pettersson and M. Josefsson, *Chromatographia*, 21 (1986) 321.
2 C. Petterson, A. Karlsson and C. Gioeli, *J. Chromatogr.*, 407 (1987) 217.
3 A. Karlsson, C. Pettersson and S. Björkman, *J. Chromatogr.*, 494 (1989) 157.
4 K. K. Unger, *Porous Silica (Journal of Chromatography Library*, Vol. 16), Elsevier, Amsterdam, 1979, p. 195.
5 M. T. Gilbert, J. H. Knox and B. Kaur, *Chromatographia*, 16 (1982) 138.
6 J. H. Knox and B. Kaur, in P. R. Brown and R. A. Hartwick (Editors), *High Performance Liquid Chromatography*, Wiley, New York, 1989, p. 189.
7 L. R. Snyder and K. K. Kirkland, *Introduction to Modern Liquid Chromatography*, Wiley, New York, 1974.
8 B. V. Laverne and H. Engelhardt, *J. Chromatogr.*, 95 (1974) 27.
9 R. E. Majors, in C. Horvath (Editor), *High Performance Liquid Chromatography* , Vol. 1, Academic Press, London, 1980, p. 86.
10 C. Pettersson and G. Schill, *Chromatographia*, 16 (1982) 192.
11 V. A. Davankov, *Chromatographia*, 27 (1989) 475.

Journal of Chromatography, 543 (1991) 299–305
Elsevier Science Publishers B.V., Amsterdam

CHROM. 23 124

Chiral high-performance liquid chromatography of aromatic cyclic dipeptides using cyclodextrin stationary phases

J. FLORANCE* and Z. KONTEATIS
BOC Group Technical Center, 100 Mountain Avenue, Murray Hill, N.J. 07974 (U.S.A.)
(First received October 18th, 1990; revised manuscript received January 16th, 1991)

ABSTRACT

A series of enantiomers of cyclic and linear dipeptides containing aromatic amino acids was prepared and chromatographed on β- and γ-cyclodextrin (CD) columns. The retention times, separation factor α and resolution values were calculated. The relevance of the distance of the chiral center from the phenyl ring for chiral resolution was studied. A model was developed using X-ray crystallographic data for an inclusion complex of β-CD and the enantiomers of cyclic(Phe-Gly).

INTRODUCTION

Separation of chiral peptides has become increasingly important due to differences in physiological activity of the resolved stereoisomers as well as regulatory requirements [1]. A variety of techniques have been used to facilitate enantiomeric separations, including chiral stationary phases, chiral eluents and chiral derivatizations [2–4]. The increasing importance of peptides as drugs has encouraged new systems for analysis of small peptide stereoisomers that are not well resolved by traditional reversed-phase columns.

Cyclic dipeptides (diketopiperazines) are an interesting class of peptides that have a variety of biological activities [5]. Previous work has been done on resolution of amino acid and dipeptide (linear and cyclic) enantiomers [6–8]. The mode of separation of enantiomers using cyclodextrin (CD) immobilized on silica high-performance liquid chromatography (HPLC) columns requires the formation of an inclusion complex that will selectively form a tighter binding complex with one isomer as opposed to the other [9–11].

Structural requirements in some systems have been defined that allow for separation of enantiomers [12–14]. In the present study a series of dipeptide compounds was synthesized. The dipeptides contained phenylalanine and phenylalanine derivatives where the phenyl ring was directly attached to the chiral center, or at one or two carbons away from the chiral center, respectively. Both linear and the cyclized dipeptides were prepared and chromatographed.

To understand better the importance of the structural requirements for separation of these dipeptides on CD, several features of these model compounds were

studied including the requirement for a phenyl ring, its proximity to the chiral center to be resolved and also the possible effects on the hydrogen bonding in CD inclusion complexes.

Molecular graphics studies of the CD inclusion complexes were also done to understand better the chromatographic results.

EXPERIMENTAL

Chromatography

Separations were performed using a Waters Assoc. (Milford, M.A., U.S.A.) HPLC system which consisted of two 510 HPLC pumps, a 481 UV detector, A WISP autoinjector and a Model 840 data acquisition and control system. The columns were β-CD and γ-CD (25 cm × 4.6 mm I.D.) from ASTEC (Whippany, N.J., U.S.A.) Mobile phases consisted of various isocratic combinations of HPLC-grade methanol and water, typically 10:90 (v/v). Additives to the aqueous phase were also tried, such as triethylamine acetate, pH 4.0. Flow-rates were 1.0 ml/min and UV detection was at 214 nm.

Materials

Solvents were HPLC grade from J. T. Baker (Phillipsburg, N.J., U.S.A.) and water was obtained from a Milli-Q system (Bedford, MA, U.S.A.). The 0.1 *M* TEAE buffer was made by titration of triethylamine with acetic acid to pH 4.0.

α-Phenyl-α-ethylglycine (racemic) was obtained from Chemical Dynamics (South Plainfield, N.J., U.S.A.). Cyclo(L-Phe-Gly) and D- and L-homophenylalanine) were purchased from Bachem (Bubendorf, Switzerland); D- and L-phenylglycine were purchased from Sigma (St. Louis, MO, U.S.A.). Boc-glycine was purchased from Peninsula Labs (Belmont, CA, U.S.A.). All other chemicals were reagent grade.

Synthesis

The linear peptides were prepared by the same general procedure as using conventional *t*-Boc peptide chemistry. Cyclic dipeptides were prepared from the corresponding linear dipeptides by cyclodehydration. This was done using phenol under non-racemizing conditions, with slight modifications from the original described by Kopple and Ghazarian [15].

Computer graphics

The molecular graphics were done on a PS390 Evans and Sutherland using SYBYL molecular modeling software [16]. The three-dimensional coordinates of β-CD were obtained from the Cambridge Crystallographic Data Base [17]. The coordinates for c(Phe-Gly) were obtained from the X-ray crystal structure of c(Tyr-Gly) which was modified by removing the hydroxyl group from tyrosine.

RESULTS AND DISCUSSION

Previous work has shown that the proximity of the chiral center to the 2'- and 3'-hydroxyls at the top of the CD cavity are important for resolution of enantiomers [12]. Modeling studies with propranolol have shown that increased hydrogen bonding allows for a more stable inclusion complex for *d*-propranolol as compared to the

l-isomer. The elution order from a β-CD column reflects this with *l*-propranolol eluting before the *d*-propranolol.

The presence of an aromatic group is beneficial but not essential for the formaion of an inclusion complex with CDs. Models show that this is the portion of the molecule that inserts into the CD cavity. In the present study, an aromatic group (*i.e.*, a phenyl group), is contained in all of the cyclic dipeptides. There is also a pseudo-aromatic ring in the form of the diketopiperazine ring in these compounds. The model suggests that as with other aromatic compounds, the aromatic phenyl ring is inserted into the CD pocket.

It has been previously suggested that the distance of the chiral center to the phenyl group seems to be important for the stability of the inclusion complex. Compounds such as racemic barbiturates, in which the chiral center is contained in rings, resulted in increased resolution of enantiomers on CD. Chiral centers farther away (*i.e.*, more than one carbon) from the phenyl ring are often not well resolved on CD, although there are exceptions. Decreased bond rotation due to a shorter side chain was one suggestion for this effect [12]. Our results also agree with this observation as cyclic dipeptides are better resolved than linear dipeptides.

Studies have been conducted on a series of hydantoin enantiomers in which the length and location (5′ and 3′) of the alkyl subtituents were varied and corresponding effects on resolution of enantiomers on CD were evaluated. The best resolution was

TABLE I

RETENTION TIMES OF LINEAR AND CYCLIC DIPEPTIDES CONTAINING AROMATIC GROUPS ON γ- AND β-CD HPLC COLUMNS

Mobile phase: water–methanol, 90:10 (v/v) at 1 ml/min, 214 nm.

Compound	Retention time	
	γ-CD	β-CD
Cyclo (L-PhenylGly-Gly)	4.1	4.8
Cyclo (D-PhenylGly-Gly)	4.1	4.8
Cyclo (L-Phe-Gly)	4.9	12.2
Cyclo (D-Phe-Gly)	4.9	8.1
Cyclo (L-homoPhe-Gly)	4.6	14.6
Cyclo (D-homoPhe-Gly)	4.6	14.6
Cyclo (L-α-Phenyl-α-ethylGly-Gly)	4.9	13.6
Cyclo (D-α-Phenyl-α-ethylGly-Gly)	4.9	12.3
L-PhenylGly-Gly	4.1	4.9
D-PhenylGly-Gly	4.1	4.9
L-Phe-Gly	4.9	8.2
D-Phe-Gly	4.9	7.8
L-HomoPhe-Gly	4.7	13.3
D-HomoPhe-Gly	4.7	13.3
L-Phenylglycine	3.9	4.1
D-Phenylglycine	3.9	4.1
L-HomoPhe	4.5	8.7
D-HomoPhe	4.5	8.7
L-Phe	4.2	4.5
D-Phe	4.2	4.5

TABLE II

CALCULATED α AND RESOLUTION VALUES ON β-CD FROM DATA IN TABLE I

Compound	β-CD	
	Resolution	α
Cyclo(L-PhenylGly-Gly) Cyclo(D-PhenylGly-Gly)	0	1.0
Cyclo(L-Phe-Gly) Cyclo(D-Phe-Gly)	1.5	1.67
Cyclo(L-homoPhe-Gly) Cyclo(D-homoPhe-Gly)	0	1.0
Cyclo(L-α-phenyl-α-ethylGly-Gly) Cyclo(D-α-phenyl-α-ethylGly-Gly)	0.5	1.12

obtained with the methyl substituent; it decreased with larger substituents. The evidence points to disruption of hydrogen bonding due to longer chain substituents on 3′ or 5′ of the phenyl ring [13].

In the present study, we observed no resolution of enantiomers with the phenyl ring attached directly to the chiral center when hydrogen is the other substituent (*i.e.*, c(D- and L-PhenylGly-Gly). Some resolution is observed when the substituent is ethyl (*i.e.*, D- and L-cyclo(α-Phe-α-ethylGly-Gly) (CPEGG) separation factor (α) = 1.12 and resolution R_s = 0.5.

The retention times of the cyclic dipeptides c(Phe-Gly), c(homoPhe-Gly) and CPEGG were in the range 8.1–14.6 min as seen in Table I. The retention times seem to be more related to the relative hydrophobicity of the compound rather than the chiral discrimination, although the enantiomers of c(Phe-Gly) seem to be an exception.

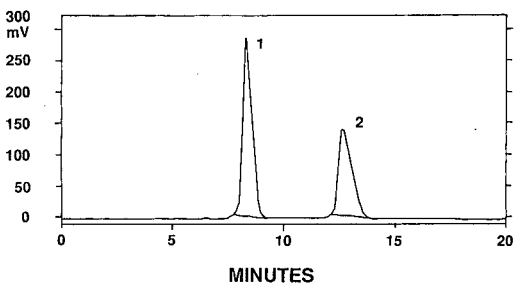

Fig. 1. Resolution of (1) c(D-Phe-Gly) and (2) c(L-Phe-Gly), on Cyclobond I, 90:10 (v/v) water–methanol at 1 ml/min.

Fig. 2. Model of the inclusion complex of c(L-Phe-Gly) (A) and c(D-Phe-Gly) (B) with β-CD using X-ray coordinates. The hydrogen bond distances in the c(L-Phe-Gly)–CD complex for the two amide hydrogens interacting with the oxygens of the 2′- and 3′-hydroxyls are 2.2 and 2.6 Å. In the D-isomer complex the same distances are 2.6 and 4.1 Å as measured with SYBYL software.

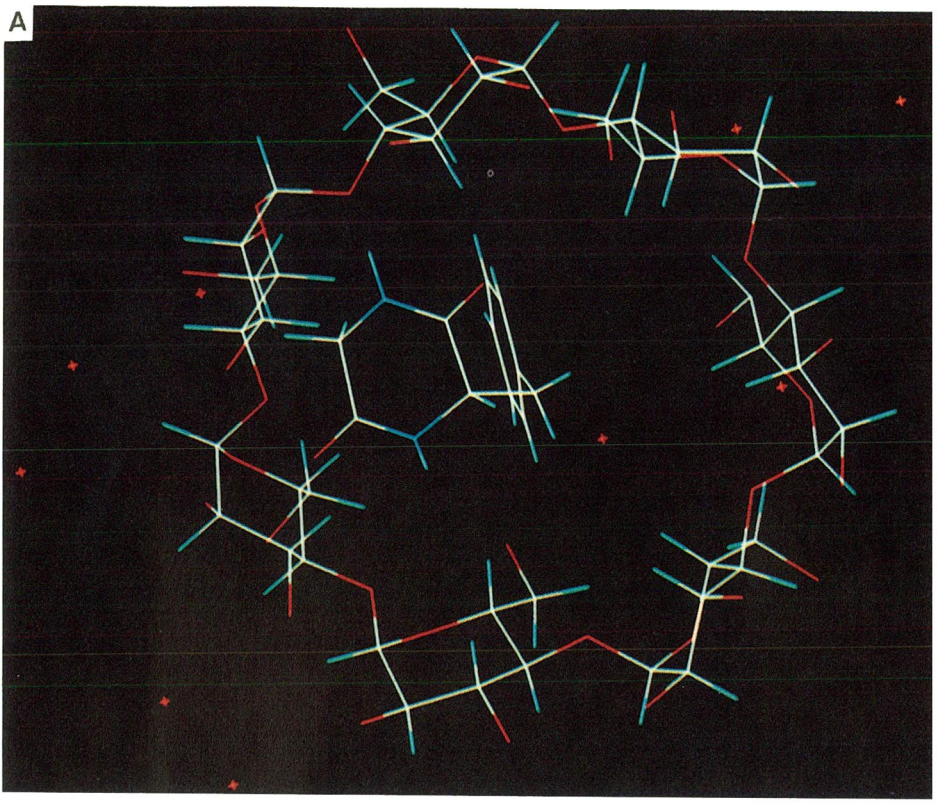
A

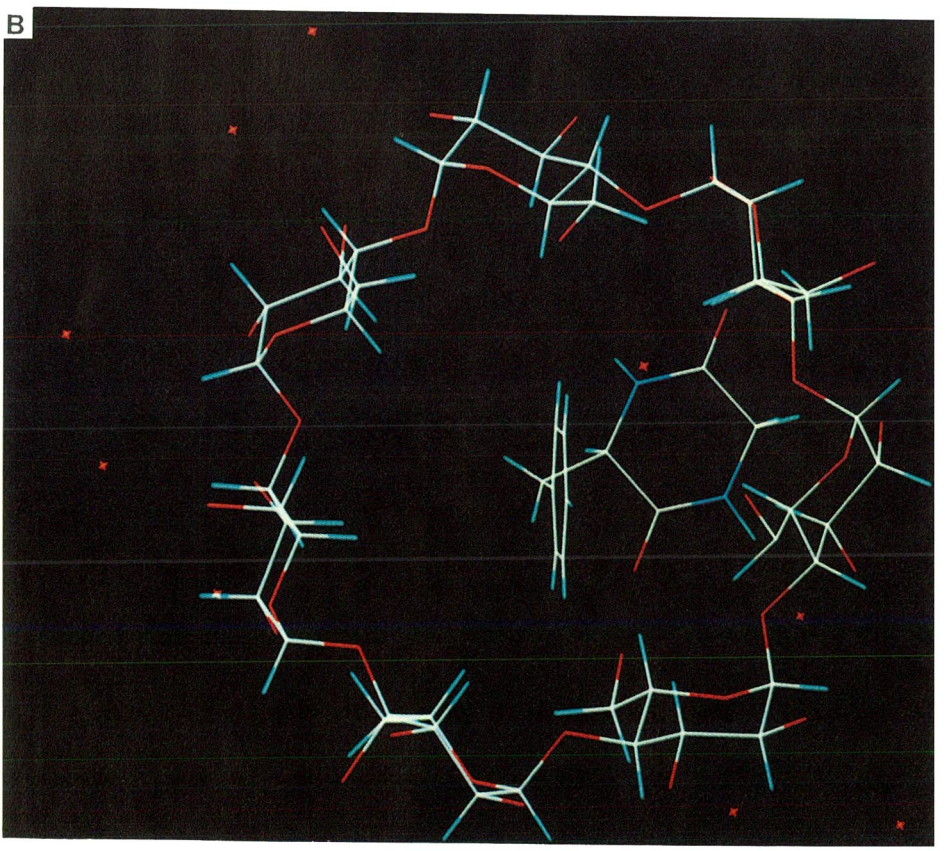
B

Enantiomers in which the phenyl ring and the chiral center are separated by two methylene units were not resolved on β-CD (*i.e.*, c(D- and L-homoPhe-Gly). This was expected in view of other studies indicating that when the chiral center is too far out of the CD pocket it will not interact with the 2′- and 3′-hydroxyls, thus not allowing for chiral recognition.

The enantiomers of c(Phe-Gly) were retained and well resolved with $\alpha = 1.67$ and $R_s = 1.5$ (Table II). The high resolution indicates a significant difference between the stability of the inclusion complex of CD with the D- versus the L-isomer. The difference is manifested in the elution times, with the c(L-Phe-Gly) eluting about 5 min after the c(D-Phe-Gly) as shown Fig. 1. These results suggest that optimal chiral resolution in this class of cyclic dipeptides is observed when the distance between the phenyl ring and the chiral center is one methylene unit.

In this study most of the chiral chromatography was performed with isocratic methanol–water combinations. In addition, cyclic dipeptides were chromatographed using an ion-pair buffer, triethylamine acetate, pH 4.0. The retention times on β-CD were increased slightly but no improvements in resolution were seen with this buffer system. No enantiomers were separated using this system that did not resolve with methanol–water.

In Fig. 2 a model of the inclusion complex of c(D-Phe-Gly) and c(L-Phe-Gly) with β-CD shows the phenyl ring inserted into the CD pocket. In this model the possible hydrogen bonds that can form with the primary and secondary hydroxyls of β-CD are the two amide protons from the cyclic dipeptide ring. The diketopiperazine ring is not linear but slightly puckered as determined from crystallographic data. It would be difficult to form optimal hydrogen bonds between the two carbonyls on the cyclic dipeptide ring and the CD hydroxyls, with the phenyl ring fully inserted. The hydrogen bond distances were measured in both D- and L-Phe isomers for the amide hydrogens. The preliminary results indicate that the L-isomer has the possibility for two optimal hydrogen bonds (about 2.5 Å) with the adjacent CD hydroxyls. The D-isomer seems to allow for only one optimal hydrogen bond with the phenyl ring fully inserted. Various rotations and translations of the cyclic dipeptide and β-CD were performed to locate possible hydrogen bonds. Molecular modeling studies are currently underway to refine this model of CD–dipeptide complexes. A full understanding of the dipeptide–β-CD complex would require crystallization of the complex and solution of the crystal structure by *X*-ray techniques.

ACKNOWLEDGEMENTS

We would like to thank Dr. Alphonse Galdes and Dr. Peter Maye for help with the Cambridge crystallographic files and with the SYBYL software.

REFERENCES

1 R. W. Souter, *Chromatographic Separations of Stereoisomers*, CRC Press, Boca Raton, FL, 1985.
2 P. Roumeliotis, K. K. Unger, A. A. Kurganov and V. A. Davankov, *J. Chromatogr.*, 255 (1983) 51.
3 N. Nimura, A. Toyama, Y. Kasahara and T. Kinoshita, *J. Chromatogr.*, 239 (1982) 671.
4 D. W. Aswad, *Anal. Biochem.*, 137 (1984) 405.
5 S. Johne and D. Groger, *Pharmazie*, 32 (1977) 1.
6 J. Florance, A. Galdes, Z. Konteatis, Z. Kosarych, K. Langer and C. Martucci, *J. Chromatogr.*, 414 (1987) 313.

7 H. J. Isaaq, *J. Liq. Chromatogr.*, 9 (1986) 229.
8 H. J. Isaaq and C. D. Ridlon, *J. Liq. Chromatogr.*, 9 (1986) 3377.
9 D. W. Armstrong, *J. Liq. Chromatogr.*,7 (Supp. 2) (1984) 353.
10 D. W. Armstrong and W. DeMond, *J. Chromatogr. Sci.*, 22 (1984) 411.
11 *The ASTEC Informer*, Vol. 1. No. 2, Advanced Separation Technologies, Whippany, NJ, 1985.
12 D. W. Armstrong, T. J. Ward, R. D. Armstrong and T. S. Beesley, *Science (Washington D.C.)*, 232 (1986) 1132.
13 J. H. Maguire, *J. Chromatogr.*, 387 (1987) 453.
14 K. G. Feitsma, J. Bosman, B. F. H. Drenth and R. A. de Zeeuw, *J. Chromatogr.*, 333 (1985) 59.
15 K. D. Kopple and H. G. Ghazarian, *J. Org. Chem.*, 33 (1968) 862.
16 *SYBYL, Version 5.2, Molecular Modeling Software*, Tripos Associates, St. Louis, MO.
17 *Cambridge Structural Database System, Version 3.6*, Cambridge Crystallographic Data Center, University of Cambridge, U.K.

Journal of Chromatography, 543 (1991) 307–314
Elsevier Science Publishers B.V., Amsterdam

CHROM. 23 117

Separation of ^{125}I-labelled derivatives of 5-hydroxy-6,8,11,14-eicosatetraenoic acid

I. MUCHA*, ILDIKÓ PALUSKA-FERENCZ and G. TÓTH
Institute of Isotopes of the Hungarian Academy of Sciences, P.O. Box 77, H-1525 Budapest (Hungary)
(First received July 5th, 1990; revised manuscript received January 14th, 1991)

ABSTRACT

Monoiodinated tyrosine methyl ester, a derivative of 5-hydroxy-6,8,11,14-eicosatetraenoic acid containing ^{125}I in the phenolic *ortho* position was prepared with high specific radioactivity and separated by column chromatography on a Sephadex LH-20 gel. The adsorption behaviour of the labelled product was studied both by adsorption chromatography using a Sephadex LH-20 adsorbent with ethanol–water as a binary eluent and by reversed-phase high-performance liquid chromatography using C_{18}-silica as a stationary phase with aqueous binary eluents containing ethanol, methanol or acetonitrile. In both separation systems, a linear relationship was found between the logarithmic capacity factor or distribution coefficient and the logarithmic concentration of the organic solvent.

INTRODUCTION

Various prostanoids can be labelled with ^{125}I through their histamine and tyramine [1] or tyrosine methyl ester (TME) [1,2] and these derivatives have widespread use in radioimmunoassay (RIA). 5-Hydroxy-6,8,11,14-eicosatetraenoic acid [5-HETE] is a key intermediate produced in the lipoxygenase pathway of arachidonic acid, and therefore the ^{125}I-labelled derivative of this compound may be useful in specific RIA, although no such RIA has previously been reported.

In the course of labelling through TME derivatives radioiodine may be incorporated via electrophilic substitution into the aromatic ring in the 3′- and/or 5′-positions, but only the monosubstituted derivatives are suitable as tracers for RIA. As we have shown previously, adsorption chromatography on Sephadex LH-20 is an efficient method for the isolation, with high specific activity, of the monoiodinated derivatives of prostanoids [3], steroids [4–8] and other bioactive compounds [9–11].

In this paper we report on the adsorption chromatographic separation of ^{125}I-labelled 5-HETE–TME from the inactive parent compound using Sephadex LH-20 as adsorbent, a method that permits a high specific activity suitable for RIA to be achieved.

According to a widely accepted model of adsorption, the displacement of solute molecules from a sorbent involves the participation of a stoichiometric number of solvent molecules used as organic modifier. Solutes that behave according to this stoichiometric displacement model are expected to give linear plots of log (distribution

0021-9673/91/$03.50

coefficient) or log (capacity factor) *vs.* log (concentration of organic solvent), with a slope that reflects the stoichiometric number of solvent molecules participating in displacement.

The adsorption behaviour of various iodinated compounds has been studied previously on Sephadex LH-20 adsorbent and a linear log k *vs.* log X relationship was found with an ethanol–water binary eluent [3–11], where k and X are the distribution coefficient and the molar fraction of ethanol, respectively. On the other hand, numerous investigations related to the mechanism of adsorption in high-performance liquid chromatography have also demonstrated a linear relationship between log k' and log X, where k' is the capacity factor. This relationship, originally verified for normal-phase high-performance liquid chromatography (HPLC) using silica as stationary phase, was extended also to reversed-phase (RP) systems using binary mobile phases consisting of water and an organic solvent modifier [12–16].

In previous work, RP-HPLC was found to be an efficient alternative to Sephadex LH-20 adsorption chromatography for the separation of various ^{125}I-labelled prostanoid derivatives and a similar chromatographic behaviour of these derivatives was observed in RP-HPLC and in Sephadex LH-20 chromatography [17,18].

In this work, the chromatographic behaviour of ^{125}I-labelled 5-HETE–TME was studied using both adsorption chromatography with Sephadex LH-20 as adsorbent and ethanol–water as eluent and RP-HPLC using C_{18}-bonded silica as stationary phase with aqueous binary eluents containing ethanol, methanol or acetonitrile as organic modifier. Highly significant linear relationships for log k *vs.* log X (Sephadex LH-20) and log k' *vs.* log X (RP-HPLC) were obtained. To our knowledge, this paper is the first to report on the linearity of log k' *vs.* log (molar fraction of organic modifier) in RP-HPLC for a representative of an important family of small molecules containing the monoiodo-TME functional group.

EXPERIMENTAL

5-(±)-HETE was synthesized from arachidonic acid according to the method of Corey *et al.* [19] (since the racemic form was used throughout this study, the chirality will not be indicated any further). In order to study the chromatographic behaviour of 5-HETE–TME used for the radioiodination, this compound was synthesized using tritium-labelled TME. [^{3}H]TME prepared as described [20] was diluted with non-radioactive TME to a specific activity of about 100 μCi/mg and coupled to 5-HETE using the carbodiimide method.

5-HETE–TME was labelled with ^{125}I by the use of the chloramine-T method. To 2–3 μg (3–4.5 nmol) of 5-HETE–TME in 50 μl of buffer, 1–2 mCi (0.5–1 nmol) of carrier-free Na^{125}I (Institute of Isotopes, Budapest, Hungary) was added, followed by the addition of 50 μl of 0.5% chloramine-T solution. After 60 s, the reaction was quenched with 100 μl of 0.7% sodium metabisulphite solution. All reagents were dissolved in 50 m*M* phosphate buffer (pH 7.4).

Monoiodinated [^{125}I]5-HETE–TME was isolated from the labelling reaction mixture by column chromatography on a preparative scale. Sephadex LH-20 dextran gel (Pharmacia, Uppsala, Sweden) swollen in distilled water was packed in a column (130 × 10 mm I.D.) to a height of 100 mm. The reaction mixture was administered on

the top of gel and allowed to soak in. After equilibration for 10 min, the elution was started with 150 ml of water, followed by 80–100 ml of 20% ethanol, and the monoiodinated product eluted with 30–35 ml of 30% ethanol. The flow-rate was 45–50 ml/h. In order to suppress the dissociation of the phenolic OH group, which would lead to a decrease in adsorption on dextran gel, the pH was adjusted to 4.0 with 0.1 *M* citrate buffer.

The effluent was passed over an NaI(Tl) scintillation crystal and its radioactivity was counted by a ratemeter and recorded by an *X–Y* plotter.

In order to measure the elution volume of [^{3}H]5-HETE–TME, the effluent was collected with a fraction collector and the ^{3}H radioactivity determined by liquid scintillation counting.

For RP-HPLC separation, a two-pump (LKB, Type 2150) gradient system controlled by an HPLC controller (LKB, Type 2152) was used. An RP-18 (Spheri-5) Aquapore Cartridge column (100 × 4.6 mm I.D.) (Pierce) equipped with a guard cartridge was attached to an NaI(Tl) scintillation crystal. Radioactive samples (0.5–1.0 μCi) dissolved in 5–10 μl of mobile phase were injected through a Rheodyne sample injector equipped with a 200-μl sample loop. The ^{125}I radioactivity of the effluent was counted by a ratemeter attached to the scintillation crystal and registered with a potentiometric recorder (LKB, Type 2210).

The elution volumes in various binary eluents were determined in duplicate. The dead volume (1 ml) was determined using Na^{125}I as the non-retained compound. In preliminary experiments the effect of pH on the retention time was studied in acetonitrile–10 m*M* citrate buffer (60:40, v/v) mobile phase in the pH range 4.0–9.0. As the retention volume remained unchanged throughout this range, the pH was unadjusted for the experiments with different binary eluents of various composition.

RESULTS AND DISCUSSION

Isolation of radioiodinated [^{125}I]5-HETE–TME by Sephadex LH-20 column chromatography

Labelling of 5-HETE–TME with ^{125}I led to the production of a complex reaction mixture. As illustrated in Fig. 1, several labelled products could be detected in the effluent collected from the Sephadex LH-20 column. Omitting the free ^{125}I$^-$ eluting at the dead volume, of the three elution peaks peak 2 was assigned to an unidentified labelled by-product. Peak 3 was attributed on the basis of the immunoreactivity to the monoiodinated [^{125}I]5-HETE–TME. On the basis of the decrease or lack of peak 4, when a large molar excess of target material was employed (*i.e.*, 40–100 nmol of 5-HETE–TME to 1 nmol of Na^{125}I), this peak can be attributed to the disubstituted derivative, [^{125}I]5-HETE–TME.

In order to achieve high specific activity, when a ^{125}I-labelled derivative is intended for use as a tracer in radioimmunoassay, perfect separations from the parent compound is of the utmost importance. When run in the same separation system as that used for the isolation of the labelled compound, tritiated 5-HETE–TME, the parent compound of monoiodinated [^{125}I]5-HETE–TME was found to elute with water near the dead volume. This experiment demonstrated that the monoiodinated product eluted with ethanol would not contain any of the unreacted parent compound. At the same time, however, when water was replaced immediately for the final eluent of

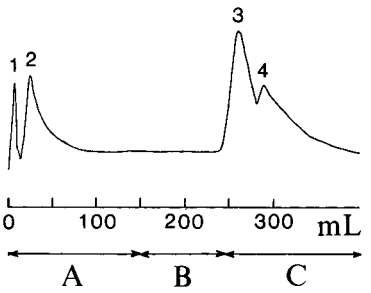

Fig. 1. Separation of ^{125}I-labelled 5-HETE–TME by column chromatography. Sorbent: Sephadex LH-20. Eluent: (A) water; (B) ethanol–water (20:80); (C) ethanol–water (30:70). Peaks: 1 = free $^{125}I^-$; 2 = unidentified labelled product; 3 = [^{125}I]5-HETE–TME; 4 = [$^{125}I_2$]-5-HETE–TME.

30% ethanol, the monoiodinated product to be isolated was usually contaminated with labelled by-products. So as to ensure the removal of these radioactive impurities, the final elution with 30% ethanol was preceded with an intermediate elution using a lower concentration of ethanol. This elution pattern, illustrated in Fig. 1, led to the isolation of monoiodinated [^{125}I]5-HETE–TME free from both the unreacted parent compound and labelled by-products. The efficacy of this separation procedure and the structure of the labelled product were further supported by the specific binding of the separated material to an antibody raised against 5-HETE–bovine serum albumin conjugate.

The monoiodinated [^{125}I]5-HETE–TME thus purified was used for studying its chromatographic properties in both column chromatography on Sephadex LH-20 and RP-HPLC on alkylated silica as the stationary phase.

Chromatographic behaviour on Sephadex LH-20

The chromatographic behaviour of monoiodinated [^{125}I]5-HETE–TME on Sephadex LH-20 was studied using aqueous ethanol eluents. As can be seen from

TABLE I

DEPENDENCE OF ELUTION VOLUME OF ^{125}I-LABELLED 5-HETE–TME ON THE COMPOSITION OF ELUENT

Sorbent: Sephadex LH-20. Eluent: aqueous ethanol–water.

Ethanol concentration		Elution volume, ml	Distribution coefficient
% (v/v)	Molar fraction, X		
35	0.144	126.7	83.05
40	0.172	60.2	37.51
45	0.203	35.8	20.79
50	0.238	21.8	11.20
55	0.276	17.3	8.12

Table I, the elution volume decreased with increasing ethanol concentration. The distribution coefficient (k) was calculated according to the equation

$$k = \frac{v_e - v_0}{w} = \frac{v_e - 5.44}{1.46} \quad (1)$$

where v_e, v_0 and w are the elution volume, the dead volume and the weight of the adsorbent, respectively.

In the range 30–55% (v/v) ethanol, the distribution coefficient as a function of ethanol concentration was calculated according to the equation

$$\log k = \log k_0 - n \log X \quad (2)$$

where X is the molar fraction of ethanol, k_0 is the distribution coefficient extrapolated to 100% ethanol and n is a constant.

As illustrated in Fig. 2, a highly significant (correlation coefficient 0.9945) linear relationship was found, with the regression line

$$\log k = -1.167 - 3.610 \log X \quad (3)$$

Chromatographic behaviour in RP-HPLC

In RP-HPLC using C_{18}-bonded silica as the stationary phase, the chromatographic behaviour of the pure monoiodinated [^{125}I]5-HETE–TME was identical with that observed with Sephadex LH-20 separation, *i.e.*, the retention time decreased with increasing proportion of organic solvent (ethanol, methanol or acetonitrile) in the aqueous binary eluent (Table II). In order to obtain a parameter suitable for direct comparison of RP-HPLC data with those determined for Sephadex LH-20, the

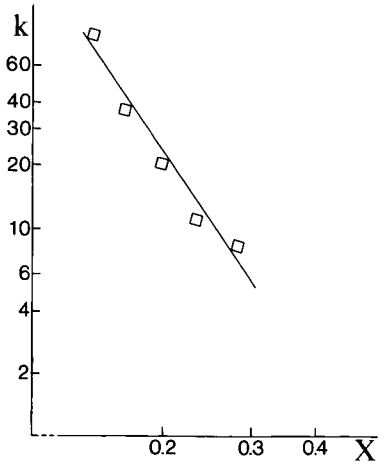

Fig. 2. Distribution coefficient of [^{125}I]5-HETE–TME as a function of ethanol concentration (x) in adsorption column chromatography. Sorbent: Sephadex LH-20. Eluent: ethanol–water. Scale: log–log.

TABLE II

CAPACITY FACTOR OF ^{125}I-LABELLED 5-HETE–TME IN RP-HPLC WITH BINARY ELUENTS

Stationary phase: C_{18}-bonded silica. Mobile phase: aqueous mixtures of organic modifiers.

Concentration				Capacity factor, k'		
% (v/v)	Molar fraction, X			Methanol	Ethanol	Acetonitrile
	Methanol	Ethanol	Acetonitrile			
50		0.238			32.5	
55		0.276	0.296		8.2	17.7
58			0.322			12.7
60		0.319	0.340		5.5	9.7
63			0.369			7.4
65		0.367	0.390		3.0	5.8
68			0.422			4.8
70		0.421	0.445		1.9	3.7
75	0.546		0.508	16.2		2.4
78	0.587			9.4		
80	0.615		0.579	6.7		1.7
82	0.646			4.8		
84	0.677			3.4		
85	0.694		0.661	2.9		1.2

capacity factor, which is directly proportional to the distribution coefficient, was calculated according to the equation

$$k' = \frac{v_e - v_0}{v_0} = \frac{v_e - 1.0}{1.0} \tag{4}$$

where k', v_e and v_0 are the capacity factor, the elution volume and the dead volume, respectively.

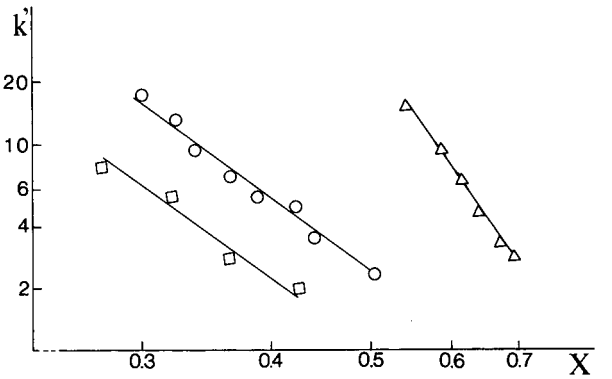

Fig. 3. Capacity factor of [^{125}I]5-HETE–TME as a function of the concentration of organic modifiers (x) in RP-HPLC. Sorbent: C_{18}-bonded silica. Mobile phase: binary mixtures of water and organic solvents (△ = methanol; □ = ethanol; ○ = acetonitrile). Scale: log–log.

Within the approximate capacity factor range 2–10, a linear relationship was found according to the equation

$$\log k' = \log k'_0 - m \log X \quad (5)$$

where X is the molar fraction of organic solvent, k'_0 is the capacity factor extrapolated to 100% organic solvent and m is constant. The regression lines fitted for different binary eluents (Fig. 3) gave the following equations:

$$\log k' = -1.052 - 3.55 \log X \text{ (ethanol)} \quad (6)$$

$$\log k' = -0.715 - 3.68 \log X \text{ (acetonitrile)} \quad (7)$$

$$\log k' = -0.674 - 7.13 \log X \text{ (methanol)} \quad (8)$$

The linearity was highly significant, with correlation coefficients of 0.9966, 0.9980 and 0.9999, respectively.

The widely accepted displacement model of adsorption predicts that solute molecules that behave according to this model will give linear plots of log (concentration) *vs.* log (distribution coefficient) and log (capacity factor). Although it cannot be regarded as direct evidence of a displacement mechanism of solute retention, the linear relationship between the concentration of organic solvents and the capacity factor (eqns. 6–8) observed in our experiments is not inconsistent with this model.

The slope of log k' *vs.* log X curve is said to be an indicator of the strength of a pure solvent used as the mobile phase. The larger slope found with methanol, which leads to a faster decrease in k' with increase in methanol concentration, may underly the good resolution obtained in RP-HPLC of the analogous monoiodo-TME derivatives of various prostanoids using a ternary eluent containing water, acetonitrile and methanol [18]. Further studies could be useful to check how the differences in elution strength could be utilized to optimize the selectivity of the separation of this family of compounds.

Comparing the slopes of fitted lines obtained from the elution on Sephadex LH-20 and RP-HPLC, the ratio was 3.61 (eqn. 3):3.55 (eqn. 6):3.68 (eqn. 7):7.13 (eqn. 8) = 1:1:1:2. The solute showed similar behaviour in terms of the retention dependence on the concentration of ethanol, as indicated by the identical slope of the plots obtained on Sephadex LH-20 (eqn. 3) and C_{18}-bonded silica (eqn. 6). Although the agreement occurred in a different range of composition for the two systems, the results are not inconsistent with the displacement model.

Linearity is normally obtained with capacity factors in the range 0.5–10. Outside this range, at extremes of k', non-linearity is frequently observed and different theoretical approaches were considered to account for this phenomenon [15,16], but none of these interpretations affected the validity of displacement mechanism. The non-linearity was observed in our experiments also in ethanol and acetonitrile below 55 and 60%, respectively, but this phenomenon was not studied in more detail. However, the divergence from linearity observed at extremes of capacity factor is not expected to affect the predictive value of solute retention based on the equations presented, as the linearity was found to be valid in the capacity factor range 2–10, a range that meets the practical requirements for applications of RP-HPLC.

REFERENCES

1 J. Maclouf, M. Pradel, Ph. Pradelles and F. Dray, *Biochim. Biophys. Acta*, 431 (1976) 139.
2 I. Mucha, G. Tóth and B. Tanács, *Izotóptechnika*, 22 (1979) 190.
3 G. Tóth, I. Mucha and B. Tanács, *J. Chromatogr.*, 189 (1980) 433.
4 G. Tóth, M. Wéber and F. Kling, *J. Chromatogr.*, 213 (1981) 511.
5 G. Tóth, *J. Chromatogr.*, 238 (1982) 476.
6 G. Tóth, *J. Chromatogr.*, 267 (1983) 420.
7 G. Tóth and J. Zsadányi, *J. Radioanal. Nucl. Chem. Lett.*, 86 (1984) 25.
8 G. Tóth, *J. Chromatogr.*, 404 (1987) 258.
9 G. Tóth, *Radiochem. Radioanal. Lett.*, 29 (1977) 207.
10 G. Tóth, *Radioanal. Chem.*, 46 (1978) 201.
11 I. Mucha, B. Tanács and G. Tóth, *J. Chromatogr.*, 478 (1989) 280.
12 E. Soczewinski and T. Dzido, *Chromatographia*, 22 (1986) 25.
13 E. Soczewinski, *J. Chromatogr.*, 388 (1987) 91.
14 F. Murakami, *J. Chromatogr.*, 178 (1979) 393.
15 X. Geng and F. E. Regnier, *J. Chromatogr.*, 332 (1985) 147.
16 A. Kalbara, T. Nakagawa, Ch. Hohda, N. Hirata and H. Tanaka, *J. Chromatogr. Sci.*, 27 (1989) 716.
17 I. Mucha and G. Tóth, *J. Chromatogr.*, 438 (1988) 111.
18 I. Mucha and G. Tóth, *J. Chromatogr.*, 483 (1989) 419.
19 E. J. Corey, J. O. Albright, A. E. Barton and S. Hashimoto, *J. Am. Chem. Soc.*, 102 (1980) 1435.
20 I. Mucha, A. Seregi, P. Serfőző, B. Tanács and J. Benkő, *Hung. Pat.*, 193 381 (1987).

Journal of Chromatography, 543 (1991) 315–326
Elsevier Science Publishers B.V., Amsterdam

CHROM. 23 133

High-performance affinity chromatography of a chick lectin on an adsorbent based on hydrophilic polymer gel

HIROTAKA KAKITA*, KOJI NAKAMURA and YOSHIO KATO
Central Research Laboratory, Tosoh Corporation, Tonda, Shin-nanyo, Yamaguchi (Japan)
and
YUKO ODA, KIYOHITO SHIMURA and KEN-ICHI KASAI
Faculty of Pharmaceutical Sciences, Teikyo University, Sagamiko, Kanagawa (Japan)
(First received August 14th, 1990; revised manuscript received January 8th, 1991)

ABSTRACT

A mouse monoclonal antibody (SIA4-5) which reacts with a chick 14K lectin (C14K) was covalently attached to a new support for high-performance affinity chromatography, TSKgel Tresyl-5PW, which is a preactivated, polymer-based particle. The immobilized antibody (SIA4-5–5PW) thus prepared proved to be useful in measuring not only the molecular properties of C14K but also specific interactions of C14K with SIA4-5 and hapten sugars. The C14K preparation was fractionated according to the oligomeric structure and with slight differences in affinity to SIA4-5 although the former was homogeneous in sodium dodecyl sulphate polyacrylamide gel electrophoresis. Application of the method for quantitative analytical purposes was successful.

INTRODUCTION

The development of suitable supports for affinity chromatography has always been required in order to extend the field of application of the method. Properties required for suitable supports are as follows: hard, small, spherical, homogeneous in size, highly porous with large pores, hydrophilic and devoid of non-specific adsorption. A new preactivated support for high-performance affinity chromatography has become commercially available under the trade-name TSKgel Tresyl-5PW. According to the manufacturer (Tosoh, Yamaguchi, Japan), it is prepared by introducing tresyl groups into TSKgel G5000PW [1], which is hydrophilic resin-based material of large pore size (particle diameter 10 μm, approximate pore size 1000 Å), intended for high-performance gel filtration. The amount of tresyl groups introduced is about 20 μmol per ml of swollen gel. Protein can be easily coupled via its ε-amino or thiol groups [2]. Affinity adsorbents prepared from this support should be useful not only for preparative but also for other purposes such as analysis and diagnosis. We intend to use this new material for investigations on specific interactions of biomolecules.

In the course of studies on vertebrate β-galactoside-binding lectins, we cloned anti-chick 14K lectin mouse monoclonal antibody (SIA4-5). Chick 14K lectin (C14K)

0021-9673/91/$03.50

has a monomer molecular weight of 14 970 [3] and an isoelectric point of 7.0 [4]. Both monomeric and dimeric forms were usually found in purified preparation. To investigate the interaction between C14K and SIA4-5, we attached SIA4-5 to TSKgel Tresyl-5PW and studied the chromatographic behaviour of C14K. Useful information such as oligomeric structure and dissociation constants between C14K and its soluble hapten sugars were obtained.

EXPERIMENTAL

The columns and proteins investigated are summarized in Table I.

Materials

Human γ-globulin (HG) and mouse γ-globulin (MG) were purchased from Miles Diagnostics Division (Elkhart, IN, U.S.A.), concanavalin A (carbohydrate-free) from Seikagaku Kogyo (Tokyo, Japan), thiodigalactoside, N-acetyl-D-lactosamine, proteins for molecular weight markers, from Sigma (St. Louis, MO, U.S.A.) and Bradford protein assay dye reagent was purchased from Bio-Rad Labs. (Richmond, CA, U.S.A.). Other reagents and solvents were of analytical-reagent grade. TSKgel Tresyl-5PW (Tosoh) with particle size 10 μm and average pore size 1000 Å was used as a support for affinity adsorbent. C14K and SIA4-5 were purified as described [4,5].

Chromatography

Chromatography was performed at ambient temperature (20–25°C) with an HLC-803D pump equipped with a variable-wavelength Model UV-8000 UV detector and a Model FS-8000 variable-wavelength fluorescence detector (all from Tosoh). Fluorescence of proteins was detected with excitation at 285 nm and emission at 340 nm. The recovery of proteins was determined from the areas of the eluted peaks [6]. As controls, we used areas obtained when the column was replaced with empty 1 mm I.D. stainless-steel tubing of 1 ml total inner volume and elution was performed isocratically at the eluent compositions at which each protein was eluted. Each protein was injected. Peak areas were measured with a Model CP-8000 data processor (Tosoh).

TABLE I

AFFINITY CHROMATOGRAPHIC COLUMNS

Column	Immobilized protein	Column size	Sample	Fig. No.
C14K–5PW	C14K	50 mm × 4.6 mm I.D.	SIA4-5	1A
C14K–5PW	C14K	50 mm × 4.6 mm I.D.	MG	1C
Non-protein–5PW	–	75 mm × 4.6 mm I.D.	SIA4-5	1B
Non-protein–5PW	–	75 mm × 4.6 mm I.D.	C14K	1F
SIA4-5–5PW	SIA4-5	75 mm × 4.6 mm I.D.	C14K	1D, 2A, 2B, 2C, 3B, 3C, 5A, 5B, 6A, 6B
HG–5PW	HG	75 mm × 4.6 mm I.D.	C14K	1E

Coupling of proteins to TSKgel Tresyl-5PW

Protein solution was applied to a Bio-Gel P-6 column that had been equilibrated with buffer [1 *M* sodium potassium phosphate buffer (pH 7.5) or 0.2 *M* $NaHCO_3$ containing 0.5 *M* NaCl (pH 8.0)] for buffer change. The protein concentration of SIA4-5 was calculated from the absorbance at 280 nm assuming a molar absorptivity (1% w/v, 1 cm) of 14 [5]. The protein concentration of C14K was determined by the protein assay method of Bradfood [7]. The protein-containing fraction obtained (4 ml) was mixed with 0.5 g (dry weight) of TSKgel Tresyl-5PW and shaken at 4°C overnight. After washing with the same buffer, unreacted tresyl groups were deactivated by resuspending the gel in 12 ml of 0.5 *M* Tris–HCl buffer (pH 8.0) at 4°C overnight. As a control, 4 ml of the buffer without protein were mixed with 0.5 g (dry weight) of TSKgel Tresyl-5PW and the same treatments were carried out. The coupling yield of protein was determined by amino acid analysis of pure and immobilized protein. After immobilization of protein, a portion of the gel and pure protein solution were treated with 6 *M* HCl for 20 h at 110°C. Hydrolysis was performed *in vacuo*. This treatment did not destroy the gel. The amino acid composition of supernatant was determined with a Hitachi Model 835 automatic amino acid analyser. As alanine is stable, its value is not easily influenced by contamination and it is a major component of the proteins investigated in this work, its value was used for determining the coupling yield. The amount of coupled protein was calculated from the protein concentration of pure solution and the coupling yield. The adsorbent thus prepared was usually stored in 0.05% sodium azide solution at 4°C. It could be used repeatedly for at least 1 year without an appreciable decrease in efficiency.

Miscellaneous methods

Sodium dodecyl sulphate polyacrylamide gel electrophoresis (SDS-PAGE) was carried out by the method of Laemmli [8] using 3% stacking gel and 12.6% separating gel. Haemagglutination activity was measured according to Nowak *et al.* [9]. In a microtitre plate (Cooke Engineering), 25 μl of serially diluted sample, 25 μl of buffer [20 m*M* sodium phosphate buffer (pH 7.2) containing 150 m*M* NaCl, 2 m*M* EDTA and 4 m*M* 2-mercaptoethanol], 25 μl of 1% bovine serum albumin and 25 μl of a 4% suspension of trypsinized glutaraldehyde-fixed rabbit erythrocytes were mixed. One unit of hemagglutination activity was defined as the reciprocal of the highest dilution of the sample which gives detectable agglutination. Concanavalin A was used as a positive control. Protein concentration was determined by using a dye reagent according to Bradford [7]. Bovine serum albumin was used as a standard. The molecular weight of C14K under non-denaturing conditions was determined by high-performance gel filtration chromatography on TSKgel G2000SWxl. Sodium phosphate buffer (0.1 *M*, pH 6.8) containing 0.1 *M* Na_2SO_4 was used.

Analysis of the interaction between C14K and immobilized SIA4-5

Interaction between C14K and immobilized SIA4-5 was analysed quantitatively according to the theory developed for frontal affinity chromatography [10,11] and that for zonal chromatography [12]. In frontal affinity chromatography, we use a relatively weak affinity adsorbent so that only retardation instead of adsorption occurs. The dissociation constant (K_d) of the complex formed between a soluble protein

(A; in this case, C14K) and its immobilized ligand (B; SIA4-5) can be described as follows:

$$K_d = [A][B]/[AB]$$
$$= \frac{B_t}{V - V_0} - [A]_0 \quad (1)$$

where B_t is total amount of the immobilized ligand, V the elution volume of A, V_0 the elution volume of A under the conditions where specific interaction is completely suppressed and $[A]_0$ the initial concentration of A, which is maintained in the column. Eqn. 1 can be rearranged to

$$V = V_0 + \frac{B_t}{[A]_0 + K_d} \quad (2)$$

If $[A]_0$ is negligibly small in comparison with K_d, V approaches the maximum value V_m, hence

$$V_m = V_0 + (B_t/K_d) \quad (3)$$

Eqn. 3 can be rearranged as follows:

$$K_d = \frac{B_t}{V_m - V_0} \quad (4)$$

This means that we can determine K_d from the elution volume provided that we apply a very dilute solution of A. Eqn. 3 is equivalent to the basic equation derived for partition chromatography (not for frontal chromatography but for zonal chromatography), although in the latter the volume of stationary phase and partition coefficient are used instead of B_t and K_d, respectively. This indicates that when we apply a very small amount of protein to the column, adsorption chromatographic techniques such as affinity chromatography can be treated by the same theory as developed for partition chromatography, because the amount of the occupied immobilized ligand becomes negligible and consequently the ratio of free and bound protein ([A]/[AB]) becomes constant. This consideration also indicates that eqn. 3 is applicable not only to frontal chromatography but also to zonal chromatography under these conditions, because frontal chromatography can be considered as a repetition of independent zonal chromatography. By expanding eqn. 3, the interactions between C14K (A) and other soluble molecules (I) that affect the binding of C14K to SIA4-5–5PW can be analysed. When chromatography is carried out in the presence of a competitive ligand I, A is eluted at an elution volume V_i which is smaller than V_m. If the concentration of I ($[I]_0$) is extremely high in comparison with $[A]_0$, we obtain the following equation [10,11]:

$$\frac{1}{1 + \frac{[I]_0}{K_i}} = \frac{V_i - V_0}{V_m - V_0} \quad (5)$$

where K_i is the dissociation constant of the AI complex. Eqn. 5 can be rearranged as follows:

$$V_i = V_0 + \frac{K_i(V_m - V_i)}{[I]_0} \quad (6)$$

When V_i is plotted against $(V_m - V_i)/[I]_0$, a straight line is obtained and K_i and V_0 can be determined from the slope and the intercept, respectively. Dunn and Chaiken [12] also proposed another analytical procedure for affinity chromatography, which was developed to analyse the effect of soluble molecules (I) which inhibit the interaction of the immobilized ligand (B) and its counterpart (A). It was originally developed for zonal chromatography and the K_i value can be obtained from the ratio of intercept and slope of the $1/(V_i - V_0)$ *versus* $[I]_0$ plot.

RESULTS

Immobilization of SIA4-5 and C14K on TSKgel Tresyl-5PW

SIA4-5–5PW and C14K–5PW were prepared as described under Experimental. The protein concentration of SIA4-5 solution was calculated as 0.9 mg/ml from the absorbance at 280 nm. The coupling yield was determined by amino acid analysis of pure and immobilized SIA4-5, using the value of alanine. A 4-ml volume of pure SIA4-5 solution contained 153.9 μg of alanine and 0.5 g (dry weight) of SIA4-5–5PW contained 144.7 μg of alanine; therefore, the coupling yield was determined as 94%.

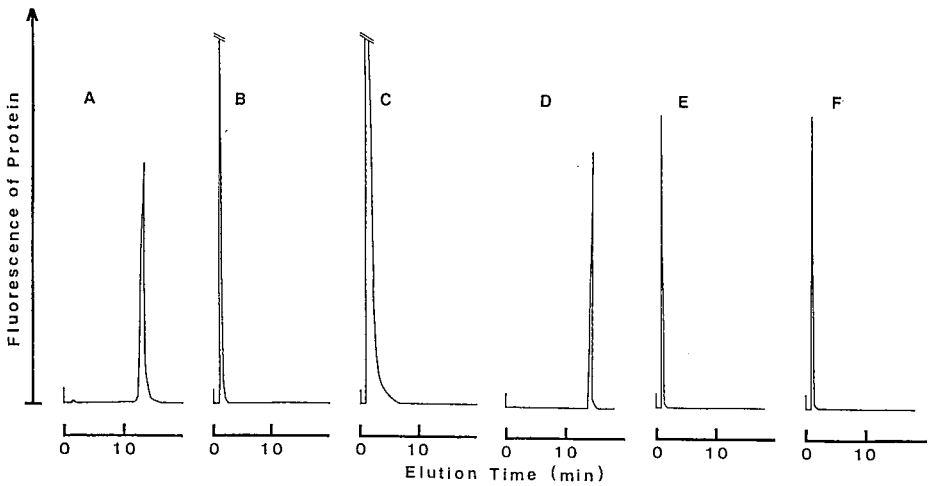

Fig. 1. Properties of several derivatized Tresyl-5PW. Columns, (A, C) C14K–5PW (50 mm × 4.6 mm I.D.), (B, F) non-protein–5PW (75 mm × 4.6 mm I.D.), (D) SIA4-5–5PW (75 mm × 4.6 mm I.D.) and (E) HG–5PW (75 mm × 4.6 mm I.D.) (containing 1.9 mg of HG). Applied samples, (A, B) SIA4-5 (100 μl, 100 μg/ml), (C) commercial MG (100 μl, 2.2 mg/ml) and (D–F) C14K (100 μl, 18 μg/ml). Flow-rate, 1 ml/min. Two elution programmes were used: for A–C, 0–10 min, 0.1 *M* sodium phosphate buffer (pH 6.8) containing 0.1 *M* Na_2SO_4 and 10–20 min, 0.1 *M* sodium citrate buffer (pH 5.0) containing 0.1 *M* Na_2SO_4; for D–F, 0–10 min, 0.1 *M* sodium phosphate buffer (pH 7.4) and 10–20 min, 0.1 *M* sodium citrate buffer (pH 5.0). Non-protein–5PW refers to derivatized Tresyl-5PW which coupled Tris base instead of protein.

The coupling yield of C14K was determined as 91% by the same method. Each gel was packed in a stainless-steel column. The column of SIA4-5–5PW (75 mm × 4.6 mm I.D.) contained 2.1 mg of SIA4-5 and that of C14K–5PW (50 mm × 4.6 mm I.D.) contained 70 μg of C14K.

SIA4-5 was adsorbed on a C14K–5PW column and eluted with sodium citrate buffer (0.1 *M*, pH 5.0) containing 0.1 *M* Na_2SO_4 (Fig. 1A). The recovery of SIA4-5 was 96%. Commercial MG was not adsorbed on the C14K–5PW column (Fig. 1C). C14K was strongly adsorbed on SIA4-5–5PW column at pH 7.4 (0.1 *M* sodium phosphate buffer) and eluted with 0.1 *M* sodium citrate buffer (pH 5.0). The recovery of C14K was more than 90% (Fig. 1D). On the other hand, C14K was not adsorbed on an HG–5PW column (Fig. 1E). No protein was adsorbed on non-protein–5PW, which coupled Tris base instead of protein (Fig. 1B and F).

Separation of C14K into several components with the SIA4-5–5PW column

Under certain conditions, C14K was separated into several peaks by SIA4-5–5PW chromatography, although the preparation used had given only one band (14K) on SDS-PAGE. Fig. 2A shows that four peaks (1–4) appeared when a descending pH gradient was applied. Apparently peak 1 has the weakest affinity to immobilized SIA4-5 and peak 4 the highest. A more detailed study showed that they can be classified into two groups, weaker (peaks 1 and 2) and stronger (peaks 3 and 4). Under the initial conditions used (pH 6.0), peaks 1 and 2 were not adsorbed on the column, whereas peaks 3 and 4 were adsorbed and eluted with 0.1 *M* sodium phosphate buffer (pH 5.0).

To characterize each peak, the C14K preparation was size-fractionated by gel filtration on TSKgel G2000SWxl and the resulting protein fractions were applied to

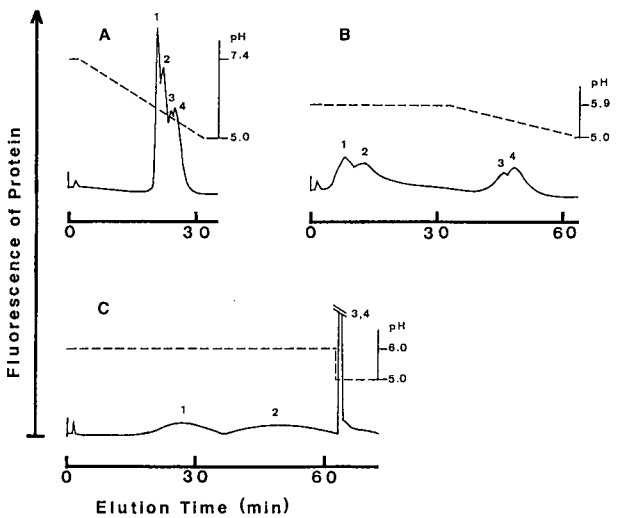

Fig. 2. Chromatograms of C14K (100 μl, 18 μg/ml) on SIA4-5–5PW column with various elution programmes. C14K protein, 1.8 μg in 100 μl, was applied. Elution programmes: (A) linear gradient from 0.1 *M* sodium phosphate buffer (pH 7.4) to 0.1 *M* sodium citrate buffer (pH 5.0) for 30 min; (B) isocratic elution with 0.1 *M* sodium citrate buffer (pH 5.9) for 30 min, then linear gradient from pH 5.9 to 5.0 in 0.1 *M* sodium citrate buffer for 30 min; (C) isocratic elution with 0.1 *M* sodium phosphate buffer (pH 6.0).

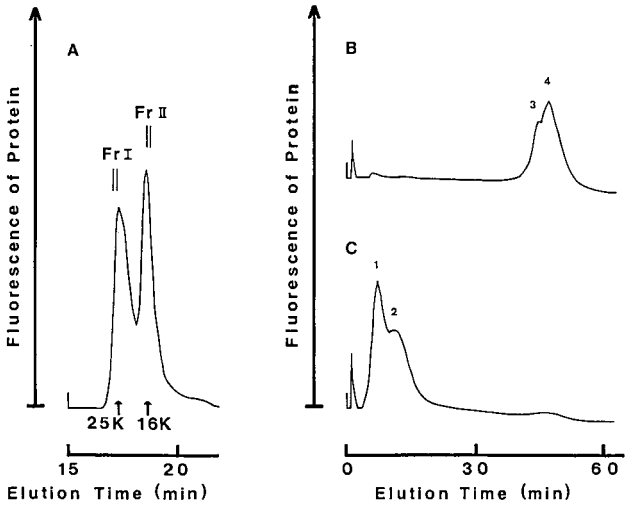

Fig. 3. (A) Gel permeation chromatography of C14K preparation on TSKgel G2000SWxl (30 cm × 7.8 mm I.D.). Mobile phase, 0.1 *M* sodium phosphate buffer (pH 6.0). Eluate between the two vertical lines of each peak was collected. Flow-rate, 0.5 ml/min. (B) and (C) chromatograms on SIA4-5–5PW of fractions I and II obtained in (A). The elution programme was the same as in Fig. 2B. Flow-rate, 1 ml/min. K = Kilodalton.

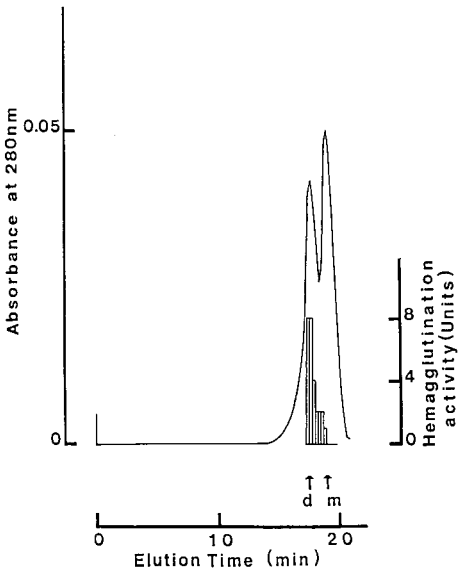

Fig. 4. Gel permeation chromatography of C14K on TSKgel G2000SWxl (30 cm × 7.8 mm I.D.). Mobile phase, 0.1 *M* sodium phosphate buffer (pH 6.8) containing 0.1 *M* Na_2SO_4. Flow-rate, 0.5 ml/min. Portions of 100 µl of column eluent were collected and haemagglutination activity was measured (indicated by histogram). Letters d and m below the chromatogram indicate C14K dimer and monomer, respectively. Elution of protein was detected by absorbance at 280 nm.

an SIA4-5–5PW column. Fig. 3A shows that C14K was separated into two peaks by gel filtration. The molecular weight of the first peak (fraction I) was calculated to be about 25 000 and that of the second peak (fraction II) about 16 000. Fraction I corresponds to C14K dimer and fraction II to C14K monomer. This was further supported because, as shown in Fig. 4, the haemagglutination activity of fraction I was much higher than that of fraction II. Fraction I gave only peaks 3 and 4, and fraction II only peaks 1 and 2 on SIA4-5–5PW chromatography under the same conditions as in Fig. 2B. Thus, peaks 1 and 2 in Fig. 2 correspond to C14K monomer. On the other hand, peaks 3 and 4 correspond to C14K dimer. It is reasonable that the dimer species has a higher affinity than the monomer species. However, the reason why each of them was further separated into two peaks has not been clarified.

Comparison of old and fresh preparations of C14K

As the behavior of C14K described above was attributable to some modification of C14K protein that occurred after purification, a C14K preparation which had been stored for 50 days at 4°C after preparation (old preparation) was applied to the column. This preparation also gave only a 14 000-dalton band on SDS-PAGE. The specific activity of the old preparation was at least eight times lower than that of freshly prepared C14K. Elution conditions that allowed only discrimination between the dimer and monomer were chosen in the experiments shown in Fig. 5. Apparently,

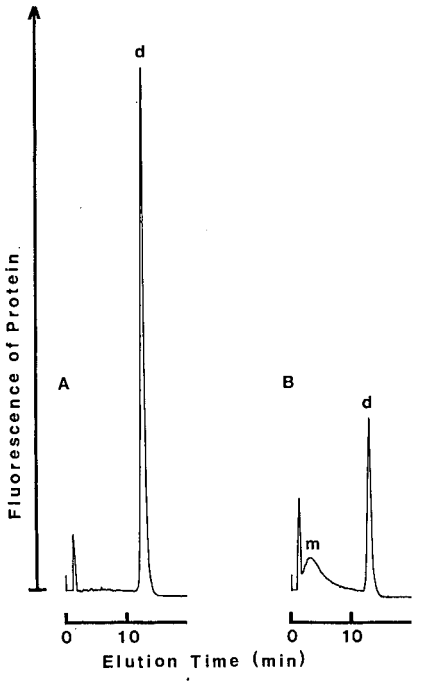

Fig. 5. Chromatograms of (A) fresh and (B) old C14K preparation on SIA4-5–5PW. C14K protein, 3 μg in 30 μl, was applied. Elution programmes were as follows; 0–10 min, 75% buffer A [0.1 *M* sodium phosphate buffer (pH 6.8) containing 0.1 *M* Na_2SO_4, 6.7 m*M* lactose] + 25% buffer B [0.1 *M* sodium citrate buffer (pH 5.0) containing 0.1 *M* Na_2SO_4]; 10–20 min, 100% buffer B. Flow-rate, 1 ml/min. Letters d and m indicate C14K dimer and monomer, respectively.

the fresh C14K preparation contained only dimer (peak d, retention time 12.5 min). On the other hand, the old preparation contained both monomer (peak m, retention time 3 min) and dimer (peak d). This suggests that C14K had partially lost its ability to form dimer during storage.

Quantitative analysis of the interaction between C14K and SIA4-5

The amount of effective immobilized ligands of the SIA4-5–5PW column (B_t) was determined as $5.5 \cdot 10^{-9}$ mol by applying an excess amount of C14K. V_0 was 1.0 ml. Under the conditions as described in Fig. 2C, when C14K monomer ($3.9 \cdot 10^{-11}$ mol, 0.59 μg) was applied to the SIA4-5–5PW column, the retention volume of peak 1 was 28 ml and that of peak 2 was 48 ml. When a smaller amount of C14K ($1.1 \cdot 10^{-12}$ mol) was applied, the same elution volume was observed. As the elution volume was unaffected by the change in the amount of protein applied, these elution volumes can be considered as V_m. Thus, K_d values were calculated to be $2.0 \cdot 10^{-7}$ M for peak 1 and $1.1 \cdot 10^{-7}$ M for peak 2 by using eqn. 4. K_d values for peaks 3 and 4 were not determined because they were adsorbed on the column.

Effect of hapten sugars

It was found that addition of hapten sugars affected the chromatographic pattern. Chromatography of C14K was carried out under conditions where peaks 1 and 2 were not adsorbed but retarded. In the presence of lactose, the elution volumes of both peaks 1 and 2 were diminished whereas sucrose and maltose had no effect (Fig.

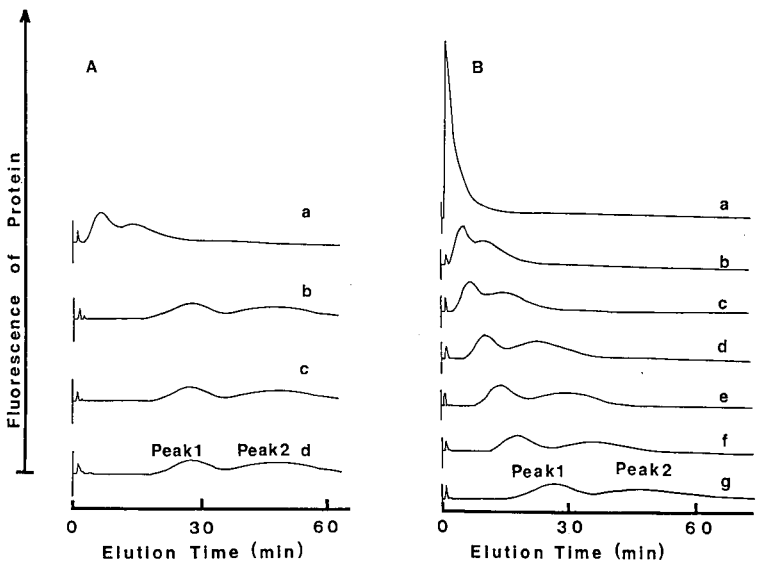

Fig. 6. (A) Effect of sugars on the chromatograms of C14K on SIA4-5–5PW. C14K protein, 0.6 μg in 100 μl was applied. Mobile phase, 0.1 M sodium phosphate buffer (pH 6.0) containing disaccharides: (a) 2 mM lactose; (b) 10 mM maltose; (c) 10 mM sucrose; (d) none. Flow-rate, 1 ml/min. (B) Effect of lactose of various concentration on chromatograms of C14K on SIA4-5–5PW. C14K protein, 0.6 μg in 100 μl, was applied. 0.1 M Sodium phosphate buffer (pH 6.0) was used. Concentration of lactose: (a) 20; (b) 3; (c) 2; (d) 1; (e) 0.6; (f) 0.3; (g) 0 mM. Flow-rate, 1 ml/min.

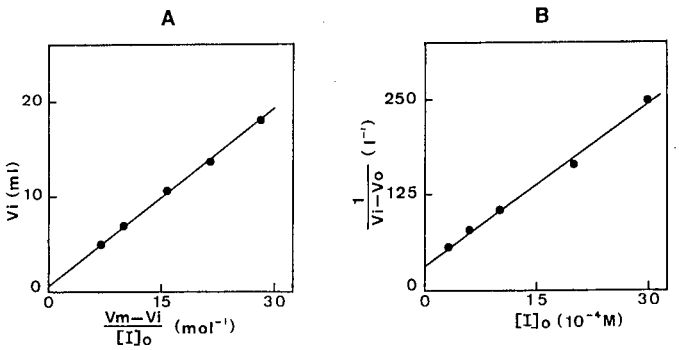

Fig. 7. Analysis of the effect of lactose. SIA4-5–5PW column was equilibrated with sodium phosphate buffer (pH 6.0) containing various concentrations of lactose. C14K protein, 0.6 μg in 100 μl was applied, then the elution volumes of C14K peak 1 were determined. Flow-rate, 1 ml/min. (A) V_i *versus* $(V_m - V_i)/[I]_0$ plot; (B) $1/(V_i - V_0)$ *versus* $[I]_0$ plot.

6A). Peaks 3 and 4 were not examined because under the conditions used they were adsorbed on the column. Other sugars containing a β-galactoside moiety, thiodigalactoside and N-acetyl-D-lactosamine, showed a similar effect. As the SIA4-5 used is sensitive to conformational changes of C14K protein, a conformational change of C14K induced by the binding with specific sugars seemed to diminish the interaction with SIA4-5. Chromatograms obtained in the presence of various concentrations of lactose (20–0.3 m*M*) are shown in Fig. 6B. A plot of V_i *versus* $(V_m - V_i)/[I]_0$, where $[I]_0$ is the concentration of lactose, according to eqn. 6 is shown in Fig. 7A. The retention volume of C14K peaks in the absence of lactose was used as V_m. Straight lines were obtained for both peaks 1 and 2 [correlation coefficients (r) were 0.999 and 0.997, respectively]. K_i values calculated for lactose were 0.6 m*M* (peak 1) and 0.88 m*M* (peak 2). K_i values for thiodigalactoside and N-acetyl-D-lactosamine were also determined and are summarized in Table II. K_i values were also calculated using the equations developed by Dunn and Chaiken [12], and similar values were obtained. Thiodigalactoside bound most strongly and lactose most weakly. These values are

TABLE II

K_i VALUES OF LECTIN PEAKS FOR β-GALACTOSIDE-CONTAINING SACCHARIDES BY QUANTITATIVE AFFINITY CHROMATOGRAPHY

Saccharide	K_i (m*M*)[a]			
	Peak 1		Peak 2	
	a	b	a	b
Lactose	0.60	0.51	0.88	0.76
Thiodigalactoside	0.063	0.060	0.12	0.12
N-Acetyl-D-lactosamine	0.14	0.15	0.25	0.25

[a] a, K_i values were calculated by plots according to eqn. 6; b, K_i values were calculated by plots according to Dunn and Chaiken [12].

consistent with previous reports [13]. Peak 1 always had a slightly stronger affinity than peak 2 for sugars.

DISCUSSION

The advantages of TSKgel Tresyl-5PW for the preparation of affinity adsorbents have been demonstrated. Proteins can be immobilized under mild conditions either at ambient temperature or in a cold room. The coupling reaction is completed within 1–2 h at 20–25°C. The procedure is simple and convenient, because it does not require aggressive reagents such as cyanogen bromide [14] or reducing agents [15]. The ratios of tyrosine and arginine to alanine particularly decreased after immobilization. The decrease in the ratio of arginine to alanine is undoubtedly due to coupling to the gel. Although tyrosine is unstable during hydrolysis in the presence of the gel, this appreciable decrease in the ratio of tyrosine to alanine may be due to coupling to the gel. Non-specific adsorption of the proteins investigated to TSKgel Tresyl-5PW was absent.

Purified C14K was separated into four peaks by the SIA4-5–5PW column in spite of apparent homogeneity in the molecular weight of the monomer. C14K is known to require a thiol-reducing agent to maintain haemagglutination activity [16,17]. However, it was suggested that no cysteine residue is involved in the sugar-binding site. Modification of cysteine residues seems to affect the dimer-forming ability of C14K, which is supported by the results shown in Fig. 5. Although the fresh C14K preparation was composed exclusively of dimer, the old preparation contained monomer in addition to dimer. The C14K preparation stored for a long period after purification seems to have been chemically modified and to have become unfavourable for forming the dimer. The reason why the monomeric C14K was separated into two peaks (peaks 1 and 2 in Fig. 2) has not been elucidated. Peak 1 seemed to have a slightly stronger affinity to saccharides than peak 2, although the former had a weaker affinity to the SIA4-5–5PW column than the latter. Some modification might have occurred which affected both sugar-binding ability and interaction with SIA4-5.

Employment of the new support for high-performance affinity chromatography proved to be promising, especially for analytical purposes. In this work, we used less than 1 μg C14K protein and each chromatographic run took less than 1 h. This method proved to be very sensitive in detecting slight differences between C14K molecules and also very powerful in determining dissociation constants. This will be also useful in a variety of applications such as diagnosis and quality control.

REFERENCES

1 T. Hashimoto, H. Sasaki, M. Aiura and Y. Kato, *J. Polym. Sci., Polym. Phys. Ed.*, 16 (1978) 1789.
2 K. Nilsson and K. Mosbach, *Biochem. Biophys. Res. Commun.*, 102 (1981) 449.
3 J. Hirabayashi, H. Kawasaki, K. Suzuki and K. Kasai, *J. Biochem (Tokyo)*, 101 (1987) 775.
4 Y. Oda and K. Kasai, *Biochim. Biophys. Acta*, 761 (1983) 237.
5 Y. Oda, J. Hirabayashi and K. Kasai, *J. Biochem (Tokyo)*, 99 (1986) 1063.
6 Y. Kato, K. Nakamura and T. Hashimoto, *J. Chromatogr.*, 354 (1986) 511.
7 M. M. Bradford, *Anal. Biochem.*, 72 (1976) 248.
8 U. K. Laemmli, *Nature (London)*, 227 (1970) 680.
9 T. P. Nowak, P. L. Haywood and S. H. Barondes, *Biochem. Biophys. Res. Commun.*, 68 (1976) 650.

10 K. Kasai, Y. Oda, M. Nishikata and S. Ishii, *J. Chromatogr.*, 376 (1986) 33.
11 K. Kasai and S. Ishii, *J. Biochem (Tokyo)*, 84 (1978) 1051.
12 B. M. Dunn and I. M. Chaiken, *Proc. Natl. Acad. Sci. U.S.A.*, 71 (1974) 2382.
13 H. Leffler and S. H. Barondes, *J. Biol. Chem.*, 261 (1986) 10119.
14 J. Porath, R. Axen and S. Ernback, *Nature (London)*, 215 (1967) 1491.
15 R. F. Borch, M. D. Bernstein and H. D. Durst, *J. Am. Chem. Soc.*, 93 (1971) 2897.
16 S. H. Barondes, *Annu. Rev. Biochem.*, 50 (1981) 207.
17 S. H. Barondes, *Science (Washington, D.C.)*, 223 (1984) 1259.

Journal of Chromatography, 543 (1991) 327–343
Elsevier Science Publishers B.V., Amsterdam

CHROM. 23 118

Chromatographic and physical studies of tropomyosin in aqueous–organic media at low pH[a]

DAN L. CRIMMINS*

Howard Hughes Medical Institute Core Protein/Peptide Facility, Washington University School of Medicine, 660 S. Euclid Avenue, Box 8045, St. Louis, MO 63110 (U.S.A.)

and

MARILYN EMERSON HOLTZER

Department of Chemistry, Washington University, 1 Brookings Drive, Box 1134, St. Louis, MO 63130 (U.S.A.)

(First received October 29th, 1990; revised manuscript received January 16th, 1991)

ABSTRACT

Non-cross-linked and disulfide-cross-linked two-chain molecules comprising the α and/or β chains of rabbit skeletal tropomyosin were studied by electrophoretic, chromatographic and physical methods. Elution order on C_4 reversed-phase high-performance liquid chromatography depends markedly on the number and position of the cross-links. In the C_4 reversed-phase elution medium, cross-linked and non-cross-linked species are >85% helical by circular dichroism, but the non-cross-linked elute later from high-performance size-exclusion chromatography (G4000) and have molecular mass of 31 000–41 000 dalton by equilibrium ultracentrifugation. The data suggest that in the C_4 reversed-phase high-performance liquid chromatography elution medium non-cross-linked tropomyosin exists as amphipathic single-chain α-helices.

INTRODUCTION

The native tropomyosin molecule is a two-chain α-helical coiled coil comprising two parallel, registered, and slightly super-twisted, amphipathic α-helical chains [1–4]. Rabbit skeletal tropomyosin (R_sTm) consists of genetically variant chains, α and β, in a 3–4:1 ratio [2,4], forming principally, two types of molecules, αα and αβ, in a ≈3:2 ratio [5,6]. Each 284 amino acid chain has a molecular mass of 33 000 dalton, and the two differ, usually by conservative substitution, at only 39 positions [7]. One important difference between the two chains is that the β chain has two cysteines, at positions 36 (C36) and 190 (C190), whereas the α chain has only one cysteine at C190. This allows the two adjacent chains of such Tm coiled-coil molecules to be covalently (disulphide) cross-linked [3,4,8–12].

In some studies, no ββ molecules were found in native R_sTm [5,6]. However, in

[a] A preliminary report of this work was presented (Abstract T146) at the *Fourth Symposium of the Protein Society, San Diego, CA, U.S.A., August 1990.*

0021-9673/91/$03.50

other studies, $\beta\beta$ molecules have been observed in disulphide-cross-linked R_sTm [11]. To determine whether or not $\beta\beta$ molecules exist in native R_sTm, and, if not, whether their absence results from thermodynamic, kinetic, or biological factors, requires a sensitive analytical assay for the relative amounts of the various molecular species. The aforementioned studies employed hydroxyapatite (HA) chromatography and sodium dodecyl sulphate–polyacrylamide gel electrophoresis (SDS-PAGE), neither of which gives sufficient resolution for accurate quantitation of the molecular species. In fact, the resolution using HA chromatography is ordinarily so poor that the 4–6% $\beta\beta$ molecules that would result from random association of the α and β chains in R_sTm could easily be masked.

In this study we investigate the efficacy of 4–20% gradient SDS-PAGE and C_4 reversed-phase high-performance liquid chromatography (RP-HPLC) in separating the various cross-linked and non-cross-linked species that can be formed from the α and β chains of Tm. *In vitro* all three possible molecular species, $\alpha\alpha$, $\alpha\beta$, and $\beta\beta$, form readily and can be selectively cross-linked [3,4,8–12] to give five different cross-linked species: C190 cross-linked α ($\alpha^{-}\alpha$); C190 cross-linked, C36 blocked $\alpha\beta$ ($\alpha^{-}\beta_{\cdot}$); C190 cross-linked, C36 blocked β ($_{\cdot}\beta^{-}\beta_{\cdot}$); C190 blocked, C36 cross-linked β ($\cdot\beta_{-}\beta\cdot$); and C190 and C36 cross-linked β ($\beta^{-}_{-}\beta$). [We use a superscript (subscript) dash to indicate cross-linking at C190 (C36), and a superscript (subscript) dot to indicate blocking at C190 (C36).] These are listed in Table I along with the non-cross-linked species studied here, *i.e.*, reduced and blocked α ($\alpha\alpha$, $\cdot\alpha\alpha\cdot$) and β ($\beta\beta$, $\cdot\beta\beta\cdot$).

We find that, although it is often possible to resolve $\beta^{-}_{-}\beta$ using 4–20% SDS-PAGE, that $\alpha^{-}\alpha$ and non-cross-linked molecules as well as $\beta^{-}_{-}\beta$ are easily resolved using C_4 RP-HPLC. Not only can small amounts of these species be detected by measuring the absorbance at 214 nm, their relative amounts in a given sample can determined by integration. Moreover, we find that the cross-linked species elute earlier

TABLE I

SUMMARY OF TROPOMYOSIN TWO-CHAIN MOLECULES

Species[a]	C36[b]	C190[b]	Elution order		Order of mobility	
			C_4 RP-HPLC	HPSEC	4–20%	9%[c]
$\alpha\alpha$	–	RD	6, 7, 8, 9	6, 7, 8, 9	1, 2	1, 2
$\cdot\alpha\alpha\cdot$	–	CAM or CM	6, 7, 8, 9	6, 7, 8, 9	1, 2	1, 2
$\beta\beta$	RD	RD	6, 7, 8, 9	6, 7, 8, 9	3, 4	3, 4
$\cdot\beta\beta\cdot$	CAM	CAM	6, 7, 8, 9	6, 7, 8, 9	3, 4	3, 4
$\alpha^{-}\alpha$	–	XL	2	1, 2, 3, 4	6, 7, 8	7
$\alpha^{-}\beta_{\cdot}$	CAM	XL	3, 4	1, 2, 3, 4	6, 7, 8	8
$_{\cdot}\beta^{-}\beta_{\cdot}$	CAM	XL	3, 4	1, 2, 3, 4	6, 7, 8	9
$\cdot\beta_{-}\beta\cdot$	XL	CAM	5	1, 2, 3, 4	5	5, 6
$\beta^{-}_{-}\beta$	XL	XL	1	5	9	5, 6

[a] We use a superscript (subscript) dash to indicate cross-linking at C190 (C36), and a superscript (subscript) dot to indicate blocking at C190 (C36).

[b] RD, XL, CAM, CM = Reduced, cross-linked, carboxyamidomethyl-blocked, carboxymethyl-blocked sulfhydryl, respectively.

[c] From ref. 11.

than the non-cross-linked contrary to expectations based on their hydrophobicities and chain lengths alone [13].

Many previous investigations have dealt with the effects of HPLC solvents and hydrophobic matrices on the secondary and quaternary structures of proteins and peptides and have attempted to elucidate the role of conformational changes and/or chain dissociation in their binding to and elution from such columns [13–17]. Whether conformational changes take place upon binding to a RP-HPLC column matrix is difficult to determine experimentally and beyond the scope of this study. However, in order to investigate whether the RP elution medium induces changes in the secondary and/or quaternary structures of Tm upon release from the column matrix, we examined circular dichroism (CD), high-performance size-exclusion chromatography (HPSEC) and equilibrium ultracentrifugation for various Tm species in a representative RP elution medium, namely, 0.0975% (v/v) trifluoroacetic acid (TFA) in 45% aqueous acetonitrile, without and with added NaCl. Using millimolarity as subscript and pH in parentheses, these media can be designated $CH_3CN_{8500}TFA_{13}NaCl_x$ (2).

MATERIALS AND METHODS

Protein preparation and characterization

Rabbit skeletal tropomyosin (R_sTm) and rabbit cardiac tropomyosin (R_cTm) were prepared and characterized as previously described [18,19]. R_cTm contains only α chains [20] and was used whenever pure $\alpha\alpha$ tropomyosin was required. Pure β-tropomyosin ($\beta\beta$) was obtained by carboxymethylcellulose ion-exchange chromatography of reduced, denatured R_sTm and subsequent renaturation of the β fraction [3].

The preparation and properties of the cross-linked homodimer species: $\alpha\text{-}\alpha$; $\beta\text{-}\beta$; $\beta^{-}\beta$.; $\beta_{-}\beta$ have been described previously [8–12]. For the samples used in this study, disulphide cross-linking was carried out by oxidation with ferricyanide [10], and sulfhydryl blocking was carried out by reaction with iodoacetamide or iodoacetic acid [12,21].

The preparation and isolation of the heterodimer species, $\alpha^{-}\beta$., was carried out as follows. R_sTm, consisting mostly of $\alpha\alpha$ and $\alpha\beta$ molecules was cross-linked at C190, then blocked at the C36 position of the β chains as previously described [12]. The resulting mixture of cross-linked dimers, mostly $\alpha^{-}\alpha$ and $\alpha^{-}\beta$., was denatured using 8 *M* urea and separated using carboxymethylcellulose ion-exchange chromatography [22]. The final product was characterized by SDS-PAGE using both non-reducing and reducing 9% Laemmli gels, and by sulfhydryl titration of the re-reduced material [23].

The preparation and properties of $\alpha\alpha$ have been described [21]. The $\beta\beta$ used in this study was produced willy-nilly, as a byproduct in the preparation of $\beta_{-}\beta$ and separated from it by SEC [11].

Gel electrophoresis and chromatography

Samples were prepared for SDS-PAGE as described earlier [24] and analyzed on 4–20% linear acrylamide gradient mini-gels of 1 mm thickness (Enprotech, Hyde Park, MA, U.S.A.) for 1.5 h at a constant voltage of 150 V. Normally, the sample size was 5–20 μl (2.5–10 μg of protein).

RP-HPLC was performed using a Vydac 214TP54 C_4 column (25 cm × 0.46 cm I.D.) and HPSEC using a TSK 4000SW column (60 cm × 0.75 cm I.D.) plus a guard

column (7.5 cm × 0.75 cm I.D.), all purchased from the Nest Group (Southborough, MA, U.S.A.). The sources of solvents, configuration of the chromatographic hardware, temperature control, and data acquisition procedures have been previously described [25,26].

The solvent program used to effect separation on the C_4 RP column was a linear gradient from 0 to 100% B in 60 min at 1 ml min^{-1}, with mobile phases A = 0.1% TFA and B = 0.095% TFA in 90% aqueous acetonitrile. HPSEC was performed isocratically at 0.5 ml min^{-1} using a 50:50 mixture of the RP solvents A and B described above. The chromatograms were monitored at 214 nm.

Protein samples were prepared by reconstituting each lyophilized sample to a protein concentration of ≈ 1 mg ml^{-1} with 1% acetic acid (Fisher Scientific, St. Louis, MO, U.S.A.); these were stored at 4°C until use. Usually, 25 μl (25 μg of protein) or 50 μl (50 μg of protein) of cross-linked and/or blocked sample was injected onto the column. To reduce disulphide bonds, 50 μl (50 μg) of samples prepared as described above were mixed with 140 μl of $NaPi_{100}EDTA_5$ (7.4) and 10 μl dithiothreitol $(DTT)_{1000}$. The mixture was blanketed with nitrogen and then incubated at 45°C overnight. Control samples were prepared by substituting 10 μl water for the reductant. For both the reduced and control samples, 150 μl (37.5 μg of protein) of the reaction mixture was injected on the column.

CD measurements

CD measurements were carried out using a Jasco J500A spectropolarimeter interfaced to a THE personal computer. Temperature control and measurement, data collection and analysis, and calculation of fraction helix from the ellipticity at 222 nm have all been described previously [8,11]. All denaturation curves were reversible.

Solutions for CD measurements were prepared by quantitative dilution of stock protein solutions (5–10 mg ml^{-1}) in 0.195% aqueous TFA (TFA_{26}). Each stock solution was passed through a 0.45-μm filter (Gelman, Fisher Scientific) before further manipulation. For concentration determination (and CD measurements in benign buffer) an aliquot of each stock was diluted tenfold with $NaCl_{433}HCl_{10}$ (2) and the absorbance at 275 nm of the resulting solution measured against a blank prepared by diluting TFA_{26} in the same manner. The protein concentration was then calculated using an extinction coefficient of 0.314 cm^2 mg^{-1} [27]. For CD measurements in the RP medium another aliquot of each stock was diluted twofold with 90% acetonitrile (CH_3CN_{17000}) resulting in a medium with composition $CH_3CN_{8500}TFA_{13}$ (2).

Equilibrium ultracentrifugation

A Spinco Model E analytical ultracentrifuge equipped with UV optics and a photoelectric scanner was used for sedimentation equilibrium molecular mass determinations of $\alpha\alpha$ and $\alpha\alpha'$ in $CH_3CN_{8500}TFA_{13}$ (2). Protein solutions having concentrations of 0.8 to 1.6 mg ml^{-1} were first dialysed against solvent for 8 h at room temperature (using dialysis bags that had been soaked successively in a series of solutions containing 13 m*M* TFA and 10, 20, 30, 40, 45% acetonitrile) and then centrifuged at 18 000 rpm for 24–48 h at *ca.* 20°C in an An-H rotor with 12-mm, double-sector cells.

The data for each run were plotted as $\ln A_{280}$ *vs.* r^2, where r is distance from the center of rotation. Where the data fell on a straight line, the molecular mass was calculated from:

$$\mathrm{d}(\ln A_{280})/\mathrm{d}(r^2) = KM \tag{1}$$

where M is the molecular mass and $K = (1 - v_\rho\rho)\omega^2/2RT$; we used $v_\rho = 0.729$ ml g^{-1} [28], and a solution density, $\rho = 0.930$ g ml^{-1}. For runs where the data showed obvious downward curvature, the data were computer-fit using a finite difference Levenberg–Marquardt algorithm (program ZXSSQ in the IMSL library of programs) to the equation:

$$r^2 = A_0 + A_1 (\ln A_{280}) + A_2(A_{280}) \quad (2)$$

The coefficients of each term in the first derivative of eqn. 2 with respect to ln A_{280} can be equated with the corresponding coefficients in the two term virial expansion of the sedimentation equilibrium equation, giving the molecular mass, $M = 1/KA_1$, and second virial coefficient, $B = K(A_2)\varepsilon l/2$, where ε is the extinction coefficient in cm^2 g^{-1} and l the optical path length in cm.

RESULTS AND DISCUSSION

SDS-PAGE and C_4 RP-HPLC analysis of Tm species

Results of a 4–20% SDS-PAGE experiment with the various cross-linked species used in this study are shown in Fig. 1 and Table I (column 6). Lanes 1–10 of the gel show, respectively, $\alpha^{-}\beta_{.}$, $\beta\text{-}\beta$, $\alpha^{-}\alpha$, $\cdot\beta\_\beta\cdot$ and $:\beta\beta:$, $_{.}\beta^{-}\beta_{.}$, $\beta\text{-}\beta$, $\alpha^{-}\beta_{.}$, $\alpha^{-}\alpha$, blank and markers. The order of electrophoretic mobility for all species is: $\alpha\alpha \approx \cdot\alpha\alpha\cdot > \beta\beta \approx :\beta\beta: \gg \cdot\beta\_\beta\cdot > \alpha^{-}\alpha \approx \alpha^{-}\beta_{.} \approx {}_{.}\beta^{-}\beta_{.} > \beta\text{-}\beta$. The band of lowest mobility, $\beta\text{-}\beta$, is often well enough resolved on scans to allow determination of its fraction in a mixture containing other cross-linked species. For comparison, column 7 of Table I gives the order of electrophoretic mobility of the various species on 9% Laemmli SDS-PAGE [11]. On that system it is often possible to resolve and quantitate the band consisting of both $\cdot\beta\_\beta\cdot$ and $\beta\text{-}\beta$.

Nevertheless, because the resolution obtained using SDS-PAGE is variable and the time required for staining, destaining, and quantitation is long, we investigated the use of C_4 RP-HPLC as a possible fast and direct analytical assay for the various Tm species. The results are shown in Figs. 2 and 3 as abscissa expansions of the 30–40 min region of each chromatogram and are summarized in Table I (column 4). The peaks were assigned by comparison to those obtained for each of the individual species in separate runs made under identical conditions. Except for the unretained solvent peak no peaks other than those shown appear in the complete chromatograms.

Fig. 2A–D shows expanded chromatograms of a mixture of $\beta\text{-}\beta$, $\alpha^{-}\alpha$, and $\alpha^{-}\beta_{.}$ as a function of temperature. The expanded chromatogram of a mixture of $\beta\text{-}\beta$, $\alpha^{-}\alpha$, $\alpha^{-}\beta_{.}$, and ${}_{.}\beta^{-}\beta_{.}$ at 28°C is shown in Fig. 3A, and that of a mixture of $\beta\text{-}\beta$, ${}_{.}\beta^{-}\beta_{.}$, $\cdot\beta\_\beta\cdot$, and $:\beta\beta:$ at 37°C in Fig. 3B.

The variations in retention times and peak resolutions for $\beta\text{-}\beta$, $\alpha^{-}\alpha$, and $\alpha^{-}\beta_{.}$ as a function of temperature are shown graphically in Fig. 2E and F as the capacity factor, k', and the resolution between pairs of samples, R_s, respectively. As the temperature increases, the retention times and k' values for all species first decrease then increase again (Fig. 2E). The resolution of the $\beta\text{-}\beta$ and $\alpha^{-}\alpha$ peaks (open dels) first increases then decreases, whereas that between the $\alpha^{-}\alpha$ and $\alpha^{-}\beta_{.}$ peaks (open diamonds) steadily decreases up to 46°C whereupon the two peaks coalesce (Fig. 2F).

In all cases, $\beta\text{-}\beta$ has the smallest retention time and, except at 55°C (Fig. 2D), is

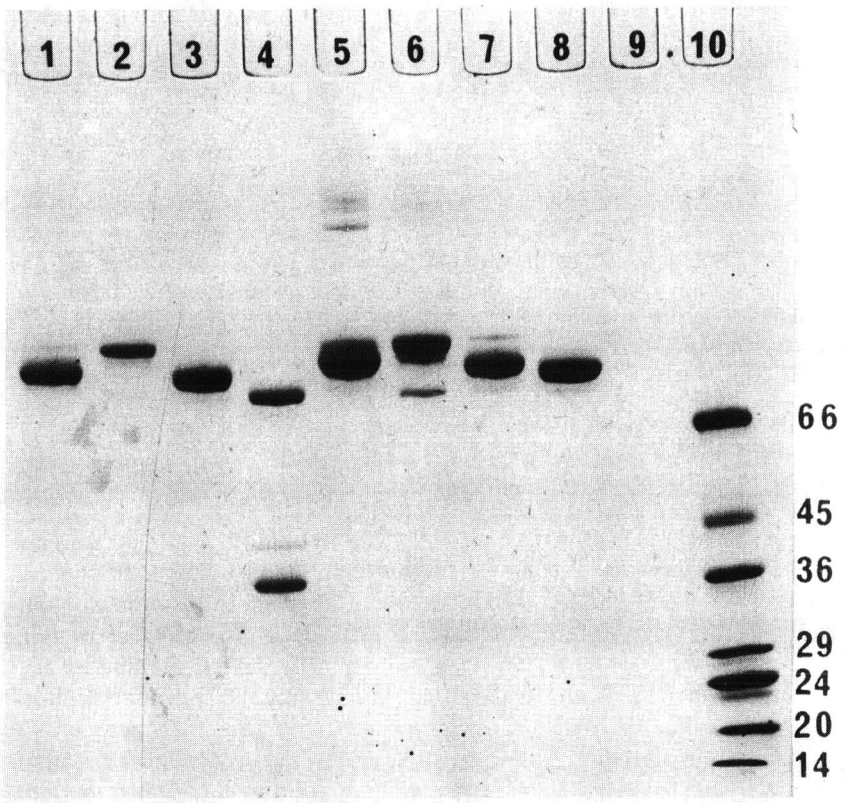

Fig. 1. Photo of 4–20% SDS-PAGE for various samples. Electrophoresis is from top to bottom. Lanes are: 1 = $\alpha^{-}\beta_{.}$; 2 = $\beta^{-}\beta$; 3 = $\alpha^{-}\alpha$; 4 = $\underline{\beta^{-}\beta}_{.}$ plus $\cdot\beta\beta\cdot$; 5 = $_{.}\beta^{-}\beta_{.}$; 6 = $\beta^{-}\beta$; 7 = $\alpha^{-}\beta_{.}$; 8 = $\alpha^{-}\alpha$; 9 = blank; 10 = protein standard mixture with indicated molecular mass (in kilodalton). The electrophoretic mobilities of the cross-linked Tm species (66 000 dalton) are lower than that of the 66 000-dalton marker on this gel system.

well separated from the other species. The retention times for the C190 singly cross-linked species are somewhat longer, and at 28°C the $\alpha^{-}\alpha$ peak is almost baseline-resolved from that of $\alpha^{-}\beta_{.}$ (Fig. 2A). On the other hand, the retention times of $\alpha^{-}\beta_{.}$ and $_{.}\beta^{-}\beta_{.}$ are almost the same, and for a mixture containing both, only one slightly broadened peak appears (Fig. 3A). The retention time for $\cdot\beta\text{-}\beta\cdot$ is even longer (Fig. 3B; the order of retention times is the same at 37°C as at 28°C). Retention times for the non-cross-linked species are longest and approximately equal for sulfhydryl-blocked and disulphide-reduced (data not shown) samples. The elution order at 28°C or 37°C is: $\beta^{-}\beta \ll \alpha^{-}\alpha < {}_{.}\beta^{-}\beta_{.} \approx \alpha^{-}\beta_{.} < \cdot\beta\text{-}\beta\cdot < \alpha\alpha = \cdot\alpha\alpha\cdot = \beta\beta = {}_{.}\beta\beta_{.}$.

The retention times for the various Tm species depend on the number and positions of the cross-links and thus cannot be accounted for wholly on the basis of their hydrophobicities and chain lengths as others have found for several proteins, including R_cTm [13]. The 284-residue α and β Tm chains differ at 39 positions, only 11 of which are interior hydrophobic positions; the chains almost match in the number of hydrophobic (104 *vs.* 102), basic (55 *vs.* 54), and acidic (80 *vs.* 81) residues [7]. Thus,

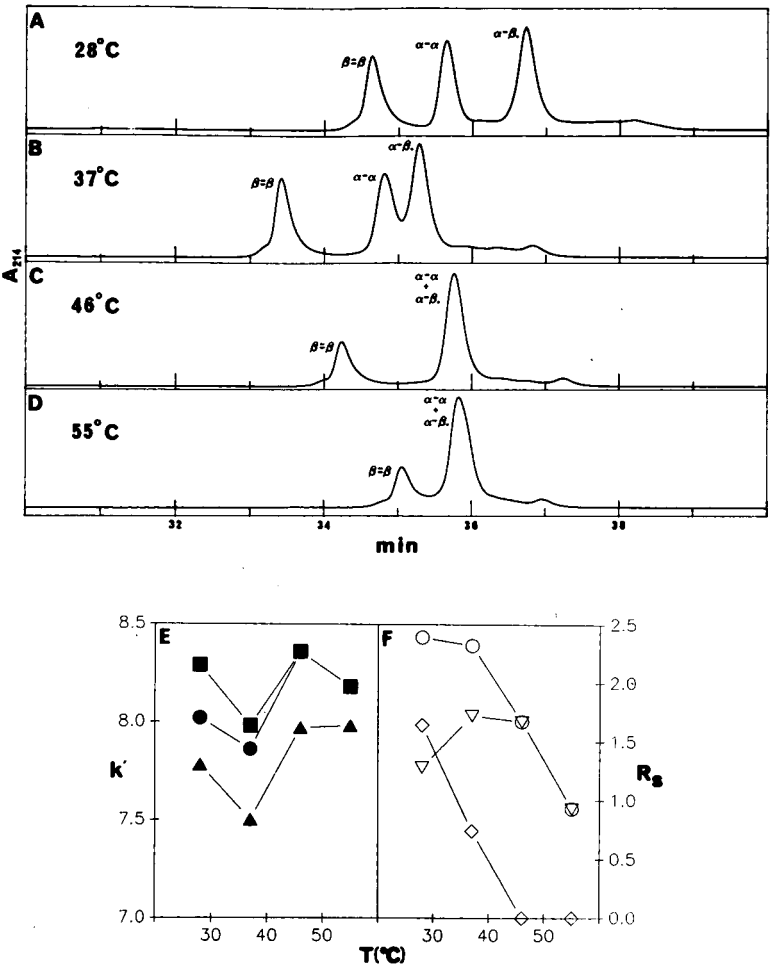

Fig. 2. Effect of temperature on the C_4 RP resolution of $\beta^-\beta$, $\alpha^-\alpha$ and $\alpha^-\beta$.; scale = 375 mV full scale; mobile phases A = 0.1% aqueous TFA and B = 0.095% TFA in 90% aqueous acetonitrile with a linear gradient from 0 to 100% B in 60 min at 1 ml min^{-1}. (A–D) C_4 RP chromatograms at 28, 37, 46 and 55°C, respectively; (E) capacity factor, k', *vs.* temperature: ▲ = $\beta^-\beta$; ● = $\alpha^-\alpha$; ■ = $\alpha^-\beta$.; (F) resolution, R_s, *vs.* temperature: ▽ = $\beta^-\beta/\alpha^-\alpha$; ○ = $\beta^-\beta/\alpha^-\beta$.; ◇ = $\alpha^-\alpha/\alpha^-\beta$.

their overall hydrophobicities should be very similar. Indeed, we observe no separation between non-cross-linked α and β using C_4 RP-HPLC.

Since there are twice as many hydrophobic sites in a cross-linked molecule as in one of its constituent chains, the overall hydrophobicities of all cross-linked species are also very similar. All cross-linked Tm species, then, would be expected to elute at approximately the same time, but, owing to their longer chain lengths, later than the non-cross-linked species. However, we find here that the cross-linked species not only elute earlier than the non-cross-linked, but at times quite different from one another.

We also find a similar inversion of expected elution positions for the cyanogen bromide (CNBr) produced C-terminal segment of $\alpha^-\alpha$. A preliminary result shows

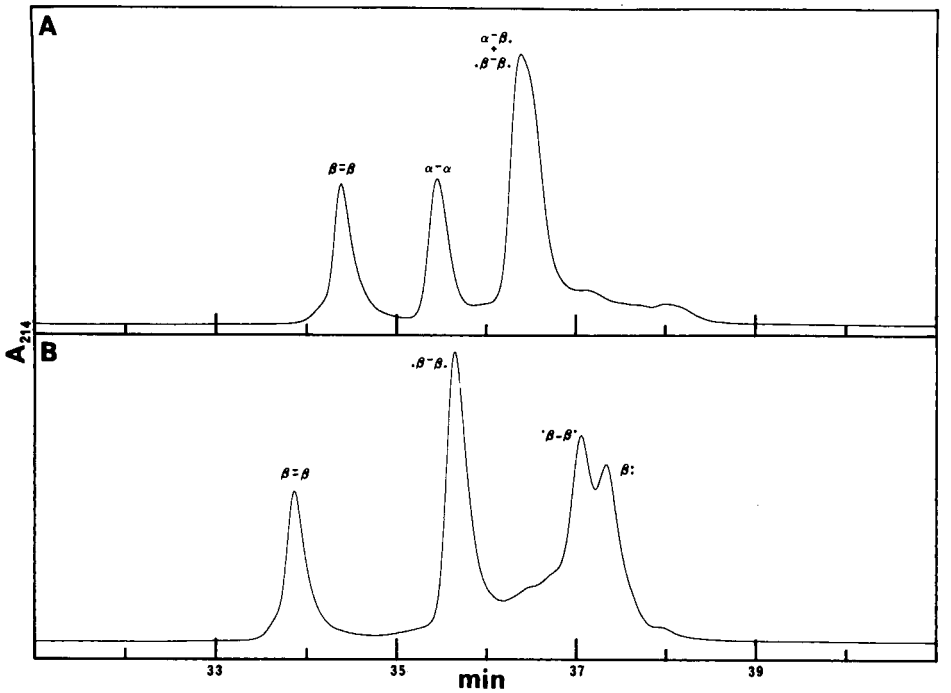

Fig. 3. (A) C_4 RP-HPLC chromatogram for $\beta\text{-}\beta$, $\alpha\text{-}\alpha$, $\alpha\text{-}\beta$. and $\beta\text{-}\beta$. at 28°C. Chromatographic conditions same as for Fig. 2, except that scale = 550 mV f.s. (B) C_4 RP-HPLC chromatogram for $\beta\text{-}\beta$, $\beta\text{-}\beta$., $\beta\text{-}\beta$·, and $\beta\beta$· at 37°C. Chromatographic conditions same as for Fig. 2, except that scale = 550 mV f.s.

that when reduced, the C-terminal segment, comprising residues 142–281 ($_{142}\alpha_{281}$), elutes later than when cross-linked, and approximately at the same time as the N-terminal segment, comprising residues 11–127 ($_{11}\alpha_{127}$). The N-terminal and reduced C-terminal segments have comparable chain lengths, almost equal fractions of positive, negative and hydrophobic residues, and similar coiled-coil conformation near room temperature in benign neutral medium [29,30], so would be expected to have similar elution behavior. However, we find cross-linking $_{142}\alpha_{281}$, as in parent Tm, leads to an inversion of expected elution positions. A similar inversion, albeit accompanied by *decreased* resolution upon cross-linking, has been observed for short Tm-analogue peptides (35 residues/chain) [31].

This inversion must arise from decreased interactions of the cross-linked species with the hydrophobic solid support. In the α-helical coiled-coil structure present in native parent Tm, excised Tm segments and Tm-analogue peptides, the amphipathicity of the helices provides strong inter-chain hydrophobic interactions that impart extraordinary stability to the structure under benign conditions [1,8,29–33]. These inter-chain interactions must be disrupted and the hydrophobes exposed for a coiled-coil molecule to interact with the hydrophobic solid support. Maximal interaction will occur when the chains are completely dissociated. For cross-linked molecules complete dissociation of the helices is, of course, impossible and, owing to conformational constraints imposed by one or more cross-links, complete exposure of the hydrophobic

residues is difficult. There are no such constraints for non-cross-linked molecules, resulting in increased binding to, and later elution from, the column.

Moreover, we find that the retention times for the cross-linked species themselves vary and that $\beta\text{-}\beta$ elutes before all the C190-cross-linked species, which, in turn, elute before β_β. It is not surprising that two cross-links are more effective than one in decreasing the accessibility of the hydrophobic sites. It is surprising, however, that a single cross-link at C190 is more effective than a single cross-link at C36, even in the two singly cross-linked $\beta\beta$ species that are identical except for the exchanged positions of the cross-linked and blocked sulfhydryls. A preliminary result shows that this order of elution persists in excised, cross-linked CNBr-produced segments of $\beta\text{-}\beta$. That is, the C190-cross-linked C-terminal segment, comprising residues 147–265 ($_{147}\beta_{265}$) elutes before the C36-cross-linked N-terminal segment, comprising residues 11–127 ($_{11}\beta_{127}$) (C_8 stationary phase, *n*-propanol mobile phase).

The complete or near-complete resolution of some Tm species, particularly $\beta\text{-}\beta$, suggests that C_4 RP can be used as an analytical assay. We determined the relative amounts of various species in a sample of cross-linked R_sTm (data not shown) and compared the results to those obtained using 4–20% SDS-PAGE and free solution capillary electrophoresis (FSCE). The presence of $\beta\text{-}\beta$ in this sample is easily detected using C_4 RP-HPLC and the relative amounts of the principal species present (7.3% $\beta\text{-}\beta$, 55.8% $\alpha\text{-}\alpha$, 32.1% $\alpha\text{-}\beta_.$, 2.3% non-cross-linked, and 2.6% unidentified) are in agreement with those obtained from 4–20% SDS-PAGE (7.6% $\beta\text{-}\beta$, and 92.4% $\alpha\text{-}\alpha$ plus $\alpha\text{-}\beta_.$). These results are also in agreement with a preliminary result obtained using FSCE (Beckman P/ACE System 2000). In $urea_{7000}NaPi_{50}\underline{SDS_{0.07}}$ (7.4) all β species in a cross-linked R_sTm sample showed the same mobility and were well resolved from $\alpha\text{-}\beta_.$, which was almost completely resolved from $\alpha\text{-}\alpha$; the relative amounts were 8.2% β (all species), 29.1% $\alpha\text{-}\beta_.$, and 62.6% $\alpha\text{-}\alpha$. Thus, we observe an amount of $\beta\beta$ molecules in R_sTm that is not inconsistent with the 4–6.25% expected for random association of α and β chains present in a 3–4:1 ratio. Since our samples were never heated (initial reduction carried out at 4°C overnight) and since chains of the native molecules do not exchange at or below room temperature [9], it is unlikely that these $\beta\beta$ species were produced through intermolecular cross-linking. However, further investigations are being carried out to exclude that possibility.

Studies of Tm species in C_4 RP-HPLC elution solvent

In order to investigate whether the elution medium itself causes secondary and/or quaternary conformational changes we carried out CD, HPSEC and equilibrium ultracentrifugation studies for several of the Tm species in $CH_3CN_{8500}TFA_{13}$ (2). The composition of this medium is very close to the average required to elute cross-linked species from the C_4 RP-HPLC solid support, and unless interaction with the solid support itself produces irreversible changes, the conformation of a given species dissolved directly in this representative RP medium should be approximately the same as it would be upon elution.

CD spectra and thermal denaturation profiles

The CD spectra at 3°C for $\beta\text{-}\beta$, $\alpha\text{-}\alpha$, and $\alpha\alpha$ in the average RP elution medium are shown in Fig. 4 and all have the characteristic double minima at 208 and 222 nm indicative of α-helical structure. For each, the ratio of the intensity of the 222 nm to

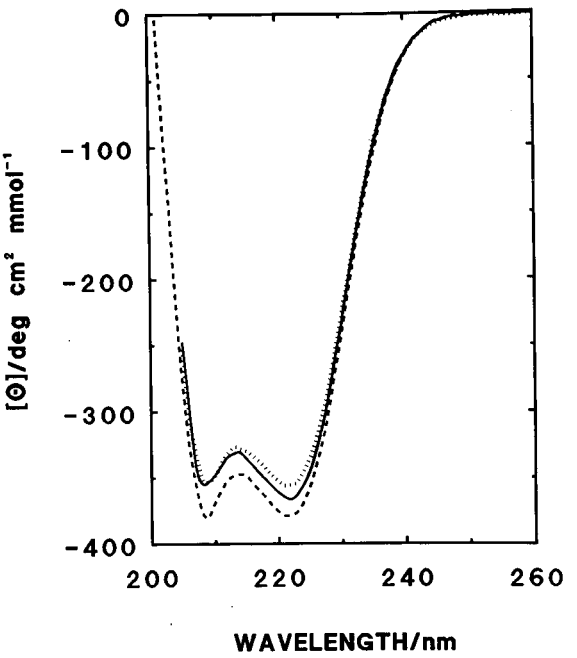

Fig. 4. CD spectra at 3°C for various Tm species in $CH_3CN_{8500}TFA_{13}$ (2). Dashed curve, 0.73 mg ml^{-1} $\alpha^{-}\alpha$; solid curve, 2.60 mg ml^{-1} ·αα·; dotted curve, 1.77 mg ml^{-1} $\beta^{-}\beta$.

that of the 208 nm minimum is approximately unity, whereas in benign aqueous media, it is ≈1.1. Approximately equal intensities of the two minima have also been observed for Tm in trifluoroethanol (TFE) [33] and in SDS [34] solutions, and for Tm-analogue peptides in acetonitrile and in TFE solutions [31–33,35]. If the decrease in $\theta_{222}/\theta_{208}$ observed here for the Tm species upon change from aqueous benign media to the RP medium is indeed associated with a change in conformation from a two-chain coiled-coil conformation to non-interacting helices as recently predicted from theory [36], then the helices must be non-interacting in non-cross-linked and cross-linked species alike, even though the latter are physically tethered.

Fraction helix, [Φ] (from CD at 222), is plotted *vs.* temperature in Fig. 5A for $\alpha^{-}\alpha$, αα, and ·αα·, and in Fig. 5B for $\beta^{-}\beta$. Thermal profiles are shown for benign aqueous as well as RP acidic media. Up to ≈40°C, both $\alpha^{-}\alpha$ (Fig. 5A) and $\beta^{-}\beta$ (Fig. 5B) are almost as helical in the RP medium (≈90% at 25°C and ≈80% at 40°C) as in benign aqueous acidic solution, wheras ·αα· (< 1.6 mg ml^{-1}) is slightly less stable in the RP elution medium (≈85% at 25°C and 75% at 40°C; Fig. 5A). Nevertheless, in the medium used here for C_4 RP-HPLC all species are highly helical and, therefore, none of them undergo major changes in secondary structure. In previous studies of the conformations of proteins both in free solution and when bound to an RP support it was also found that the helical forms of those proteins constitute the eluted forms and that those proteins were less helical when bound to the RP-HPLC support [14,15].

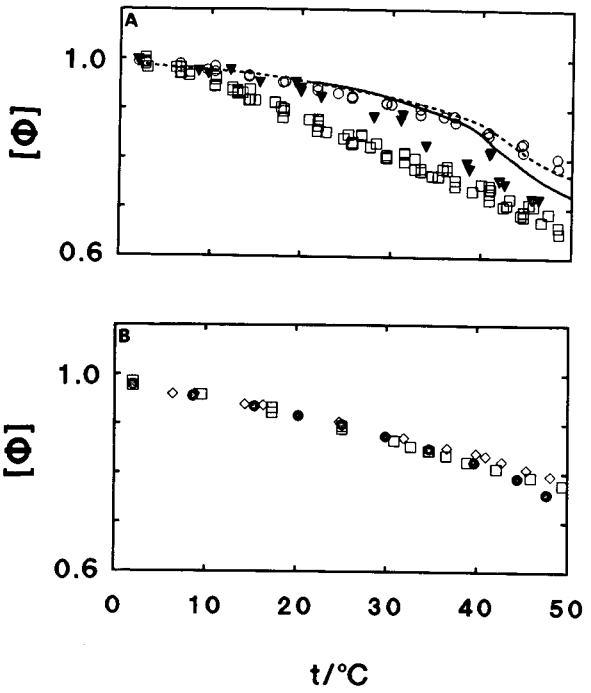

Fig. 5. Fraction helix, [Φ], (from CD at 222) *vs.* temperature. (A) $\alpha\alpha$ species: dashed (solid) curve is spline curve through data for $\alpha\alpha$ ($\alpha^{-}\alpha$) in $NaCl_{390-590}HCl_{10}$ (2) [37]. ○ = ·$\alpha\alpha$·, 0.59 mg ml^{-1} in $NaCl_{390}HCl_{10}$ (2); □ = ·$\alpha\alpha$·, 0.017–1.6 mg ml^{-1} in $CH_3CN_{8500}TFA_{13}$ (2); ▼ = $\alpha^{-}\alpha$, 0.0126, 0.73 and 0.90 mg ml^{-1} in $CH_3CN_{8500}TFA_{13}$ (2). (B) $\beta\text{-}\beta$ solutions: □ = 0.315 mg ml^{-1} in $NaCl_{390}HCl_{10}$ (2); ◇ = 1.77 mg ml^{-1} in $CH_3CN_{8500}TFA_{13}$ (2); ● = 0.133 mg ml^{-1} in $CH_3CN_{9440}TFA_{4.1}NaCl_{146}HCl_5$ (2).

Size-exclusion chromatography

To determine whether the RP elution medium causes quaternary structural changes we carried out HPSEC for the Tm species in the RP medium at 25°C. The elution profiles for $\alpha^{-}\alpha$, ·$\alpha\alpha$· and a mixture thereof (Fig. 6A), and those for $\beta\text{-}\beta$, $\beta^{-}\beta$., ·$\beta\text{-}\beta$·, and :$\beta\beta$: (Fig. 6B) show a sharp peak for each of the principal species. The elution order is: $\alpha^{-}\alpha = \alpha^{-}\beta$. (data not shown) = $\beta^{-}\beta$. = ·$\beta\text{-}\beta$· $\approx \beta\text{-}\beta < \alpha\alpha$ (data not shown) = ·$\alpha\alpha$· = $\beta\beta$ (data not shown) = :$\beta\beta$: and is given in column 5 of Table I. Samples of $\alpha^{-}\beta$., ·$\beta\text{-}\beta$·, ·$\alpha\alpha$·, and :$\beta\beta$: that had been subjected to RP-HPLC were collected and then subjected to HPSEC (data not shown). The results are the same as those for samples that had not previously been subjected to RP-HPLC. Thus, interaction with the support during C_4 RP-HPLC produces no irreversible changes in these species that affect their HPSEC behavior.

We find here that in the RP medium, the cross-linked species elute before the non-cross-linked, indicating that the former have larger Stokes' radii than the latter. Since both have similar, highly helical, secondary structures in the RP medium, the differences in HPSEC elution times must be caused by diferences in the quaternary structure, *i.e.*, by further association of the cross-linked molecules to higher aggregates or by dissociation of the non-cross-linked molecules into single-chain α-helices. The former is highly unlikely; the presence or absence of a cross-link should have little

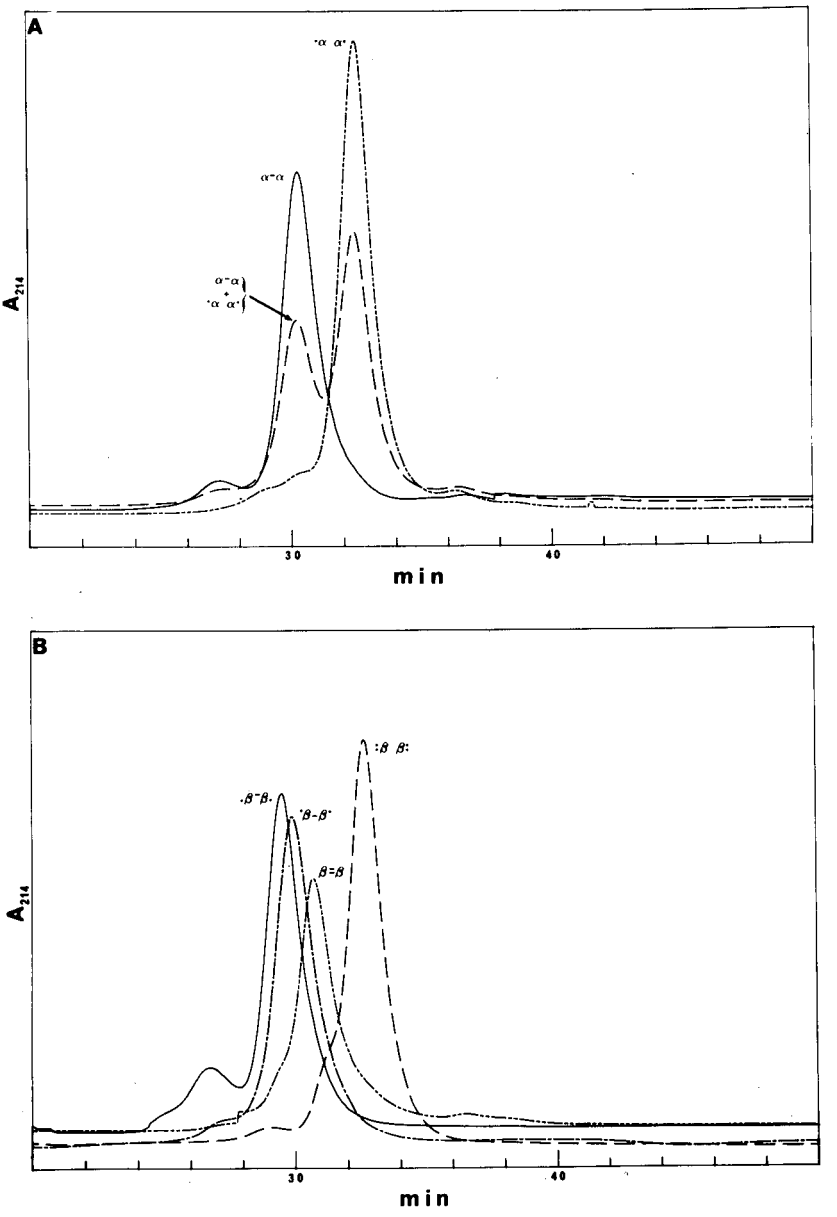

Fig. 6. HPSEC chromatograms of Tm species. Mobile phase is $CH_3CN_{8500}TFA_{13}$ (2) for all. (A) Overlay of three separate chromatograms for $\alpha^{-}\alpha$ (solid curve), ·αα· (long-short-short dashed curve), and a mixture thereof (long dashed curve); scale = 500 mV f.s. (B) Overlay of four separate chromatograms for $\beta^{-}\beta$ (solid curve), ·β-β· (long-short dashed curve), β-β (long-short-short dashed curve), and ·ββ· (long dashed curve); scale = 700, 450, 300 and 450 mV f.s., respectively.

affect on the formation of higher aggregates. In order to investigate whether the chains, indeed, dissociate in the RP medium we carried out additional HPSEC experiments of Tm species in the presence of added salt. The addition of NaCl should increase the helix–helix hydrophobic interactions as well as decrease the chain dipole–chain dipole repulsions [38], and at high enough salt concentration cause the chains to reassociate.

Additional HPSEC experiments were carried out on ·αα·, αα, and α⁻α in $NaCl_{390}HCl_{10}$ (2) and in the average RP elution medium containing 50 and 100 m*M* NaCl; the elution profiles are shown in Fig. 7. In $NaCl_{390}HCl_{10}$ (2) (Fig. 7A) all three species show the same elution profile: one main peak flanked by two considerably smaller peaks. The two small flanking peaks are probably aggregated and monomeric Tm, or some unrelated impurities. In any case their amounts are small. In benign acidic aqueous medium αα has the same intrinsic viscosity [34] as R_sTm which has been shown to be a two-chain α-helical molecule [27]. Thus, it seems reasonable to conclude that in benign media ·αα·, αα, and α⁻α all exist predominantly as two-chain coiled coils.

The effect of added salt in the RP elution medium is shown in Fig. 7B, which gives elution profiles of α⁻α, αα and ·αα· in $CH_3CN_{8500}TFA_{13}NaCl_{100}$ (2). The profile for α⁻α is similar to that observed in benign acidic aqueous solution (Fig. 7A), ~~except that elution times for corresponding peaks are shorter~~. The profile for ·αα·, however, shows two broad overlapping peaks, a larger one that elutes at the same position as α⁻α (≈38 min; peak I) and a smaller one that elutes later (≈44 min; peak II). The eluent from each peak was collected and reinjected onto the column. The results are also shown in Fig. 7B. The elution profile of reinjected peak I is similar to the original; reinjected peak I elutes as two peaks —a larger one with elution time ≈38 min and a much smaller one with elution time ≈44 min. Reinjected peak II elutes as a single peak with elution time ≈44 min.

Fig. 7C shows ·αα· and α⁻α in $CH_3CN_{8500}TFA_{13}NaCl_{50}$ (2). Again, the elution behavior of α⁻α is similar to that observed in benign acidic solution (Fig. 7A) or in $CH_3CN_{8500}TFA_{13}NaCl_{100}$ (2) (Fig. 7B), except that the elution times for corresponding peaks are shorter. As in 100 m*M* NaCl, the profile for ·αα· shows two broad overlapping peaks, but the peak that elutes at the same time as α⁻α is considerably diminished. We also find that the elution time for a given species and a given mobile phase is independent of the medium of the injected sample, indicating that equilibrium with the column mobile phase is achieved in a much shorter time than is required for elution, *i.e.*, ≪30–40 min. For example, the elution time of ·αα· is the same whether the sample was in $NaCl_{390}HCl_{10}$ (2) or $CH_3CN_{8500}TFA_{13}NaCl_{50}$ (2) prior to injection onto a column with mobile phase $CH_3CN_{8500}TFA_{13}NaCl_{50}$ (2) (Fig. 7C).

The data are consistent with the existence of an equilibrium between two-chain α-helical ·αα· species and single-chain α-helical α· species in the RP elution medium containing added salt. Increasing the salt concentration favors two-chain species and decreasing it favors single-chain species, and in the absence of added salt the single-chain species are overwhelmingly favored.

Equilibrium ultracentrifugation

Fig. 8 shows sedimentation equilibrium data for αα and for ·αα· in $CH_3CN_{8500}TFA_{13}$ (2) plotted as ln A_{280} *vs.* r^2. The values for αα fall on a straight line (correlation coefficient = 0.9997), and give an apparent molecular mass of 31 000 dal-

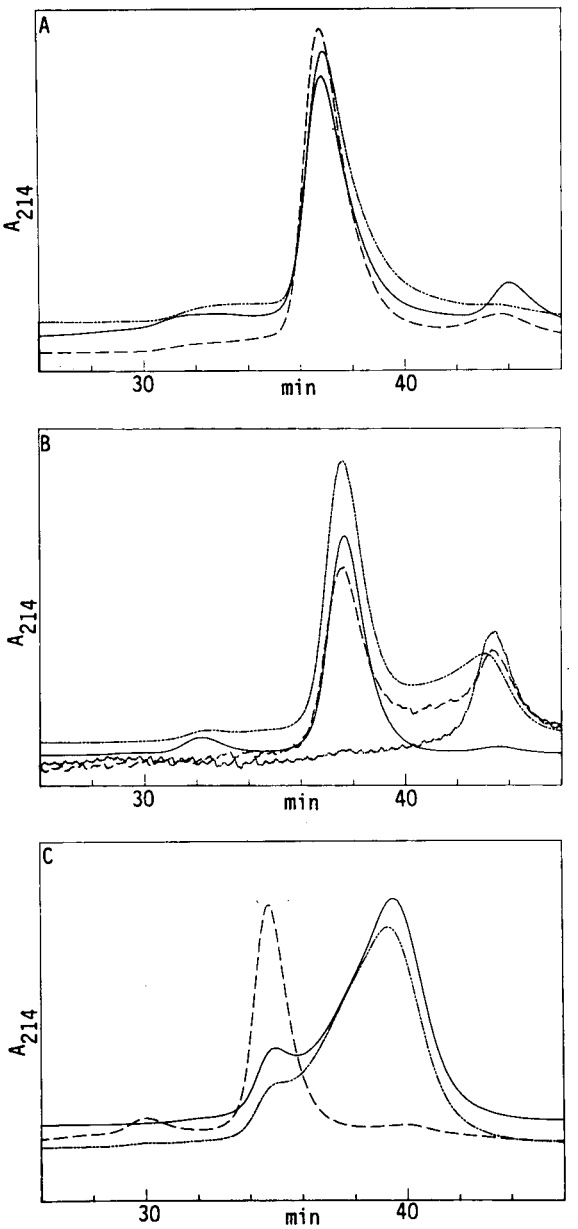

Fig. 7. HPSEC chromatograms of Tm species. (A) Mobile phase is $NaCl_{390}HCl_{10}$ (2). Overlay of three separate chromatograms for ·αα· in $NaCl_{390}HCl_{10}$ (2) (solid curve), αα in $CH_3CN_{8500}TFA_{13}$ (2) (dashed curve), and $\alpha^-\alpha$ in $CH_3CN_{8500}TFA_{13}NaCl_{100}$ (2) (long-short-short dashed curve); scale = 325, 500 and 100 mV f.s., respectively. (B) Mobile phase and sample buffer for all is $CH_3CN_{8500}TFA_{13}NaCl_{100}$ (2). Overlay of four separate chromatograms for ·αα· (long-short-short dashed curve), reinjected ≈38 min ·αα· peak (dashed curve), reinjected ≈44 min ·αα· peak (short-long curve), and $\alpha^-\alpha$ (solid curve); scale = 250, 10, 7.5 and 375 mV f.s., respectively. (C) Mobile phase is $CH_3CN_{8500}TFA_{13}NaCl_{50}$ (2). Overlay of three separate chromatograms for ·αα· in $NaCl_{390}HCl_{10}$ (2) (solid curve), and ·αα· (long-short-short dashed curve) and $\alpha^-\alpha$ (dashed curve) in $CH_3CN_{8500}TFA_{13}NaCl_{50}$ (2); scale = 150, 200 and 250 mV f.s., respectively.

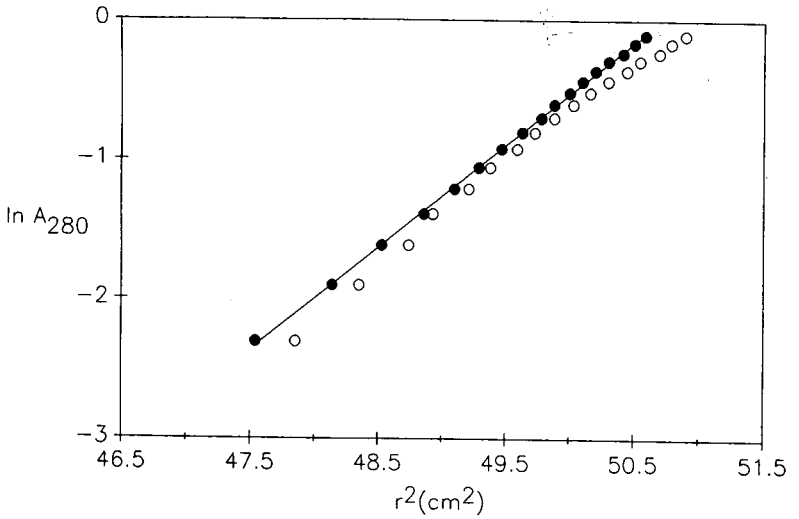

Fig. 8. Sedimentation equilibrium data plotted as the natural logarithm of A_{280} *vs.* the square of the radial distance: ● = αα, and ○ = ·αα·, in $CH_3CN_{8500}TFA_{13}$ (2). Initial concentrations, temperatures, and times for αα (·αα·) were 1.0 (0.87) mg ml^{-1}, 17.2 (19.6)°C and 24 (45 h), respectively. Rotor speed was 18 000 rpm for both.

ton (eqn. 1). Those for ·αα· fall on a slightly curved line that is concave downward. Downward curvature in such a plot indicates non-ideality, whereas heterogeneity in the system will cause upward curvature. Thus, it is possible that the straight line observed for αα results from fortuitous cancellation of the two and that the curved line for ·αα· results from predominance of the former. A straight line fit to the data for ·αα· (eqn. 1) gives an apparent molecular mass of 29 000 dalton and correlation coefficient of 0.9953, whereas a computer fit to eqn. 2 above gives a molecular mass of 41 000 dalton (infinite dilution), second virial coefficient of $4.4 \cdot 10^{-4}$ mol cm^3 g^{-2}, and root mean square (r.m.s.) residual 0.022. Using this second virial coefficient to calculate a corrected molecular mass for the αα sample gives 32 000 dalton.

For comparison we also examined the sedimentation equilibrium behavior of $\alpha^{-}\alpha$ (1.6 mg ml^{-1}; data not shown) in $CH_3CN_{8500}TFA_{13}$ (2). The data were fit using eqn. 2 above which gives molecular mass of 58 000 dalton, second virial coefficient of $28 \cdot 10^{-4}$ mol cm^3 g^{-2}, and r.m.s. residual 0.0155. Although the molecular mass of the cross-linked sample is less than the two-chain value (66 000 dalton), it is distinctly greater than those for the non-cross-linked species, indicating that the non-cross-linked species are highly dissociated in the RP medium.

CONCLUSIONS

We find here that C_4 RP-HPLC is useful as an analytical tool for detecting various non-cross-linked and disulphide-cross-linked dimers formed from the α and β chains of R_sTm, and for quantitating the relative amounts of $\beta^{-}\beta$, $\alpha^{-}\alpha$, and non-cross-linked material in a given sample. The method should be applicable to mixtures of other cross-linked coiled coils as well.

We also find that in the RP elution medium both the cross-linked and non-cross-linked species are highly α-helical, and that the non-cross-linked species are highly dissociated into single-chain α-helices, which, upon addition of salt, reassociate. Although long chain synthetic polypeptide have long been known to form single-chain α-helical structures [39] and short, synthetic amphipathic peptides have more recently been shown to form such structures [31,33,40], to our knowledge this is the first observation of a naturally occurring protein single-chain α-helix.

ACKNOWLEDGEMENTS

M.E.H. was supported in part by Grant No. GM-20064 from the Division of General Medical Sciences, United States Public Health Service and by a grant from Muscular Dystrophy Association. The authors thank Mr. William Clay Bracken for preparing several of the samples; Mr. Walter Nulty of the Biochemistry Department, Washington University School of Medicine for performing the sedimentation equilibrium experiments; and Professor Alfred Holtzer for helpful discussions, particularly concerning treatment of the sedimentation equilibrium data.

REFERENCES

1 C. Cohen and D. A. D. Parry, *Proteins*, 7 (1990) 1–15.
2 P. Cummins and S. Perry, *Biochem. J.*, 133 (1973) 765–777.
3 P. Johnson and L. B. Smillie, *Biochem. Biophys. Res. Commun.*, 64 (1975) 1316–1322.
4 S. Lehrer, *Proc. Natl. Acad. Sci. U.S.A.*, 72 (1975) 3377–3381.
5 E. Eisenberg and W. Kielly, *J. Biol. Chem.*, 249 (1974) 4742–4748.
6 G. Strasburg and M. Greaser, *FEBS Lett.*, 72 (1976) 11–14.
7 A. Mak, L. Smillie and G. Stewart, *J. Biol. Chem.*, 255 (1980) 3647–3655.
8 M. E. Holtzer, A. Holtzer and J. Skolnick, *Macromolecules*, 16 (1983) 173–180.
9 M. E. Holtzer, T. Breiner and A. Holtzer, *Biopolymers*, 23 (1984) 1811–1833.
10 M. E. Holtzer, K. Askins and A. Holtzer, *Biochemistry*, 25 (1986) 1688–1692.
11 M. E. Holtzer, W. C. Bracken and A. Holtzer, *Biopolymers*, 29 (1990) 1045–1056.
12 W. C. Bracken, J. Carey, M. E. Holtzer and A. Holtzer, *Biopolymers*, 27 (1988) 1223–1237.
13 C. T. Mant, N. E. Zhou and R. S. Hodges, *J. Chromatogr.*, 476 (1989) 363–375.
14 A. J. Sadler, R. Micanovic, G. E. Katzenstein, R. V. Lewis and C. R. Middaugh, *J. Chromatogr.*, 317 (1984) 93–101.
15 G. E. Katzenstein, S. A. Vrona, R. J. Wechsler, B. L. Steadman, R. V. Lewis and C. R. Middaugh, *Proc. Natl. Acad. Sci. U.S.A.*, 83 (1986) 4268–4272.
16 S. Y. M. Lau, A. K. Taneja and R. S. Hodges, *J. Chromatogr.*, 317 (1984) 129–140.
17 A. F. Drake, M. A. Fung and C. F. Simpson, *J. Chromatogr.*, 476 (1989) 159–163.
18 M. E. Noelken, *Ph.D. Thesis*, Washington University, St. Louis, MO, 1962.
19 B. F. P. Edwards and B. D. Sykes, *Biochemistry*, 19 (1980) 2577–2583.
20 W. G. Lewis and L. Smillie, *J. Biol. Chem.*, 255 (1980) 6854–6859.
21 M. E. Holtzer, A. Holtzer and D. L. Crimmins, *Biochem. Biophys. Res. Commun.*, 166 (1990) 1279–1283.
22 M. E. Holtzer, W. C. Bracken and A. Holtzer, unpublished results.
23 G. Ellman, *Arch. Biochem. Biophys.*, 82 (1959) 70–77.
24 D. L. Crimmins, D. W. McCourt, R. S. Thoma, M. G. Scott, K. Macke and B. D. Schwartz, *Anal. Biochem.*, 187 (1990) 27–38.
25 D. L. Crimmins, J. Gorka, R. S. Thoma and B. D. Schwartz, *J. Chromatogr.*, 443 (1988) 63–71.
26 D. L. Crimmins, F. S. Thoma, D. W. McCourt and B. D. Schwartz, *Anal. Biochem.*, 176 (1989) 255–260.
27 A. Holtzer, R. Clark and S. Lowey, *Biochemistry*, 4 (1965) 2401–2411.
28 C. M. Kay, *Biochim. Biophys. Acta*, 38 (1960) 420–427.
29 M. D. Pato, A. S. Mak and L. B. Smillie, *J. Biol. Chem.*, 256 (1981) 593–598.
30 M. E. Holtzer and A. Holtzer, *Biopolymers*, 30 (1990) 985–993.

31 R. S. Hodges, P. D. Semchuk, A. K. Taneja, C. M. Kay, J. M. R. Parker and C. T. Mant, *Pept. Res.*, 1 (1988) 19–30.
32 R. S. Hodges, A. K. Saund, P. C. S. Chong, S. A. St.-Pierre and R. E. Reid, *J. Biol. Chem.*, 256 (1981) 1214–1224.
33 S. Y. M. Lau, A. K. Taneja and R. S. Hodges, *J. Biol. Chem.*, 259 (1984) 13253–13261.
34 M. E. Holtzer and A. Holtzer, unpublished results.
35 R. S. Hodges, N. E. Zhou, C. M. Kay and P. D. Semchuk, *Pept. Res.*, 3 (1990) 123–137.
36 T. M. Cooper and R. W. Woody, *Biopolymers*, 30 (1990) 657–676.
37 M. E. Holtzer, A. Holtzer and J. Skolnick, *Macromolecules*, 16 (1983) 462–465.
38 J. Mo, M. E. Holtzer and A. Holtzer, *Biopolymers*, 30 (1990) 921–927.
39 P. M. Doty, J. H. Bradbury and A. Holtzer, *J. Am. Chem. Soc.*, 78 (1956) 947–954.
40 N. E. Zhou, C. T. Mant and R. S. Hodges, *Pept. Res.*, 3 (1990) 8–20.

Journal of Chromatography, 543 (1991) 345–354
Elsevier Science Publishers B.V., Amsterdam

CHROM. 23 165

Chiral copper–chelate complexes alter selectivities in metal affinity protein partitioning

G. E. WUENSCHELL, E. WEN, R. TODD, D. SHNEK and F. H. ARNOLD*
Division of Chemistry and Chemical Engineering, 210-41, California Institute of Technology, Pasadena, CA 91125 (U.S.A.)
(Received December 13th, 1990)

ABSTRACT

Proteins can be distinguished by exploiting complementarity between a histidine's microenvironment and a metal–chelate ligand in metal-affinity separations. The partitioning behavior of three myoglobins was investigated in aqueous two-phase polyethylene glycol–dextran systems containing polyethylene glycol derivatized with Cu(II) complexes of the L- and D-isomers of methionine and aspartate. TSK chromatographic supports derivatized with the methionine complexes were used to study retention of these proteins in metal-affinity chromatography. In the partitioning studies, the amino acid metal chelates exhibit selectivities for the myoglobins that are different from that of Cu(II)-iminodiacetate. Significant differences in selectivity based on the chiral nature of the amino acid complexes were also observed. The chromatographic selectivities of the chelating ligands exhibit little variation, however, suggesting that interactions occurring in solution but not on a surface play an important role in protein binding to the Cu(II)-amino acid–PEG complexes. In solution, the Cu(II)-amino acid complexes are sensitive probes of the microenvironments of surface histidines. The choice of the metal chelate affinity ligand offers a powerful means by which the selectivity of metal-affinity separations can be altered.

INTRODUCTION

The development of cost-effective affinity separations will eventually require that expensive and labile biological affinity ligands be replaced by small chemicals capable of selective binding interactions. Metal-affinity separations, which use chelated metals to bind proteins and other biological materials, afford an excellent example of the advantages of a separation process based on small chemical affinity ligands. Metal chelate ligands are inexpensive and stable; they can be chemically modified and formulated into columns with extremely high loading capacities; they are easy to regenerate and recycle; and product elution is carried under conditions that do not normally harm sensitive biological products. As a result, the applications of metal-affinity separations are rapidly expanding. To be most effective, however, small chemical ligands must exhibit affinities and selectivities for the molecules of interest that are comparable to biological binding interactions. A major drawback of metal-affinity separations for large-scale purification is the limited selectivity that can be achieved with currently-used materials.

0021-9673/91/$03.50

In order to expand the potential applications of metal-affinity techniques in biological separations, we are investigating methods by which the selectivity for a particular protein can be modified and enhanced. Various means for altering selectivity, including engineering metal-binding residues into recombinant proteins, have recently been reviewed [1]. In this paper we demonstrate that significant changes in selectivity in metal-affinity partitioning can be effected through the choice of the metal chelate affinity ligand.

Metal-affinity chromatography with iminodiacetate-bound copper ion [Cu(II) IDA] distinguishes proteins primarily based on their surface histidine content. Proteins with several surface histidines are easily separated from those with no exposed histidines. However, to easily differentiate among proteins bearing similar numbers of exposed histidines, modifications which influence the strength of individual metal–histidine interactions are required. Since Cu(II)IDA is small, hydrophilic, achiral, and bears no net charge, its affinity for histidine is minimally influenced by the protein environment in the vicinity of the histidine. However, this environment is necessarily chiral and will have a particular character imparted to it by the nature of the surrounding amino acid residues. To investigate the feasibility of exploiting the chiral nature and specific properties of the microenvironments of surface histidine residues for protein recognition, we synthesized polyethylene glycol (PEG) derivatives of the L- and D-isomers of aspartic acid and methionine and metallated them with Cu(II) for use in metal-affinity aqueous two-phase partitioning [2]. The L- and D-isomers of methionine were also immobilized onto TSK supports and loaded with Cu(II) in order to determine their binding selectivities in metal-affinity chromatography.

MATERIALS AND METHODS

MPEG-5000 [PEG monomethyl ether, relative molecular mass (M_r)5000] was purchased from Fluka, Dextran T-500 from Pharmacia, epichlorohydrin from Aldrich, and amino acids and proteins from Sigma. Materials were used as purchased, without further purification. TSK G6000PW (15–19 μm porous beads) was the kind gift of Dr. Y Kato, Tosoh. Microchemical analyses were performed at the Caltech Microanalytical Laboratory. Copper contents were determined spectrophotometrically by dissolving the samples in 0.10 *M* EDTA, pH 7, and comparing the absorbance at 800 nm with 0.10 *M* EDTA solutions of known Cu(II) concentration.

Synthesis of Cu(II)IDA–PEG

MPEG-5000 was chlorinated by the procedure of Buckmann *et al.* [3]. Cl-PEG (25.40 g, 5.1 mmols), anhydrous potassium carbonate (3.97 g, 28.7 mmols) and iminodiacetic acid (3.87 g, 29.1 mmols) were dissolved in 225 ml of distilled water and gently refluxed for 53 h. Anhydrous sodium sulfate (37.5 g) was dissolved in the warm reaction mixture, which was transferred to a separatory funnel to cool and separate into two phases. The lower phase, containing most of the inorganic salts and unreacted iminodiacetic acid, was discarded. The upper phase was diluted with an equal volume of distilled water and exhaustively dialyzed, first against dilute bicarbonate, then against distilled water, to remove the low-molecular-weight impurities. The dialyzed solution was lyophilized, giving the product as a white solid. Yield: 23.15 g (89%). IDA–PEG (**1**) and excess copper(II) sulfate pentahydrate were dissolved in

distilled water and exhaustively dialyzed. The dialyzed solution was lyophilized, giving the product as a light blue solid. Yield: 86%. Anal. ($C_{231}H_{459}NO_{117}Cu \cdot 3H_2O$) C, H, N, Cu.

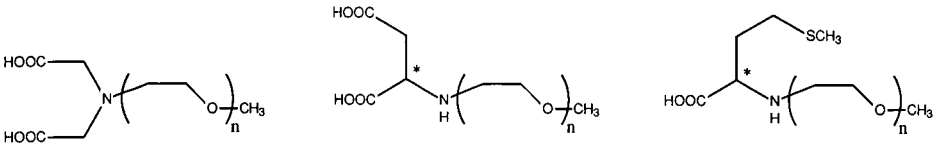

1 2 3

Synthesis of Cu(II)Asp–PEG (L- and D-isomers)

Cl-PEG (5.04 g, 1.00 mmol), L-aspartic acid (0.82 g, 6.2 mmols), and anhydrous potassium carbonate (2.00 g, 14.5 mmols) were dissolved in 45 ml of distilled water and gently refluxed for 67 h. Anhydrous sodium sulfate (3.5 g) was dissolved in the warm reaction mixture, which was transferred to a separatory funnel to cool and separate into two phases. The two phases were treated as described above. Yield (L-isomer): 4.36 g (85%). The same procedure was performed using D-aspartic acid (0.79 g, 6.0 mmols). Yield (D-isomer): 4.38 g (85%). The specific rotation was determined for each product and found to be $-0.454°$ and $+0.453°$ for the L- and D-isomers, respectively (room temperature, 0.07 *M* phosphate, pH 7.0, using the sodium D line).

Asp-PEG (**2**) and excess copper(II) sulfate pentahydrate were dissolved in distilled water and exhaustively dialyzed. The dialyzed solution was lyophilized, giving the product as a light blue solid. Anal. L-isomer: ($C_{231}H_{459}NO_{117}Cu_{0.5} \cdot 2H_2O$) C, H, N, Cu. D-isomer: ($C_{231}H_{459}NO_{117}Cu_{0.5} \cdot 2H_2O$) C, H, N, Cu.

Synthesis of Cu(II)Met–PEG (L- and D-isomers)

Cl-PEG (5.46 g, 1.09 mmols), L-methionine (0.86 g, 5.6 mmols), and anhydrous potassium carbonate (0,84 g, 6.1 mmols) were dissolved in 40 ml of distilled water and gently refluxed for 96 h. Anhydrous sodium sulfate (7.0 g) was dissolved in the warm reaction mixture, which was transferred to a separatory funnel to cool and separate into two phases. The two phases were treated as described above. The dialyzed solution was lyophilized, giving the product as an off-white solid. Yield (L-isomer): 4.36 g (85%). The same procedure was performed using Cl-PEG (5.43 g, 1.08 mmols), D-methionine (0.83 g, 5.8 mmols), and anhydrous potassium carbonate (0.81 g, 5.8 mmols). Yield (D-isomer): 4.84 g (88%). The specific rotations was determined for each product and found to be $+0.315°$ and $-0.336°$ for the L- and D-isomers, respectively (room temperature, 0.07 *M* phosphate, pH 7.0, using the sodium D line).

Met–PEG (**3**) and excess copper(II) sulfate pentahydrate were dissolved in water and exhaustively dialyzed. The dialyzed solution was lyophilized, giving the product as a light blue solid. Anal. L-isomer: ($C_{232}H_{464}NO_{115}SCu_{0.5} \cdot 4H_2O$) C, H, N, Cu. D-isomer: ($C_{232}H_{464}NO_{115}SCu_{0.5} \cdot 4H_2O$) C, H, N, Cu.

Protein partitioning

Aqueous two-phase partitioning experiments were performed as described previously [4]. Two-phase systems were generated by combining appropriate amounts of

stock solutions: (1) 13.54% (w/w) dextran T-500 in distilled water, (2) 0.5 mg/ml protein in 0.046 *M* sodium phosphate, 0.45 *M* sodium chloride, pH 7.6 (3) 40% (w/w) MPEG-5000 in distilled water [used for the determination of the partition coefficient of the protein in the absence of the metal complex (K_0)], and (4) 40% (w/w) MPEG-5000 containing PEG-derivatized Cu(II) chelate to $5.6 \cdot 10^{-3}$% [used for the determination of the protein partition coefficient in the presence of the metal complex (K)]. Each phase system consisted of 1.30 g of the dextran solution (1), 2.00 g of buffered protein solution (2), and 0.70 g of the appropriate PEG solution, (3) or (4). This gave a final 4.00 g phase system composed of 4.4% (w/w) dextran, 1 mg total protein, 7% (w/w) total PEG, and $9.8 \cdot 10^{-4}$% ($1.6 \cdot 10^{-4}$ M) copper, buffered to pH 7.6. The total concentrations of Cu(II) were identical in all partitioning experiments.

The phase systems were gently mixed for 30 min, then centrifuged for 30 min to separate the phases. An aliquot of 200 μl of each phase was diluted to 3.00 ml with distilled water and their absorbances were read at the Soret maximum for the heme proteins (*ca.* 409 nm). The partition coefficient is the ratio of the absorbance derived from the upper phase to the absorbance derived from the lower phase.

Surface histidine contents of the myoglobins were determined from the X-ray crystal structure of sperm whale myoglobin and from the sequences of homologous proteins, as described previously [2]. A histidine was defined as exposed if it exhibited at least 1 Å^2 of surface accessible to a 3 Å radius probe.

Preparation of metal-affinity TSK derivatives

The TSK G6000PW beads were epoxidated using a method similar to that of Matsumoto *et al.* [5]. After extensive washing with distilled water, 9.3 g beads in 9 ml water were combined with 5 ml of 15 *M* NaOH and 6 ml epichlorohydrin, and the mixture was stirred for 2 h at room temperature. The activated beads were washed extensively with water and suction dried before coupling to the chelating agents. For coupling, 3 g of the dried epoxidated beads were added to 6 ml of L- of D-methionine (0.5 *M*, pH 10). An amount of 3.4 g beads were combined with 7 ml iminodiacetic acid (0.5 *M*, pH 11). The three reaction mixtures were shaken at 55°C overnight. (In a separate control experiment, L-methionine showed no tendency towards racemization under these conditions.) The derivatized beads were extensively washed with water.

Metal-affinity chromatography

A 40 × 5 mm column was packed with a quantity of the derivatized beads to give approximately equal total copper loading of 4 μmol for each experiment. The columns were then subjected to the following protocol to determine copper loading and to regenerate the column between experiments (0.4 ml/min flow-rate): 0.1 *M* EDTA, pH 8.0: 10 min; 0.2 *M* $CuSO_4$: 10 min; distilled water: 2 min; 0.05 *M* sodium phosphate, 0.5 *M* NaCl, 0.02 *M* imidazole, pH 7.6: 10 min; 0.05 *M* sodium phosphate, 0.5 *M* NaCl, pH 7.6: 10 min.

The amount of copper loaded onto each column was determined by washing with 0.1 *M* EDTA, pH 7.0, and comparing the absorbance at 800 nm with standard copper solutions. The columns were loaded with approximately 100 μg ($5 \cdot 10^{-9}$ mol) protein, folowed by an imidazole gradient at a flow-rate of 0.2 ml/min. The experiments were repeated with samples of mixed proteins to ensure that the correct elution order was maintained.

RESULTS AND DISCUSSION

Protein recognition by copper chelates can be readily investigated through the measurement of partition coefficients in aqueous dextran–PEG two-phase systems containing metal chelate covalently bound to PEG. Histidines exposed on protein surfaces are available for interaction with chelated copper at neutral and alkaline pH. Since the side chains of other amino acids bind copper with much less affinity (see discussion below), metal-affinity partitioning with Cu^{2+} chelated by IDA at neutral pH reflects the protein's surface histidine content. The addition of Cu(II)IDA–PEG to a two-phase PEG–dextran of PEG–salt system increases the partitioning of proteins which contain surface histidines, and the increase in the logarithm of the partition coefficient in the presence of the the metal-affinity ligand, $\ln(K/K_0)$, is linearly proportional to the number of histidines exposed on the protein surface over a very wide range [2]. This behavior is expected when surface histidines bind equally and independently to the metal complex [4]. Similar behavior is observed in metal-affinity chromatography; proteins are eluted from Cu(II)IDA supports according to their surface histidine contents [6].

The partitioning of three myoglobins from horse, whale, and sheep were studied using copper complexes of IDA–PEG and chiral aspartate and methionine derivatives of PEG. The results are summarized in Table I. The contribution to partitioning that is due to interactions between the protein and the metal-affinity ligand is indicated by $\ln(K/K_0)$, the difference between the logarithms of the partition coefficient in the presence (K) and absence (K_0) of affinity ligand [4,7]. As observed in earlier studies, the metal-affinity partitioning of horse myoglobin to the PEG phase with Cu(II)IDA–PEG is less favorable [as measured by $\ln(K/K_0)$] than the partitioning of whale or sheep myoglobin.

The relative affinities of these proteins for the PEG-rich phase are dramatically

TABLE I

MYOGLOBIN PARTITION COEFFICIENTS IN PEG–DEXTRAN TWO-PHASE SYSTEMS CONTAINING PEG-DERIVATIZED Cu(II) CHELATES

K_0 = partition coefficient in the absence of PEG–copper chelate, K = partition coefficient in the presence of PEG–copper chelate. Each partition coefficient is an average of at least five measurements, with a standard deviation of approximately 3% of the mean. Mb = Myoglobin.

	Derivative	Horse Mb	Whale Mb	Sheep Mb
K_0		0.39	0.47	0.38
K	IDA	0.75	0.97	1.10
	L-Asp	0.53	0.60	0.52
	D-Asp	0.54	0.53	0.50
	L-Met	0.73	0.55	0.73
	D-Met	0.49	0.53	0.49
$\ln(K/K_0)$	IDA	0.66	0.73	1.07
	L-Asp	0.32	0.25	0.32
	D-Asp	0.33	0.13	0.28
	L-Met	0.64	0.17	0.66
	D-Met	0.24	0.12	0.27

altered when the chiral metal-chelating polymers derived from aspartic acid and methionine are used. $\text{Ln}(K/K_0)$ for whale myoglobin is the least favorable of the three proteins in all four two-phase systems containing the amino acid-copper–PEG complexes. This is particularly striking for partitioning with the methionine-derivatized PEG; the apparent affinity of both optical isomers of Cu(II)Met–PEG towards whale myoglobin is approximately equivalent to (Cu(II)IDA–PEG binding to a protein possessing only one exposed histidine as opposed to five. In contrast, the apparent affinity of the Cu(II)-L-Met–PEG complex towards the myoglobins from horse and sheep in only slightly smaller than that of Cu(II)IDA–PEG. Furthermore, there is a distinct chiral effect in the protein partitioning; partitioning with complexes derived from L-isomers of the amino acids results in $\ln(K/K_0)$ values significantly different from those obtained using the D-isomers. For the methionine-based complexes, this chiral effect is most significant for the myoglobins from horse and sheep.

To determined whether the altered selectivities observed for metal-affinity partitioning also occur in metal-affinity chromatography, a TSK chromatographic support was derivatized with Cu(II)IDA, Cu(II)-L-Met, and Cu(II)-D-Met. The concentrations of imidazole required to elute the three myoglobins from these supports are reported in Table II. For these experiments, the column lengths were adjusted to maintain similar copper loadings. On all three Cu(II)-chelating supports, the whale protein requires a greater concentration of imidazole for elution than do the horse and sheep proteins. Since the elution order remains the same for the myoglobins on all three supports, there are no significant differences in binding selectivity for the copper chelates in the solid phase. If anything, the selectivity of Cu(II)-methionine is reduced with respect to Cu(II)IDA; the horse and sheep myoglobins are indistinguishable on both methionine-based supports. The fact that the myoglobins require smaller concentrations of imidazole for elution from the L- and D-methionine supports as compared to Cu(II)IDA probably reflects the lower Cu(II)-binding affinity of methionine. Cu(II) is more easily removed from these columns than from the IDA-derivatized material.

Imidazole competes with binding sites on the protein for coordination to the bound copper ion. Elution with a gradient of imidazole at pH 7.6 allows us to identify the relative binding affinities based on interactions between the copper chelates and

TABLE II

COLUMN CHARACTERISTICS AND CONCENTRATIONS OF IMIDAZOLE REQUIRED TO ELUTE MYOGLOBINS FROM TSK METAL-AFFINITY COLUMNS

Column diameter is 0.5 cm, flow-rate = 0.2 ml/min.

Chelating ligand	Column volume (ml)	Copper loading (μmol)	Concentration of imidazole at elution (mM)		
			Horse	Sheep	Whale
IDA[a]	0.63	4.2	7.3	8.5	9.3
L-Met[b]	0.51	3.6	4.9	4.9	6.4
D-Met[b]	0.78	3.7	5.3	5.3	6.1

[a] Gradient: 0–10 mM imidazole in 150 min, pH 7.6.
[b] Gradient: 2–8 mM imidazole in 100 min, pH 7.6.

surface histidine residues. Direct binding by chelated Cu(II) to other functional groups such as the N-terminus or lysine residues are small because these groups are still largely protonated at this pH. Copper coordination to carboxylic acid moieties is weak relative to histidine [8]. There is no evidence that copper directly coordinates aromatic side chains; the apparent influence of aromatic residues in metal-affinity chromatography is due to indirect effects on solvation and metal electronegativity [1,9]. Thus it is unlikely that direct binding interactions with residues other than histidine are contributing to the observed altered selectivity order in metal-affinity partitioning. While Cu(II)IDA appears to bind all accessible histidines with more-or-less equal affinity [4], the altered selectivities of Cu(II)-L-Met and Cu(II)-D-Met most likely reflect the effects of neighboring amino acid residues on Cu(II)-histidine binding. However, these interactions manifest themselves only in solution, not upon interaction with the surface-immobilized chelates.

Possible origins of the differences in binding selectivity observed for the various Cu(II) chelates in metal-affinity partitioning must be discussed in light of the structures of the protein-chelate complexes. Cu(II) and IDA form a 1:1 (metal–ligand) complex, whereas most amino acids form a 1:2 (bis-glycinate-like) complex in solution [10,11] (Fig. 1). When the derivatized PEGs are metallated with excess Cu(II), followed by exhaustive dialysis to remove unbound metal, the free, dialyzable Cu(II) becomes negligible as the Cu(II)–(IDA–PEG) ratio approaches 1:1. In contrast, significant quantities of free copper are present until the Cu(II)–(Asp–PEG) and Cu(II)–(Met–PEG) ratios approach 1:2. This indicates that the stability constants [13] and structures of the soluble PEG-derivatized chelates are similar to those of their underivatized counterparts. 1:2 Cu(II)–amino acid complexes cannot form on the TSK surface because all the amino acids are covalently attached, and the distance between ligands (>40 Å) is much greater, on average, than the length of epoxide spacer arm and Cu(II)Met ligand (7.5 Å).

We expect a surface histidine to coordinate Cu(II)IDA equatorially in a 1:1 complex, similar to the coordination seen in the crystal structure of Cu(II)IDA–bipyridine [14]. Although two equatorial sites are available for histidine coordination,

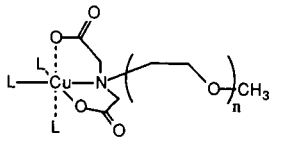

Cu(II)IDA-PEG

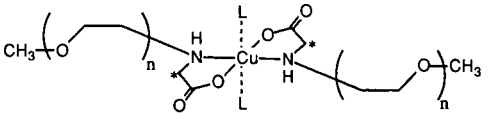

Cu(II)bis-(amino-acid)-PEG

Fig. 1. Expected structures of Cu(II)IDA–PEG and Cu(II)bis(amino acid–PEG) complexes. Structures are assumed to be analogous to those of Cu(II)iminodiacetate dihydrate [10] and bis(L-methionato)Cu(II) [11,12]. "L" indicates sites available for ligand binding (protein or solvent). * = Stereogenic center.

protein complexation with Cu(II)IDA–PEG is sterically limited to single histidine residues, unless multiple histidines are arranged according to precise geometric requirements, such as the His-X_3-His arrangement in an α-helix [15,16]. Thus, in solution, the protein can associate with as many Cu(II)IDA–PEG molecules as there are accessible histidines. This simple binding behavior leads to the linear dependence of $\ln(K/K_0)$ on surface histidine content.

The nature of complex formation between a histidine residue and a Cu(II)bis-glycinate-like amino acid complex is less clear. A histidine could coordinate to the weak axial site of the bis-complex. Such binding would be weaker than to a Cu(II) IDA complex, a result of both the weaker nature of the axial bond and the greater steric hindrance from the bisamino acid complex, which depends on the histidine microenvironment. However, this weaker binding may not necessarily be apparent in the partitioning, since two PEG molecules associated at a single histidyl site could offset the negative effects of the reduced affinity on partitioning. Alternatively, the histidine could displace one amino acid to take up a more strongly-bound equatorial position, yielding a 1:1 Cu(II)chelate–histidine complex similar to that expected for Cu(II)IDA. Cu(II) complexes of amino acids (1:1 mixed) are known: the crystal structure of Cu(II)aspartic acid–phenanthroline is similar to that of the Cu(II)IDA–bipyridine complex cited above [17]. However, a complex of this type, which can form on the solid support as well as in solution, cannot explain the difference between partitioning and chromatography.

The complexes derived from the L- and D-isomers of aspartic acid exhibit similar affinities for the different myoglobins in partitioning, although the affinity for whale myoglobin is somewhat reduced. Aspartic acid is isomeric with IDA and, if a 1:1 Cu(II)aspartate–histidine complex is formed, it would be expected to have properties very similar to those of the IDA complex and should exhibit little tendency to be influenced by the protein environment in the vicinity of the histidine. The properties of the methionine-derived complexes should be quite different from those derived from aspartic acid. These complexes bear a greater positive charge than do their aspartate-derived counterparts, and the methyl thioether side chain confers both steric bulk and a greater hydrophobic character to the complex. Both forms of the Cu(II) Met–PEG have low apparent affinity for whale myoglobin in metal-affinity partitioning.

Although the structures of myoglobins from horse, whale, and sheep are highly conserved [18], they differ slightly in the content and placement of surface histidine residues. Horse, whale and sheep myoglobin share five histidines that are accessible to solvent (amino acid positions 36, 48, 81, 113 and 116). The whale and sheep proteins each have one additional surface histidine. Histidines 113 and 116 in all three myoglobins are separated by a very short distance, and it appears that only one Cu(II)IDA–PEG can bind at this position [2]. As discussed previously [16], there is no evidence that the His 113–His 116 arrangement forms a special high-affinity binding site for Cu(II). Myoglobin partitioning with Cu(II)IDA is fully explained by binding interactions with non-interacting histidines [4].

Using protein sequence data for horse, sheep and whale myoglobins [7], and crystallographic data for sperm whale myoglobin [19,20], the surface environments within 6 Å of the exposed histidines were compared. The amino acid residues within this radius are 100% conserved for three of the exposed histidines (His 36, 48, and 81)

in horse and sheep myoglobin. In contrast, the environment is 100% conserved for only one of the surface histidine residues in whale myoglobin (His 81). In two of four of the surface histidine environments which differ from those of the sheep and horse proteins (His 36 and 48), the whale myoglobin either has an additional positive charge in the vicinity (a lysine residue), or lysine has been substituted by a larger, positively-charged arginine. The effect of these substitutions may be to move a positive charge closer to, or add an additional charge in the vicinity of, the potential histidine binding sites. The reduction in affinity for whale myoglobin is much more pronounced for the more positively charged Cu(II)methionine complexes than for the Cu(II) aspartate ones. The increase in positive charge near the histidine residues in the whale myoglobin could effectively reduce the number of histidines available for complexation to Cu(II)Met–PEG.

Cu(II)-L-Met–PEG has a higher apparent affinity for the horse and sheep myoglobins than does the complex derived from D-methionine in the partitioning experiments. The protein environment surrounding a histidine is chiral, and it is certainly feasible that these surroundings can differentiate between copper chelate complexes that differ in their chirality. [The effective size of the chelate that is available for interactions with the protein surface and, therefore, the distinction between the D- and L-forms are enhanced if the protein is binding a 1:2 copper–(amino acid–PEG) complex.] However, at this point we are unable to identify specific structural origins for the differences in the abilities of the complexes derived from the D- and L-amino acids to bind to exposed histidines. Further work will be necessary to explain the observed chiral selectivity.

We have shown that selectivities in protein binding by copper chelate complexes can differ significantly from solution to solid phase. A possible explanation for this behavior is that, in solution, the amino acid chelates form larger 1:2 copper–chelate complexes which are capable of discriminating among histidines on the surface of the myoglobins. Cu(II)Met–PEG and Cu(II)Asp–PEG complexes are sensitive probes of the microenvironments of surface histidines in metal-affinity partitioning.

ACKNOWLEDGEMENTS

This research is supported by the National Science Foundation, Grant No. EET-8807351, and a NSF Presidential Young Investigator Award. F.H.A. is the recipient of a David and Lucile Packard Foundation Fellowship. E.W. is the recipient of a Caltech Summer Undergraduate Research Fellowship. R.T. acknowledges the support of a predoctoral training fellowship in biotechnology from the National Institute of General Medical Sciences, NRSA 1 T32 GM 08346-01, Pharmacology Sciences Program.

REFERENCES

1 F. H. Arnold, *Bio/Technology*, 9 (1991) 151.
2 G. E. Wuenschell, E. Naranjo and F. H. Arnold, *Bioprocess Eng.*, 5 (1990) 199.
3 A. F. Buckmann, M. Morr and M.-R. Kula, *Biotechnol. Appl. Biochem.*, 9 (1987) 258.
4 S.-S. Suh and F. H. Arnold, *Biotechnol. Bioeng.*, 35 (1990) 682.
5 Matsumoto, I., Y. Ito and N. Seno, *J. Chromatogr.*, 239 (1982) 747.
6 E.S. Hemdan, Y. Zhao, E. Sulkowski and J. Porath, *Proc. Natl. Acad. Sci., U.S.A.*, 86 (1989) 1811.

7 A. Cordes, J. Flossdorf and M.-R. Kula, *Biotechnol. Bioeng*, 30 (1987) 514.
8 A. E. Martell and R. M. Smith, *Critical Stability Constants*, Vol. 3, Plenum, New York, 1977.
9 E. J. Leporati, *Chem. Soc., Dalton Trans.*, (1986) 199.
10 A. Podder, J. K. Dattagupta and N. N. Saha, *Acta Cryst.*, B35 (1979) 53.
11 M. V. Veidis and G. J. Palenik, *J. Chem. Soc., Chem. Commun.*, (1969) 1277.
12 C.C. Ou, D. A. Powers, J. A. Thich, T. R. Felthouse, D. N. Hendrickson, J. A. Potenza and H. J. Schugar, *Inorg. Chem.*, 17 (1978) 34.
13 A. E. Martell and R. M. Smith, *Critical Stability Constants*, Vol. 1, Plenum, New York, 1974.
14 G. Nardin, L. Randaccio, R. P. Bonomo and E. Rizzarelli, *J. Chem. Soc. Dalton Trans.*, (1980) 369.
15 R. Todd, M. Van Dam, D. Casimiro, B. L. Haymore and F. H. Arnold, *Proteins: Struct. Funct. Genet.*, (1991) in press.
16 S.-S. Suh, B. L. Haymore and F. H. Arnold, *Protein Engineering*, 4 (1991) 301.
17 L. Antolini, L. P. Battaglia, A. Bonamartini Corradi, C. Marcotrigiano, L. Menabue, G. C. Pellacani, M. Saladini and M. Sola, *Inorg. Chem.*, 25 (1986) 2901.
18 M. O. Dayhoff (Editor) *Atlas of Protein Sequence and Structure*, Vol. 5, Supplement 2, National Biomedical Research Foundation, Washington, D.C., 1972, pp. 206–208.
19 T. Takano, *J. Mol. Biol.*, 110 (1977) 537.
20 T. Takano, *J. Mol. Biol.*, 110 (1977) 569.

Journal of Chromatography, 543 (1991) 355–366
Elsevier Science Publishers B.V., Amsterdam

CHROM. 23 132

Chromatographic separation of the optical isomers of naproxen

JOHN R. KERN

Analytical and Environmental Research Laboratory, Syntex Research, 3401 Hillview Ave., Palo Alto, CA 94304 (U.S.A.)

(First received September 19th, 1990; revised manuscript received January 22nd, 1991)

ABSTRACT

Naproxen, (*S*)-6-methoxy-α-methyl-2-naphthyleneacetic acid, is a non-steroidal anti-inflammatory drug, which is administered as a single enantiomer. Two different approaches applying high-performance liquid chromatography for the determination of the optical purity of naproxen are described. One method involves the derivatization of naproxen with 3,5-dinitroaniline and separation of the amide derivatives on a (*R*)-N-(2-naphthyl)alanine chiral stationary phase. The second method is a direct separation of naproxen optical isomers using α-1-acid glycoprotein columns. The latter method has been studied in detail to address the effects of temperature, ionic strength, pH and concentration of mobile phase buffer on enantiomeric resolution.

INTRODUCTION

The use of high-performance liquid chromatography (HPLC) for the determination of the optical purity of chiral substances is now a well developed analytical technique. The past 15 years have given rise to a profusion of new analytical developments such as chiral stationary phases (CSPs), derivatizing reagents, and chiral mobile phase additives, all of which have been proven effective in achieving chiral separation.

Four major approaches involving the separation of optical isomers by HPLC are: (1) direct separation on a CSP, (2) derivatization with an achiral reagent and separation on a CSP, (3) direct separation on an achiral stationary phase with the use of a chiral mobile phase additive, and (4) derivatization with a chiral reagent and separation of the resulting diastereomers using an achiral support. Similar techniques for the determination of optical purity by gas chromatography (GC) have also been reported.

Many of the separation types described above have been successfully applied to separate the optical isomers of the α-methylarylacetic acid series of non-steroidal anti-inflammatory drugs (NSAIDs), such as naproxen and ibuprofen. The majority of NSAIDs have one chiral center α to the carboxylic acid moiety, and most NSAIDs in this category are administered as the racemic mixture, with the exception of naproxen, which is administered as the resolved (*S*) enantiomer.

0021-9673/91/$03.50

The majority of enantiomeric resolutions of NSAIDs reported in the literature are achieved by formation of diastereomeric derivatives with an optically active reagent and subsequent separation using either gas chromatography (GC) or HPLC. Separation via the diastereomeric amide derivatives is by far the most applied method. Of all the applicable chiral amines used as derivatizing reagents, α-methylbenzylamine has been the most widely published in conjunction with GC [1–6] or HPLC [7–10] analysis. The use of a number of other chiral amines e.g. L-1-(4-dimethylamino-1-naphthyl)ethylamine (DANE) and L-leucinamide in such applications has also been extensively reported [11–32] and, in many cases, these diastereomeric separations are preferred to the direct resolution on chiral columns. Other reported diastereomeric separations of the optical isomers of NSAIDs have included ester derivatives [9,33].

Derivatization of NSAIDs with various achiral amines combined with separation on CSPs has been applied to effect chiral separations of NSAIDs on numerous occasions [34–41]. The majority of these separations have been accomplished on "Pirkle-type" CSPs [34,35,37–41]. Other CSPs used have included cellulose based CSPs [39] and a CSP which contained either (*R*)- or (*S*)-1-(α-naphthyl)ethylamine with (*S*)-valine chemically bonded to γ-aminopropyl silanized silica [36]. Chiral separations of ester derivatives of NSAIDs have also been reported [34,42] using the Pirkle-type CSPs.

Protein based CSPs offered direct chiral separations of NSAIDs [43,44] while ion-pair chromatography employing chiral amine counter-ions on an achiral support [45,46] failed to facilitate enantiomeric resolution of naproxen. Nonetheless, a CSP that contains acetylquinine bonded to silica has been reported to separate the optical isomers of naproxen with the addition of quinine in the mobile phase [47,48].

Mixed advantages and disadvantages may be identified with the methods reported to date, therefore, method development was continued in order to develop a rugged chiral separation method for naproxen with good sensitivity and high efficiency. An important criterion is that this method can be easily adopted in a quality control environment. Two suitable methods considered to be most rugged are reported in this manuscript.

EXPERIMENTAL

Apparatus

The HPLC equipment consisted of a Spectra-Physics Model 8100 liquid chromatograph equipped with a Valco fixed-loop injector and a Kratos 757 UV detector. The detector output was monitored using a Spectra-Physics SP 4200 recording integrator.

Materials

Naproxen, its enantiomer and the racemic mixture were synthesized by the Institute of Organic Chemistry, Syntex Research (Palo Alto, CA, U.S.A.). 3,5-Dinitroaniline (98% +) and N,N-dimethyloctylamine were obtained from Aldrich (Milwaukee, WI, U.S.A.). Thionyl chloride was obtained from J. T. Baker (Phillipsburgh, NJ. U.S.A.). HPLC-grade hexane, isopropanol, acetonitrile and methanol were obtained from Burdick and Jackson (Muskegon, MI, U.S.A.). NaH_2PO_4, Na_2HPO_4,

and NaCl were obtained from Mallinckrodt (Paris, KY, U.S.A.). Doubly distilled deionized water was used throughout the experiments.

Chiral HPLC columns

The chiral HPLC columns used were: (1) Pirkle covalent (*R*)-N-(3,5-dinitrobenzoyl)phenylglycine (Regis, Morton Grove, IL, U.S.A.); (2) Pirkle covalent (*R*)-N-(2-naphthyl)alanine (Regis); (3) Cyclobond β-cyclodextrin (Astec, Whippany, NJ, U.S.A.); (4) Resolvosil bovine serum albumin (Macherey-Nagel, Düren, Germany); (5) Enantiopak α_1-acid glycoprotein (AGP) (LKB, Bromma, Sweden); (6) Chiral AGP (ChromTech, Stockholm, Sweden); (7) Chiralpak OT(+) (J. T. Baker); (8) Chiralcel OB (J. T. Baker); (9) Chiralcel OD (J. T. Baker); (10) Chiralcel OJ (J. T. Baker); (11) Chiralcel CA-1 (J. T. Baker).

Derivatization procedure

The 3,5-dinitroanilide derivative of naproxen was prepared by converting the acid functionality of naproxen into the acid chloride with thionyl chloride followed by the addition of excess 3,5-dinitroaniline.

Naproxen acid chloride: naproxen (0.05 g, 0.22 mmol) was gently refluxed in 5.0 ml of freshly distilled thionyl chloride for 5 min. The excess thionyl chloride was then removed, *in vacuo*, to give a viscous yellow oil.

Naproxen 3,5-dinitroanilide: the acid chloride of naproxen was diluted with 5.0 ml of dry dichloromethane and (0.037 g, 0.24 mmol) of 3,5-dinitroaniline was added.

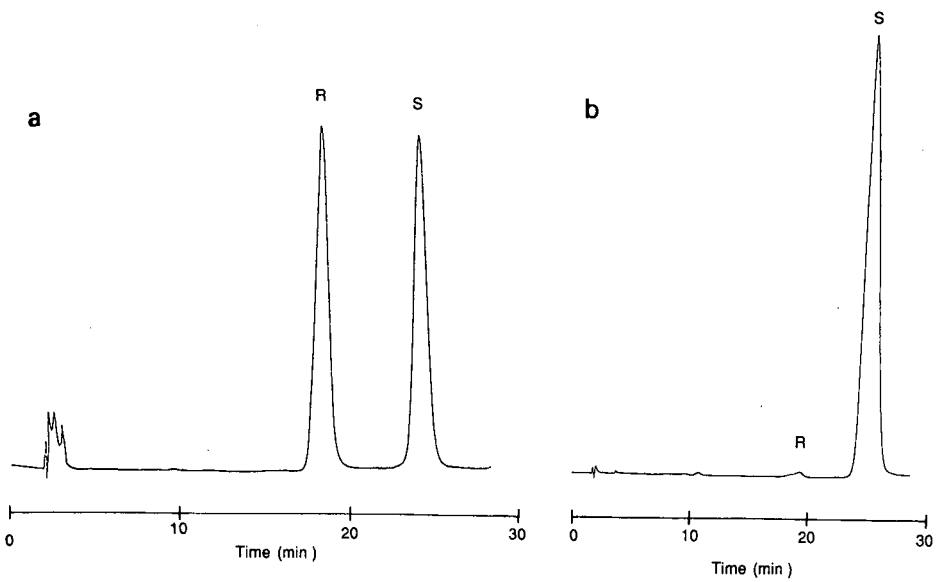

Fig. 1 (a). Chromatographic separation of the 3,5-dinitroanilide derivatives of *R,S*-naproxen on the (*R*)-N-(2-naphthyl)alanine CSP. Mobile phase: hexane–isopropanol (90:10). Flow-rate: 2.0 ml/min. UV detection at 254 nm. Temperature: ambient. (b) Chromatographic separation of the 3,5-dinitroanilide derivative of *S*-naproxen containing *ca.* 1.0% *R*-naproxen on the (*R*)-N-2-(naphthyl)alanine CSP. Chromatographic conditions same as in Fig. 1a.

The reaction mixture was stirred at room temperature for 10 min. A 1.0 ml aliquot of the reaction mixture was diluted to 50 ml with mobile phase and injected onto the HPLC system.

Chromatography

Naproxen 3,5-dinitroanilide: the separation of the 3,5-dinitroanilide of naproxen was accomplished using a Pirkle covalent (*R*)-N-(2-naphthyl)alanine (250 × 4.6 mm I.D.) HPLC column (Fig. 1). The mobile phase was hexane–isopropanol (90:10, v/v) and the flow-rate was 2.0 ml/min. The column eluent was monitored at 263 nm and the chromatography was accomplished under ambient temperature conditions. Sample concentrations were approximately 0.2 mg/ml and the injection volume was 20 μl.

Naproxen: the direct separation of naproxen isomers was accomplished using the Enantiopak AGP (100 × 4.6 mm I.D.) column or a second generation, Chiral AGP (100 × 4 mm I.D.) column. Mobile phases consisted of phosphate buffers at different pHs and ionic strengths with isopropanol as the organic modifier. Flow-rates were maintained between 0.3 and 0.8 ml/min. The eluent was monitored at 263 nm and column temperature was maintained in the range of 5 to 40°C using water-jacket thermostated control. Sample concentrations were approximately 0.05 mg/ml and the injection volume was 20 μl.

RESULTS AND DISCUSSION

Initial reports in the literature on the use of CSPs for the separation of the optical isomers of naproxen and other NSAIDs involved formation of amide derivatives followed by separation on a CSP. Wainer and Doyle [34] resolved the optical isomers of naproxen (separation factor, $\alpha = 1.23$) and other NSAIDs as the 1-naphthylenemethylamide derivatives using the Pirkle covalent (*R*)-N-3,5-(dinitrobenzoyl)phenylglycine (DNBPG) CSP. Nicoll-Griffith [38] reported the resolution of twelve amide derivatives of ibuprofen using the DNBPG CSP, and McDaniel and Snider [39] compared the Pirkle 3,5-DNBPG column and the chiralcel OC (cellulose triphenylcarbamate coated on macroporous silica) column for the separation of amide derivatives of ibuprofen and two other α-methylarylacetic acids.

Pirkle [37] recently introduced a new CSP, covalent (*R*)-N-(2-naphthyl)alanine and reported numerous separations of 3,5-dinitrophenyl derivatives of alcohols, amines and acids (ibuprofen, $\alpha = 1.33$). Encouraged by the results obtained by Pirkle, the 3,5-dinitroanilide of *R,S*-naproxen was prepared and chromatographed using the (*R*)-N-(2-naphthyl)alanine CSP. Baseline resolution, $\alpha = 1.34$ was achieved using the conditions described in Fig. 1a. The resolution between the naproxen isomer peaks could be improved by decreasing the amount of the organic modifier, isopropanol, but, at the same time, the isomer peaks broadened, making quantitation of the minor *R*-isomer more difficult. It was determined by derivatizing and chromatographing each individual isomer of naproxen that the elution order was the *R*-isomer first (retention time, $t_R = 18$ min) and the *S*-isomer second ($t_R = 24$ min).

The precision of this method was addressed by performing six replicate injections of the same reaction product of a sample of *S*-naproxen containing 1% of *R*-naproxen (Fig. 1b). The ratios of the two isomer peaks gave a standard deviation of

0.1%, demonstrating the chromatographic method to be precise and repeatable. The detection limit was determined to be ca. 0.1%.

Direct resolution of the optical isomers of naproxen and other NSAIDs was reported using the Enantiopak AGP CSP [45,46], wherein the enantioselectivity of strong acids such as naproxen was regulated by the addition of a tertiary amine, N,N-dimethyloctylamine (DMOA) to the mobile phase. In this laboratory, the baseline separation (α = 1.25) of naproxen isomers with the Enantiopak column could only be achieved upon addition of DMOA to the mobile phase. An example of the best separation achieved with this column is illustrated in Fig. 2. However, the long retention times of up to 65 min, broad peaks and generally poor peak shape encountered with the Enantiopak CSP prohibited the quantitation of small (<1.0%) amounts of the *R*-naproxen present in *S*-naproxen. Column to column variability was observed with the Enantiopak CSP and, in many cases severe peak fronting was observed for the Enantiopak CSP.

The difficulties experienced with the Enantiopak CSP were not observed when using a "second generation" AGP CSP, the Chiral AGP column. This CSP has been reported to give superior results [49], for a series of chiral dihydropyridine compounds as compared to the Enantiopak column and, appears to be more durable as well.

The chromatographic conditions for the resolution of the optical isomers of naproxen with the Chiral AGP were optimized by changing mobile phase conditions such as pH, buffer strength, temperature and ionic strength. The optimal conditions as shown in Fig. 3a and b allowed for the baseline resolution (α = 1.71) of the naproxen optical isomers in less than five minutes! The *R*-isomer was determined to elute first and the *S*-isomer second. As can be seen in Fig. 3a and b, the peak shapes are much improved from those obtained on the Enantiopak column (Fig. 2). In addition, quantitation of small amounts (<1%) of *R*-naproxen was more feasible with the Chiral AGP column than with the Enantiopak column.

The effects of pH, temperature, ionic strength, buffer strength and organic modifier on retention times and resolution of the naproxen enantiomers were studied using the Chiral AGP column.

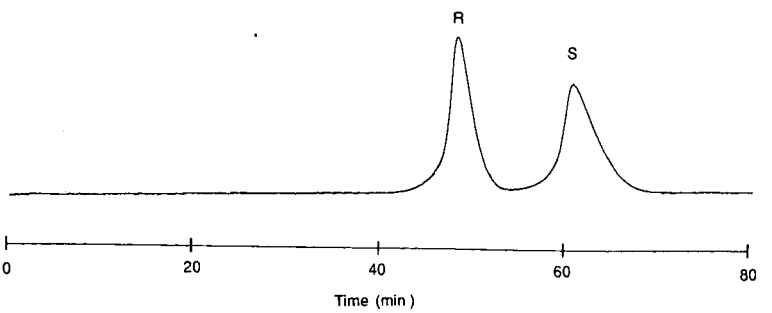

Fig. 2. Direct chromatographic separation of the optical isomers of naproxen on the Enantiopak AGP CSP. Mobile phase: 20 m*M* phosphate buffer with 8 m*M* DMOA at pH 7.0–isopropanol (99:1). Flow-rate: 0.3 ml/min. UV detection at 263 nm. Temperature: ambient. Sample loading: 1.0 μg.

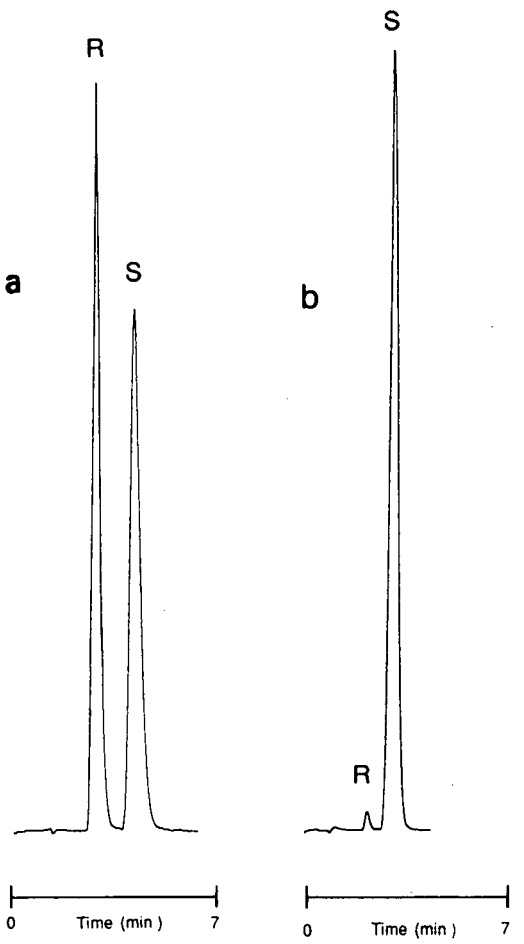

Fig. 3 (a). Direct chromatographic separation of the optical isomers of naproxen on the Chiral AGP CSP. Mobile phase: 4 m*M* phosphate buffer, pH 7.0–isopropanol (99.5:0.5). Flow-rate: 0.8 ml/min. UV detection at 263 nm. Temperature: ambient. Sample loading 1.0 μg. (b) Chromatographic separation of *S*-naproxen containing 1.5% *R*-naproxen on the Chiral AGP CSP. Chromatographic conditions as in (a).

Effect of buffer concentration

The effects of buffer strength were studied at pH 7.0 using six phosphate buffer concentrations ranging from 40 to 1 m*M*. All the mobile phases contained 0.5% isopropanol as the organic modifier. At higher buffer strengths, capacity factors (k') were increased, peak shape was broadened and α-values increased. The data are depicted in Fig. 4a and b. In general, the retention behavior of the *S*-isomer was slightly more sensitive than that of the *R*-isomer to changes in the buffer concentration.

Effect of pH and ionic strength

The effect of mobile phase pH was studied in the range between 5.0 and 7.5 while maintaining a 4.0 m*M* phosphate buffer concentration in a buffer–isopropanol

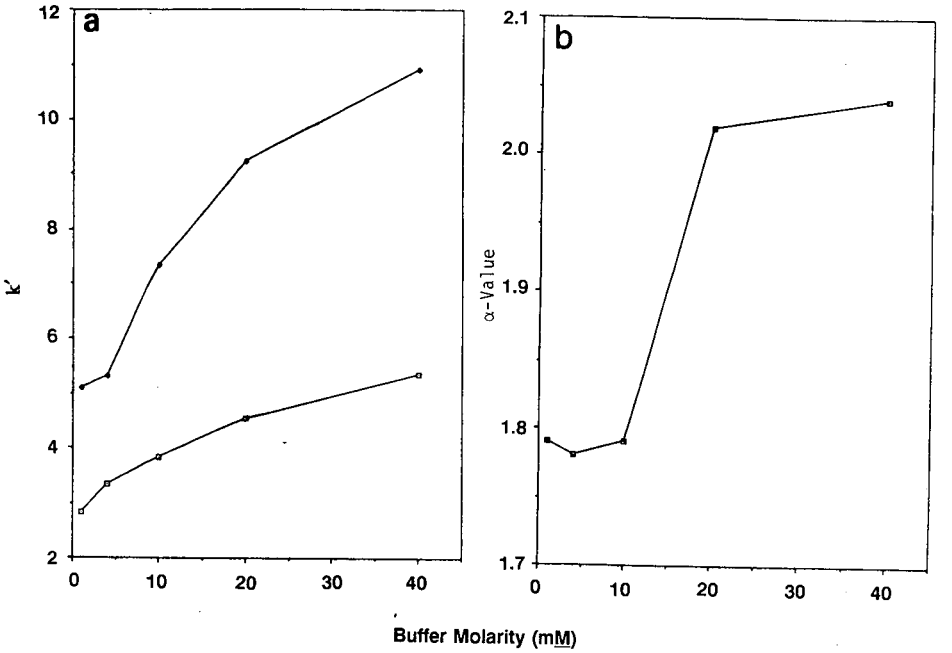

Fig. 4. Effect of buffer concentration on (a) k': □ = *R*-isomer, ◆ = *S*-isomer; and (b) resolution of *R*- and *S*-naproxen. Chromatographic conditions as in Fig. 3a, except buffer concentrations.

(99.5:0.5, v/v) composition. In addition, at each pH value studied, 10 m*M* NaCl was added to the mobile phase to evaluate the effect of ionic strength at the respective pH values. The results as shown in Fig. 5 indicate increased resolution with decreasing pH. Retention times for the *S*-isomer ranged from 5.7 min at pH 7.5 to greater than 3 h at pH 5.0. However, no apparent effect was observed when 10 m*M* NaCl was present in the mobile phase. Baseline resolution between the enantiomers was achieved throughout the 5.0 to 7.5 pH range.

Effect of temperature

The chromatography was evaluated at temperatures from 5 to 40°C. The HPLC conditions and mobile phase are those described in Fig. 3. As expected, the resolution increased at the expense of lengthened retention times as well as broadened peak shape when the column temperature was decreased. However, no significant column degradation was observed upon operation at higher temperatures. The retention time of the *S*-isomer, which was the longer retained enantiomer, was significantly increased at temperatures below 20°C. In the 20–25°C range, the chromatography was not effected by slight changes in temperature. These data are depicted in Fig. 6.

Effect of organic modifier

Evaluation of the retention characteristics of the enantiomers as a function of the amount of isopropanol in the mobile phase established that the AGP CSP, in addition to chiral recognition, appeared to operate in a reversed-phase mode as well (*i.e.*, the retention times decreased in response to increased levels of isopropanol).

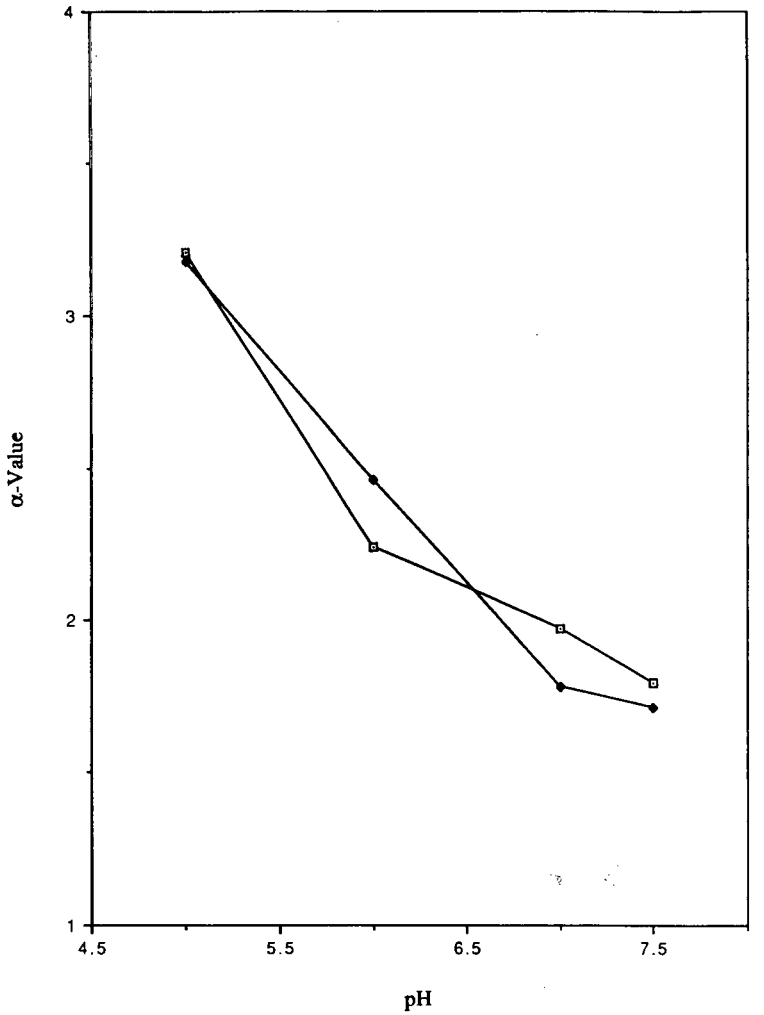

Fig. 5. Effect of pH and ionic strength on resolution of *R*- and *S*-naproxen. Chromatographic conditions as in Fig. 3a, except pH and NaCl concentration. □ = 10 m*M* NaCl; ◆ = no NaCl.

While isopropanol acted as an effective regulator of retention times, resolution of enantiomers could be manipulated by varying the isopropanol content in that the longer retained *S*-isomer showed more response in its retention time towards the organic modifier. Specifically, a total loss of resolution between the naproxen enantiomers was observed by increasing the isopropanol content to amounts greater than 2.0% (v/v).

From the above evaluation, the optimal chromatographic conditions for the direct resolution of the optical isomers of naproxen using the Chiral AGP column were defined as follows: a mobile phase composed of 99.5% 4 m*M* phosphate at pH 7.0 and 0.5% isopropanol operating at a column temperature of 25°C, at a flow-rate

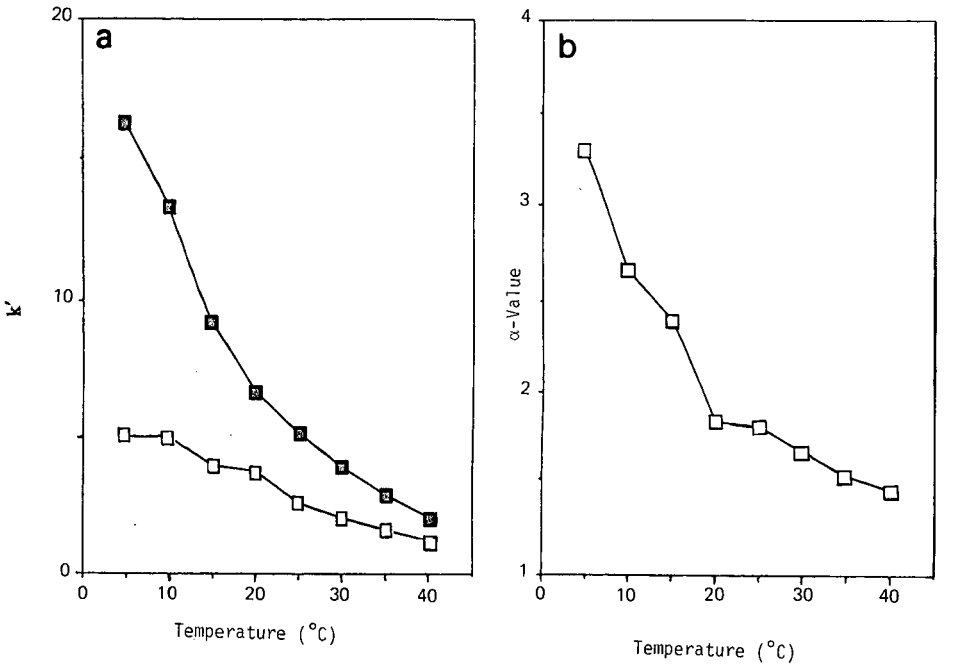

Fig. 6. Effect of temperature on (a) k': □ = *R*-isomer, ■ = *S*-isomer; and (b) resolution of *R*- and *S*-naproxen. Chromatographic conditions as in Fig. 3a, except temperature.

of 0.8 ml/min. Typically, UV detection at 263 nm and a sample loading of 1.0 μg should be used.

The method was examined for precision, linearity and limits of detection under the above conditions. The precision of the method was evaluated by performing six replicate injections of a solution of *S*-naproxen containing *ca.* 1.3% *R*-naproxen. The mean value for *S*-naproxen was 98.71% and the standard deviation was 0.1% indicating that the method is precise. The intended application of this chiral separation method is to quantitate low levels of *R*-naproxen present in the *S*-naproxen product. Therefore, linearity of the method was determined by analyzing spiked solutions of 0.2, 0.5, 1.0, 2.0, 4.0 and 5.0% of *R*-naproxen in the presence of *S*-naproxen. Fig. 7 depicts the experimentally determined linearity plot from these spiked samples. This method exhibits good linearity over the range tested, following the derived linear equation of $y = 0.00198 + 0.998778x$, where y = observed response and x = theoretical response of % *R*-naproxen. The average deviation from a theoretical calibration line having a slope of 1.00, expressed as the standard error of estimate, is 0.05%. The coefficient of correlation is 0.9998. The method is, therefore considered to be linear in the examined range of concentration. The limit of detection was determined to be ca. 0.1% of either enantiomer in the presence of its enantiomeric counterpart.

Finally, for comparison, four resolved *S*-naproxen samples of varying optical purities were separately subjected to the two optical purity determination methods described in this work. The results (Table I) showed good correlation between the

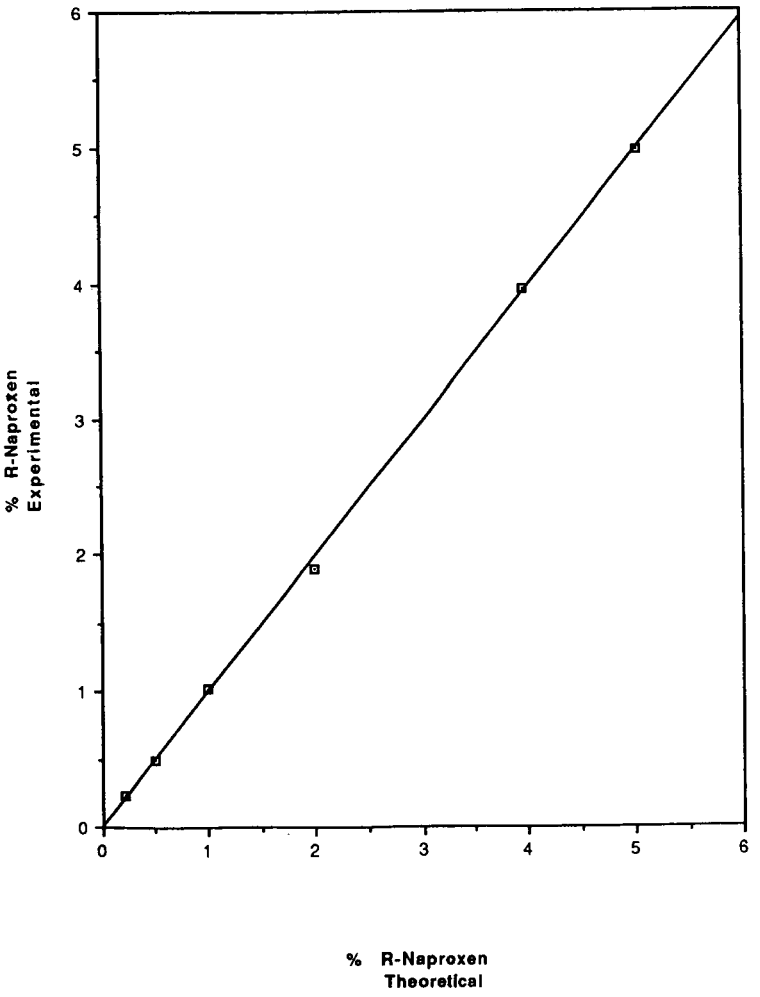

Fig. 7. Linearity plot for *R*-naproxen spiked in *S*-naproxen.

TABLE I

COMPARISON OF CHROMATOGRAPHIC RESULTS OF THE ENANTIOMERIC PURITY OF NAPROXEN USING THE PIRKLE CSP AND CHIRAL AGP CSP

Sample	(%*S*-Naproxen)	
	Chiral AGP	Pirkle CSP
A	99.87	99.55
B	99.55	99.06
C	98.65	98.50
D	95.82	95.62

methods using the Pirkle (*R*)-N-(2-naphthyl)alanine column and the Chiral AGP column.

Other chiral stationary phases

Seven other commercially available chiral stationary phases were evaluated for their ability to separate the optical isomers of naproxen. These included β-cyclodextrin, bovine serum albumin, Chiralpak OT(+) and four cellulose based CSPs, namely, Chiralcel OB, OD, OJ, and CA-1. In all cases, the attempted separations were performed on naproxen using mobile phases suggested by the respective column manufacturer. Chiral separations of derivatives of naproxen were not attempted with these columns. No separation of the optical isomers of naproxen was observed with any of these seven columnms.

CONCLUSIONS

Two chromatographic methods for the separation of the optical isomers of naproxen were presented. Both methods offer advantages over existing literature methods in both separation factors and ease of use. In particular, the Chiral AGP CSP gave direct resolution of the optical isomers of naproxen in less than 5 min. This CSP has been shown to be superior to the Enantiopak AGP CSP with regard to column stability, peak shape and separation efficiency. The methods reported in this manuscript may prove applicable to other α-methylarylacetic acid NSAIDs since these compounds all share common functional groups and often share similar chromatographic characteristics towards chiral separations.

ACKNOWLEDGEMENT

The author would like to thank Dr. T. Yang for helpful comments on the preparation of this manuscript.

REFERENCES

1 G. P. Tosolini, E. Moro, A. Forgione, M. Ranghieri and V. Mandelli, *J. Pharm. Sci.*, 63 (1974) 1072.
2 G. J. Vangiessen and D. G. Kaiser, *J. Pharm. Sci.*, 64 (1975) 798.
3 C. J. Brooks and M. T. Gilbert, *J. Chromatogr.*, 99 (1974) 541.
4 D. G. Kaiser, G. J. Vangiessen, R. J. Reischer and W. J. Wechter, *J. Pharm. Sci.*, 65 (1976) 269.
5 R. J. Bopp, J. F. Nash, A. S. Ridolfo and E. R. Shepard, *Drug Metab. Disp.*, 7 (1979) 356.
6 S. W. McKay, D. N. B. Mallen, P. R. Shrubsall, B. P. Swann and W. R. N. Williamson, *J. Chromatogr.*, 170 (1979) 482.
7 J. K. Stoltenborg, C. V. Puglisi, F. Rubio and F. M. Vane, *J. Pharm. Sci.*, 70 (1981) 1207.
8 J. M. Maitre, G. Boss and B. Testa, *J. Chromatogr.*, 299 (1984) 397.
9 T. Tamegai, M. Ohmae, K. Kawabe and M. Tomoeda, *J. Liq. Chrom.*, 2 (1979) 1229.
10 T. Tamegai, T. Tanaka, T. Kaneko, S. Ozaki, M. Ohmae and K. Kawabe, *J. Liq. Chromatogr.*, 2 (1979) 551.
11 J. K. Kemmerer, F. A. Rubio, R. M. McClain and B. A. Koechlin, *J. Pharm. Sci.*, 68 (1979) 1274.
12 J. Goto, N. Goto, A. Hikichi, T. Nishimaki and T. Nambara, *Anal. Chim. Acta*, 120 (1980) 187.
13 J. Goto, N. Goto and T. Nambara, *J. Chromatogr.*, 239 (1982) 559.
14 H. Nagashima, Y. Tanaka and R. Hayashi, *J. Chromatogr.*, 345 (1985) 373.
15 S. Bjorkman, *J. Chromatogr.*, 339 (1985) 339.
16 J. Goto, M. Ito, S. Katsuki, N. Saito and T. Nambara, *J. Liq. Chromatogr.*, 9 (1986) 683.

17 A. J. Hutt, S. Foumel and J. Caldwell, *J. Chromatogr.*, 378 (1986) 378.
18 N. N. Singh, F. Jamali, F. M. Pasutto, A. S. Russel, R. T. Coutts and K. S. Drader, *J. Pharm. Sci.*, 75 (1986) 439.
19 N. N. Singh, F. M. Pasutto, R. T. Coutts and F. Jamali, *J. Chromatogr.*, 378 (1986) 125.
20 R. T. Coutts, F. M. Pasutto, F. Jamali and N. Singh, in J. W. Gorrod (Editor), *Development of Drugs and Modern Medicines*, Ellis Horwood, Chichester, 1986, p. 232.
21 B. C. Sallustio, A. Abas, P. J. Hayball, Y. J. Purdie and P. J. Meffin, *J. Chromatogr.*, 374 (1986) 329.
22 J. M. Maitre, G. Boss, B. Testa and K. Hostettman, *J. Chromatogr.*, 356 (1986) 341.
23 H. Spahn, *J. Chromatogr.*, 423 (1987) 334.
24 A. Sioufi, D. Colussi, F. Marfil and J. P. Dubois, *J. Chromatogr.*, 414 (1987) 131.
25 R. T. Foster and F. Jamali, *J. Chromatogr.*, 416 (1987) 388.
26 K. Shimada, E. Haniuda, T. Oe and T. Nambara, *J. Liq. Chromatogr.*, 10 (1987) 3161.
27 A. Avgerinos and A. J. Hutt, *J. Chromatogr.*, 415 (1987) 75.
28 Y. Fujimoto, K. Ishi, H. Nishi, N. Tsumagari, T. Kakimoto and R. Shimizu, *J. Chromatogr.*, 402 (1987) 344.
29 P. Slegel, G. Vereczkey-Donath, L. Ladanyi and M. Toth-Lauritz, *J. Pharm. Biomed. Anal.*, 5 (1987) 665.
30 R. Behvar and F. Jamali, *Pharm. Res.*, 5 (1988) 53.
31 R. Mehvar, F. Jamali and F. M. Pascutto, *J. Chromatogr.*, 425 (1988) 135.
32 H. Spahn, D. Krauss and E. Mutschler, *Pharm. Res.*, 5 (1988) 107.
33 D. M. Johnson, A. Reuter, J. M. Collins and G. F. Thompson, *J. Pharm. Sci.*, 68 (1979) 112.
34 I. W. Wainer and T. W. Doyle, *J. Chromatogr.*, 284 (1984) 117.
35 J. B. Crowther, T. R. Covey, E. A. Dewey and J. D. Henion, *Anal. Chem.*, 56 (1984) 2921.
36 N. Oi and H. Kitahara, *J. Liq. Chromatogr.*, 9 (1986) 511.
37 W. H. Pirkle and T. C. Pochapsky, *J. Chromatogr.*, 434 (1986) 233.
38 D. A. Nicoll-Griffith, *J. Chromatogr.*, 402 (1987) 179.
39 D. M. McDaniel and B. G. Snider, *J. Chromatogr.*, 404 (1987) 123.
40 B. Blessington, N. Crabb and J. O'Sullivan, *J. Chromatogr.*, 396 (1987) 177.
41 D. A. Nicoll-Griffith, T. Inaba, B. K. Tang and W. Kalow, *J. Chromatogr.*, 428 (1988) 103.
42 R. Dernoncour and R. Azerad, *J. Chromatogr.*, 410 (1987) 355.
43 J. Hermansson and M. Eriksson, *J. Liq. Chromatogr.*, 9 (1986) 621.
44 R. Bishop, I. Hermansson, B. Jaderlund, G. Lindgren and C. Pernow, *Am. Lab. (Fairfield, Conn.)*, 3 (1986) 138.
45 C. Petterson and K. No, *J. Chromatogr.*, 282 (1983) 671.
46 C. Pettersson and G. Schill, *J. Liq. Chromatogr.*, 9 (1986) 269.
47 C. Pettersson and C. Gioeli, *J. Chromatogr.*, 398 (1987) 247.
48 C. Pettersson and C. Gioeli, *J. Chromatogr.*, 435 (1988) 225.
49 E. Delee, I. Jullien and L. LeGarrec, *J. Chromatogr.*, 450 (1988) 191.

Journal of Chromatography, 543 (1991) 367–374
Elsevier Science Publishers B.V., Amsterdam

CHROM. 23 147

Assay for both ascorbic and dehydroascorbic acid in dairy foods by high-performance liquid chromatography using precolumn derivatization with methoxy- and ethoxy-1,2-phenylenediamine

N. BILIC
Federal Dairy Research Institute, Schwarzenburgstrasse 161, 3097 Liebefeld-Berne (Switzerland)
(First received December 10th, 1990; revised manuscript received January 30th, 1991)

ABSTRACT

A procedure for the simultaneous determination of both ascorbic and dehydroascorbic acid in dairy foods by high-performance liquid chromatography using precolumn derivatization with 4-methoxy- and 4-ethoxy-1,2-phenylenediamine is presented. The derivatives are isolated by solid-phase extraction and analysed by fluorescence detection on a resin-type reversed-phase column at pH 9. Retention times are 2 and 3.2 min for the derivatives of ascorbic and dehydroascorbic acid, respectively. Relative standard deviations of the within- and between-assay tests are 7.1 and 5.5%, respectively, for ascorbic and 11 and 9%, respectively, dehydroascorbic acid. The limits of detection are 50 and 70 fmol per 5-μl injection for ascorbic and dehydroascorbic acid, respectively.

INTRODUCTION

Milk and dairy products are a valuable source of vitamins for human nutrition. These foods may be heated by a range of processes and stored for various periods of time. Vitamin C, consisting of both ascorbic acid (AA) and dehydroascorbic acid (DHAA), is known to be labile during both processing and storage. It seems important to measure the effects on vitamin C and to ensure that losses are at a minimum, if possible. Also, it is of interest for the consumer to know the final level of vitamin C.

A variety of methods for the assay of vitamin C in foods and biological samples are available. They include biological, chemical, polarographic, enzymatic and chromatographic procedures. The literature in this area has been reviewed by Jaffe [1] and by Bui-Nguyén [2]. Chemical techniques combined with spectrophotometric or spectrofluorimetric detection are still in use. Oxidation–reduction titration of AA with dichlorophenolindophenol is still very popular, although unspecific [3]. Another class of colorimetric reactions involves the reaction of AA with metal ions such as Fe^{3+} [4,5]. Enzymatic assays for AA utilize the ability of ascorbic acid oxidase to deplet ascorbic acid. The depletion may be followed by spectrophotometric [6] or polarographic methods [7]. Total vitamin C (AA + DHAA) may be measured by ox-

0021-9673/91/$03.50

idation of AA to DHAA, followed by derivatization of the DHAA with either 2,4-dinitrophenylhydrazine [8] or 1,2-phenylenediamine [9] to give a coloured or a fluorescent derivative.

New developments in this area include high-performance liquid chromatography (HPLC) on anion-exchange [10–13], reversed-phase [14–16] and bonded-phase NH_2 [17] columns. Either ultraviolet [13,17] or electrochemical [14–16] detection is applied. However, these techniques are sensitive to AA only.

A precolumn derivatization procedure includes the reaction of DHAA with 1,2-phenylenediamine, followed by HPLC [18,19]. With prior oxidation of AA to DHAA, total vitamin C may be measured in the second run.

Using a post-column derivatization technique, both AA and DHAA may be measured separately in one run [20]. In this instance, the post-column reagent solution contains both 1,2-phenylenediamine and an oxidizing agent. After separation by HPLC, DHAA is derivatized and AA is oxidized and derivatized, to give the fluorescent quinoxaline. However, disadvantages include both the use of 20-m heated (65–70°C) and cooled coils and retention times of up to 20 min.

In this work, 4-methoxy- and 4-ethoxy-1,2-phenylenediamine were applied to the sequential precolumn derivatization of both AA and DHAA. The derivatives formed exhibit at least a 10-fold increase in fluorescence, compared with the quinoxaline derived from 1,2-phenylenediamine. They can be selectively isolated by solid-phase extraction and analysed by HPLC at pH 9 in a single run. The retention times are 2 and 3.2 min.

EXPERIMENTAL

Apparatus

The HPLC system consisted of Beckman (Berkeley, CA, U.S.A.) Model 100A precision-flow metering pumps, a Hamilton (Reno, NV, U.S.A.) PRP-1 column (150 × 4.1 mm I.D.) with a 5-μm polystyrene–divinylbenzene copolymer packing, a 5-μl loop, a Shimadzu (Kyoto, Japan) C-R1A data processor and a Merck–Hitachi (Darmstadt, Germany) Model F1000 spectrofluorimeter for HPLC applications, equipped with both a 150-W high-pressure xenon lamp and a 12-μl flow cell. The excitation and emission wavelength were set at 375 and 475 nm, respectively. The mobile phase was delivered at 1 ml/min. A Perkin-Elmer (Beaconsfield, U.K.) LS-5 luminescence spectrometer was used to scan the excitation and emission wavelengths of the methoxy- and ethoxyquinoxaline derivatives of DHAA.

Reagents and chemicals

Unless stated otherwise, analytical-reagent grade chemicals were used. Ascorbic acid, oxalic acid, 70% perchloric acid, 85% orthophosphoric acid, 25% ammonia solution, methanol, ethanol, bromine, 1,2-phenylenediamine and palladium phthalocyanine and HPLC-grade acetonitrile, dipotassium hydrogenphosphate and 1-propanesulphonate were obtained from E. Merck (Darmstadt, Germany). Column chromatographic grade C_{18} silica gel LiChroprep (particle size 25–40 μm) and Florisil (100–200 mesh) were from Merck. 4-Methoxy-1,2-phenylenediamine dihydrochloride (98%) and 4-ethoxy-2-nitroaniline (97%) were from Aldrich (Steinheim, Germany) and Aminex 50W-X2 (Na^+) (200–400 mesh) from Bio-Rad Labs. (Richmond, CA, U.S.A.).

Stock solutions were 0.5% oxalic acid, 150 mmol/l H_3PO_4, 1 mol/l KH_2PO_4, 1 mol/l K_2HPO_4 for HPLC stored in a refrigerator, C_{18} silica gel LiChroprep in ethanol (10 g in 95 ml), saturated aqueous bromine, phosphoric acid buffer (150 mmol/l H_3PO_4 adjusted to pH 2 with 1 mol/l KH_2PO_4) and a 30% (v/v) slurry of Aminex 50W-X2 (H^+) in water.

Solutions prepared on the day of use were mobile phase for HPLC, consisting of 16% acetonitrile in both 50 mmol/l K_2HPO_4 and 5 mmol/l 1-propanesulphonate, adjusted to pH 9 with 150 mmol/l H_3PO_4, 10 mmol/l ascorbic acid made by dissolving 1 mmol of ascorbic acid in 100 ml of 0.5% oxalic acid and 1 μmol/l dehydroascorbic acid as a standard solution. The last solution was prepared by transferring 100 μl of 10 mmol/l ascorbic acid into a 10-ml screw-capped volumetric flask (Pierce Europe, Oud-Beijerland, The Netherlands), half-filled with 0.5% oxalic acid, followed by addition of aqueous bromine as an oxidizing agent. The excess of bromine was removed by streaming nitrogen over the fluid surface. The flask was diluted to the mark with water, sealed and shaken. The resulting solution contained 100 μmol/l DHAA. A 100-μl volume of this solution was diluted in 10 ml of phosphoric acid buffer.

Solutions prepared just prior to use were 100 mg per 100 ml 4-ethoxy-1,2-phenylenediamine ditrifluoroacetic acid in phosphoric acid buffer (pH 2) and 100 mg per 100 ml 4-methoxy-1,2-phenylenediamine ditrifluoroacetic acid in phosphoric acid buffer (pH 2).

Solid-phase extraction columns were made on the day of use by filling 1-ml filtration tubes (containing frits only) with 1 ml of a suspension of C_{18} silica gel in ethanol. The filled tubes were allowed to drain. The packed adsorbent was rinsed twice with 1 ml of water.

Cation-exchange columns were made on the day of use by filling filtration tubes with 1 ml of a suspension of 30% Aminex 50W-X2.

Derivatization reagents

4-Methoxy-1,2-phenylenediamine dihydrochloride (3 g) was dissolved in 100 ml of water, decolorized with Florisil and filtered through a 0.45-μm pore membrane filter. The solution was loaded onto a 25 × 5 cm I.D. Prepbar column (E. Merck) filled with reversed-phase C_{18} silica, particle size 7 μm. Gradient elution with ethanol was performed at 10 ml/min (gradient from 0 to 60% in 60 min) in the presence of 0.5% trifluoroacetic acid. The 4-methoxy-1,2-phenylenediamine peak at 280 nm was identified by reacting one drop of effluent with 5 ml of 100 mmol/l disodium α-ketoglutarate in 1 mol/l KH_2PO_4 and observing blue-green fluorescence under UV light. The fraction was evaporated to dryness and the residue was dissolved in 100 ml of water and freeze-dried. The substance was stored in a 250-ml glass bottle under nitrogen at room temperature.

4-Ethoxy-1,2-phenylenediamine was prepared from 4-ethoxy-2-nitroaniline. 4-Ethoxy-2-nitroaniline (3 g) was dissolved in 200 ml of methanol and hydrogenated with hydrogen on 250 mg of palladium phthalocyanine as catalyst. The fluid was passed through a 0.45-μm PTFE membrane to remove palladium, decolorized with Florisil, evaporated to dryness, the residue dissolved in 100 ml of water, purified by HPLC using gradient elution with ethanol as described above (gradient from 0 to 80% in 60 min), evaporated to dryness, the residue dissolved in water, freeze-dried and stored under nitrogen.

Sample preparation, derivatization and extraction

A 1-g cheese sample or 1 ml of milk was homogenized in or mixed with, respectively, 18 ml of 0.5% oxalic acid, 1 ml of 70% perchloric acid was added and the precipitate was removed by centrifugation at 1600 *g*.

The supernatant (0.5 ml) was transferred into a test-tube, followed by addition of 0.8 ml of 1 mol/l KH_2PO_4 for buffering at pH 2 and 0.5 ml of 100 mg per 100 ml 4-ethoxy-1,2-phenylenediamine for derivatization. The reaction time was 45 min in the dark at room temperature. The solution was passed through a solid-phase extraction column and a cation-exchange column, attached to one another by means of an adapter, and collected in a test-tube. Two 1-ml volumes of water were passed through the columns for rinsing and collected in the same test-tube. Saturated aqueous bromine (50 μl) was added to oxidize AA. The excess of bromine was removed by bubbling with nitrogen for 10 min. [A manifold for delivering nitrogen to ten test-tubes held in a rack was constructed from a length of polyethylene tubing (30 cm × 1.2 cm I.D. × 1.4 cm O.D.) and ten pieces of PTFE capillary tubing (100 mm × 1.8 mm I.D. × 2 mm O.D.). The polyethylene tubing was sealed at one end with a stopper and punctured a long its length in ten places, corresponding to the positions of the ten test-tube holes in the rack. The PTFE capillaries were then forced into the puncture holes. The unit was attached at one end to the nitrogen source and fixed in position, allowing immersion of capillary tubing tips into the test-tube fluid for nitrogen bubbling.]

A 0.5-ml volume of 100 mg per 100 ml 4-methoxy-1,2-phenylenediamine was added and allowed to react for 45 min in the dark. The solution was passed through the solid-phase extraction column used previously. The column was rinsed with 1 ml of water. The derivatives of interest were recovered from the adsorbent by elution with 1 ml of 15% acetonitrile and 0.5% of trifluoroacetic acid in water, and immediately neutralized by adding 5 μl of 25% ammonia solution. (For this purpose, a 25% ammonia solution was stored in a 30-ml serum-type reaction vial sealed with a 13.5 mm O.D. polyethylene stopper. When in use, the stopper was replaced with one having a 1 mm diameter hole, through which the ammonia solution was sampled with a 5-μl syringe-pipette with a disposable PTFE-tip.) HPLC analysis was performed within a few hours.

RESULTS AND DISCUSSION

1,2-Phenylenediamine reacts with α-keto acids and with DHAA to yield fluorescent quinoxaline derivatives under mild conditions [21]. The present derivatization reagents also undergo this type of reaction to generate presumably methoxy- and ethoxyquinoxalines. However, these derivatives exhibit at least a 10–13-fold higher fluorescence than the quinoxaline of DHAA. Excitation and fluorescence maxima are observed at 375 and 475 nm, respectively.

Two-step sequential derivatization is applied to the simultaneous assay of both AA and DHAA by HPLC. First, the sample is derivatized with 4-ethoxy-1,2-phenylenediamine, followed by isolation of both products of derivatization and removal of excess of reagent. The latter is removed by adsorption on a cation-exchange resin. The derivatives are retained by the reversed-phase adsorbent. The AA in the sample is oxidized to DHAA and then derivatized with 4-methoxy-1,2-phenylenediamine.

Each derivatization reaction could be followed by measuring the increase in fluorescence. Stable plateau values of fluorescence were attained within 45 min at pH 2, 3, 4 and 5 at room temperature.

The derivatives were recovered from the reversed-phase adsorbent by elution with 15% acetonitrile and 0.5% trifluoroacetic acid in water. Under these conditions, the derivatives of keto acids and orange-coloured products are largely retained by the adsorbent. Usually colourless eluates were obtained. These were immediately neutralized with a 25% ammonia solution, with which pH 8–8.5 was easily obtained. When neutralized, the derivatives were found to be very stable at room temperature, and could be analysed by HPLC within 24 h without noticeable changes in the fluorescence.

A typical chromatogram representing 5 pmol each of AA and DHAA per 5-μl injection is shown in Fig. 1. Separation at pH values between 3 and 5.5 on both resin- and silica-based reversed-phase columns was unsatisfactory, as the elution profile of each derivative gave a major peak with a shoulder on both sides. This drawback could not be corrected by ion-pair reagents in the mobile phase.

In the extract, AA should remain constant during derivatization of DHAA. This requirement was fulfilled by performing the derivatization at pH 2, as shown in recovery experiments (Table I). Different amounts of both AA and DHAA were added to oxalic acid–perchloric acid extracts of milk, buffered with 1 mol/l KH_2PO_4 at pH 2, and with 1 mol/l potassium oxalate (pH 5) at pH 3 and 4, followed by two-step derivatization, extraction and HPLC. The recoveries of AA ranged between

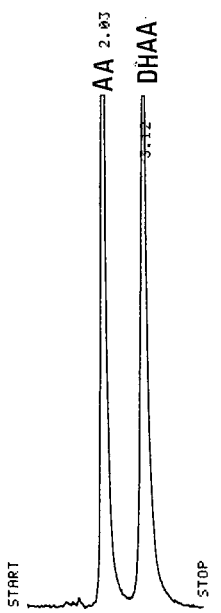

Fig. 1. Separation of methoxy- and ethoxyquinoxaline of DHAA, with retention times of 2.03 and 3.12 min as indicated. Peaks represent 5 pmol each of AA and DHAA. Elution at 1 ml/min; injection volume, 5 μl; recording attenuation, 8 mV full-scale. For other details, see text.

TABLE I

RECOVERIES OF AA AND DHAA ADDED TO 0.4-ml VOLUMES OF OXALIC ACID–PERCHLORIC ACID EXTRACTS OF MILK

Procedure	Amount added (pmol)		Amount measured (pmol) (mean ± S.D.)		Recovery (%)	
	AA	DHAA	AA	DHAA	AA	DHAA
Derivatization at pH 2 ($n=5$ at each level)	0	0	612±68	167±29		
	100	100	715±52	265±24	103	98
	200	200	850±67	345±43	119	89
	400	400	1050±78	532±51	108	91
	800	800	1432±45	913±36	103	93
Derivatization at pH 3 ($n=5$ at each level)	0	0	276±13	167±7		
	100	100	339±26	301±13	63	134
	200	200	450±14	395±19	87	114
	400	400	641±39	589±26	91	106
	800	800	908±49	1064±27	79	112
Derivatization at pH 4 ($n=5$ at each level)	0	0	244±19	200±7		
	100	100	235±7	411±19	0	211
	200	200	250±26	635±33	0	217
	400	400	204±11	1050±30	0	213
	800	800	20±3	2281±99	0	260

103 and 119% at pH 2 and 63 and 91% at pH 3. No recovery of AA was observed at pH 4. The AA losses were recovered as DHAA.

Dairy foods such as raw and pasteurized milk, yoghurt, UHT-processed milk and cheese were analysed by derivatization at pH 2. Results with details of the origin of the foods and type of heat treatment are given in Table II.

TABLE II

AA AND DHAA CONTENTS OF DAIRY FOODS EXPRESSED IN mg PER 1000 ml OR 1000 g, RESPECTIVELY

Results are means ± S.D. ($n=6$).

Food	AA	DHAA
Raw cow's milk[a]	5.9 ±0.3	1.52±0.2
Pasteurized milk[b,c]	4.0 ±0.25	0.39±0.03
Yoghurt[b]	0.27±0.3	1.52±0.2
UHT milk by indirect heating[b,d,e]	1.1 ±0.05	0.21±0.03
UHT milk by indirect heating[b,d,f]	0.14±0.03	0.07±0.007
UHT milk by direct heating[b,d,g]	4.15±0.21	0.28±0.014
UHT milk by direct heating[b,d,h]	3.90±0.13	0.28±0.02
Pasteurized milk[b,h]	5.0 ±0.3	0.46±0.03
Tilsiter cheese[b]	1.76±0.3	0.32±0.04

[a] Obtained from the herd at our institute.
[b] On retail sale.
[c,e,f,g,h] Local dairy plants.
[d] Ultra-high-temperature-processed milk (135–150°C).

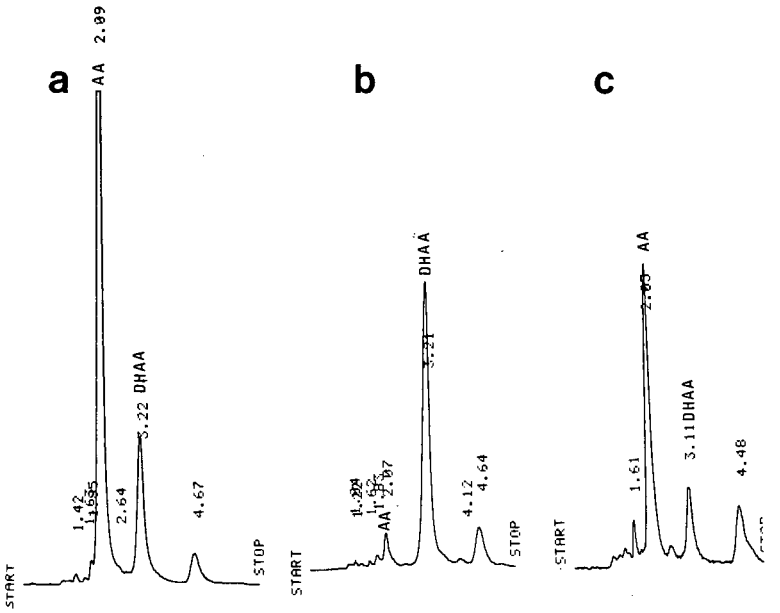

Fig. 2. Elution profiles for the analysis of (a) raw milk, (b) yoghurt and (c) Tilsiter cheese. Peaks for AA and DHAA are indicated. Numbers at peaks indicate retention times in min.

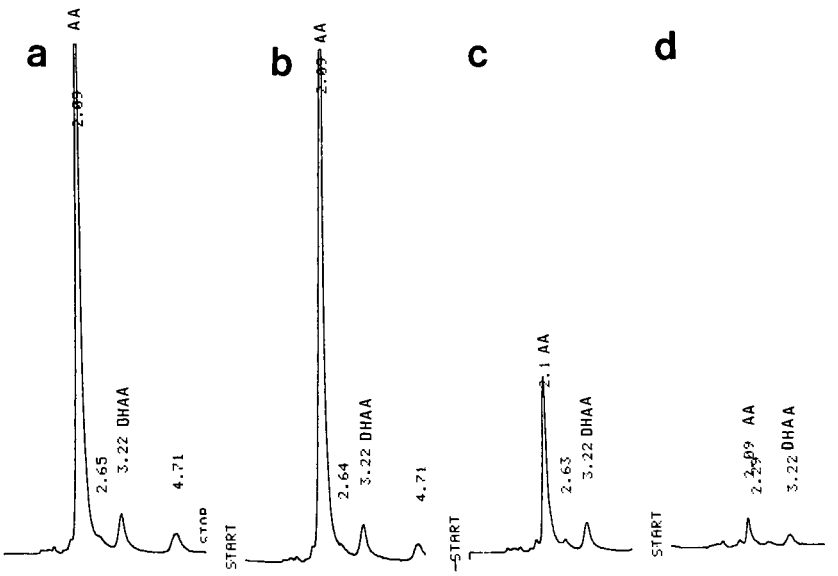

Fig. 3. Elution profiles for the analysis of UHT milk by (a,b) direct and (c,d) indirect heating at dairy plants given in Table II. Numbers at peaks indicate retention times in min.

TABLE III

PRECISION OF THE ASSAY

Parameter	Amount in 1-ml aliquot of Tilsiter cheese (pmol) (mean ± S.D.)	
	AA	DHAA
Within-assay ($n=9$)	500 ± 36	90 ± 6
Relative standard deviation	7.1%	5.5%
Between-assay ($n=6$)	479 ± 45	93 ± 8
Relative standard deviation	11%	9%

Typical chromatograms for the analysis of dairy foods given in Table II are shown in Figs. 2 and 3. As expected, the highest values were found in both raw and pasteurized milk, with as much as 80% in the form of AA. The yoghurt contained a quarter of the amount found in pasteurized milk, mostly in the form of DHAA. UHT-processing by indirect heating with heat exchangers destroyed as much as 80–90% of the vitamin in raw milk, in contrast to processing by direct heating with steam. In contrast to Emmental and Gruyère cheese, which contained less then 0.2 mg/kg, Tilsiter cheese showed concentrations of about 2 mg/kg, with 80% in the form of AA.

The reproducibility of the procedure was tested on a Tilsiter cheese, which was stored in a refrigerator for 10 days. The results are given in Table III. The within- and between-assay relative standard deviations were 7.1 and 5.5%, respectively for AA and 11 and 9%, respectively, for DHAA. These values are within acceptable limits.

At a signal-to-noise ratio of 3, the detection limits were calculated to be about 50 and 70 fmol of AA and DHAA, respectively, per 5-μl injection.

REFERENCES

1 G. M. Jaffe, in L. J. Machlin (Editor), *Handbook of Vitamins*, Marcel Dekker, New York, Basle, 1984, p. 199.
2 M. H. Bui-Nguyén, in A. P. De Leenheer, W. E. Lambert and M. G. M. De Ruyter (Editors), *Modern Chromatographic Analysis of the Vitamins*, Marcel Dekker, New York, Basle, 1985, p. 267.
3 R. J. Henry, D. C. Cannon and J. W. Winkleman, *Clinical Chemistry–Principles and Technics*, Harper & Row, New York, 1974.
4 S. T. Omaye, J. D. Turnbull and H. E. Sauberlich, *Methods Enzymol.*, 62 (1979) 3.
5 W. C. Butts and H. J. Mulvihill, *Clin. Chem.*, 21 (1975) 1493.
6 T. Z. Liu, N. Chin, M. D. Kiser and W. N. Bigler, *Clin. Chem.*, 28 (1982) 2225.
7 R. Stevanato, L. Avigliano, A. Finazzi-Agro and A. Rigo, *Anal. Biochem.*, 149 (1985) 537.
8 L. W. Mapson, *Biochem J.*, 80 (1961) 459.
9 M. J. Deutsch and C. E. Weeks, *J. Assoc. Off. Agric. Chem.*, 48 (1965) 1248.
10 R. C. Williams, D. R. Baker and J. A. Schmit, *J. Chromatogr. Sci.*, 11 (1973) 618.
11 L. A. Pachla and P. T. Kissinger, *Anal. Chem.*, 48 (1976) 364.
12 M. Grün and F. A. Loewus, *Anal. Biochem.*, 130 (1983) 191.
13 L. L. Lloyd, F. P. Warner, C. A. White and J. F. Kennedy, *Chromatographia*, 24 (1987) 371.
14 W. A. Behrens and R. Madère, *Anal. Biochem.*, 165 (1987) 102.
15 M. A. Kutnik, W. C. Hawkes, E. E. Schaus and S. T. Omaye, *Anal. Biochem.*, 166 (1987) 424.
16 P. W. Washko, W. O. Hartzell and M. Levine, *Anal. Biochem.*, 181 (1989) 276.
17 M. H. Bui-Nguyén, *J. Chromatogr.*, 196 (1980) 163.
18 A. J. Speek, J. Schrijver and W. H. P. Schreurs, *J. Chromatogr.*, 305 (1984) 53.
19 A. J. Speek, J. Schrijver and W. H. P. Schreurs, *J. Agric. Food Chem.*, 32 (1984) 352.
20 A. Lopez-Anaya and M. Mayersohn, *Clin. Chem.*, 33 (1987) 1874.
21 R. W. Keating and P. R. Haddad, *J. Chromatogr.*, 245 (1982) 249.

Journal of Chromatography, 543 (1991) 375–387
Elsevier Science Publishers B.V., Amsterdam

CHROM. 23 026

Determination of ginkgolides and bilobalide in *Ginkgo biloba* leaves and phytopharmaceuticals

T. A. VAN BEEK*, H. A. SCHEEREN, T. RANTIO, W. Ch. MELGER and G. P. LELYVELD
Phytochemical Section, Laboratory of Organic Chemistry, Agricultural University, Dreijenplein 8, 6703 HB Wageningen (The Netherlands)
(First received July 18th, 1990; revised manuscript received January 29th, 1991)

ABSTRACT

A method has been developed for the determination of the pharmacologically active terpenoids ginkgolide A, B and C and bilobalide in *Ginkgo biloba* leaves and phytopharmaceutical preparations containing ginkgo extracts. The leaves (400–800 mg) are selectively extracted with methanol–water (10:90) and the resulting extract is purified by means of a polyamide and a C_{18} solid-phase extraction column. After concentration, the terpenoids are determined by high-performance liquid chromatography on a C_{18} column with methanol–water (33:67) as eluent and refractive index detection. Benzyl alcohol is used as an internal standard. The recovery of the method is 95 ± 5%. The reproducibility is dependent on the concentration and varies from 2 to 15%. The minimum concentration that can be determined in leaves is 10 μg of terpenoid/g of dry leaves. With a small modification the method can be used equally well for phytopharmaceuticals. Several ginkgo medicines were investigated and the total concentration of terpenoids was found to vary by a factor 18. The concentration in leaves varied by a factor 40.

INTRODUCTION

Ginkgolides, which occur in the leaves of the tree *Ginkgo biloba*, possess unique pharmacological properties and are part of many phytopharmaceutical preparations. Reviews have been published by Braquet [1], Schilcher [2] and Hosford *et al.* [3] and in a special issue of *La Presse Medicale* [4] and a multi-author book on ginkgolides [5].

Their analysis and that of the closely related sesquiterpenoid bilobalide is difficult because of the poor UV characteristics of these compounds and the highly complex matrix. Guth and co-workers [6,7] were the first to publish two different reversed-phase high-performance liquid chromatographic (RP-HPLC) methods with UV detection. Both methods have in common time-consuming purification steps prior to HPLC analysis, a high detection limit of 30 μg and unsatisfactory results.

In 1988 Teng [8] published a good chromatogram of a *Ginkgo biloba* extract with a baseline separation of bilobalide and ginkgolide A, B, C and J and no other visible peaks. Separation was achieved by RP-HPLC with refractive index detection. Unfortunately, no details of the work-up procedure or recovery were given so the work cannot be reproduced. Komoda *et al.* [9] also reported an RP-HPLC method with refractive index detection. Their purification procedure involved two partitions, among other steps. No recovery data or extraction efficiencies were given.

0021-9673/91/$03.50

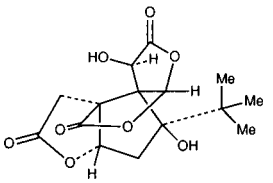

Bilobalide

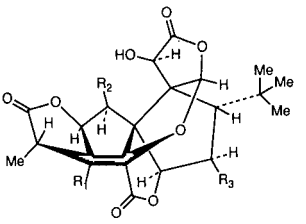

Ginkgolide A	R_1=OH, R_2=R_3=H
Ginkgolide B	R_1=R_2=OH, R_3=H
Ginkgolide C	R_1=R_2=R_3=OH
Ginkgolide J	R_1=R_3=OH, R_2=H

Recently, Wagner *et al.* [10] published a method for the determination of flavonoids and ginkgolides in leaves and phytopharmaceuticals by means of HPLC and thin-layer chromatography (TLC) followed by detection with a chromogenic reagent. Prior to detection they used a lengthy purification procedure including column chromatography. After investigating several phytopharmaceuticals they concluded that ginkgolides were either absent or present in extremely low concentrations. This statement prompted a polemic in the same journal by one of the producers of the extracts [11], who stated that the extracts do contain at least 3% of ginkgolides and that these can be determined with sufficient accuracy if the proper analytical techniques are employed. The method used by Wagner *et al.*, especially the TLC part, was considered to be inadequate.

Finally, Pietta *et al.* [12] recently published a simple purification step for ginkgolides followed by RP-HPLC with UV detection. Unfortunately, using this type of detection, several trace impurities co-eluting with ginkgolide C and A are determined at the same time, which gives rise to too high values for these two compounds. This follows from the on-line UV spectra which show too much absorption in the 200–220 nm range, and the baseline of the chromatogram, which returns to zero only after elution of ginkgolide B. No recoveries were given.

In summary, there are no reliable methods that will allow smaller companies and pharmacies to compare different batches of leaves, to control extracts or to standardize phytopharmaceuticals. Phytopharmaceuticals could thus be lacking in the important ginkgolides. Nothing is so far known about differences in the content of ginkgolides as a function of harvest time, age, sex or geographic origin of the tree or weather conditions.

In this paper we report a simple method for the determination of ginkgolides and bilobalide in ginkgo leaves and phytopharmaceuticals containing ginkgo extracts.

EXPERIMENTAL

Plant materials and phytopharmaceuticals

Dutch ginkgo leaves were collected in the botanical garden of the Agricultural University, Wageningen, from a 55-year-old male tree. The year and month of harvest are mentioned with the individual samples. German ginkgo leaves were collected in mid-September, 1989, from two trees near the Organic Chemistry building of the University of Heidelberg. For the Chinese and French leaves no details are known.

Phytopharmaceutical preparations were provided by the producers or bought in a pharmacy.

Drying

Dutch and German leaves were dried as soon as possible after collection for 24 h at 70°C in an oven with forced ventilation.

Standards

Ginkgolide A, B and C and bilobalide used for some of the recovery experiments and the determination of the response factors were supplied by Prof. K. Weinges. The purity was checked by means of RP-HPLC, UV spectroscopy and 200-MHz ^{1}H NMR spectroscopy.

Solvents

Methanol (M4058), acetonitrile and tetrahydrofuran (THF), all from Fisons (Loughborough, U.K.), were of HPLC quality. Methyl acetate was of synthetic quality (Merck, Darmstadt, Germany) and was redistilled prior to use. Hexane was of analytical-reagent grade (Merck). Water was doubly distilled in an all-glass apparatus. All solvents used for HPLC were filtered (0.45 μm) and ultrasonically degassed before use.

Instrumentation

All separations were carried out isocratically at room temperature (20°C) with a Kratos (Manchester, U.K.) Spectroflow 400 HPLC pump, equipped with a MUST (Spark, Emmen, The Netherlands) injector with a 50-μm (analytical) or 250-μm (preparative) loop. Detection was carried out with a Gilson (Villiers le Bel, France) Model 131 refractive index (RI) detector ($3 \cdot 10^{-5}$ refractive index units full-scale). In some initial experiments detection was carried out with a Kratos Spectroflow 773 UV detector at 219 nm. Integration was performed with a Shimadzu (Kyoto, Japan) C-R3A Chromatopac integrator. The analytical column (231 × 4.6 mm I.D.) packed with Spherisorb (Clwyd, U.K.) 5-μm C_{18}-modified silica gel was prepared in our laboratory. The preparative column (250 × 10 mm I.D.) packed with Microsorb 5-μm C_{18}-modified silica gel was prepared by Rainin (Woburn, MA, U.S.A.).

Chromatographic conditions

Three different eluents were used: (1) water–methanol–THF (7:2:1), flow-rate 1.0 ml/min; (2) water–acetonitrile–THF (7:2:1), flow-rate 1.0 ml/min; (3) water–methanol (67:33), flow-rate 1.0 ml/min (analytical) or 4.0 ml/min (preparative).

Identification and purity of peaks

Ginkgolide A, B and C and bilobalide were identified by comparing the retention times of the various peaks with those of authentic reference samples. Ginkgolide J was identified by comparing its chromatographic behaviour in the different eluents with literature data [7,8].

The purity of the peaks was checked by working up a 1-g amount of French leaves according to the standard procedure (see below) and, after evaporation of the ethyl acetate–hexane extract, injecting the ginkgolides onto the preparative HPLC column. Each peak was collected separately and after several injections the solvent was removed. The five residues were investigated by means of analytical HPLC with solvents 1 and 2 with refractive index detection. When only one peak was observed the ginkgolide or bilobalide peak in solvent 3 was considered to be pure.

Extraction and purification procedure

(a) Phytopharmaceuticals. A Bond Elut (Analytichem International, Harbor City, CA, U.S.A.) 500-mg C_{18} solid-phase extraction column (Art. No. 607 303) is placed below a similar extraction tube packed with 500 mg of MN-polyamid SC 6 for column chromatography (Macherey, Nagel & Co., Düren, Germany). The combination of the two purification columns is first washed with 10 ml of methanol and then conditioned with 10 ml of 2% aqueous methanol. Unless stated otherwise, the column is never allowed to run dry. A 1.00-ml volume of the medicine is diluted with 4 ml of water in a 20-ml conical flask and boiled for 5 min in an oil-bath of 150°C without a reflux condenser. After cooling, the solution is transferred to another flask. The first flask is washed three times with 1.5 ml of 2% aqueous methanol.

The diluted ginkgo extract and the washings (*ca.* 8 ml) are transferred to the polyamide column and sucked through the two columns at a rate of 1 drop/s. The flask is washed three times with a total of 5 ml of 2% aqueous methanol and the washings are transferred to the column as well. The two columns are then washed with 5 ml of 5% aqueous methanol and dried by sucking air through the columns for 2 min with a water pump at maximum suction. The polyamide column is discarded, the C_{18} column is washed with 1 ml of water and again dried for 2 min.

The dried C_{18} column is first washed with 6 ml hexane (washings discarded) and then eluted with 7 ml of hexane–methyl acetate (60:40) into a 20-ml conical flask. After evaporation of the solvent, the residue is dissolved in 70–350 μl of methanol. Subsequently 1.00 μl of benzyl alcohol is added with a Hamilton (Bonaduz, Switzerland) zero-dead-volume Model 7001 injection needle, followed by 130–650 μl of water. The flask is stoppered and placed in a water bath at 50°C. After 5 min, the solution is ready for injection in the HPLC system.

(b) Leaves. The dried leaves are pulverised either mechanically or with a pestil and mortar. Leaves (400–800 mg) are carefully weighed and placed in a 20-ml conical flask, 5 ml of 10% aqueous methanol and a boiling stone are added and the solution is refluxed for 15 min. During the last minute the condenser is removed. The hot solvent is filtered under vacuum over a small Büchner funnel (3.3 cm I.D.) with a filter-paper (Schut, Heelsum, The Netherlands). The flask and the leaves are washed with 2 ml of 2% aqueous methanol. After 1 min of suction the leaves are replaced in the flask and extracted a second time in the same way with 4 ml of 10% aqueous methanol. After filtration the flask and the residue of leaves are washed twice with 1.5 ml of 2% aqueous methanol.

The combined filtrates (*ca.* 12 ml) are transferred to the polyamide column (see above) and drawn through the two columns at a rate of 1 drop/s. The flask is washed three times with a total of 3 ml of 2% aqueous methanol and the washings are transferred to the column.

The remainder of the procedure for the leaves is the same as that for the phytopharmaceuticals from "The two columns are then washed with 5 ml ...".

Determination of response factor

Benzyl alcohol (Aldrich, Milwaukee, WI, U.S.A.) was used as an internal standard. Response factors were calculated for ginkgolide A, B and C and bilobalide by plotting for each of the ginkgo compounds the ratio of the area of the ginkgo peak to that of the internal standard peak (benzyl alcohol) against the ratio of the weight of the ginkgo compound to that of the internal standard. The slope of each line gives the relative response factor. For each ginkgolide seven different weight ratios, varying from 0.00 to 2.1, were used.

Reproducibility of integration

The reproducibility of the integration of the RI signals was determined for each ginkgolide at six different concentrations. Each solution was injected five times and relative standard deviations were calculated.

Recovery experiments

Known amounts of the ginkgolides and bilobalide in aqueous methanol were submitted to the extraction and purification procedure and the recovery was determined. Three different amounts of starting material were investigated. For each amount the purification process was repeated three times. Each extract obtained was injected three times for HPLC analysis.

Quantification

The ginkgo leaves and phytopharmaceuticals to be investigated were analysed two to five times according to the above purification procedure. The concentrations of ginkgolide A, B and C and bilobalide were calculated with the following equation:

$$\text{concentration (ppm)} = \frac{\text{area (G)}}{\text{area (I.S.)}} \times \frac{10^6}{R} \times \frac{1.045}{M}$$

where area (G) is the peak area of the ginkgo compound of interest, area (I.S.) is the peak area of the internal standard (benzyl alcohol), R is the relative response factor of the ginkgo compound (see Table I) and M is either the sample volume of the phytopharmaceutical preparation (μl) or the weight of the ginkgo leaves (mg).

Owing to the poor separation of bilobalide and ginkgolide J in some chromatograms the concentration given for bilobalide includes ginkgolide J, whereas in other chromatograms it was possible to give a separate value for ginkgolide J. As no pure ginkgolide J was available to determine the response factor relative to benzyl alcohol, an estimated value of 1.21 was chosen (average of R_{GB} and R_{GC}).

RESULTS AND DISCUSSION

Although ginkgolides can be determined by gas chromatography (GC) [1] as their trimethylsilyl derivatives, HPLC seems a more logical choice for these relatively polar compounds. All the earlier investigations used RP-HPLC, which gives good separations of the ginkgo compounds [7]. Initially we choose UV detection because of the ready availability of UV detectors, high stability and good sensitivity. The ginkgolides and bilobalide all have poor UV characteristics with $\lambda_{max} = 219$ nm and $\varepsilon \approx 300$ l/mol · cm [13]. Nevertheless, the detection limit was 30 ng, which was more than sufficient for our purposes. Water–methanol (67:33) was used as eluent, which gives a good separation of, in order of increasing retention time, bilobalide and ginkgolide J, C, A and B in 20 min. Only bilobalide and ginkgolide J nearly coelute.

With pure reference compounds several purification procedures were developed using different combinations of solid-phase extraction columns and extraction procedures. Combinations showing adequate recovery were then tested on leaves and sometimes phytopharmaceuticals. Interfering compounds present in ginkgo leaves include many phenolics, *e.g.*, flavonoids and tannins, and more apolar compounds, *e.g.*, chlorophyl, anacardic acids and lipids. Although ginkgolides and especially ginkgolide B are not very soluble in cold water, they are soluble in boiling water and this was found to be a selective primary extraction solvent.

However, many flavonoids are co-extracted and have to be removed because of their high concentration and their much stronger UV absorption, but no single purification column or combination of two or even three solid-phase extraction columns gave an extract that could be analysed by RP-HPLC with UV detection. Purification columns used include C_{18} silica, Diol, Extrelut, polyamide and phenylboronic types. Precipitation agents for phenolics such as Pb^{2+} ions and polyvinylpolypyrollidone (PVPP) did not improve the chromatograms.

The best results were eventually obtained with a combination of a polyamide and a C_{18} column. The polyamide column removes most of the phenolics. The non-retained ginkgolides are then retained by the C_{18} purification column if the methanol content is low enough. By increasing the elution strength the ginkgolides can easily be removed from the C_{18} column. However, even leaves with a high content of ginkgolides gave poor chromatograms with this procedure and UV detection. Fig. 1a shows the chromatogram of an already partially purified phytopharmaceutical with a high content of terpenoids after the polyamide–C_{18} column work-up. Only at the end of the chromatogram is the baseline back to zero. Leaves could not be analysed at all.

We therefore tried this clean-up procedure in combination with RI detection. This immediately gave much better results and, after some modifications, this method was also usable for leaves and phytopharmaceuticals with a low yield of ginkgolides. Fig. 1b shows the same purified extract as in Fig. 1a analysed under identical conditions except that RI detection instead of UV detection was used. The noise level is naturally much higher but the baseline immediately returns to zero after the solvent and essentially no peaks other than those of the terpenoids of interest are observed. Apparently the unwanted compounds still present in the purified extract occur in low concentrations relative to the ginkgolides but possess ε values at 219 nm which are *ca.* 100 times higher than those for the ginkgolides. Hence the RI detector, which shows much less variation in response factors, is better suited even though the sensitivity and

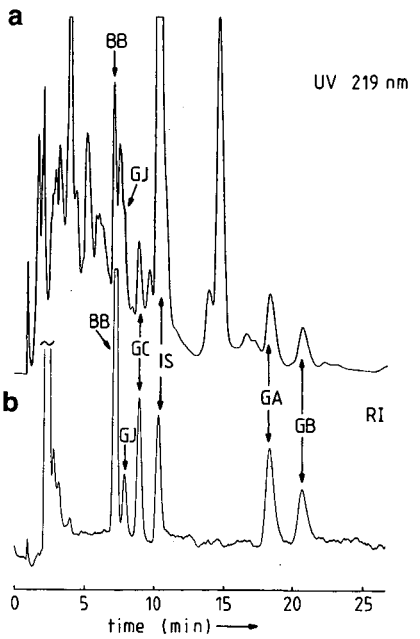

Fig. 1. HPLC traces of 1.00 ml of Tanakan preparation purified according to extraction and purification procedure (a). Solvent 3; flow-rate, 1.0 ml/min. BB = Bilobalide; IS = internal standard (benzyl alcohol); GJ, GC, GA, GB = ginkgolide J, C, A and B, respectively. (a) UV detection (220 nm); (b) RI detection.

baseline stability are much poorer. The detection limit was 0.5 μg for bilobalide and ginkgolide C and 1 μg for ginkgolide A and B. For quantitative purposes ten times more is needed, which means that the purified extract obtained after the last purification column is usually too dilute for direct analysis by HPLC. The final extract has to be evaporated and the residue dissolved in a small volume (0.2–1.0 ml) of the HPLC eluent before injection. Because water is difficult to evaporate quickly we tried to elute the ginkgolides with a purely organic solvent. Hexane–ethyl acetate (6:4) or hexane–methyl acetate (6:4) gave good results. As ethyl acetate is more difficult to evaporate and appeared as an additional peak in the chromatogram near ginkgolide J and C, methyl acetate, which lacks these disadvantages, was chosen. A wash step with hexane just prior to the hexane–methyl acetate elution was necessary to remove the water still present on the C_{18} column after drying. Hexane does not remove ginkgolides because they are totally insoluble in this solvent.

Another modification was the addition of a few percent of methanol to the primary extraction solvent, which increased the extraction efficiency. Removal of the methanol before transferring the extract onto the polyamide by boiling briefly without a reflux condenser was necessary to retain as much impurities as possible on the polyamide column. A small percentage of methanol was left in the various conditioning, washing and elution solvents to increase the retention of the C_{18} solid-phase extraction column. This method could also be used for phytopharmaceutical preparations if their initial high alcohol content (50–60%) was lowered almost to zero by boiling for 5 min in an open flask.

TABLE I

RESPONSE FACTORS OF GINKGOLIDE A, B AND C AND BILOBALIDE

Compound	Response factor	Correlation coefficient
Ginkgolide A	1.12	0.9988
Ginkgolide B	1.16	0.9972
Ginkgolide C	1.26	0.9989
Bilobalide	1.11	0.9984

To avoid fixed end volumes and to make the method usable by laboratories which do not possess pure ginkgolides, benzyl alcohol as an internal standard was added just prior to the HPLC analysis. Relative response factors for ginkgolide A, B and C and bilobalide were determined and are reported in Table I. The relative standard deviation in the integration process is dependent on the concentration and becomes considerable at concentrations of 100 ppm or lower (see Table II).

The recovery of the whole filtration and purification process was determined for various initial concentrations of the ginkgo constituents. The results are presented in Table III. The recovery was 95 ± 5% for all concentrations except for very high concentrations of ginkgolide B. The reason for this is the very poor solubility of this compound in water (0.01%). Concentrated solutions of ginkgolide B in water have a tendency to form crystals which do not redissolve easily. Most of the ginkgolide B in the most concentrated test solutions remained as tiny crystals on the polyamide column. With leaves or phytopharmaceutical preparations containing higher concentrations than the reference solutions there was never any evidence of crystallization of ginkgolide B. Probably other substances present in ginkgo leaves keep ginkgolide B in solution. Only in the final solution for injection into the HPLC system, which sometimes contains high concentrations of the ginkgolides (> 0.1%), could crystallization again be observed. This could be prevented by warming the solution in a closed flask at 50°C.

The efficiency of the extraction of the leaves was determined by extracting the leaves for 30 min a third time after the first two times. It was found that an additional 1.8% of ginkgolide C and bilobalide, 3.5% of ginkgolide A and 4.5% of ginkgolide B

TABLE II

RELATIVE STANDARD DEVIATIONS OF INTEGRATION RESULTS FOR GINKGOLIDE (G) A, B AND C AND BILOBALIDE (BB) (n = 3)

Concentration (μg/ml)	Relative standard deviation (%)			
	G-A	G-B	G-C	BB
100	3.8	14.3	5.6	6.0
200	7.5	4.8	3.4	3.8
300	5.2	3.4	5.2	2.4
435	3.7	2.4	3.6	1.6
625	2.2	3.4	1.5	0.8
800	2.0	1.5	1.3	1.4

TABLE III

RESULTS OF RECOVERY EXPERIMENTS

For conditions, see Experimental (n = 3)

Compound	Initial amount (μg)	Recovery (%)	Relative standard deviation (%)
Bilobalide	2140	98.8	2.2
	719	98.5	2.9
Ginkgolide C	1160	102.5	9.2
	615	90.1	3.1
	290	97.3	5.8
Ginkgolide A	1300	96.6	0.6
	738	94.8	2.6
	320	97.0	8.9
Ginkgolide B	708	86.9	2.5
	590	92.3	2.5
	150	99.5	7.9

could be extracted. Thus in the normal procedure 95–98% of the ginkgolides and bilobalide are extracted.

As there is always a possibility that an impurity which is not removed during the purification process coelutes with one of the compounds of interest, the purity of the peaks was assessed. A larger amount of leaves with a high content of ginkgolides was purified in the usual manner and then separated on a preparative column. The peaks corresponding with ginkgolide A, B, C and J and bilobalide were collected, evaporated and then reinjected onto an analytical column with a tetrahydrofuran-containing solvent. Such solvents have a large influence on the capacity factors of ginkgolide A, B and C and bilobalide [7]. The chance that a possible interfering compound undergoes exactly the same shift in retention can be considered small. The appearance of one or more peaks in addition to the ginkgolide peak is then evidence for an impurity co-eluting in the standard water–methanol (67:33) solvent. No peaks larger than the noise level were observed, so no major impurities co-elute.

Finally, the reproducibility of the method when applied to leaves with a high ginkgolide content was determined. For this purpose four samples of 500 mg of leaves were extracted and purified according to the standard procedure. Each of the four extracts was analysed three times by HPLC. The results are given in Table IV. For leaves and phytopharmaceuticals with a low content of ginkgolides the relative errors become larger owing to larger integration errors (see also Table II). If "electronic noise" and not "chemical noise" is the main problem, decreasing the volume of the final solution from 1.0 to 0.3 ml gives more reliable data.

The method was applied on some commercial ginkgo preparations. The results are given in Table V. Two corresponding chromatograms are shown in Fig. 2. Tebonin and Rökan look similar to Tanakan in Fig. 1b. It is immediately clear that controlled partially purified ginkgo medicines (Rökan, Tanakan, Tebonin) contain much higher concentrations of ginkgolides and bilobalide than Dutch phytopharma-

TABLE IV

REPRODUCIBILITY OF EXTRACTION AND PURIFICATION PROCESS FOR 500 mg OF GINKGO LEAVES (n = 4)

Compound	Weight (μg)					Standard deviation (μg)	Relative standard deviation (%)
	1	2	3	4	Average		
Bilobalide	531	507	517	520	519	10	1.9
Ginkgolide C	316	313	321	327	319	6	1.9
Ginkgolide A	226	224	218	232	225	6	2.6
Ginkgolide B	197	196	205	196	198	4	2.2

ceuticals (see Fig. 2a), which are prepared according to the homeopathic pharmacopoeia. This is not surprising as, according to this pharmacopoeia, 10 kg of fresh leaves, which correspond to *ca.* 2.5 kg of dry leaves, give *ca.* 20 l of ginkgo tincture. The partially purified French and German preparations contain far more "leaves"/ml. The ginkgogink preparation is entirely different from all the others. It contains high concentrations of all the ginkgolides but bilobalide could not be detected. As bilobalide is the major terpenoid in all the leaves and other phytopharmaceuticals investigated, this suggests that the bilobalide has been selectively removed during the manufacturing process. Some extra peaks not present in any other sort of leaves or phytopharmaceuticals can be observed at the beginning of the chromatogram (see Fig. 2b).

According to Stumpf [11], Tebonin extract contains at least 0.12% of "ginkgolides". We found a total of 0.115% (excluding bilobalide) or 0.21% (including bilobalide), which is in agreement with his claim. Hence the HPLC–TLC procedure put forward by Wagner *et al.* [10] is indeed not usable. According to Drieu [14], Tanakan contains 0.24% of ginkgolides and bilobalide. We found 0.22%. As we do not know how they determined these compounds, it is difficult to say whether their determination gives systematically slightly higher results than ours or whether the

TABLE V

GINKGOLIDE (G) A, B, C AND J AND BILOBALIDE (BB) CONCENTRATIONS IN GINKGO PHYTOPHARMACEUTICALS

For Dutch preparations only a combined value for bilobalide and ginkgolide J is given.

Phytopharmaceutical	Concentration in μg/ml fluid					Total (%)
	BB	G-J	G-C	G-A	G-B	
Geriaforce A (Dutch)	98		20	26	24	0.017
Geriaforce B (Dutch)	80		22	23	21	0.015
Ginkgoplant (Dutch)	72		18	27	16	0.013
Naphyto DØ (Dutch)	58		22	24	19	0.012
Ginkgogink (French)	<20	120	363	372	256	0.111
Tanakan (French)/	943	184	336	460	278	0.220
Rökan (German)	921	174	280	360	180	0.192
Tebonin (German)	988	167	302	398	279	0.213

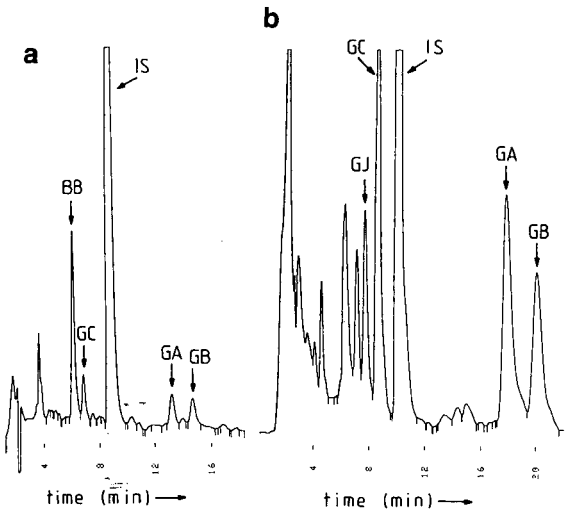

Fig. 2. HPLC traces of 1.00 ml of commercial fluid ginkgo phytopharmaceuticals after purification according to extraction and purification procedure (a). Solvent 3; flow-rate, 1.0 ml/min; RI detection. Abbreviations as in Fig. 1. Sample: (a) Geriaforce; (b) Ginkgogink.

batch is below their specification. If we make a 3–4% correction for the usual losses (see recovery experiments) the difference is hardly significant.

Some different leaves were compared and large variations were found (see Table VI). French leaves contained the highest amount of ginkgolides. Dutch leaves from the good summer of 1989 contained almost as much bilobalide but *ca.* 40% less ginkgolides, whereas Chinese leaves, German leaves (1989) and Dutch leaves (1987) contained much less. Dutch leaves from May 1990 contained a small amount of bilobalide and no detectable ginkgolides. Apparently the sun and the time of harvest play an important role in the yield of these terpenoids. In all instances the bilobalide

TABLE VI

GINKGOLIDE (G) A, B, C AND J AND BILOBALIDE (BB) CONCENTRATION IN GINKGO LEAVES

For Chinese leaves only a combined value for bilobalide and ginkgolide J is given.

Origin of leaves	Date of collection	Concentration in μg/g dry leaf					Total (%)
		BB	G-J	G-C	G-A	G-B	
Chinese	–	758		162	265	155	0.134
Dutch	Oct. 1987	318	7	9	17	21	0.037
Dutch	Sept. 1989	1100	42	260	380	220	0.196
Dutch	May 1990	65	<2	<2	<3	<3	0.006
French	–	1250	190	424	646	348	0.266
French	Aug. 1982	964	74	638	450	396	0.252
German	Sept. 1989	290	<4	<4	<4	29	0.032

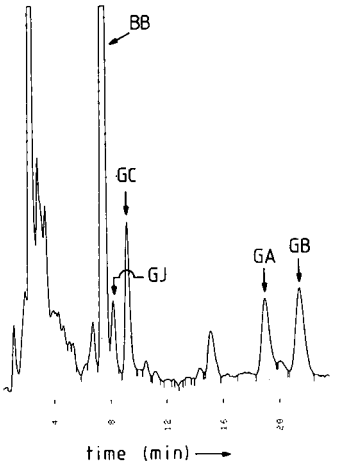

Fig. 3. HPLC trace of 1.000 g of Dutch *Ginkgo biloba* leaves (September 1989) after purification according to extraction and purification procedure (b). Solvent 3; flow-rate, 1.0 ml/min; RI detection. Abbreviations as in Fig. 1.

content was equal to or higher than that of the total ginkgolides. A typical chromatogram is presented in Fig. 3.

CONCLUSION

Selective extraction of ginkgo leaves with methanol–water (10:90) followed by a sample clean-up with a polyamide and a C_{18} solid-phase extraction column in series gives an extract that can be readily analysed by RP-HPLC with RI detection. All the leaves and phytopharmaceuticals investigated were found to contain bilobalide and ginkgolides, although large differences between different leaf batches or ginkgo preparations from different manufacturers were observed.

Owing the intrinsic poor stability and sensitivity of the RI detector, the minimum concentration that can be determined with acceptable accuracy is fairly high (*ca.* 10 ppm). Improvements to the proposed analytical procedure should in the first place concentrate on this aspect.

ACKNOWLEDGEMENTS

We thank Professor K. Weinges (University of Heidelberg) for his repeated and generous gifts of bilobalide and ginkgolide A, B and C, without which this work could not have been carried out. We also thank Professor K. Nakanishi (University of New York) for his gift of some of the original ginkgolide A, B and C, Dr. P. Braquet and Dr. B. P. Teng (Institut Henri Beaufour) for their gifts of Tanakan and a sample of French ginkgo leaves, Dr. G. Massiot (University of Reims) for his gift of ginkgogink, Dr. D. O. Wijnands and T. J. Stoker (Botanical Garden, University of Wageningen) for their gifts of Dutch ginkgo leaves, Mr. A. van Veldhuizen for recording the NMR spectra and F. Griepink for technical assistance.

REFERENCES

1 P. Braquet, *Drugs Future*, 12 (1987) 643.
2 H. Schilcher, *Z. Phytother.*, 9 (1988) 119.
3 D. Hosford, J. M. Mencia-Huerta, C. Page and P. Braquet, *Phytother. Res.*, 2 (1988) 1.
4 *Presse Med.*, 15 (1986) 1438 [special issue on extract of *Ginkgo biloba* (EGb 761)].
5 P. Braquet (Editor), *Ginkgolides —Chemistry, Biology, Pharmacology and Clinical Perspectives*, J. R. Prous Science, Barcelona, 1988.
6 A. Guth, F. Briançon-Scheid, M. Haag-Berrurier and R. Anton, *Planta Med.*, 42 (1981) 129.
7 A. Lobstein-Guth, F. Briançon-Scheid and R. Anton, *J. Chromatogr.*, 267 (1983) 431.
8 B. P. Teng, in P. Braquet (Editor), *Ginkgolides —Chemistry, Biology, Pharmacology and Clinical Perspectives*, J. R. Prous Science, Barcelona, 1988, p. 37.
9 Y. Komoda, H. Nakamura and M. Uchida, *Iyo Kizai Kenkyusho Hokoku*, 22 (1988) 83.
10 H. Wagner, S. Bladt, U. Hartmann, A. Daily and W. Berkulin, *Dtsch. Apoth.-Ztg.*, 129 (1989) 2421.
11 H. Stumpf, *Dtsch. Apoth.-Ztg.*, 129 (1989) 2794.
12 P. G. Pietta, P. L. Mauri and A. Rava, *Chromatographia*, 29 (1990) 251.
13 K. Okabe, K. Yamada, S. Yamamura and S. Takada, *J. Chem. Soc. C*, (1967) 2201.
14 K. Drieu, *Presse Med.*, 15 (1986) 1455.

Journal of Chromatography, 543 (1991) 389–395
Elsevier Science Publishers B.V., Amsterdam

CHROM. 23 131

Separation and quantification of 1,4-benzoxazin-3-ones and benzoxazolin-2-ones in maize root extract by high-performance liquid chromatography

Y. S. XIE
Ottawa-Carleton Institute of Biology, University of Ottawa, Ottawa, Ontario K1N 6N5 (Canada)
J. ATKINSON
Ottawa-Carleton Institute of Chemistry, University of Ottawa, Ottawa, Ontario K1N 6N5 (Canada)
J. T. ARNASON*
Ottawa-Carleton Institute of Biology, University of Ottawa, Ottawa, Ontario K1N 6N5 (Canada)
P. MORAND
Ottawa-Carleton Institute of Chemistry, University of Ottawa, Ottawa, Ontario K1N 6N5 (Canada)
and
B. J. R. PHILOGÈNE
Ottawa-Carleton Institute of Biology, University of Ottawa, Ottawa, Ontario K1N 6N5 (Canada)
(First received July 2nd, 1990; revised manuscript received January 16th, 1991)

ABSTRACT

A high-performance liquid chromatography method is described for the separation and quantification of 1,4-benzoxazin-3-ones and benzoxazolin-2-ones in maize root extract. The four compounds, 2,4-dihydroxy-7-methoxy-1,4-benzoxazin-3(4H)-one, 2,4-dihydroxy-7,8-dimethoxy-1,4-benzoxazin-3(4H)-one, 2-hydroxy-7-methoxy-1,4-benzoxazin-3(4H)-one and 6-methoxybenzoxazolinone, were separated and identified within 30 min on a C_{18} reversed-phase column using a gradient of methanol and phosphoric acid. The technique has useful applications in studies of the chemical ecology of plant root and subterranean pest interactions.

INTRODUCTION

It is well known that 1,4-benzoxazin-3-ones are present in several species of Gramineae, such as maize, wheat [1] and rye [2]. Some of these compounds and their decomposition products have been found to play an important role in the resistance of plants to insect pests such as European corn borer, *Ostrinia nubilalis* (Hübner) [3], cereal aphids, *Rhopalosiphum maidis* (Fitch) [4], *Metopolophium graminum* (Walker) [5] and to plant pathogenic fungi, *Helminthosporium turcicum* [6] and bacteria, *Erwina carotovia* [7]. We recently found 2,4-dihydroxy-7-methoxy-1,4-benzoxazin-3-one (DIMBOA), a major 1,4-benzoxazin-3-one in maize, to be toxic to western corn rootworm, *Diabrotica virgifera virgifera* (LeConte) [8].

During the past three decades, several methods have been developed to separate

0021-9673/91/$03.50

and to quantify 1,4-benzoxazin-3-ones and related compounds. The simplest method available is to measure total hydroxamic acid content by measuring the absorbance of the blue complex formed between hydroxamic acids and $FeCl_3$ [9–11]. This method can only estimate total cyclic hydroxamic acids as $FeCl_3$ does not react with benzoxazolinones. Another method is based on the assumption that 1 mole of hydroxamic acid (2,4-dihydroxy-7-methoxy-1,4-benzoxazin-3(4H)-one, DIMBOA) produces 1 mole of benzoxazolinone (6-methoxybenzoxazolinone, MBOA) after degradation, and measures hydroxamic acid content as benzoxazolinones. The benzoxazolinones were quantified by isotopic dilution [3], infrared spectrophotometry [12], fluorometry [13], gas chromatography (GC) [14] and by high-performance liquid chromatography (HPLC) [15]. However, it has been found that the amount of MBOA formed from DIMBOA varies with temperature, pH and composition of the reaction medium and always yields less than 75% of MBOA from DIMBOA [16]. Therefore, it is clear that these methods can lead to erroneous estimates of DIMBOA content in plant extracts. More recently, GC and HPLC methods have been developed which can separate and quantify individual cyclic hydroxamic acids and related compounds [14,17–20].

Most of the authors cited above used plant leaves (corn or wheat) as experimental materials to quantify the compounds concerned, although Klun and Robinson [21] have reported that corn root, compared with corn stalk, whorl and leaf, contains the highest concentration of 1,4-benzoxazinones. Corn roots have been used as experimental materials to quantify total cyclic hydroxamic acids [22,23], but none of these studies has quantified the individual hydroxamic acids and/or related compounds. Our previous work [8] has demonstrated that DIMBOA, the main hydroxamic acid in maize, plays an important role in the defence of maize to the western corn rootworm, a serious insect pest which damages the corn root system. To understand the chemical ecology of corn root subterranean pest interactions, it is necessary to develop a method for the quantitative determination of the content of individual hydroxamic acids and related compounds in corn root.

In this paper we report an accurate HPLC method for separation and quantification of two hydroxamic acids, 2,4-dihydroxy-7-methoxy-1,4-benzoxazin-3(4H)-one (DIMBOA), 2,4-dihydroxy-7,8-dimethoxy-1,4-benzoxazin-3(4H)-one (DIM_2BOA), one lactam, 2-hydroxy-7-methoxy-1,4-benzoxazin-3(4H)-one (HMBOA) and one benzoxazolinone, 6-methoxybenzoxazolinone (MBOA) (Fig. 1) in corn root extracts.

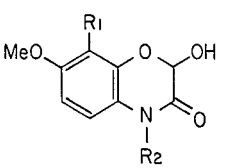

1,4-benzoxazin-3-ones

R1	R2	Abbreviation
H	OH	DIMBOA
MeO	OH	DIM_2BOA
H	H	HMBOA

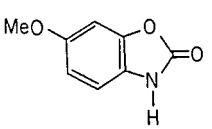

benzoxazolin-2-one
(MBOA)

Fig. 1. 1,4-Benzoxazin-3-ones and benzoxazolin-2-one found in maize root extracts. Me = Methyl.

It represents the first gradient HPLC method to separate a variety of hydroxamates and derivatives in maize root extracts.

EXPERIMENTAL

Standard compounds

All standard compounds (DIMBOA, DIM_2BOA, HMBOA and MBOA) were synthesized in our laboratory, and the complete synthetic details were described by Atkinson [24].

Extract sample preparation

Seeds of maize (*Zea mays* L.) (hybrid 359GC3-6 × 46-43) were soaked in tap water for 24 h and planted in a plastic pot (15 cm × 15 cm) with growing medium of one part perlite and one part vermiculite. Greenhouse temperature was maintained at approximately 22/20°C day/night and the photoperiod was 12L:12D (12 h light:12 h dark; 12 h light provided by natural sunlight plus 3 h artificial light at the beginning and at the end of the photoperiod). After two weeks of growth under these conditions, corn roots were taken out and washed with tap water, then with distilled water. One gram of this fresh root material was cut in small pieces and homogenized with 2 × 5 ml distilled water using a mortar and pestle. The slurry was extracted by a modification of the method described by Gutierrez *et al.* [18].

Apparatus and HPLC procedures

The root extract in methanol was analyzed using a Perkin-Elmer HPLC system equipped with a Model 250 binary pump, and a Model LC-480 auto scan diode-array detector. A 20-μl volume of the extract sample in methanol was injected into the liquid chromatography system. The sample was run under the following conditions: Ultrasphere ODS 5 μm, 25 cm × 4.6 mm reversed-phase C_{18} column (Beckman); a flow-rate of 1 ml/min; detection wavelength of 265 nm; an online UV scan of 190–400 nm; and a two-solvent system, solvent A 100% methanol and solvent B 20 m*M* H_3PO_4 (pH 2.3), was used as a mobile phase. A gradient program was processed as follows: Solvent A at the initiation was 10%; then when sample was injected, 10% A was linearly altered to 56% A in 25 min, and then to 100% A in 2 min. This ratio was held for 4 min to clean the column, after which the mobile phase was returned to the starting concentration (10% A) in 2 min. This ratio was maintained for 2 min to equilibrate the column.

Identification and quantitation of 1,4-benzoxazin-3-ones and benzoxazolin-2-ones

Identification of 1,4-benzoxazin-3-ones and benzoxazolin-2-ones in corn root extract was carried out by comparison of retention times, UV spectra and by peak enrichment of known standard compounds. Quantitation of related compounds was derived from standard curves created by a dilution series (0–20 μg) of different compounds. Three replicates were prepared for each concentration.

Recovery efficiencies

A triplicate of different concentrations of DIMBOA, DIM_2BOA, HMBOA and MBOA were separately added to an erlenmeyer (7 cm × 7 cm) containing 1 g of

homogenated tissue from corn root and the extraction was processed as described above. In order to detect how much of the reference compounds was lost by binding to the tissue, a triplicate of different concentrations of the reference compounds were added to an erlenmeyer containing solvent (ethyl acetate) alone and the same extraction procedure was carried out.

RESULTS AND DISCUSSION

The purity of DIMBOA, DIM_2BOA, HMBOA and MBOA standards were checked by HPLC. Under the HPLC procedures described above, each of the standards showed one peak. When a standard mixture of DIM_2BOA, HMBOA, DIMBOA and MBOA was injected into the HPLC system, four peaks were resolved within 25 min with a retention time of 18.95 min (DIM_2BOA), 20.10 min (HMBOA), 20.83 min (DIMBOA) and 24.32 min (MBOA), respectively. The retention times of the mixture of four standards were almost identical as when they were injected individually.

A typical chromatogram of a corn root sample extracted for 1,4-benzoxazin-3-ones and related compounds is shown in Fig. 2. DIM_2BOA, HMBOA, DIMBOA and MBOA were identified as the major compounds in corn root extracts based on comparison of retention times and spectra. Other minor hydroxamates appear to be present in the extract sample shown in Fig. 2, but we have, so far, no available data for the identification and quantification.

Fig. 3 shows typical UV spectra of 1,4-benzoxazin-3-ones and related compounds in corn root extracts which are useful in confirmation of the identification of the compounds concerned. DIM_2BOA, HMBOA and DIMBOA have similar but distinct UV spectra with absorbance maxima at wavelengths of 264 nm, 261 nm (shoulder 289 nm) and 264 nm (shoulder 292 nm), respectively. MBOA has two absorbance peaks with maxima of 230 nm and 292 nm.

Quantitative estimates of the identified compounds were derived from standard curves for DIM_2BOA, HMBOA, DIMBOA and MBOA. Regression formulas for the quantitation of different compounds in practical samples were: y (μg DIM_2BOA/ml sample) = 31.99 + 7548.50 · (absorbance units) (r = 0.99, $P < 0.001$); y (μg

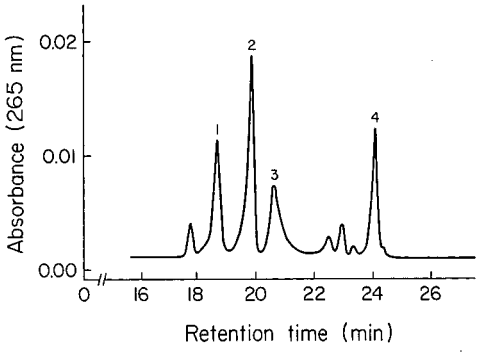

Fig. 2. Chromatogram of maize root extracts separated by the conditions as described in the text. 1 = DIM_2BOA; 2 = HMBOA; 3 = DIMBOA; 4 = MBOA.

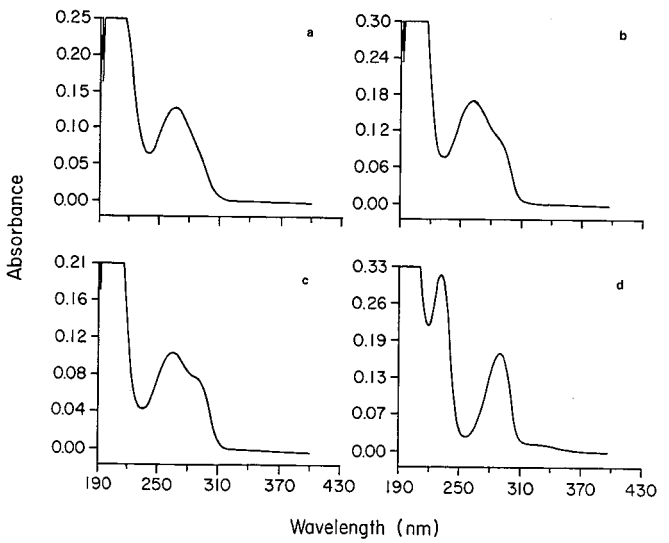

Fig. 3. UV spectra of 1,4-benzoxazin-3-ones and benzoxazolin-2-one in a maize root extract. (a) DIM_2BOA; (b) HMBOA; (c) DIMBOA; (d) MBOA.

HMBOA/ml sample) = 11.42 + 2627.00 · (absorbance units) (r = 0.98, $P <$ 0.0001); y (μg DIMBOA/ml sample) = 96.29 + 10898.50 · (absorbance units) (r = 0.99, $P < 0.0001$; y (μg MBOA/ml sample) = 63.79 + 12360.50 · (absorbance units) (r = 0.99, $P < 0.0001$). By using these formulas, concentrations of compounds in practical samples were calculated, and Table 1 shows the analysis of two different corn lines which were used for the study of corn resistance to western corn rootworm [8]. ITR 3872 contains considerably more of all the hydroxamates, which we believe explains its demonstrated resistance to rootworm [8].

The limits of detection of the present method were determined from a dilution series. It appears that this method can detect 1 μg/ml for DIM_2BOA, DIMBOA and MBOA, and 0.5 μg/ml for HMBOA. The accuracy of the present method was evaluated by a recovery test. Triplicate known amounts of each compound were individually added to an erlenmeyer containing 1 g of homogenated root sample and processed according to the extraction procedure. The results are shown in Fig. 4. The intercept values in these plots represent the original amounts of each known compound found in the root sample without adding any known compounds. The recoveries are represented by the slopes of the regressions. The recoveries of

TABLE I

CONTENTS OF 1,4-BENZOXAZIN-3-ONES AND BENZOXAZOLIN-2-ONES IN TWO DIFFERENT MAIZE LINES (μg/g FRESH ROOT)

Maize line	DIM_2BOA	HMBOA	DIMBOA	MBOA
ITR 3872	120.95	86.96	718.48	214.14
NTR-2 Ger. 4042	2.72	9.78	36.20	69.64

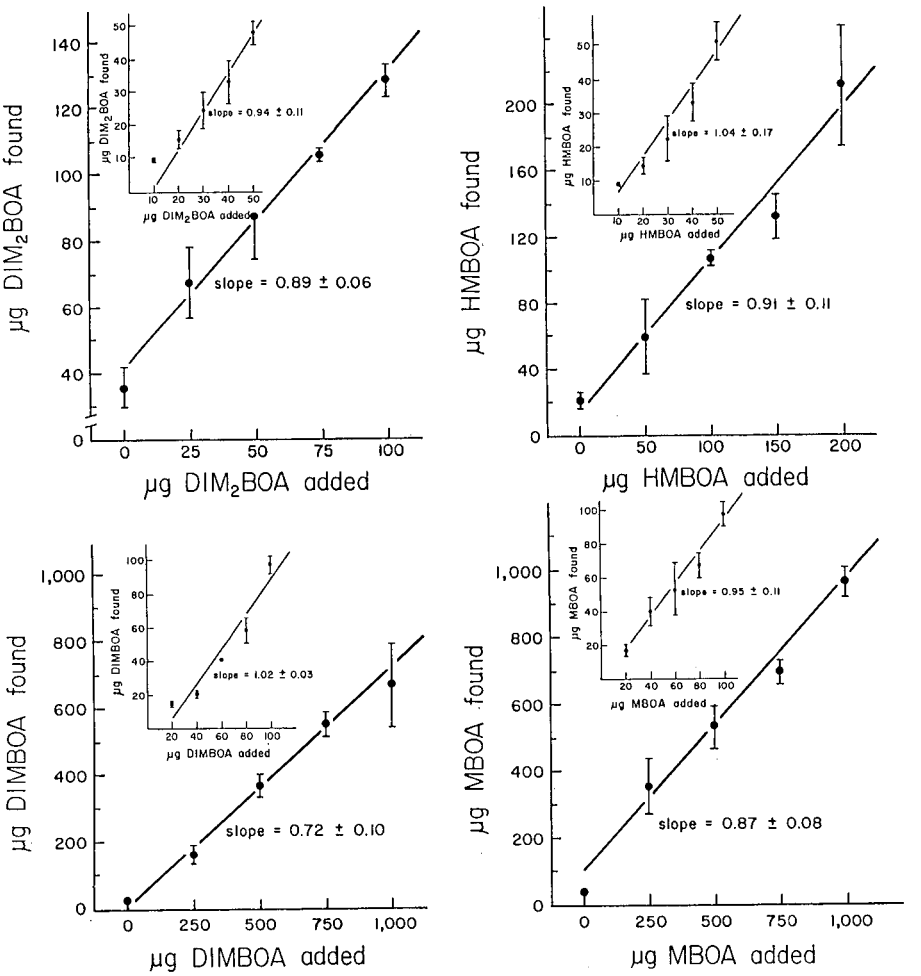

Fig. 4. Recovery of DIM_2BOA, HMBOA, DIMBOA and MBOA added to maize root samples prior to extraction and HPLC analysis. In each plot, the intercept values with *y* axes represent the original amount of the compounds present in the samples; the slope of each regression is equal to the fraction of the compounds recovered. The figures in the corners show the recovery of the compounds added to solvent (ethyl acetate) alone prior to extraction and HPLC analysis. Bars indicate standard deviation.

DIM_2BOA, HMBOA, DIMBOA and MBOA were 89 ± 4%, 91 ± 11%, 72 ± 10% and 87 ± 8% (mean ± S.D.). The recovery of DIMBOA was relatively low, due to decomposition of DIMBOA to MBOA. When the extraction was carried out with solvent (ethyl acetate) alone (no added plant tissue), the recoveries of DIM_2BOA, HMBOA, DIMBOA and MBOA were obviously increased (Fig. 4). This may be the result of cyclic hydroxamic acids reacting with plant tissue. It has been reported that cyclic hydroxamic acids react with protein thiol groups, which is one possible cause of yield loss and one of the unavoidable problems in quantification of cyclic hydroxamic acids [25,26].

The standard deviations in Fig. 4 are large for most data points. In comparison with the standard deviation in standard curves (>0.5%), it indicates that the main source of error appeared in the extraction procedure rather than in the separation method used.

The HPLC procedure reported here is a rapid and accurate method for separation and quantification of individual 1,4-benzoxazin-3-ones and related compounds in corn root extracts. Compared with GC, the present HPLC method eliminates the derivatization step and can separate and quantify at least four 1,4-benzoxazin-3-ones and related compounds within 30 min.

ACKNOWLEDGEMENTS

This research was supported by the Ontario Ministry of Agriculture and Food, and the Natural Sciences and Engineering Research Council of Canada.

REFERENCES

1 Ö. Wahlroos and A. I. Virtanen, *Acta Chem. Scand.*, 13 (1959) 1906.
2 E. Honkanen and A. I. Virtanen, *Acta Chem. Scand.*, 14 (1960) 504.
3 J. A. Klun and T. A. Brindley, *J. Econ. Entomol.*, 59 (1966) 711.
4 B. J. Long, G. M. Dunn, J. S. Bowman and D. G. Rouley, *Crop Sci.*, 17 (1977) 55.
5 V. H. Argandoña, J. G. Luza, H. M. Niemeyer and L. J. Corcuera, *Phytochem.*, 19 (1980) 1665.
6 B. J. Long, G. M. Dunn and D. G. Routley, *Crop Sci.*, 15 (1975) 333.
7 L. J. Corcuera, M. D. Woodward, J. P. Helgeson, A. Kelman and C. D. Upper, *Plant Physiol.*, 61 (1978) 791.
8 Y. S. Xie, J. T. Arnason, B. J. R. Philogène, J. D. H. Lambert, J. Atkinson and P. Morand, *Can. Ent.*, 122 (1990) 1177.
9 R. H. Hamilton, *J. Agric. Food Chem.*, 12 (1964) 14.
10 B. J. Long, G. M. Dunn and D. G. Routley, *Crop Sci.*, 14 (1974) 601.
11 V. H. Argandoña, H. M. Niemeyer and L. J. Corcuera, *Phytochem.*, 20 (1981) 673.
12 A. J. Scism, J. N. Bemiller and A. L. Caskey, *Anal. Biochem.*, 58 (1974) 1.
13 M. C. Bowan, M. Beroza and J. A. Klun, *J. Econ. Entomol.*, 61 (1968) 120.
14 C. S. Tang, S. H. Chang, D. Hoo and K. H. Yanagihara, *Phytochem.*, 14 (1975) 2077.
15 A. Pessi and D. Scalorbi, *J. Chromatogr.*, 177 (1979) 162.
16 M. D. Woodward, L. J. Corcuera, J. P. Helgeson and C. D. Upper, *Plant Physiol.*, 61 (1978) 796.
17 M. D. Woodward, L. J. Corcuera, J. P. Helgeson, A. Kelman and C. D. Upper, *Plant Physiol.*, 63 (1979) 14.
18 C. Gutierrez, A. Guerrero, P. Castanera and J. V. Torres, *J. Agric. Food Chem.*, 30 (1982) 1258.
19 P. C. Lyons, J. D. Hipskind, K. V. Wood and R. L. Nicholson, *J. Agric. Food Chem.*, 36 (1988) 57.
20 H. M. Niemeyer, E. Pesel, S. Franke and W. Franke, *Phytochem.*, 28 (1989) 2307.
21 J. A. Klun and T. A. Robinson, *J. Econ. Entomol.*, 62 (1969) 214.
22 L. Jr. Thompson, F. W. Slife and H. S. Butler, *Weed Sci.*, 18 (1970) 509.
23 V. H. Argandoña and L. J. Corcuera, *Phytochem.*, 24 (1985) 177.
24 J. K. Atkinson, *Ph.D. Thesis*, University of Ottawa, Ottawa, 1989.
25 H. M. Niemeyer, L. J. Corcuera and F. J. Pèrez, *Phytochem.*, 21 (1982) 2287.
26 F. J. Pèrez and H. M. Niemeyer, *Phytochem.*, 24 (1985) 2963.

Journal of Chromatography, 543 (1991) 397–404
Elsevier Science Publishers B.V., Amsterdam

CHROM. 23 116

Chromatographic analysis of some commercial samples of camphene via cyclodextrin inclusion processes

DANUTA SYBILSKA*, JOANNA KOWALCZYK, MONIKA ASZTEMBORSKA, TOMASZ STANKIEWICZ and JANUSZ JURCZAK

Institute of Physical Chemistry and Institute of Organic Chemistry, Polish Academy of Sciences, Kasprzaka 44/52, 01-224 Warsaw (Poland)

(First received October 31st, 1990; revised manuscript received January 14th, 1991)

ABSTRACT

A gas–liquid chromatographic system containing α-cyclodextrin in formamide medium (coated on Celite) was found to be useful for the separation of camphene enantiomers, with a separation factor α $[t'_R(-)/t'_R(+)]$ equal to 3.6 (at 30°C). The packing was applied in the analytical mode for a study of the composition of five commercial camphenes, and in the micropreparative mode to establish the enantiomeric composition of separated camphenes.

INTRODUCTION

Terpenes are found in large amounts in most plants, and are of special interest because of their industrial uses and on account of their chemical properties and biological activity. The very large number of possible stereoisomers within each group of terpenes makes it very difficult to obtain pure reference compounds, especially enantiomers. In fact, most commercially available terpenes derived from natural sources are of variable composition and variable enantiomeric purity. Hence methods for their exact analysis and the determination of their enantiomeric purity are of crucial importance.

Nevertheless, the chromatographic separation of enantiomeric hydrocarbons presents a number of difficulties, because they are very resistant to diastereoisomer formation. The use of optically active organic stationary phases cannot be applied on the basis of the 'three-point attachment' concept of Dalgliesh [1] because hydrocarbon molecules do not contain any functional groups able to form the necessary hydrogen bonds for specific attachment of enantiomers.

Recently, chiral metal complexes were applied in high-performance liquid chromatography (HPLC) and gas–liquid chromatography (GLC) for the resolution of some olefins into enantiomers [2–7]. However, in this instance π-donor–acceptor interactions, being possible only for unsaturated hydrocarbons, take place. Chiral saturated hydrocarbons cannot be recognized in this way.

Subsequently it was discovered that the stereoselective fitting of α- and β-pi-

0021-9673/91/$03.50

nenes and *cis*- and *trans*-pinanes to the α-cyclodextrin (α-CD) cavity permits the very efficient resolution of their enantiomers under GLC conditions [8–11]. Another approach was initiated recently by König and co-workers [12,13] and subsequently by Armstrong and co-workers [14,15] involving the use of some molten CD derivatives of relatively low fusibility in capillary GC. Although numerous efficient separations of various chiral compounds have been reported [12–15], only one example concerns terpenoic hydrocarbons, *viz.*, limonene.

This paper reports some further systematic studies on the application of CD solutions to enantioselective separations of various hydrocarbons and it focuses attention on the enantiomeric camphenes.

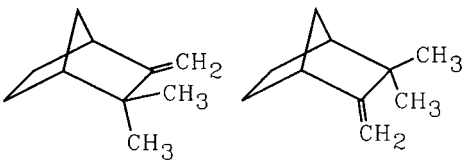

(+)-camphene (-)-camphene

EXPERIMENTAL

Reagents

CDs were supplied by Chinoin (Budapest, Hungary), Celite for GLC by BDH (Poole, U.K.) and samples of camphenes by Fluka (Buchs, Switzerland), Aldrich (Milwaukee, WI, U.S.A.), S.C.M. Glidco (Jacksonville, FL, U.S.A.) and Chemipan (Warsaw, Poland). All materials were used as received.

Apparatus and procedures

Analytical chromatographic studies were performed using a Hewlett-Packard Model 5890 gas chromatograph equipped with duel flame ionization detectors. The peak areas and retention times were measured by means of a Hewlett-Packard Model 3390A integrator. Glass columns (2 m × 4 mm I.D.) were used. The compounds were injected with Hamilton microsyringes (0.02 μl). A constant inlet pressure (2.75 ± 0.05 atm) and helium flow-rate (40 ± 0.5 ml/min) were maintained.

Micropreparative separations were performed on a Hewlett-Packard Model 7620A gas chromatograph, adapted for this purpose, equipped with a thermal conductivity detector and a glass column (8 m × 7 mm I.D.) [16].

The amount of coated support in each analytical column was *ca.* 11 g, and the micropreparative column was filled with *ca.* 100 g of packing.

The column packings, *i.e.* Celite (30–80 mesh) coated with a formamide solution of α-, β- or γ-CD, were prepared as described previously [8]. The amounts of formamide (4.54 g) and Celite (20 g) were constant. The amounts of CDs used were as follows: (I) none (reference); (II) α-CD, 0.60 g (0.79 mol%); (III) β-CD, 0.23 g (0.22 mol%); and (IV) γ-CD, 0.90 g (0.79 mol%).

As indicated previously [17], an α-CD then acts as an efficient separating agent under GLC conditions when its formamide solution contains 3–4% of water. Hence

the packing for column II contained *ca.* 4% of water and lithium nitrate (0.45 g) was added as a stabilizing agent. The contents of formamide and water in the final column packings were determined by thermogravimetric analysis with a DuPont Type 1090B apparatus.

Optical rotation was measured using a JASCO DIP 360 polarimeter.

^{1}H and ^{13}C NMR spectra were recorded with a Bruker AM-500 spectrometer at 500.14 and 125.76 MHz, respectively.

RESULTS AND DISCUSSION

Analytical approach

Fig. 1a shows a chromatogram obtained on the chiral column II containing α-CD solution (0.79 mol%) in formamide medium.

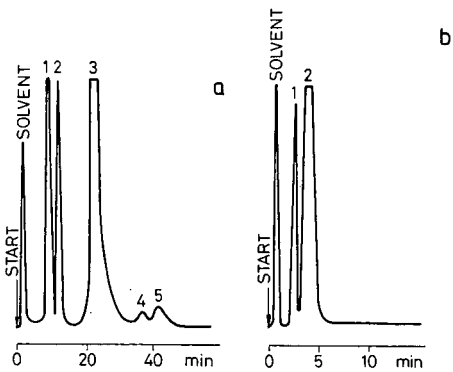

Fig. 1. Chromatograms of a heptane solution of (+)-camphene from Fluka obtained at 40°C on (a) chiral column II (2 m × 4 mm I.D.) loaded with Celite (30–80 mesh) covered with a solution of α-CD (0.79 mol%) in formamide and (b) a reference achiral column with Celite (30–80 mesh) covered with formamide only. Injected samples, 0.02 μl; helium flow-rate, 40 ml/min.

The sample was (+)-camphene from Fluka, dissolved in heptane. It is seen that in addition to the peak of the solvent, several peaks were unregistered. At first, it was very difficult to identify the maxima of elution of camphene enantiomers from chiral column II or even to answer the question of whether resolution of the enantiomers had been achieved or not. In order to elucidate this matter, a second reference achiral column was used, working in parallel, as shown in Fig. 1b. This achiral reference column, containing pure matrix medium, *i.e.*, formamide, should permit the elution of the sum of (+)- and (−)-camphene. In this simplified consideration, impurities by other hydrocarbons that may be eluted together with camphene were not taken into account. Thus, on the basis of the results shown in Fig. 1a and b, it was possible to suggest tentatively that maybe peaks 1 and 3 in Fig. 1a and 2 in Fig. 1b are the suspected ones, but it was very uncertain. For this reason we undertook further studies on other camphene samples, derived from different sources. Their chromatograms, obtained on chiral column II (0.79 mol% α-CD), are presented in Fig. 2.

The adjusted retention times (t'_R) of the components of the investigated samples

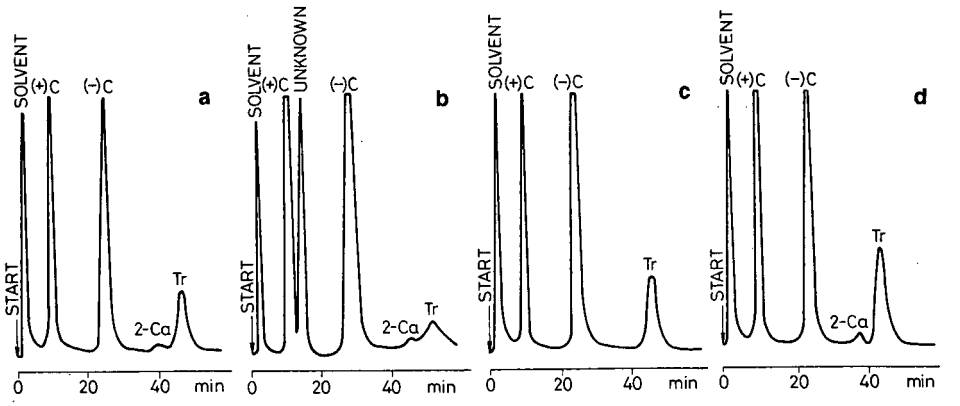

Fig. 2. Chromatograms of heptane solutions of camphenes obtained under the same conditions as in Fig. 1a. (+)C, (+)-camphene; (−)C, (−)-camphene; 2-Ca, 2-carene; Tr, tricyclene. (a) (+)-Camphene from Aldrich; (b) (−)-camphene from Aldrich; (c) camphene from S.C.M. Glidco; (d) camphene from Chemipan.

TABLE I

ADJUSTED RETENTION TIMES (t'_R) OF THE MAIN COMPONENTS OF THE COMMERCIAL CAMPHENES DETERMINED AT 40°C ON CHIRAL COLUMN II (0.79 mol% α-CD) AND THEIR CONTENTS EVALUATED FROM THE PEAK AREAS

Flow-rate, 40 ml/min

Source	t'_R (min)	Content (%)
Aldrich (+)	5	60
	7	–
	14	28
	23	1
	26	11
Aldrich (−)	5	40
	7	13
	14	43
	23	1
	26	6
Chemipan	5	56
	7	–
	14	31
	23	1
	26	12
Fluka	5	42
	7	11
	14	44
	23	1
	26	3
S.C.M. Glidco	5	41
	7	2
	14	43
	23	–
	26	13

as eluted from the α-CD column, and their percentage contents calculated from peak areas, are given in Table I. In the calculations the share of the solvent was subtracted and it was not taken into account.

Total declared and found contents of (+)- and (−)-camphene enantiomers are given in Table II. The found values were evaluated at 60°C using the γ-CD (0.79 mol%) column IV, which separates camphene from impurities of other terpenoic hydrocarbons especially well.

TABLE II

TOTAL CONTENTS OF (+)- AND (−)-CAMPHENE DETERMINED AT 60°C ON COLUMN IV WITH γ-CD (0.79 mol%)

Source	Total content of camphene (%)	
	Declared	Determined
Aldrich (+)-	80	79
Aldrich (−)-	95	80
Chemipan	Not given	75
Fluka	90–95	83
S.C.M. Glidco	Not given	76

The chromatograms in Figs. 1 and 2 and the data in Tables I and II lead to the conclusion that in fact peaks with adjusted retention times of 5 and 14 min (peaks 1 and 3, respectively, in Fig. 1a) correspond to enantiomers of camphene. Nevertheless, the absolute configuration of the enantiomeric camphenes, *i.e.a*, the sequence of their elution, remained unsolved. Our earlier experiments on α- and β-pinenes and *cis*- and *trans*-pinanes indicated that the compounds of *R* configuration form more stable complexes with α-CD than those of *S* configuration. In order to make this aspect clear, we have indicated the enantiomers of camphene in Fig. 2 according to this supposition, although this statement precedes true verification, which will be discussed late.

Enantiomeric compositions found using column II with 0.79 mol% α-CD are presented in Table III.

In fact the enrichment of the samples denoted (+) or (−) is poor, and they seemed to be closer to a racemic mixture. From a comparison of the data in Tables II and III, it is seen that the total contents of camphene determined on the γ-CD column IV are always smaller than those found as the sum of (+) and (−)-camphenes using the α-CD column II. This may suggest that some small impurities are eluted from column II together with enantiomers. In some instances rationalization of the measured optical rotation with the true enantiomeric composition suggests that there must be another component involved, imposing its optical activity. This may be exemplified by camphene from Fluka or (−)-camphene from Aldrich.

In additional chromatographic runs we have identified peaks with retention times (Figs. 1a and 2a–d) of 23 and 26 min as 2-carene (2-Ca) and tricyclene (Tr), respectively, while that with a retention time of 7 min remained unidentified.

The values of the separation factor α $[t'_R(-)/t'_R(+)]$ determined on column II

TABLE III

ENANTIOMERIC COMPOSITION OF (+)- AND (−)-CAMPHENE IN THE SAMPLES INVESTIGATED

Source	Optical rotation (°)		Enantiomeric composition from chromatograms evaluated on α-CD column II	
	Declared	Measured directly	(+)-	(−)-
Aldrich (+)-	+12.6	+13.7	60	28
Aldrich (−)-	− 6.6	−20.7	40	43
Chemipan	Not given	+10.7	56	31
Fluka	+17	−19.5	42	44
S.C.M. Glidco	Not given	−21.5	41	43

(α-CD) at different temperatures are given in Table IV. Two aspects are notable. The first is the remarkable enantioselectivity of the α-CD inclusion process towards camphene, *e.g.*, $\alpha = 3.6$ at 30°C. Such values are very rarely achieved for enantiomers, where separation factors of the order of 1.1–1.2 are considered satisfactory. Second, the considerable changes in the values of the selectivity factor with temperature should be mentioned. This phenomenon may suggest that the enantioselective differentiation processes of camphenes via α-CD complexation are mainly enthalpic.

Micropreparative approach

Micropreparative attempts were made to confirm the absolute configuration of enantiomeric camphenes, *i.e.*, to verify the sequence of their elution from the α-CD column assumed above and to identify the compound denoted (Figs. 1 and 2) as unknown on the chromatograms.

Fig. 3 shows an example of the separation of 10 μl of *ca.* 60% camphene in heptane solution, performed on a micropreparative scale. The inset shows a chromatogram of a heptane solution of a collected fraction of (−)-camphene.

Starting from the Fluka camphene, using the micropreparative approach, we obtained (+)-camphene of 82% optical purity and of 90% chemical purity (both

TABLE IV

VALUES OF ENANTIOSELECTIVITY FACTOR α AT DIFFERENT TEMPERATURES

Temperature (°C)	α
30	3.6
35	3.1
40	2.9
45	2.3

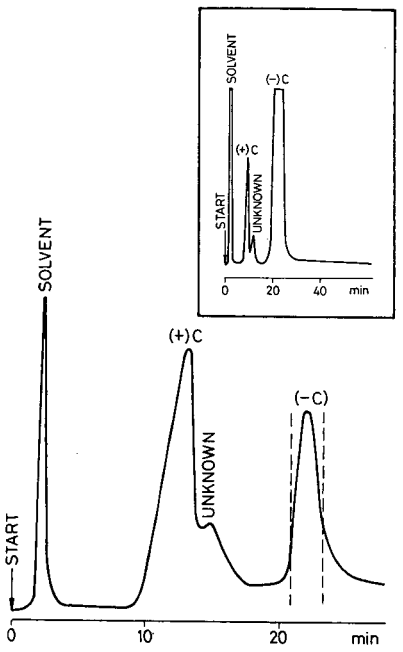

Fig. 3. Micropreparative separation of 10 μl of camphene from Fluka at 40°C on a column (8 m × 1 cm I.D.) filled with Celite (30–80 mesh) covered with α-CD solution (0.59 mol%) in formamide. Helium flow-rate, 40 ml/min. Inset: chromatogram of indicated collected fractions of (−)-camphene.

determined chromatographically) and (−)-camphene of 94% optical purity and 98% chemical purity (both determined chromatographically). The optical rotations of (+)- and (−)-camphene were $[\alpha]_D^{20} = +7.8°$ ($c = 1$, CCl_4) and $[\alpha]_D^{20} = -8.5°$ ($c = 1$, CCl_4), respectively. Supplementary ^1H and ^{13}C NMR spectra confirmed the above-mentioned purities.

Hence the earlier assumed absolute configuration of camphenes appeared unequivocally to be correct. Unfortunately, our attempts to identify the 'unknown' compound have so far failed. Nevertheless, both the contents of camphenes in the collected fractions and their optical purity seem to be worthy of mention, especially with regard to our analytical data for commercial samples.

ACKNOWLEDGEMENTS

This work was supported by Grants C.P.B.R. 3.20 and C.P.B.P. 01.13 from the Polish Academy of Sciences.

REFERENCES

1 C. E. Dalgliesh, *J. Chem. Soc.*, (1952) 3940.
2 V. Schurig, *Angew. Chem., Int. Ed. Engl.*, 16 (1977) 110.
3 V. Schurig, *Chromatographia*, 13 (1980) 263.

4 J. Köhler and G. Schomburg, *Chromatographia*, 14 (1981) 559.
5 J. Köhler and G. Schomburg, *J. Chromatogr.*, 255 (1983) 331.
6 J. Köhler, A. Deege, G. Schomburg, *Chromatographia*, 18 (1984) 119.
7 V. Schurig and R. Weber, *J. Chromatogr.*, 289 (1984) 321.
8 T. Kościelski, D. Sybilska and J. Jurczak, *J. Chromatogr.*, 280 (1983) 131.
9 T. Kościelski, D. Sybilska, S. Belniak and J. Jurczak, *Chromatographia*, 19 (1984) 292.
10 T. Kościelski, D. Sybilska, S. Belniak and J. Jurczak, *Chromatographia*, 21 (1986) 413.
11 T. Kościelski, D. Sybilska and J. Jurczak, *J. Chromatogr.*, 364 (1986) 299.
12 W. A. König, S. Lutz and G. Wenz, *Angew. Chem., Int. Ed. Engl.*, 27 (1988) 979.
13 W. A. König, S. Lutz, C. Colberg, N. Schmidt, G. Wenz, E. van der Bey, A. Mosandl, G. Günther and A. Kustermann, *J. High Resolut. Chromatogr. Chromatogr. Commun.*, 11 (1988) 621.
14 D. A. Armstrong, W. Li and J. Pitha, *Anal. Chem.*, 62 (1990) 217.
15 D. W. Armstrong, W. Li, C.-D. Chang and J. Pitha, *Anal. Chem.*, 62 (1990) 914.
16 D. Sybilska, J. Goronowicz and M. Cieślak, *Pol. Pat. Appl.*, P-277627, 1989.
17 D. Sybilska and J. Jurczak, *Carbohydr. Res.*, 192 (1989) 243.

Journal of Chromatography, 543 (1991) 405–411
Elsevier Science Publishers B.V., Amsterdam

CHROM. 23 141

Derivatization of hydroxyeicosatetraenoic acid methyl esters with pentafluorobenzoic anhydride and analysis with supercritical fluid chromatography–chemical ionization mass spectrometry[a]

DONALD V. CRABTREE* and ALICE J. ADLER
Eye Research Institute, 20 Staniford Street, Boston, MA 02114 (U.S.A.)
(Received September 19th, 1990)

ABSTRACT

Analysis by supercritical fluid chromatography, in conjunction with chemical ionization mass spectrometry shows that methyl 5-O-pentafluorobenzoyl eicosatetraenoate is the stable product of the derivatization of methyl 5-hydroxyeicosatetraenoate with pentafluorobenzoic anhydride. This method may be useful in the analysis of hydroxy lipids.

INTRODUCTION

The measurement of small quantities of hydroxy lipids continues to increase in importance as more of them are discovered [1]. The ocular effects of eicosanoids, most of which are hydroxy lipids, is a nascent and rapidly growing field [2].

Previously, we developed a method for the gas chromatographic (GC) analysis of alcohols and hydroxy fatty acid methyl esters that utilized electron-capture detection (ECD) and pentafluorobenzoic anhydride (PFBA) as a derivatizing reagent [3]. After derivatization, methyl ricinoleate (12-OH-18:1ω9), a mono-unsaturate, as well as some saturated compounds, were found to be stable at temperatures high enough to elute them from a GC column [3]. Using that method, we attempted to analyze 5- and 15-hydroxyeicosatetraenoic acid methyl esters (5- and 15-HETE-Me). We were not able to elute the products of these derivatization reactions from our GC column. Instead, the chromatogram consisted of numerous small peaks with retention times much less than one would anticipate for the expected product, indicating that the derivative decomposed at the temperatures required for elution. Using thin-layer chromatography (TLC), we observed that derivatization of methyl ricinoleate, 5-HETE-Me and 15-HETE-Me yielded products having polarities between triolein and methyl oleate.

[a] Presented in part at a satellite meeting (*The Ocular Effects of Eicosanoids and Other Lipid Mediators*) of the *International Conference on Eye Research, Helsinki, August 1990.*

0021-9673/91/$03.50

Using supercritical fluid chromatography (SFC)–mass spectrometry (MS), we show here that the product of derivatization of 5-HETE-Me is stable under the conditions required to elute it from an SFC column and that the product is the anticipated methyl 5-O-pentafluorobenzoyl eicosatetraenoate. Derivatized 15-HETE-Me was also analyzed using SFC–MS, but because of the complexity of its mass spectrum we are somewhat uncertain of the identity of derivatized 15-HETE-Me.

EXPERIMENTAL

Chemicals

Racemic methyl 5-hydroxy-6,8,11,14-(*E*,*Z*,*Z*,*Z*)-eicosatetraenoate and methyl 15(*S*)-hydroxy-5,8,11,13-(*Z*,*Z*,*Z*,*E*)-eicosatetraenoate were obtained from Sigma (St. Louis, MO, U.S.A.). Methyl *tert.*-butyl ether was obtained from Aldrich (Milwaukee, WI, U.S.A.), and ethyl acetate from Fluka (Ronkonkoma, NY, U.S.A.). Acetonitrile, hexane, methylene chloride, and tetrahydrofuran were J. T. Baker HPLC grade (purchased from Doe and Ingalls, Medford, MA, U.S.A.). Silylation grade pyridine was obtained from Pierce (Rockford, IL, U.S.A.); because of its shelf life, it was redistilled prior to use. Dimethyldichlorosilane and methyl ricinoleate were purchased from Alltech (Deerfield, IL, U.S.A.). TLC standards [18-4-A (a mixture of cholesterol, cholesteryl oleate, triolein, oleic acid and methyl oleate) and 18-5-A (a mixture of cholesterol, cholesteryl oleate, triolein, oleic acid and lecithin)] were obtained from Nu-Chek Prep (Elysian, MN, U.S.A.) and fatty acid methyl ester standards were from Supelco (Bellefonte, PA, U.S.A.).

Instrumentation and equipment

SFC with flame ionization detection was done on a Lee Scientific Series 600 Supercritical Fluid Chromatograph (Salt Lake City, UT, U.S.A.). A 0.2-μl fixed-loop injector having an injection time of 0.6 s and a split ratio of 2.6:1 was used to introduce samples into the column. The column was 10 m × 375 μm O.D. × 50 μm I.D. SB-Phenyl-5 (0.25-μm film) from Lee Scientific. The mobile phase was SFC-grade carbon dioxide. The column temperature was held constant at 120°C. The mobile phase was subjected to the following pressure program: 115 atm for 10 min, then ramped at 10 atm/min to 415 atm.

SFC–MS was performed at Oneida Research Services (Whitesboro, NY, U.S.A.). The chromatograph was the same as described above except that the sample loop was 0.1 μl and the column was 8 m × 100 μm I.D. SB-Methyl (0.25-μm film). The mobile phase and its temperature and pressure parameters were also the same. The MS apparatus was a Finnigan TSQ-70. It was scanned from 100–700 a.m.u. in 0.6 s. The electron multiplier was 2000 V. Methane was the reagent gas for both positive ion (PI) and negative ion (NI) chemical ionization (CI). The pressure in the ion source was maintained at 210 mtorr. Both the NICI and PICI measurements were made with the ion source at 250°C.

High-performance liquid chromatography (HPLC) was performed using a Beckman Model 344 interfaced to a Spectra-Physics (San Jose, CA, U.S.A.) SP-4250 integrator. A reversed-phase ODS column (250 × 4.6 mm I.D.) was obtained from Beckman. Ultraviolet (UV) detection was done with a cadmium lamp and 229-nm filter. Mobile phase was acetonitrile–water (75:25, v/v) with a flow-rate of 1.0 ml/min [4].

TLC plates were E. Merck high-performance plates with a silica gel 60 stationary phase (thickness: 0.2 mm) having dimensions of 10 × 10 cm. They were purchased from Alltech.

Silica gel Sep-Pak cartridges were obtained from Waters Assoc. (Milford, MA, U.S.A.). They were used in conjunction with a 10-ml glass syringe purchased from Scientific Products (Bedford, MA, U.S.A.).

Procedures

TLC plates were activated at 115°C for 10–15 min just prior to use. Samples were applied manually with a 25-μl TLC syringe (Alltech). The TLC mobile phase was hexane–methyl *tert.*-butyl ether–ethyl acetate (80:20:2) [5]. After developing, the plates were dried at 115°C for 2 min. Bromothymol Blue (Alltech) was used to visualize the spots.

PFBA was synthesized as previously described [3]. It was recrystallized in tetrahydrofuran rather than diethyl ether.

Just prior to derivatization, the HETE-Mes were brought to dryness with a gentle flow of nitrogen. The PFBA derivatization reaction was run as previously described [3] with the following modifications: acetonitrile or methylene chloride was used to dissolve the alcohols rather than toluene, since toluene was found not to be a polar enough solvent to dissolve HETE-Mes. The reaction time was increased to 2.5 h, the reaction volume was decreased to 0.5 ml, and 15 μl of pyridine were used. Silanized (with dimethyldichlorosilane) 6 ml glass scintillation vials were used to carry out reactions and for any subsequent transfers of products. (Caution is recommended in storing and using dimethyldichlorosilane. During storage, it easily corrodes the plastic of a PTFE-lined cap.)

After derivatization, the reaction solution was cleaned up with a (600 mg) silica Sep-Pak cartridge. The mobile phase was the same as was used for TLC (see above). The cartridge was rinsed with 10 ml of mobile phase before introducing the reaction solution. The products were then eluted with 5 ml of mobile phase. The sample was then concentrated under a stream of nitrogen to a final volume of *ca.* 0.4 ml.

RESULTS

Chromatography

We observed that PFBA derivatization of the HETE-Mes occurred more slowly than that of the saturated 2-hydroxy fatty acid methyl esters or methyl ricinoleate. This was somewhat surprising considering that allylic hydroxyl groups typically are acylated more easily than isolated hydroxyls [6]. Increasing the reaction time to 2.5 h and using 50% more pyridine provided satisfactory results.

TLC chromatograms (not shown) indicated that the relative polarity of the products is derivatized 5-HETE-Me > derivatized 15-HETE-Me > derivatized methyl ricinoleate. All three products migrate between triolein and methyl oleate. Consistent with previous results on a normal-phase HPLC column for 5- and 15-HETE [4], the same relative polarity was observed for the starting materials. The underivatized alcohols have R_f values close to that of cholesterol.

Fig. 1 indicates that both 5-HETE-Me and derivatized 5-HETE-Me are stable when subjected to the conditions of SFC. The two small peaks observed in both

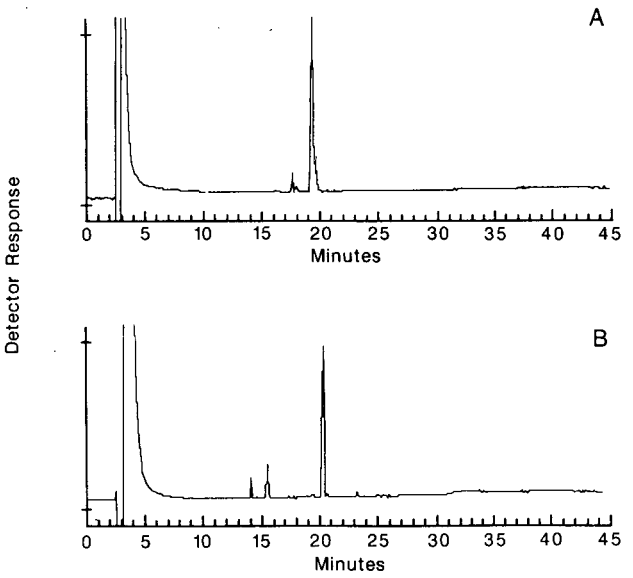

Fig. 1. Supercritical fluid chromatograms. Mobile phase: carbon dioxide. Column temperature: 120°C. Pressure program: 115 atm for 10 min, then 10 atm/min to 415 atm. (A) 5-HETE-Me; (B) derivatized 5-HETE-Me.

chromatograms were not identified but most probably can be attributed to impurities. Small impurity peaks are also observed when underivatized 5-HETE-Me is analyzed with HPLC using UV (229 nm) detection (data not shown). These minor peaks were not present in the blank (derivatization reaction run without 5-HETE-Me).

With the same chromatographic conditions as in Fig. 1, the retention times of methyl stearate (18:0), methyl arachidicate (20:0), methyl behenate (22:0), methyl ricinoleate and derivatized methyl ricinoleate were 17.7, 19.2, 20.4, 18.0 and 19.8 min, respectively. Methyl stearate was not resolved from 18:1, 18:2 or 18:3 methyl esters and methyl behenate was not resolved from 22:1 methyl ester. The chromatographic conditions were not optimized for maximum separation. SFC enables much better resolution [7] but that was not required for these experiments. The retention times of 5-HETE-Me and derivatized 5-HETE-Me were consistent with what one would expect based on the fatty acid methyl ester standards, methyl ricinoleate and derivatized methyl ricinoleate. As is common on silica-based columns, the underivatized alcohol tails to a greater extent than the derivatized compound.

Mass spectrometry

To identify the derivatized compounds, the positive chemical ionization mass spectra were measured (Fig. 2). For derivatized 5-HETE-Me (*m/z* 528), the base peak is *m/z* 317 (Fig. 2A, Table I). This indicates that the major pathway of fragmentation begins with loss of an electron from the alkyl oxygen adjacent to C_6F_5 and includes subsequent heterolytic α-cleavage of the C–O bond, leading to an allylic secondary carbocation (*m/z* 317). Formation of the acyl ion, $[C_6F_5CO]^+$ (*m/z* 195) is not observed. Since the relative abundance of *m/z* 213 is 9.7%, double H-transfer (associ-

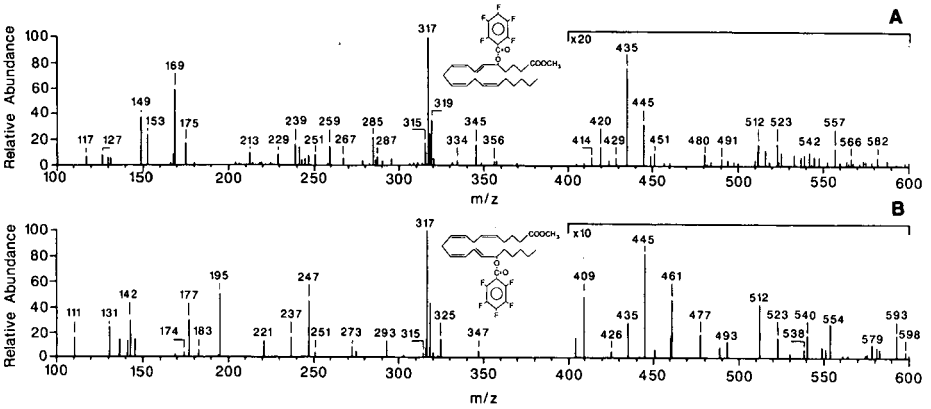

Fig. 2. Positive-ion chemical ionization mass spectra. Ion source temperature is 250°C. Reagent gas: methane. (A) Derivatized 5-HETE-Me; (B) derivatized 15-HETE-Me.

ated with the pentafluorobenzoyl ester) appears to compete slightly with heterolytic α-cleavage. Probably, *m/z* 435 is formed via the neutral McLafferty [8] fragment associated with the methyl ester [9] that subsequently loses a fluorine. other than these, most of the peaks appear to stem from $[M - C_7F_5O_2]^+$ (See Table I).

The PICI-MS of derivatized 15-HETE-Me (Fig. 2B) also had *m/z* 317 as its base peak. With the exception of *m/z* 523, 512, 445 and 435, which all have small

TABLE I

PICI-MS FRAGMENTATION PATTERN OF DERIVATIZED METHYL 5-HYDROXYEICOSA-TETRAENOATE

M is the molecular ion *m/z* 528. Ion source temperature was 250°C and the reagent gas was methane.

m/z	Relative abundance (%)	Positive ion assignment
557	0.7	$M + C_2H_5$
525	0.6	$[M + C_2H_5] - CH_3OH$
497	0.1	$M - CH_3O$
451	0.6	$[M - CO_2CH_3] - F + H$
435	3.8	$[M - 74] - F$
345	15.8	$[M - C_7F_5O_2] + CO$?
334	2.9	$[M - C_7F_5O_2] + CH_5$ or $[M - C_7F_5O] + H$
319	35.6	$[M - C_7F_5O_2] + 2H$
318	24.3	^{13}C and ^2H isotopes
317	100.0	$M - C_7F_5O_2$
285	22.2	$[M - C_7F_5O_2] - CH_3OH$
259	14.7	$[M - C_7F_5O_2] - CO_2CH_3 + H$
213	9.7	$C_6F_5CO_2H_2$
169	59.6	$C_6F_5H + H$
153	23.8	?
149	38.5	C_6F_4H

relative abundances, the remainder of the spectrum does not correlate with the derivatized 5-HETE-Me mass spectrum. We hypothesize that the secondary carbocation (*m/z* 317) cyclizes to an aromatic intermediate (*m/z* 273) with concurrent loss of CO_2. This fragment then goes on to form the series: 273, 247, 221, 195, 169 and possibly 142 (with loss of H). A series of *m/z* values differing by 26 daltons from one another is typical of aromatic compounds [10].

When the NICI mass spectra were measured, it would have been desirable to maintain the ion source temperature at 80°C. At that temperature, we probably would have observed the molecular ion. But, because of Joule–Thompson cooling of the mobile phase when it eluted from the column [11], with this instrument it was necessary to maintain the ion source of the mass spectrometer at 250°C so that eluting components did not precipitate at the interface [12]. Consistent with our previous NICI-MS measurements on derivatized 2-hydroxy fatty acid methyl esters [3], at this high of a temperature, the only fragments observed for both derivatized 5- and 15-HETE-Me were: *m/z* 148, C_6F_4; *m/z* 167, C_6F_5; and *m/z* 196, C_6F_5CO + H.

DISCUSSION

The advantages and disadvantages of SFC relative to GC and HPLC have been considerably discussed in the past [13]. Also, the extremely good sensitivity of ECD has been known since the middle sixties [14]. With our derivatizing reagent and GC–ECD we were able to measure hydroxy lipids in the femtomole range [3]. Only very recently has anyone attempted to couple ECD to SFC. SFC–ECD was first shown to be a viable technique by Kennedy and Wall in 1988 [15]. In this early work, a rising baseline prevented them from obtaining a sensitivity better than 35 pg for a triazole fungicide metabolite standard. Subsequent work by Richter *et al.* [16] indicated that baseline rise could be reduced. More recently, Chang and Taylor [17] have reported a detection limit for 2,3′,4′-trichlorobiphenyl of 0.64 pg and a linear range of 10^4. These results along with the results we show here suggest that without resorting to complex chemical procedures and extremely expensive instrumentation (NICI-MS), but using SFC–ECD instead, the chromatographic analysis and detection limits of hydroxy lipids can now be significantly improved.

ACKNOWLEDGEMENTS

The authors would like to acknowledge Drs. Vernon Reinhold and Margaret Merritt of Harvard Medical School for the assistance they provided in measuring the supercritical fluid chromatograms.

REFERENCES

1 B. Samuelsson, S.-V. Dahlen, J. A. Lindgren, C. A. Rouzer and C. N. Serhan, *Science (Washington, D.C.)*, 237 (1987) 1171.
2 N. G. Bazan, *Prog. Clin. Biol. Res.*, 312 (1989) 15.
3 D. V. Crabtree, A. J. Adler and G. J. Handelman, *J. Chromatogr.*, 466 (1989) 251.
4 M. Van Rollins and R. C. Murphy, *J. Lipid Res.*, 25 (1984) 507.
5 J. G. Hamilton and K. Comal, *Lipids*, 23 (1988) 1146.
6 L. F. Fieser and M. Fieser, *Advanced Organic Chemistry*, Reinhold, New York, 1961, p. 292.

7 J. A. Crow and J. P. Foley, *J. High Resolut. Chromatogr.*, 12 (1989) 467.
8 F. W. McLafferty, *Anal. Chem.*, 31 (1959) 82.
9 A. G. Sharkey, Jr., J. L. Shultz and R. A. Friedel, *Anal. Chem.*, 31 (1959) 87.
10 W. Schonfeld, *Org. Mass Spectrom.*, 10 (1975) 321.
11 R. D. Smith, J. L. Fulton, R. C. Petersen, A. J. Kopriva and B. W. Wright, *Anal. Chem.*, 58 (1986) 2057.
12 J. A. G. Roach, J. A. Sphon, J. A. Easterling and E. M. Calvey, *Biomed. Environ. Mass Spectrom.*, 18 (1989) 64.
13 K. D. Bartle, in R. M. Smith (Editor), *Supercritical Fluid Chromatography*, The Royal Society of Chemistry, London, 1988, pp. 1–28.
14 C. F. Poole and S. K. Poole, *J. Chromatogr. Sci.*, 25 (1987) 434.
15 S. Kennedy and R. J. Wall, *LC · GC*, 6 (1988) 930.
16 B. E. Richter, D. J. Bornhop, J. T. Swanson, J. G. Wangsgaard and M. R. Andersen, *J. Chromatogr. Sci.*, 27 (1989) 303.
17 H.-C. K. Chang and L. T. Taylor, *J. Chromatogr. Sci.*, 28 (1990) 29.

Journal of Chromatography, 543 (1991) 413–424
Elsevier Science Publishers B.V., Amsterdam

CHROM. 23 078

Supercritical fluid extraction from a brown alga by stagewise pressure increase

PASCALE SUBRA* and PATRICK BOISSINOT
Laboratoire d'Ingéniérie des Matériaux et des Hautes Pressions, CNRS, Avenue Jean-Baptiste Clément, 93430 Villetaneuse (France)
(First received September 25th, 1990; revised manuscript received December 27th, 1990)

ABSTRACT

The use of supercritical carbon dioxide as an extractant for biological materials is described. Extractions from a mediterranean brown alga were conducted with commercial micro-scale equipment, improved by introducing a sapphire extraction cell, and coupled to a high-pressure vessel in order to collect the extracts. By applying a controlled stagewise pressure increase one obtains separate fractions, the colours of which range from colourless to green, depending on the temperature of the extraction. The results, in terms of weight, colour and analysis by high-performance liquid chromatography and by high-performance thin-layer chromatography, are discussed.

INTRODUCTION

Recent concern about the hazardous nature of many commonly used solvents as well as the costs and environmental dangers of waste solvent disposal have led to the development of alternative sample extraction methods. The limitations of conventional methods such as liquid–liquid or liquid–solid extractions, which are time and solvent consuming, have fuelled interest in the development of high-pressure extraction by supercritical gases, especially for compounds intended for human consumption. Many research groups have reported extractions of a variety of compounds from natural products, including flavouring materials from leaves and needles [1,2] and from citrus and orange peels [3–5], food colours from dried grass and turmeric roots [6,7] and flavours from milk fat [8], but no reports on marine materials, especially algae, have been published.

Algae are widely exploitated owing on the one hand to their technological and nutritional properties (asiatic nutritional algae industry), and on the other to their content of specific polysaccharides (colloids industry), with a world production of 1 600 000 tons of collected algae [9]. There are also many prospects for new developments, as described in a recent review [10], including the use of algae in the medical field, where numerous studies have confirmed the antifungal, anticoagulative and antimicrobial activities of algae extracts [11,12]. Screenings of such activities have been obtained from crude extracts, but only a few active molecules have so far yet been isolated [13–15].

0021-9673/91/$03.50

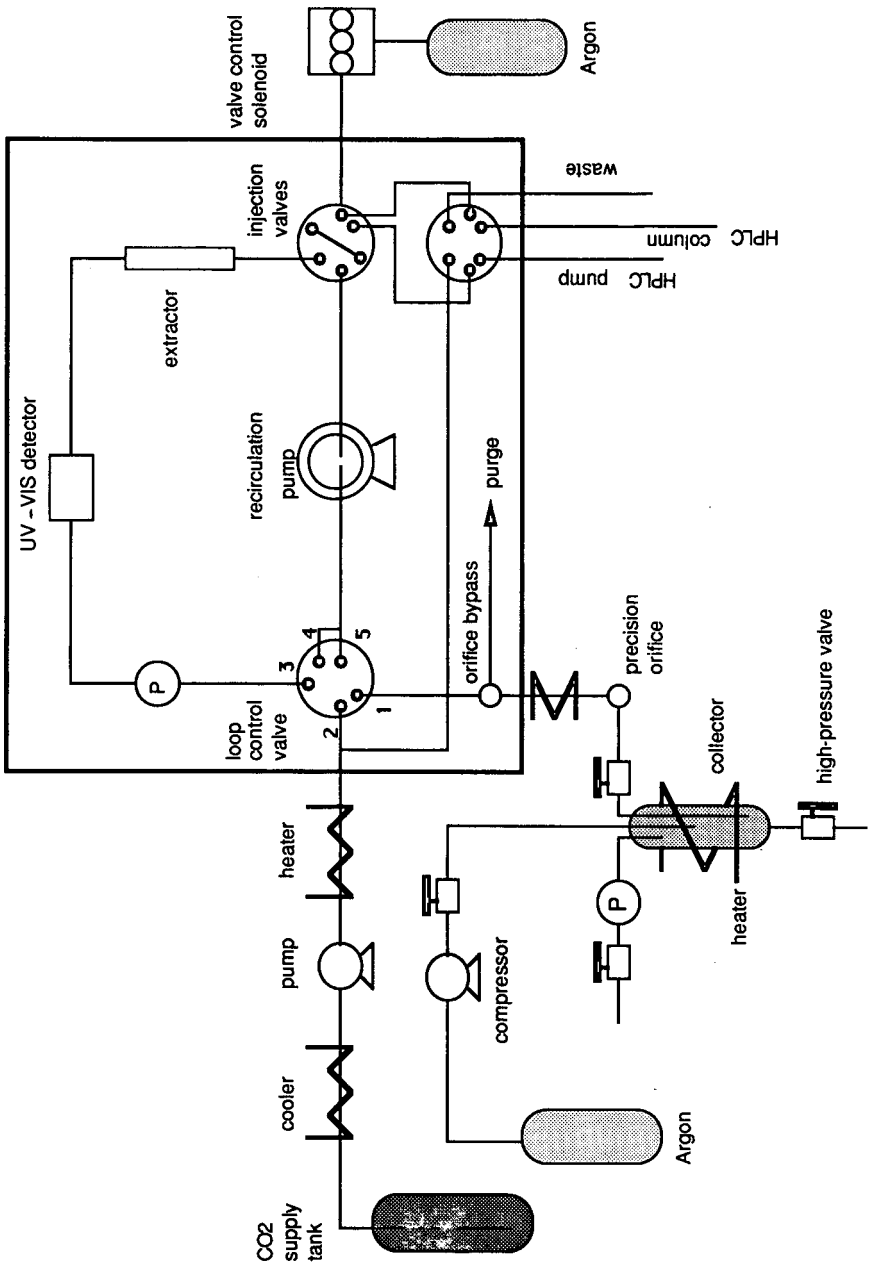

Fig. 1. Supercritical fluid extraction apparatus.

Classical purifications often require numerous steps, such as liquid extraction and flash chromatographic techniques [16], including evaporations and sample transfers which may induce losses and contamination risks. For such purification of active molecules from complex natural matrices, supercritical fluids may offer some advantages over liquid organic solvents; from a brown mediterranean alga, supercritical carbon dioxide leads to extracts similar to those obtained by liquid extraction in terms of antifungal properties, but they contain interfering compounds with a narrower range of polarity, and they are obtained in a shorter analysis time [17]. Selectivity may be adjusted by controlling the solvent strength of the fluid, depending on the pressure and the temperature of the extraction; at a constant temperature, extraction at lower pressures will favour less polar analytes, while higher pressures will favour more polar and higher molecular weight analytes [18].

In this paper, we present the results of supercritical carbon dioxide extraction from a brown mediterranean alga, *Dilophus ligulatus*, which exhibits a wide range of antifungal activities. By applying a stagewise pressure increase, from 8 to 25 MPa, differents fractions, in terms of colour and composition are obtained.

EXPERIMENTAL

Supercritical fluid extraction (SFE) is conceptually simple to perform, particularly on an analytical scale. A micro-scale extractor offers many advantages: (1) ease of construction with components available for liquid or gas chromatography, (2) low cost of the optimization because of the small sizes of samples and fluids, (3) on-line monitoring of extract by UV during the extraction step and (4) through the use of switching valves, on-line analysis of extracts by chromatography. The sample preparation accessory (SPA) from LDC Analytical (Thermo Instrument Division) combines most of these advantages.

SFE can be performed in either a dynamic or a static mode. In the dynamic mode, the fluid is constantly flowing through the cell containing the raw material, while a flow restrictor maintains pressure in the system and allows the fluid to depressurize into the collection device (most of the published examples are performed in such a mode). The static mode is performed by pressurizing the cell and extracting the sample with no outflow of the fluid. Specific criteria for selecting dynamic or static modes are not yet clear, and both methods have been used for quantitative SFE of a variety of samples [19]; the commercial extractor we used combines both techniques, as described below.

Micro-SFE apparatus

The SPA is shown in Fig. 1. Carbon dioxide (N 45 grade, Air Liquide) from the supply tank was cooled to the liquid state and then compressed to the desired pressure, up to 35 MPa, by a constant-pressure pump. The compressed carbon dioxide was preheated to the desired temperature, up to 333 K, before being introduced into the oven. The oven houses the extraction loop, which is made up of the loop control valve, recirculating pump, switching valves, extractor and high-pressure UV detection cell. Two modifications were carried out: the original extraction cell, which was a 5-ml 316 stainless-steel cup with a porous bottom and lid with frits, was replaced with an empty column, because an amount of cosolvent always remained in the bottom of

the cell; and a sapphire cell [20] was introduced into the extraction loop in order to observe various phenomena.

The original purpose of this extraction system is to provide both modes of extraction (dynamic or static), depending on the position of the loop control valve. When 3–4, and therefore 1–2, are connected, the extraction loop is isolated from the supply tank and becomes a closed system, filled with a known volume of carbon dioxide of density precisely controlled by the pressure and the temperature parameters. When the recirculating pump is activated, the fluid continuously cycles though the closed loop until extraction of the desired analytes has occurred, as indicated by the UV–VIS detector. After a set period of time, the loop control valve is switched, so that 2–5 and therefore 3–1, are connected. A constant flow-rate of fresh carbon dioxide delivered by the main pump, enters the loop to sweep out the carbon dioxide enriched with analytes through a flow restrictor into a collection device; this orifice is temperature controlled to prevent ice build-up due to rapid depressurization.

Collection device

A quickly and easily dismantled device, made of 316 stainless steel, is shown in Fig. 2. The vessel head is securely fastened to the body by two half-circle nuts and sealed with anti-extrusion O-rings; the nuts themselves are confined in a lid. The lid, nuts and head can be removed by hand, without using any tools.

Three tubes of 1/8 in. O.D. pass through the vessel head; the compressor tube (not drawn in Fig. 2) is connected to an air compressor, which pressurizes the vessel with argon above the set pressure. Through the inlet tube, connected to the extractor,

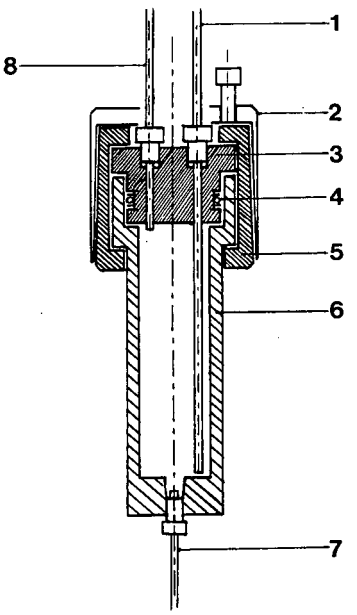

Fig. 2. Collection device. 1 = Tubing of 1/8 in. O.D. connected to the extractor; 2 = lid; 3 = vessel head; 4 = anti-extrusion O-rings; 5 = half-circle nuts; 6 = body of the collector; 7 = tubing of 1/8 in. O.D. connected to the collection valve; 8 = outlet port.

supercritical carbon dioxide enriched with analytes is introduced into the vessel, which generally contains a few milliliters of hexane. Extracts are dissolved in the organic solvent and carbon dioxide flows out from the outlet port.

Analysis

High-pressure thin-layer chromatography (HPTLC). Extracts are dissolved in 100 μl of the developing solvent [hexane–ethyl acetate (80:20, v/v)]; 5 μl are applied to a glass plate (5 cm × 5 cm) precoated with silica (Silica gel 60 F_{254}; Merck, Nogent sur Marne, France). Separated substances are revealed using a spray reagent (sulphuric acid–methanol).

High-performance liquid chromatography (HPLC). Extracted substances are separated, after dilution in 3 ml of ethyl acetate, on a Spherisorb ODS-2 column (15 cm × 0.46 cm I.D.). Pumps, column oven, single-wavelength UV detector and integrator were obtained from LDC Analytical.

Sample matrix

A brown alga, *Dilophus ligulatus*, was collected from the Mediterranean at Villefranche sur Mer, France, during May and June 1989. If the algae were then stored in ethanol, the weights of the supercritical extracts were too low for subsequent quantitative analysis. However, if fresh algae were stored in a dark room until they were dry, repeated samplings showed that storage did not alter the antifungal properties. Algae were therefore stored at 255 K in a freezer.

For each experiment, 2.7 g of the alga were crushed into pieces of about 0.5 mm, mixed with an equal volume of 50-μm glass beads and introduced into an empty column (8.3 cm × 1.05 cm I.D.).

Procedure

The extraction cell was connected to the extraction loop and the carbon dioxide was then pressurized to the set pressure of 8 MPa. The system was allowed to equilibrate for 30 min before the recirculating pump was activated for 30 min. This time corresponds to the altainment of a constant UV detector response, indicating that the maximum amount of dissolved compounds had been reached. Subsequently, a constant flow-rate of fresh carbon dioxide swept the extract into the collector, previously pressurized to the extraction pressure. The collection device was then isolated by shutting off the two high-pressure regulating valves, while the extraction loop was pressurized to the second set pressure value. The collector was depressurized by opening the collection valve and the hexane containing solutes flowed out. The organic solvent was gently evaporated under a stream of nitrogen; extracts were weighed and analysed by both types of chromatography.

Pressure values investigated during the stagewise pressure increase were 8, 10, 15, 20 and 25 MPa; three temperatures of extraction were also investigated, 308, 318 and 328 K.

RESULTS AND DISCUSSION

The densities and amounts of carbon dioxide used in the experiment are listed in Table I. Because the SPA extractor consists mainly of a closed loop of finite

TABLE I

VALUES OF DENSITY AND MASS OF CARBON DIOXIDE AS A FUNCTION OF PRESSURE AND TEMPERATURE

Density (ρ) is expressed in g cm^{-3} and mass of CO_2 (m_f) in g.

T (K)	Pressure (MPa)									
	8		10		15		20		25	
	ρ	m_f	ρ	m_f	ρ	m_f	ρ	m_f	ρ	m_f
308	0.505	9.52	0.678	12.78	0.816	15.39	0.856	16.14	0.895	18.80
318	0.294	5.55	0.490	9.24	0.740	13.97	0.800	15.08	0.857	16.16
328	0.205	3.88	0.338	6.37	0.655	12.35	0.756	14.26	0.802	15.46

volume, each density corresponds to a precise amount of fluid. This point depends on the fact that density cannot be dissociated from the mass of the extraction fluid; therefore, the effect of the density parameter on the solubilization has to be counterbalanced by the effect of the mass of carbon dioxide used for the extraction.

Colours and weights of extracts

As indicated in Table II, the colours of the extracts range from colourless to green, depending on the carbon dioxide density; for densities less than 0.74 g cm^{-3}, most extracts are colourless excepted that at 15 MPa and 328 K, which is slightly orange; up to a density of 0.8 g cm^{-3} the extracts are yellow and at higher densities green pigments are extracted.

As noted in Table III, the total amount of fluid used for each isotherm decreases

TABLE II

COLOURS OF EXTRACTS AS A FUNCTION OF PRESSURE AND TEMPERATURE

T (K)	Pressure (MPa)				
	8	10	15	20	25
308	Colourless	Colourless	Yellow	Light green	Green
318	Colourless	Colourless	Colourless	Yellow	Green
328	Colourless	Colourless	Orange	Yellow	Green

TABLE III

TOTAL AMOUNTS OF EXTRACTS (M_e, mg) AND CO_2 (M_f g), AND RATIO OF THESE TWO VALUES FOR EACH ISOTHERM

T (K)	M_e	M_f	M_e/M_f
308	36.1	70.72	0.510
318	74.5	60.01	1.241
328	88.5	52.33	1.691

TABLE IV

WEIGHTS OF EXTRACTS (mg) COLLECTED FOR EACH PRESSURE INCREASE

T (K)	Pressure (MPa)				
	8	10	15	20	25
308	1.4	1.4	21.3	7.5	4.5
318	2.9	13.5	38.4	12.8	6.9
328	1.1	2.6	44.3	22.4	18.1

with increasing temperature, while the total weight of extracted material increases. Therefore, a temperature of 328 K was chosen in order to obtain a greater amount of extract with a smaller consumption of carbon dioxide.

Weights of the extracts are listed in Table IV. For a constant temperature, an increasing pressure up to 15 MPa leads to an increase in the weight of the extracts, owing to the general influence of pressure (and density) on the solubility of compounds in a supercritical fluid. For higher pressure, the amounts decrease; this may be due to the depletion of the algae in soluble analytes, which does not overcome the possible increase in solubility of more polar compounds. This depletion in soluble analytes is also observed when several extractions are performed on a same sample, with a constant density of carbon dioxide.

By representing the distribution of extraction yields with pressure in the form of fractions (Fig. 3), one observes that the fraction corresponding to a pressure of 15 MPa (and also to an extraction time of 3 h), contains about 50% of the total amount, whatever the temperature. Hence temperature seems to be a parameter influencing

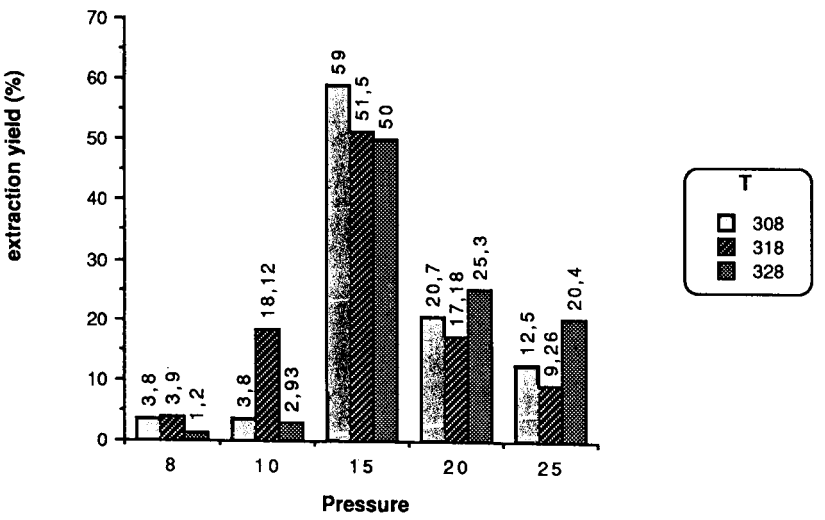

Fig. 3. Distribution of extraction yields by fractions depending on extraction temperature. Yield is defined by the ratio between the extracted amount in a fraction i and the sum of amounts obtained at constant temperature. Temperature in K, pressure in MPa.

mainly the amount of extractable material, but not the distribution of yields by pressure. The HPTLC and HPLC results confirm these tendencies.

HPTLC

TLC plates of extracts are shown schematically in Fig. 4. For a pressure of 8 MPa, only a few compounds are revealed; because of their migration zone, these species are fairly non-polar or moderately polar analytes; for example, compounds 9 and 5 are eluted as standards of β-carotene and cholesterol respectively. By increasing the pressure, compounds with a wider range of polarity are extracted by carbon dioxide; the third fraction contains the nine solutes, in increasing concentration with temperature. For higher pressures, the concentration of each solute generally decreases, except for a green compound eluted between 2 and 3 and which appears in the fourth and the fifth fractions depending on temperature. Refering to Table III, the presence of this compound may be compared with the green colour of extracts.

The influence of temperature is not clearly defined: it modulates the distribution of solutes by fractions, but generally it does not induce important changes in selectivities.

HPLC

Four chromatograms corresponding to fractionation along the isotherm at 318 K are shown in Fig. 5. Whatever the pressure, there is a lack of polar compounds which might be eluted rapidly under such conditions. When the pressure is increasing, several modifications in terms of concentration and selectivity are observed: a pressure of 15 MPa leads to the extraction of compounds with retention times less than 45 min, whereas materials collected at higher pressures show fewer compounds present. The variations also depend on the isotherm considered. As shown in Fig. 6, the first fraction obtained at 8 MPa and 308 K contains compounds with a wider range of retention times than the corresponding fraction obtained at 318 K. For a quantitative description, peaks have been collected into groups numbered from I to VII; these groups are determined by their responses to a change in extraction pressure or tem-

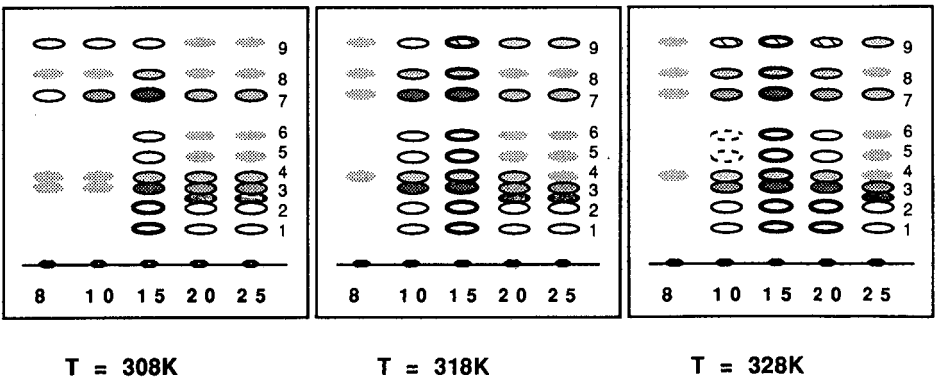

Fig. 4. HPTLC plates of fractions obtained for each isotherm (fractions are identified by pressure, in MPa). Experimental conditions are described in the text.

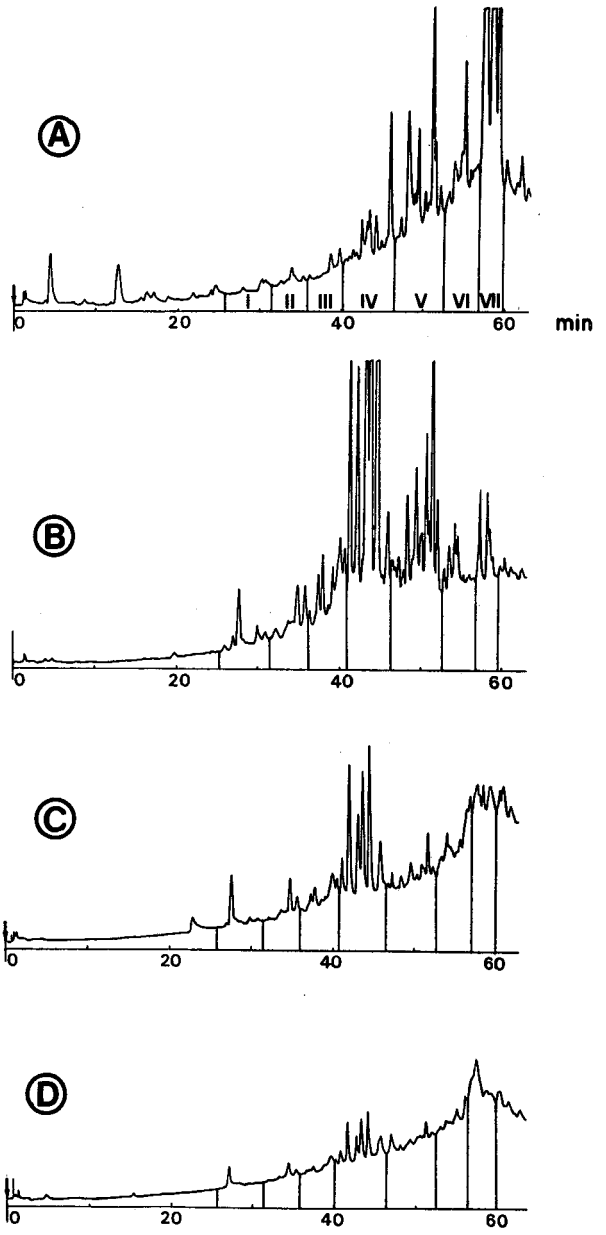

Fig. 5. HPLC of fractions obtained for the isotherm 318 K. Corresponding pressures: (A) 8 MPa; (B) 15 MPa; (C) 20 MPa; (D) 25 MPa. Conditions: column, 15 × 0.46 cm I.D.; stationary phase, Spherisorb ODS-2 d_p 5 μm; mobile phase: methanol–water with a methanol content of initially 44% for 5 min, reaching 84% in 50 min and then remaining constant for 10 min; flow-rate 1.5 ml min^{-1}; UV detection wavelength, 254 nm; attenuation, 64.

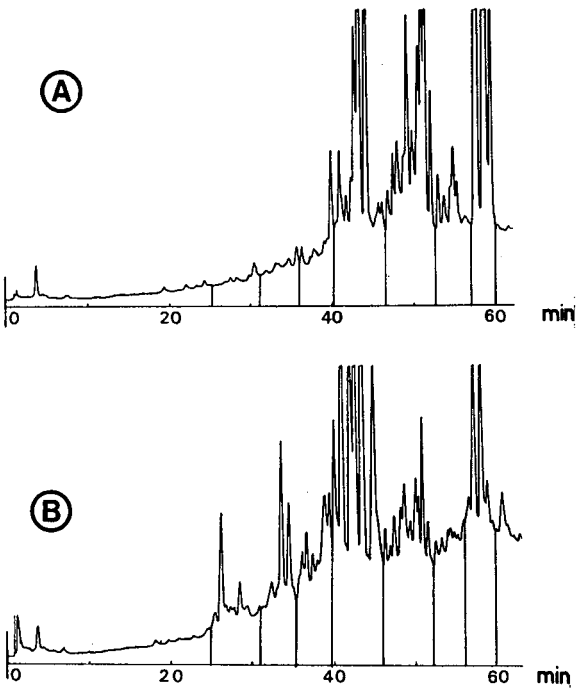

Fig. 6. HPLC of fractions corresponding to a pressure of (A) 8 MPa and (B) 15 MPa and to a temperature of 308 K. Conditions are as in Fig. 5.

TABLE V

DISTRIBUTION (%) OF GROUPS FOR EACH SUPERCRITICAL FRACTION, FOR A CRUDE SAMPLE AND FOR A PURIFIED EXTRACT AND SELECTIVITY OF GROUP V

Selectivity is the % of group V divided by the sum of % of other groups.

Group number	Supercritical fractions								Crude sample	Purified extract
	T = 308 K				T = 318 K					
	8 MPa	15 MPa	20 MPa	25 MPa	8 MPa	15 MPa	20 MPa	25 MPa		
I	1	4	4	3	1	2	4	3	2	0
II	3	9	9	2	1	5	4	5	3	3
III	4	10	3	3	4	9	14	16	11	0
IV	22	39	35	18	7	42	45	58	37	7
V	27	18	15	16	15	28	8	7	10	65
VI	1	1	10	5	11	3	13	8	30	14
VII	42	19	24	53	61	11	12	3	7	11
Selectivity	0.37	0.22	0.18	0.19	0.18	0.39	0.09	0.07	0.11	1.86

perature. The distributions of groups for each extracted fraction are listed in Table V and may be correlated with the selectivity; results for a crude sample extracted by a conventional method (two organic solvents, hexane and dichloromethane) and for a purified fraction (the isolation of which involved selective elutions by flash chromatography [17]) are also given. With the supercritical extracts, most of compounds are distributed mainly among three groups, IV, V and VII, whereas the content of the crude sample is distributed among more groups. A further purification of this crude sample led to a narrow distribution, with a high content of 65% for the fifth group; the presence of compounds in this fraction has to be correlated with the antifungal activities of this extract. Hence terms of selectivity between this group and the six others (Table V), supercritical extraction does not allow the production of highly purified fraction, but it may compete favourably in a first step to the achievement of a crude extract of better quality than is obtainable with organic solvents.

CONCLUSION

The small amounts of sample and fluids used in this modified commercial extractor were useful in optimizing the carbon dioxide extraction of compounds from a complex matrix such as an alga. By increasing the pressure stagewise, extracts of different contents in terms of selectivity and amount can be obtained; the choice of operating conditions will depend on the purpose and on the demands of the extraction process. Therefore, these results indicate that an extraction process with a supercritical fluid in order to obtain different active compounds from algae is practicable and that this process will compete favourably with classical processes such as liquid extraction.

Further experiments will be performed in order to increase the selectivity of the extraction. We have already used a modifier such as ethyl acetate in addition to carbon dioxide, but it does not induce noticeable modifications. Future studies will concern the use of packed beds to fractionate the extract during the collection step.

REFERENCES

1 S. B. Hawthorne, M. S. Krieger and D. J. Miller, *Anal. Chem.*, 60 (1988) 472.
2 P. Pellerin, in M. Perrut (Editor), *Proceedings of the 1st International Symposium on Supercritical Fluids, Nice, October 17–19, 1988*, Institut National Polytechnique de Lorraine, Nancy, 1988, p. 677.
3 K. Sugiyama and M. Saito, *J. Chromatogr.*, 442 (1988) 121.
4 F. Temelli, J. P. O'Connell, C. S. Chen and R. J. Braddock, *Ind. Eng. Chem. Res.*, 29 (1990) 618.
5 D. M. Kassim and M. S. Hameed, *Sep. Sci. Technol.*, 24 (1990) 1427.
6 A. J. Jay, T. W. Smith and P. Richmond, in M. Perrut (Editor), *Proceedings of the 1st International Symposium on Supercritical Fluids, Nice, October 17–19, 1988*, Institut National Polytechnique de Lorraine, Nancy, 1988, p. 821.
7 A. Manabe, T. Tokumori, Y. Sumida, T. Yoshida, T. Hatano, K. Yazaki and T. Okuda, *Yakugaku Zasshi*, 107 (1987) 506.
8 A. B. de Haan, J. de Graauw, J. E. Schaap and H. T. Badings, *J. Supercrit. Fluids*, 3 (1990) 15.
9 J. De la Noue, D. Proulx, P. Dion and C. Gudin, *Aquaculture 1989*, European Aquaculture Society, in press.
10 S. Mabeau, O. Vallat and C. Rochas, *Biofutur*, 88 (1990) 30.
11 J. Moreau, D. Pesando and B. Caram, *Hydrobiologia*, 116/117 (1984) 521.
12 S. de Rosa, S. de Stephano, S. Macura, E. Trivellane and N. Zavodnik, *Tetrahedron*, 23 (1984) 499.
13 S. Caccamese and R. Azzolina, *Planta Med.*, 37 (1979) 333.

14 F. Cafieri, L. De Napoli, E. Fattorusso and C. Santacroce, *Phytochemistry*, 27 (1988) 621.
15 S. Caccamese, O. Cascio and A. Campagnini, *J. Chromatogr.*, 478 (1989) 255.
16 N. Bouaïcha and D. Pesando, personal communication.
17 P. Subra, N. Bouaïcha and D. Pesando, in preparation.
18 E. Stahl, W. Schilz, E. Schütz and E. Willing, in G. Schneider, E. Stahl and G. Wilke (Editors), *Extraction with Supercritical gases*, Verlag Chemie, Weinheim, Deerfield Beach, FL, and Basle, 1980, p. 100.
19 S. B. Hawthorne, *Anal. Chem.*, 62 (1990) 633A.
20 P. Subra and R. Tufeu, *J. Supercrit. Fluids*, 3 (1990) 20.

Journal of Chromatography, 543 (1991) 425–438
Elsevier Science Publishers B.V., Amsterdam

CHROM. 23 135

Anomalous retention behaviour of some synthetic nucleosides on aluminium oxide layers

TIBOR CSERHÁTI

Central Research Institute for Chemistry, Hungarian Academy of Sciences, P.O. Box 17, H-1525 Budapest (Hungary)

(First received October 11th, 1990; revised manuscript received January 24th, 1991)

ABSTRACT

The retention of 21 nucleoside derivatives with various alkyl substituents at the 5'-position was determined on unimpregnated and paraffin oil-impregnated alumina layers using dichloroethane–methanol, water–methanol, water–ethanol and water–2-propanol eluent systems. The nucleosides showed anomalous retention behavior in each system: their retention first decreased with increasing concentration of the stronger component in the eluent, reached a maximum, and then increased with further increase in the concentration of the stronger component in the eluent. The data indicate a mixed (adsorption and reversed-phase) retention mechanism independently of the impregnation of the alumina surface. A quadratic equation described well the dependence of the R_M value on the concentration of the stronger component in the eluent; the parameters of the quadratic equation showed a high intercorrelation. The chain length of the alkyl substituent and the number of triple bonds in the alkyl chain governed the retention of nucleoside derivatives in each eluent system.

INTRODUCTION

In recent years quantitative structure–activity relationship (QSAR) studies have often promoted the design of novel bioactive compounds [1]. QSAR methods may also help in the elucidation of the role of hydrophobic interactions in various biochemical [2] and biophysical processes [3]. In the search for the best correlation between chemical structure and biological activity, a wide range of molecular parameters have been applied [4] and many of these parameters can readily be determined by various chromatographic techniques [5]. Chromatographic methods have several advantages: they are rapid and relatively simple, very small amounts of the substances are required and the compounds used need not be very pure. Lipophilicity as the molecular parameter used most frequently in QSAR studies can also be determined by reversed-phase high-performance liquid chromatography [6], reversed-phase thin-layer chromatography (RPTLC) [7] and gas chromatography [8].

The R_M value (related to the molecular lipophilicity), determined through the use of RPTLC, generally depends on the concentration of the organic component in the eluent [9]. In most instances the correlation is linear. The R_M value extrapolated to zero organic phase concentration (R_{M0}) was regarded as the most accurate estimate

0021-9673/91/$03.50

of lipophilicity. However, marked deviations from linearity have been observed with quaternary amino steroids [10], crown ether derivatives [11] and peptides [12]. The R_M value decreased with increasing organic component concentration in the lower concentration range, reached a maximum and then increased with further increase in the proportion of organic component. This phenomenon was tentatively explained in terms of a silanophilic effect: at higher organic component concentrations, the solute molecules have an enhanced probability of access to the silanol groups uncovered by the impregnating agent. The interaction with the free silanol groups results in an increased retention and an increased apparent lipophilicity [13,14]. It was further established that the relative polarity of the mobile and stationary phases is the main distinguishing attribute for the classification of different chromatographic systems; in other words, in RPTLC, the stationary phase has to be less polar than the mobile phase [14]. This means that the impregnation or chemical bonding of hydrophobic substituents to the support is not a prerequisite in RPTLC. The validity of the hypothesis outlined above was proved to be correct for unimpregnated cellulose [15]. For example, the application of water–alcohol mixtures on unimpregnated layers may result in an adsorption or reversed-phase retention mode depending on the relative polarity of the stationary and mobile phases.

It has additionally been stated that not only the R_M value extrapolated to zero organic phase concentration but also the slope (b) value of the linear correlation is characteristic of molecular lipophilicity [15]. With a homologous series of compounds the slope and the R_{M0} value exhibited a significant intercorrelation [16], but for a non-homologous series both parameters were needed to describe the lipophilicity accurately [17]. The slope has been regarded as a characteristic of the hydrophobic surface of the compounds [18].

The various molecular parameters determined by means of adsorption chromatography (relative energy of adsorption, specific adsorption surface) have found only limited application in QSAR. A good correlation was found between the tumour-inhibiting activity and the relative energy of adsorption for a series of benzofluorene derivatives [19].

Synthetic nucleosides have many biological effects [20]; they can be incorporated into DNA [21], resulting in the modification of some enzymatic processes [22]. The dependence of their biological activity on certain chromatographic parameters has recently been demonstrated [23]. The adsorption capacity, the specific adsorptive surface, the lipophilicity and the specific hydrophobic surface of some nucleosides have recently been determined using a silica support [24].

Nucleosides may be partially ionized in an aqueous environment, with the result that the pH and the ionic strength of the eluent may influence their retention. As the nature of the buffer [25] and the buffer mobility [26] also influence the retention, we assumed that the inclusion of so many variables (pH, ionic strength, buffer type and buffer mobility) would overcomplicate the experimental design and the calculation. Accordingly, we used unbuffered, ion-free eluent systems. Our choice was also guided by the fact that the adsorptive, non-aqueous systems were also unbuffered and ion free, and hence the comparison of the systems is facilitated. The objectives of our investigations were to determine some hydrophilic and hydrophobic parameters of nucleosides using alumina as a support, to select the molecular substructures that significantly influence the parameters and to find correlations between the various parameters.

EXPERIMENTAL

DC-Fertigplatten Aluminiumoxid 60 F_{254} plates (Merck, Darmstadt, Germany) were used for adsorptive TLC without any pretreatment. For RPTLC the plates were impregnated with paraffin oil as described earlier [27]. The nucleosides were the 5′-alkylated derivatives of deoxyuridine (**1**), *i.e.*, methyl (**2**), ethyl- (**3**), *n*-propyl- (**4**), butyl- (**5**), hexyl- (**6**), heptyl- (**7**), octyl- (**8**), vinyl- (**9**), pentenyl- (**10**), hexenyl- (**11**), heptenyl- (**12**), octenyl- (**13**), propynyl- (**14**), butynyl- (**15**), pentynyl- (**16**), hexynyl (**17**), heptynyl- (**18**), octynyl- (**19**), isopropyl- (**20**) and bromovinyldeoxyuridine (**21**). They were synthesized by the research group of Dr. J. Sági at the Central Research Institute for Chemistry of the Hungarian Academy of Sciences (Budapest, Hungary).

The nucleoside derivatives were dissolved separately in methanol to give a concentration of 5 mg/ml, and 2 μl of solution were spotted on the plates with a Camag (Muttenz, Switzerland) applicator. The developments were carried out in sandwich chambers, the running distance being about 16 cm. Dichloroethane–methanol (1:0, 3:1, 1:1, 1:3 and 0:1, v/v) and water–methanol, water–ethanol and water–2-propanol mixtures (15–90%, v/v, alcohol in steps of 5%) were applied as eluents for adsorption TLC. The application of the uncommon water–alcohol mixtures as adsorption-mode eluents was motivated by the considerations mentioned in the Introduction about the distinguishing features of adsorption and reversed-phase separation modes. For RPTLC, ethanol was applied as the organic mobile phase in the concentration range 0–90% (v/v) in steps of 10%.

After development the plates were dried at 105°C and the nucleoside spots were detected under a CAMAG UV lamp at 254 nm. Each determination was run in quadruplicate. The R_M values were calculated for both TLC and RPTLC systems.

When in a given chromatographic system the nucleoside spot remained at the start or was very near to the front (deformed spot shape) or when the relative standard deviation of parallel determinations was higher than 8%, the data were omitted from the calculations. As the linear correlation between the R_M value of the nucleosides and the alcohol concentration in the eluent did not fit the experimental data well, quadratic correlations were calculated for each nucleoside–organic modifier pair:

$$R_M = R_{M0} + b_1C + b_2C^2 \quad (1)$$

where R_M = actual R_M value of a compound at an alcohol concentration C in the eluent, R_{M0} = R_M value extrapolated to zero alcohol concentration, C = alcohol concentration in the eluent (%, v/v), b_1 = change in R_M value caused by a unit change in alcohol concentration and b_2 = change in R_M value caused by a unit change in the alcohol concentration squared.

To assess the contributions of the nucleoside lipophilicity and the nature of the organic component to the anomalous retention behaviour, the organic compound concentration corresponding to minimum retention (C_M) was calculated with the parameters of eqn. 1. Mathematically, C_M corresponds to the point where the first derivative of eqn. 1 is equal to zero.

To elucidate the similarities and dissimilarities between the retention behaviour of the nucleosides and the parameters of eqn. 1, principal component analysis (PCA)

was applied [28]. The nucleosides were taken as observations, and the parameters (R_{M0}, b_1, b_2 and C_M values separately for methanol, ethanol and 2-propanol on unimpregnated alumina; a total of twelve variables) served as variables. Two-dimensional non-linear mapping of the PC loadings and variables was also carried out [29].

To find the molecular substructures accounting for the retention behaviour, stepwise regression analysis was applied [30]. The calculation was carried out sixteen times; the R_{M0}, b_1, b_2 and C_M values of eqn. 1. determined in methanol, ethanol and 2-propanol as organic mobile phases on unimpregnated alumina and in ethanol on impregnated alumina were the dependent variables. The length of the alkyl chain, the number of double and triple bonds in the chain and the number of branching and bromo substitutions were the independent variables in each instance. The acceptance limit for the individual independent variables was set to the 95% significance level.

RESULTS AND DISCUSSION

Solvent demixing was not observed in the eluent systems; in each instance the first and second eluent fronts were very near to each other and the nucleoside spots were always under the second eluent front.

The nucleosides showed anomalous retention behaviour even under strictly adsorption conditions (unimpregnated alumina, dichloroethane–methanol mixtures as eluents). They remained at the start in pure dichloroethane and pure methanol and showed low mobility in eluents of 1:3 and 3:1 (v/v). The lowest retention was observed in the 1:1 (v/v) eluent. This phenomenon is similar in character to the silanophilic effect. It has been customary to use this term for the attraction (retention) of solutes by SiOH groups. However, in this instance the support was unimpregnated alumina, which does not contain any silanol groups. We are well aware that the application of the term "silanophilic effect" to describe the anomalous retention behaviour of nucleosides is somewhat misleading. As the phenomenon is similar we subsequently use the term "silanophilic-like effect", bearing in mind the differences between the two retention mechanisms discussed above.

It was expected that the mobility of the nucleosides would increase with increasing concentration of methanol. The data contradict this supposition. We have no valid hypothesis to explain this anomalous retention behaviour. The R_M value decreased with increasing length of the alkyl chain (Fig. 1), which indicates a normal-phase separation mode.

The relationship between the chain length and the R_M value was not linear. The presence of a double bond in the alkyl chain increased the retention slightly and a triple bond increased it strongly; the difference between the effects of double and triple bonds was higher than expected from their physico-chemical characteristics.

In water–alcohol eluents on unimpregnated alumina the nucleosides showed typical silanophilic-like retention behaviour; the R_M value decreased or did not change in the lower concentration range, then increased with increasing alcohol concentration (Fig. 2). Methanol had the smallest and 2-propanol the greatest impact on the retention at higher alcohol concentrations. This order corresponds to the order of reversed-phase eluent strengths; however, higher concentrations of water with respect to alcohol caused a decrease in R_M, which would be compatible with a normal-phase mechanism. These observations indicate a mixed mode of retention that is not well

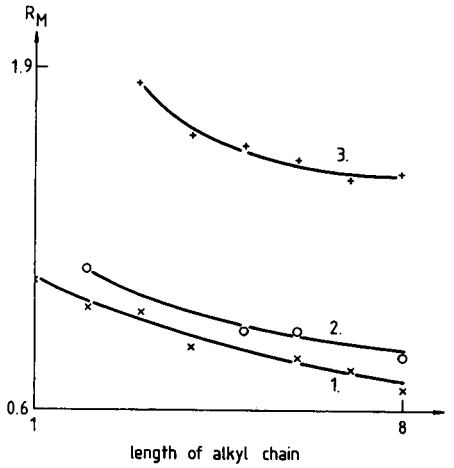

Fig. 1. Effect of the length of the alkyl chain on the R_M values of some synthetic nucleosides. Eluent: dichloroethane–methanol (1:1, v/v). 1 = Saturated alkyl chain; 2 = double bond in the alkyl chain; 3 = triple bond in the alkyl chain.

understood. The water–alcohol eluents at higher alcohol concentrations behaved similarly to dichloroethane–methanol (1:1, v/v) eluent; the nucleosides with the longest alkyl chain showed the highest mobility and the difference between the retentions of nucleosides with saturated and unsaturated chains was the same (Fig. 3). This finding suggests that the retention is governed by the adsorption separation mechanism; however, the eluent is of reversed-phase character.

The retention order of nucleosides changed continuously with changing alcohol concentration and it showed a curious picture at the lowest alcohol concentration (Fig. 4). The R_M value decreased with increasing length of the alkyl chain for the shorter chains, which indicates an adsorption-type separation. It increased again with

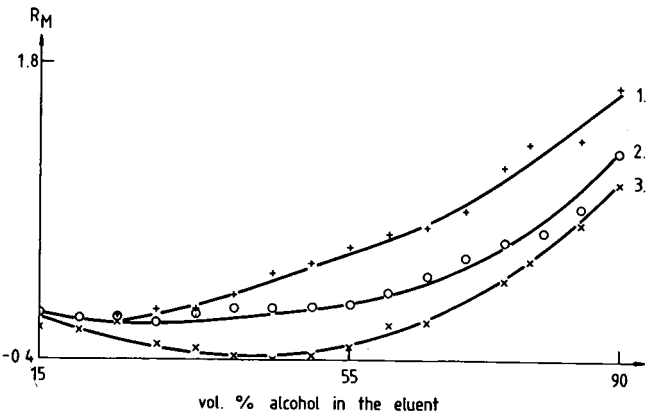

Fig. 2. Effect of the alcohol concentration in the eluent on the R_M value of 5'-hexynyldeoxyuridine. Unimpregnated alumina, water–alcohol eluents. 1 = Methanol; 2 = ethanol; 3 = 2-propanol.

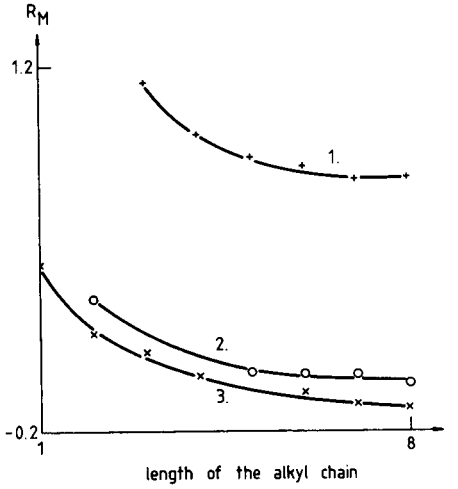

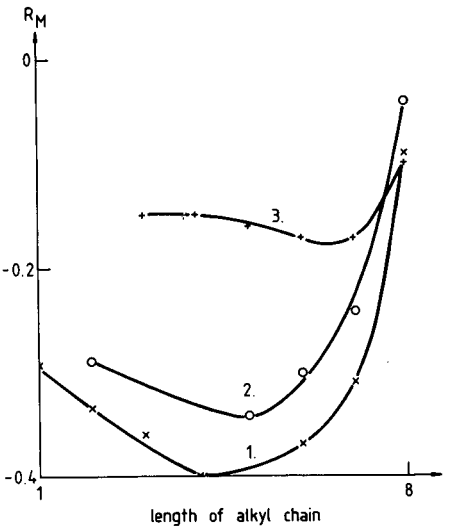

Fig. 3. Effect of the length of the alkyl chain on the R_M values of some synthetic nucleosides. Eluent, water–2-propanol (1:9, v/v). 1 = Saturated alkyl chain; 2 = double bond in the alkyl chain; 3 = triple bond in the alkyl chain.

Fig. 4. Effect of the length of the alkyl chain on the R_M values of some synthetic nucleosides. Eluent, water–2-propanol (85:15, v/v). 1 = Saturated alkyl chain; 2 = double bond in the alkyl chain; 3 = triple bond in the alkyl chain.

increasing length of the alkyl chain at longer chain lengths, which indicates a reversed-phase separation mechanism. This result can be explained by the assumption that the retention mechanism in the same chromatographic system may depend heavily on the type of solute because its partitioning between the stationary and mobile phases may depend on the length and lipophilicity of the alkyl chain substituents.

The substantial role of triple bonds in determining retention prevails for the shorter alkyl chains and disappears with longer alkyl chains.

The results indicate that the retention of nucleosides is highly irregular on unimpregnated alumina; at least two retention mechanism (adsorption and reversed-phase) are involved, their relative importance depending on the type and composition of the eluent and on the character of the alkyl substituent. The data do not exclude the possibility that the change in intermolecular forces (caused by the changing dielectric constant of the eluents) may also influence the retention, as was observed with silica-based supports [31].

Similar anomalies were observed on impregnated alumina (Fig. 5). The R_M values decreased with growing ethanol concentration in water in the lower concentration range, reached a minimum, then increased again.

The importance of triple bonds is manifested only at higher ethanol concentrations (adsorption-like separation mechanism). In this instance the anomaly can be explained by the silanophilic-like effect when we assume that for the appearance of the silanophilic-like effect a support with uncovered adsorption centres is sufficient and the adsorption centres need not to be silanol groups. However, this explanation is

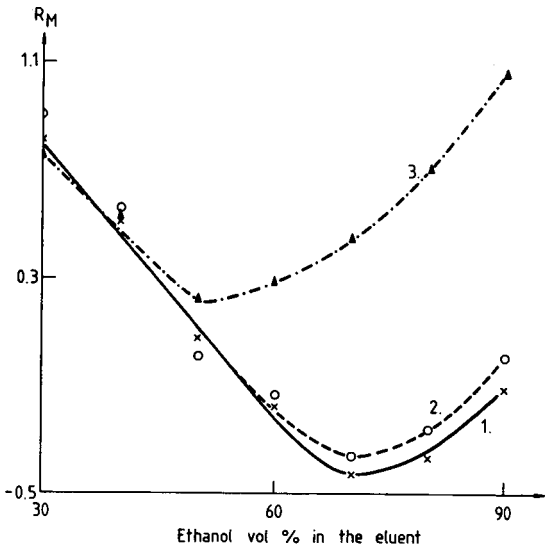

Fig. 5. Effect of ethanol concentration in the water–ethanol eluent on the R_M value of (1) hexyl-, (2) hexenyl- and (3) hexynyldeoxyuridine. Impregnated alumina.

not valid for the unimpregnated alumina, showing similar retention behaviour. We suggest two possible mechanisms to account for the irregularities:

(a) The water or the alcohol is adsorbed on the alumina depending on their relative concentrations in the eluent. The quasi-stationary phase of water or alcohol behaves as an adsorption or reversed-phase support, respectively, depending on the equilibrium of the various nucleoside derivatives between the stationary and mobile phases.

(b) The extent of dissociation of the nucleosides depends strongly on the dielectric constant of the eluent, which decreases with increasing proportion of organic component in the mobile phase. The dissociated and undissociated nucleosides may be retained in the same eluent by an adsorption or reversed-phase retention mechanism, the retention being influenced by the changing intramolecular forces.

We assume that both processes have a considerable impact on the retention and the retention order is the result of the interplay of the processes outlined above.

The parameters of eqn. 1 are compiled in Tables I–IV. Blanks in Table I indicate that the linear regression coefficient did not differ significantly from zero. The quadratic function fits the experimental data well, the significance level in each instance being higher than 99.9%, confirming the applicability of eqn. 1 (see F values). The equation accounted for about 92–99% of the total variance (see r^2 values). The normalized slope values (b'_1 and b'_2 values) clearly show that the contribution of the linear and quadratic parameters to the retention is commensurable. The numerical values of the slope (b_1) increased in the order methanol < ethanol < 2-propanol on unimpregnated alumina. As this order corresponds to the reversed-phase elution strength of the alcohols, this phenomenon indicates a reversed-phase separation mechanism. For deoxyuridine derivatives with a saturated alkyl chain and with a double bond in the alkyl chain the intercept (R_{M0}) values generally increased with

TABLE I

PARAMETERS OF THE QUADRATIC RELATIONSHIP BETWEEN THE R_M VALUES OF NUCLEOSIDES AND THE METHANOL CONCENTRATION (C) IN THE ELUENT USING UNIMPREGNATED ALUMINA

$R_M = R_{M0} + b_1C + b_2C^2$.

Parameter	No. of nucleoside						
	1	**2**	**3**	**4**	**5**	**6**	**7**
R_{M0}	50.4	−1.38	11.1	6.49	−5.27	9.81	39.9
b_1	−4.02	−1.55	−2.12	−2.08	−1.65	−2.54	−3.52
$b_2 \cdot 10^2$	4.96	2.79	2.99	3.03	2.57	3.48	4.23
F	104.9	136.1	72.3	67.8	100.4	77.5	73.6
r^2	0.9589	0.9612	0.9393	0.9250	0.9481	0.9337	0.9305
b'_1(%)	41.01	32.28	37.88	37.13	35.50	38.56	41.69
b'_2(%)	58.99	67.72	62.12	62.87	64.50	61.44	58.31
	8	**9**	**10**	**11**	**12**	**13**	**14**
R_{M0}	51.1	−45.5	56.1	32.0	38.3	79.6	−24.3
b_1	−3.83	–	–	−3.21	−3.60	−4.65	–
$b_2 \cdot 10^2$	4.45	1.50	1.56	4.23	4.72	5.26	2.14
F	102.2	190.5	162.0	182.1	173.7	180.4	709.6
r^2	0.9489	0.9407	0.9310	0.9707	0.9693	0.9704	0.9834
b'_1(%)	42.53	–	–	39.46	39.58	43.15	–
b'_2(%)	57.47	–	–	60.54	60.42	56.85	–
	15	**16**	**17**	**18**	**19**	**20**	**21**
R_{M0}	−25.9	−24.7	−22.9	−23.4	−21.5	−58.1	−52.6
b_1	–	–	–	–	–	–	–
$b_2 \cdot 10^2$	2.10	2.02	2.15	1.92	1.89	1.21	1.86
F	756.8	463.2	616.6	323.5	292.6	155.9	291.6
r^2	0.9844	0.9748	0.9809	0.9672	0.9606	0.9285	0.9605
b'_1(%)	–	–	–	–	–	–	–
b'_2(%)	–	–	–	–	–	–	–

increasing length of the alkyl substituent, which also supports the reversed-phase retention mechanism. However, the derivatives with triple bonds did not show a similar retention behaviour, that is, for these the reversed-phase retention mechanism is not valid. The unsubstituted deoxyuridine deviates considerably from the retention order. It shows a higher retention than would be expected under reversed-phase conditions. We assume that the free hydrogen can form hydrogen bonds with the free adsorption centres of alumina, resulting in increased retention.

Only one background variable explains the majority of the variance in the data matrix for PCA (Table V). It means that may exists only one chromatographic parameter that accounts for about 80% of variance. We must stress that the PCA did not state that such a parameter really exists, it only indicates the mathematical possibility of it. Each parameter has a high loading in the first component, which demon-

TABLE II

PARAMETERS OF THE QUADRATIC RELATIONSHIP BETWEEN THE R_M VALUES OF NUCLEOSIDES AND THE ETHANOL CONCENTRATION (C) IN THE ELUENT USING UNIMPREGNATED ALUMINA

$R_M = R_{M0} + b_1C + b_2C^2$.

Parameter	No. of nucleoside						
	1	**2**	**3**	**4**	**5**	**6**	**7**
R_{M0}	183.1	2.96	30.8	47.2	5.50	64.3	100.6
b_1	−8.71	−1.76	−3.02	−3.81	−2.63	−5.08	−6.45
$b_2 \cdot 10^2$	7.53	2.36	3.12	3.78	2.77	4.78	5.89
F	81.6	97.9	75.4	108.2	188.8	79.7	140.1
r^2	0.9477	0.9377	0.9263	0.9516	0.9667	0.9300	0.9589
b'_1(%)	47.89	41.11	46.45	46.41	47.00	48.76	49.53
b'_2(%)	52.11	58.89	53.55	53.59	53.00	51.24	50.47
	8	**9**	**10**	**11**	**12**	**13**	**14**
R_{M0}	106.7	14.4	41.7	51.3	58.2	102.1	16.8
b_1	−6.73	−2.29	−4.06	−4.36	−4.75	−6.50	−1.52
$b_2 \cdot 10^2$	6.10	2.74	4.09	4.23	4.67	6.07	2.79
F	76.9	110.2	89.4	105.1	77.8	95.7	254.1
r^2	0.9276	0.9443	0.9322	0.9417	0.9229	0.9677	0.9750
b'_1(%)	49.72	43.85	48.12	49.10	48.73	50.02	33.76
b'_2(%)	50.28	56.15	51.88	50.90	51.27	49.98	66.24
	15	**16**	**17**	**18**	**19**	**20**	**21**
R_{M0}	16.8	17.3	24.6	25.7	34.7	5.19	6.66
b_1	−1.52	−1.94	−2.22	−2.39	−2.70	−2.48	−2.38
$b_2 \cdot 10^2$	2.79	3.11	3.40	3.48	3.62	2.57	2.89
F	254.1	138.4	216.0	208.8	145.3	149.2	99.7
r^2	0.9751	0.9551	0.9708	0.9698	0.9572	0.9582	0.9388
b'_1(%)	33.76	36.81	37.88	39.76	41.11	47.46	43.55
b'_2(%)	66.24	63.19	62.12	60.24	58.89	52.54	56.45

strates again the strong intercorrelation between them. The linear regression coefficients form a distinct cluster on the two-dimensional non-linear map of PC loadings, whereas the other parameters form another cluster (Fig. 6). This finding suggests that the intercept value, the quadratic regression coefficient and the critical alcohol concentration contain similar information. As the slope value is generally related to the lipophilicity, we assume that these three parameters are related to the lipophilicity of the nucleoside derivatives. The nucleosides form three separate clusters on the two-dimensional non-linear map of PC variables (Fig. 7). The nucleosides with triple bonds in the alkyl chain (cluster C) form the most compact group, indicating the important role of triple bonds in the retention of nucleosides on unimpregnated alumina. The nucleosides with a saturated alkyl chain form a separate group (cluster A), whereas the nucleosides with double bonds and with branching or bromo sub-

TABLE III

PARAMETERS OF THE QUADRATIC RELATIONSHIP BETWEEN THE R_M VALUES OF NUCLEOSIDES AND THE 2-PROPANOL CONCENTRATION C IN THE ELUENT USING UNIMPREGNATED ALUMINA

$R_M = R_{M0} + b_1C + b_2C^2$.

Parameter	No. of nucleoside						
	1	**2**	**3**	**4**	**5**	**6**	**7**
R_{M0}	269.3	16.8	25.2	45.2	53.0	96.1	136.0
b_1	−14.4	−2.58	−3.47	−4.66	−5.53	−8.15	−9.99
$b_2 \cdot 10^2$	12.7	3.05	3.58	4.52	5.30	7.66	9.25
F	96.9	197.4	135.6	88.4	115.4	173.7	132.8
r^2	0.9556	0.9681	0.9542	0.9315	0.9467	0.9639	0.9533
b'_1(%)	48.73	44.18	47.58	49.03	49.38	49.87	50.24
b'_2(%)	51.27	55.82	52.42	50.97	50.62	50.13	49.76
	8	**9**	**10**	**11**	**12**	**13**	**14**
R_{M0}	154.3	17.7	96.4	124.8	153.1	165.7	7.85
b_1	−10.6	−3.04	−7.64	−9.19	−10.9	−11.3	−1.95
$b_2 \cdot 10^2$	9.67	3.29	7.25	8.64	10.3	10.4	3.44
F	93.7	110.5	95.8	120.0	83.7	104.6	110.5
r^2	0.9351	0.9444	0.9365	0.9486	0.9279	0.9415	0.9526
b'_1(%)	50.61	46.38	49.60	49.85	49.87	50.22	34.38
b'_2(%)	49.39	53.62	50.40	50.15	50.13	49.78	65.62
	15	**16**	**17**	**18**	**19**	**20**	**21**
R_{M0}	8.95	18.5	31.0	45.8	67.7	57.0	75.3
b_1	−2.06	−2.71	−3.57	−4.36	−5.29	−5.10	−5.80
$b_2 \cdot 10^2$	3.37	3.78	4.67	5.15	5.93	4.61	5.48
F	126.4	83.2	80.9	186.6	144.9	144.3	108.9
r^2	0.9583	0.9380	0.9363	0.9664	0.9571	0.9569	0.9437
b'_1(%)	36.26	39.83	41.38	44.20	45.47	50.83	49.73
b'_2(%)	63.74	60.17	58.62	55.80	54.53	49.17	50.27

stitution in the alkyl chain form the third cluster (cluster B). This means that branching and bromo substitution of the alkyl chain have a similar effect to the double bond on the retention of nucleosides.

The significant correlations between the chromatographic parameters and structural characteristics of the nucleoside derivatives are collected in Table VI. As the PCA proved that the chromatographic parameters did not show large differences and are strongly intercorrelated, it was reasonable to assume that the structure–chromatographic parameter correlations will be very similar. The calculation entirely supported this assumption; the equations did not differ considerably from each other. Therefore, only the equations derived from the 2-propanol–unimpregnated alumina system are presented. Each chromatographic parameter was related to the structural characteristics of the nucleoside derivatives and the significance level was over 99.9%

TABLE IV

PARAMETERS OF THE QUADRATIC RELATIONSHIP BETWEEN THE R_M VALUES OF NUCLEOSIDES AND THE ETHANOL CONCENTRATION (C) IN THE ELUENT USING IMPREGNATED ALUMINA

$R_M = R_{M0} + b_1C + b_2C^2$.

Parameter	No. of nucleoside						
	1	**2**	**3**	**4**	**5**	**6**	**7**
R_{M0}	974.1	47.5	83.4	125.4	167.2	322.9	441.5
b_1	−24.9	−3.11	−4.40	−5.80	−6.26	−9.78	−12.9
$b_2 \cdot 10^2$	15.6	3.47	4.16	5.12	4.89	6.68	8.61
F	483.8	79.8	59.6	47.4	131.1	63.2	168.9
r^2	0.9979	0.9580	0.9445	0.9405	0.9740	0.9693	0.9883
b'_1(%)	55.18	48.97	53.09	55.04	57.81	54.71	55.19
b'_2(%)	44.82	51.03	46.91	44.96	42.19	45.29	44.81
	8	**9**	**10**	**11**	**12**	**13**	**14**
R_{M0}	526.9	60.2	231.6	346.5	467.2	536.6	63.8
b_1	−14.9	−3.08	−7.48	−10.5	−13.7	−15.2	−2.66
$b_2 \cdot 10^2$	9.83	3.00	5.47	4.34	9.37	10.2	3.71
F	182.0	116.1	159.0	77.2	185.0	153.3	41.8
r^2	0.9747	0.9707	0.9815	0.9747	0.9979	0.9871	0.9227
b'_1(%)	55.56	52.41	57.16	54.10	54.59	55.18	43.45
b'_2(%)	44.44	47.59	42.84	45.90	45.41	44.82	56.55
	15	**16**	**17**	**18**	**19**	**20**	**21**
R_{M0}	123.2	180.9	313.7	303.2	421.9	129.9	168.1
b_1	−4.70	−6.67	−9.85	−9.37	−12.5	−6.69	−7.27
$b_2 \cdot 10^2$	5.14	6.60	8.46	7.82	9.80	5.94	6.54
F	98.4	75.2	38.1	69.0	38.5	40.9	81.8
r^2	0.9657	0.9619	0.9384	0.9787	0.9506	0.9424	0.9703
b'_1(%)	49.48	52.18	51.01	49.65	51.20	54.61	54.31
b'_2(%)	50.52	47.82	48.99	50.35	48.80	45.39	45.69

in each instance (see F values). The substructures accounted for about 81–94% of the total variance (see r^2 values). The normalized slope values (b') indicate that the length of the alkyl chain and the number of triple bonds in the chain have the greatest impact on the retention. The role of the triple bond is higher than would be expected. We do not have any valid explanation for the phenomenon. It is probable that the triple bond specially binds to the adsorption site on the alumina surface, but the character of the binding is not known.

TABLE V

RESULTS OF PRINCIPAL COMPONENT ANALYSIS USING UNIMPREGNATED ALUMINA

No. of PC	Eigenvalue	Explained variance (%)
1	9.57	79.76
2	1.06	8.86
3	0.92	7.68

Principal component loadings

No. of variable[a]	No. of principal component		
	1	2	3
1	0.82	0.48	0.22
2	−0.93	−0.11	−0.33
3	0.92	0.24	0.24
4	0.84	0.05	0.52
5	0.85	0.28	−0.35
6	−0.97	0.01	0.16
7	0.94	0.14	−0.27
8	0.86	−0.43	0.15
9	0.93	−0.03	−0.32
10	−0.95	0.17	0.17
11	0.94	−0.07	−0.22
12	0.72	−0.66	0.12

[a] 1–4 = Water–methanol eluents: 1 = intercept (a) value; 2 = linear regression coefficient (b_1); 3 = quadratic regression coefficient (b_2); 4 = critical alcohol concentration (C_M). 5–8 = Water–ethanol eluents: 5 = intercept (a) value; 6 = linear regression coefficient (b_1); 7 = quadratic regression coefficient (b_2); 8 = critical alcohol concentration (C_M). 9–12 = Water–2-propanol eluents: 9 = intercept (a) value; 10 = linear regression coefficient (b_1); 11 = quadratic regression coefficient (b_2); 12 = critical alcohol concentration (C_M).

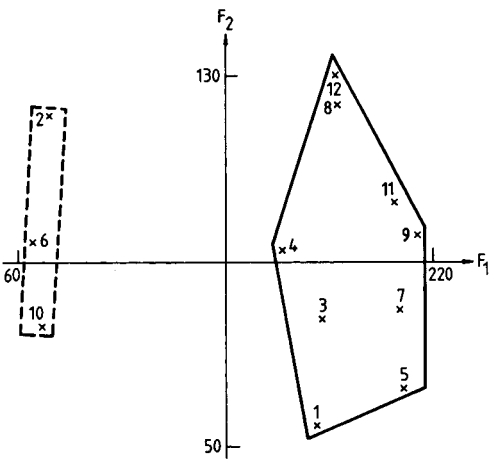

Fig. 6. Two-dimensional non-linear map of PC loadings. Number of iterations, 116 Maximum error, $1.83 \cdot 10^{-3}$. 1–4 = Water–methanol eluents: 1 = intercept (a) value; 2 = linear regression coefficient (b_1); 3 = quadratic regression coefficient (b_2); 4 = critical alcohol concentration (C_M). 5–8 = Water–ethanol eluents: 5 = intercept (a) value; 6 = linear regression coefficient (b_1); 7 = quadratic regression coefficient (b_2); 8 = critical alcohol concentration (C_M). 9–12 = Water–2-propanol eluents: 9 = intercept (a) value; 10 = linear regression coefficient (b_1); 11 = quadratic regression coefficient (b_2); 12 = critical alcohol concentration (C_M).

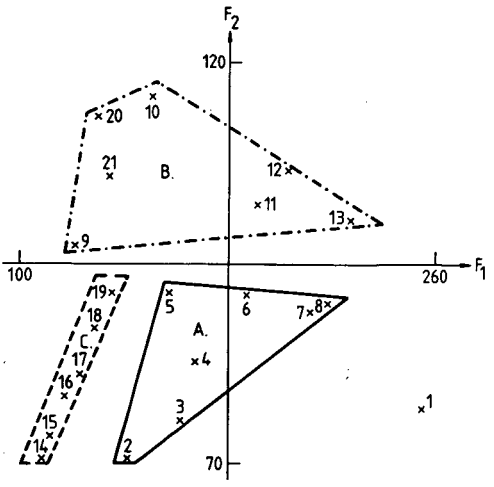

Fig. 7. Two-dimensional non-linear map of PC variables. Number of iterations, 73. Maximum error, $9.59 \cdot 10^{-3}$. Numbers refer to nucleosides given in Experimental.

TABLE VI

PARAMETERS OF SIGNIFICANT CORRELATIONS BETWEEN THE CHROMATOGRAPHIC PARAMETERS AND STRUCTURAL CHARACTERISTICS OF SOME NUCLEOSIDE DERIVATIVES

Results of stepwise regression analysis. Unimpregnated alumina; eluent, water–2-propanol mixtures.
(I) $R_{M0} = a + b_1x_1 + b_2x_2 + b_3x_3 + b_4x_4$.
(II) Regression coefficient (linear) $= a + b_1x_1 + b_3x_3 + b_4x_4$.
(III) Regression coefficient (quadratic) $= a + b_1x_1 + b_3x_3 + b_4x_4$.
(IV) $C_M = a + b_1x_1 + b_2x_2 + b_3x_3$.
x_1 = length of the alkyl chain; x_2 = number of double bonds in the alkyl chain; x_3 = number of triple bonds in the alkyl chain; x_4 = number of bromo substituents in the alkyl chain.

Parameter	Equation No.			
	I	II	III	IV
a	−8.37	−1.10	0.017	44.2
b_1	19.13	−1.21	0.010	1.86
b_2	16.43	–	–	−4.61
b_3	−66.88	4.49	−0.030	−17.75
b_4	45.39	−2.26	0.017	–
F	64.7	79.4	67.4	25.4
r^2	0.9418	0.9334	0.9225	0.8175
b'_1(%)	47.11	51.71	56.96	28.86
b'_2(%)	8.30	–	–	14.67
b'_3(%)	33.78	39.03	33.96	56.47
b'_4(%)	10.81	9.26	9.08	–

REFERENCES

1 C. Hansch, in C.J. Cavallito (Editor), *Structure–Activity Relationships*, Pergamon Press, Oxford, 1973, p. 73.
2 A. Lopata, F. Darvas, K. Valkó, Gy. Mikite, É. Jakucs and A. Kiss-Tamás, *Pestic. Sci.*, 14 (1983) 513.
3 T. Cserháti, J. Bojarski, É. Fenyvesi and J. Szejtli, *J. Chromatogr.*, 351 (1986) 356.
4 R. Franke, in J. K. Seydel (Editor), *QSAR and Strategies in the Design of Bioactive Compounds*, VCH, Weinheim, 1985, p. 59.
5 R. Kaliszan, *Quantitative Structure–Chromatographic Retention Relationships*, Wiley, New York, 1987.
6 T. Braumann, *J. Chromatogr.*, 373 (1986) 191.
7 R. F. Rekker, *J. Chromatogr.*, 300 (1984) 105.
8 B. Rittich and H. Dubsky, *J. Chromatogr.* 209 (1981) 7.
9 L. Ekiert, Z. Grodzinska-Zachvieja and J. Bojarski, *Chromatographia*, 13 (1980) 472.
10 É. János, T. Cserháti and E. Tyihák, *J. High Resolut. Chromatogr. Chromatogr. Commun.*, 5 (1982) 634.
11 T. Cserháti, M. Szögyi and L. Györfi, *Chromatographia*, 20 (1985) 253.
12 T. Cserháti, Gy. Ösapay and M. Szögyi, *J. Chromatogr. Sci.*, 27 (1989) 540.
13 A. Nahum and Cs. Horváth, *J. Chromatogr.*, 203 (1981) 53.
14 K. E. Bij, Cs. Horváth, W. R. Melander and A. Nahum, *J. Chromatogr.*, 203 (1981) 65.
15 T. Cserháti, *Chromatographia*, 18 (1984) 18.
16 T. Cserháti, *Chromatographia*, 18 (1984) 318.
17 K. Valkó, *J. Liq. Chromatogr.*, 7 (1984) 1405.
18 Cs. Horváth, W. R. Melander and I. Molnár, *J. Chromatogr.*, 125 (1976) 129.
19 Z. Peřina, M. Šaršúnová, K. Schmidt and J. Křepelka, *Pharmazie*, 41 (1986) 236.
20 E. De Clercq, *Methods Findings Exp. Clin. Pharmacol.*, 2 (1980) 253.
21 L. Ötvös, J. Sági, T. Kovács and R. T. Walker, *Nucleic Acid Res.*, 15 (1987) 1763.
22 J. Sági, A. Szabolcs, A. Szemzö and L. Ötvös, *Nucleic Acid Res.*, 4 (1977) 2767.
23 K. Valkó, T. Cserháti, I. Fellegvári, J. Sági and A. Szemzö, *J. Chromatogr.*, 507 (1990) 35.
24 T. Cserháti and K. Valkó, *J. Biochem. Biophys. Methods*, 20 (1990) 81.
25 T. Cserháti, M. Szögyi and L. Lelkes, *J. Biochem. Biophys. Methods*, 16 (1988) 263.
26 T. Cserháti and J. Gasparic, *J. Chromatogr.*, 394 (1987) 368.
27 T. Cserháti, B. Bordás, É. Fenyvesi and J. Szejtli, *J. Chromatogr.*, 259 (1983) 107.
28 K. V. Mardia, J. T. Kent and J. M. Bibby, *Multivariate Analysis*, Academic Press, London and New York, 1969, p. 213.
29 J. W. Sammon, Jr., *IEEE Trans. Comput.*, C18 (1969) 401.
30 H. Mager, *Moderne Regressionsanalyse*, Salle, Sauerlander, Frankfurt am Main, 1982, p. 135.
31 W. E. Hammers, M. C. Spanjer and C. L. Ligny, *J. Chromatogr.*, 174 (1979) 291.

Journal of Chromatography, 543 (1991) 439–449
Elsevier Science Publishers B.V., Amsterdam

CHROM. 23 130

Z-Shaped flow cell for UV detection in capillary electrophoresis

J. P. CHERVET*, R. E. J. VAN SOEST and M. URSEM
LC Packings, Baarsjesweg 154, 1057 HM Amsterdam (The Netherlands)
(First received November 27th, 1990; revised manuscript received January 25th, 1991)

ABSTRACT

A longitudinal (Z-shaped) flow cell for improved UV detection for capillary electrophoresis was examined and compared with perpendicular (on-column) detection. Bending of a small section of the capillary column into a Z-shaped flow cell has no adverse influence on the electrophoresis process. With enhancements in signal-to-noise ratio of up to 6-fold for 3-mm Z-shaped flow cells, a considerable improvement in detectability is possible. The increase in signal of up to 14-fold in comparison with on-column UV detection illustrates the potential of this new type of capillary flow cell. The loss in resolution caused by the extended path length is less pronounced than expected, and can be tolerated in many of the CE separation modes.

INTRODUCTION

A wide variety of detection techniques have been developed for capillary electrophoresis (CE) and have been reviewed recently [1–3]. Owing to its universal nature and its ease of use, UV detection is still the most popular method. In order to minimize band spreading and to cope with the nanolitre zone volumes, on-column UV detection is mainly used. Nevertheless, with capillaries of I.D. less than 100 μm, considerable loss in sensitivity is encountered. Recently, several attempts have been made to extend the path length for UV detection in CE. Tsuda *et al.* [4] described the use of rectangular tubing with widths of up to 1 mm, while Grant and Steuer [5] extended the path length up to 3 mm by axial illumination of the capillary using laser-induced fluorescence with indirect UV detection. Owing to the presence of high background noise, however, the advantage of an increased path length could not be fully exploited with this approach.

In capillary LC the successful use of longitudinal flow cells with volumes of $\leqslant$90 nl and path lengths of up to 20 mm resulting in enhancements in the signal-to-noise ratio of up to 100-fold have been described [6]. It was therefore of interest to know if similar types of flow cells with shorter path lengths (maximum 3–4 mm) could be used for UV detection in CE, where the maximum tolerable path length is determined by the width of the zone rather than the peak volume. Further, the influence of the bends (Z shape) on the electrophoretic process and the peak distortion caused by

0021-9673/91/$03.50

the extended path length have to been established.

The aim of this work was to evaluate the performance of longitudinal (Z-shaped) capillary flow cells. The advantages and drawbacks are discussed.

EXPERIMENTAL

Reagents

Nucleosides (2′-deoxycytidine, 2′-deoxyguanosine), nucleotides (2′-deoxyguanosine-5′-monophosphate, 2′-deoxycytidine-5′-monophosphate) and peptides (met-enkephalin, leu-enkephalin, val-5-angiotensin II, angiotensin II) were purchased from Sigma (St. Louis, MO, U.S.A.). Other reagents and solvents were of analytical-reagent grade.

The compounds were dissolved in water at concentrations of 50 μg/ml each. For electrophoresis of the nucleosides and nucleotides a 75 m*M* sodium dodecyl sulphate (SDS)–10 m*M* phosphate–6 m*M* borate buffer (pH 8.5) was used and for the peptides a 50 m*M* SDS–10 m*M* borate buffer (pH 8.5). Buffer solutions and samples were filtered through 0.2-μm membrane filters (Chromafil; Macherey, Nagel & Co., Düren, Germany) and were stored at 4°C.

Flow cell construction

In order to minimize zone dispersion and to facilitate handling, the Z-shaped flow cell is constructed as part of the capillary column by bending a small section of the capillary into a Z shape. The bending of fused-silica tubing into Z or U configurations has been described elsewhere [7].

The flow cell (Fig. 1) is prepared by sandwiching a shim (made of alumina) with the bent capillary between two plastic disks (black polyethylene). The thickness of the shim and the sharpness of the capillary bends determine the total path length of the flow cell. For shims of 1 mm thickness, and for sharp bends, flow cells of *ca.* 3 mm path length can be obtained. The shim has a centred hole of 300 μm that is adapted to match the O.D. of the fused-silica capillary. Each plastic disk has a groove to fix the capillary with epoxy resin in order to obtain a stable capillary flow cell. For on-column detection the same type of shims and plastic disks was used. Thus, the 300-μm hole of the shim served as an aperture for on-column detection, placed directly in front of the perpendicular capillary. The distance between the flow cell and the photodiode was *ca.* 3–4 mm and was equal for both types of flow cell.

Capillary column pretreatment

Capillary columns were made of fused-silica tubing of 50 or 75 μm I.D. and 280 μm O.D. (Polymicro Technologies, Phoenix, AZ, U.S.A.). Typically, the columns had a length of 60 cm, with 40 cm to the detector.

The columns were pretreated with 0.1 *M* sodium hydroxide solution for 5 min (*ca.* 25× capillary volume), followed by a 5-min rinse with water. After each injection, the column was rinsed with 0.1 *M* sodium hydroxide solution for 1 min (*ca.* 5× capillary volume), followed by a 1-min rinse with water.

Instrumentation

The basic electrophoretic apparatus was similar to that described in detail by

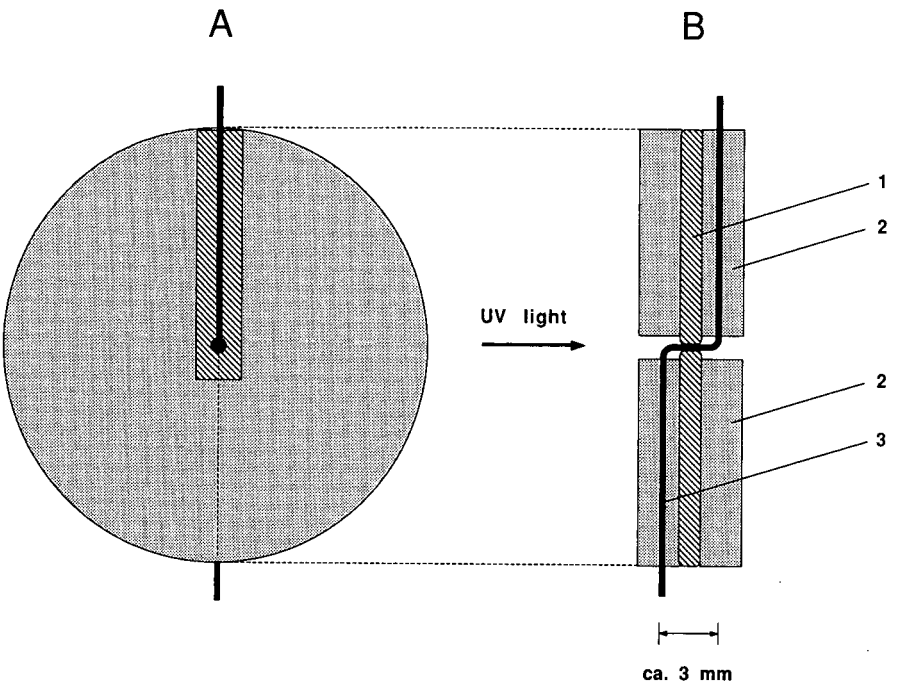

Fig. 1. Schematic diagram of the 3-mm Z-shaped capillary flow cell. (A) Front view; (B) cross-sectional view. 1 = Shim (alumina) with centred 300 μm I.D. hole; 2 = plastic disks (black polyethylene or Plexiglas); 3 = fused-silica capillary of 50 or 75 μm I.D., 280 μm O.D.

Jorgenson and Lukacs [8,9]. A variable-wavelength UV detector (Model 433; Kontron Instruments, Milan, Italy) equipped with a flow-cell holder was used for all measurements. The holder guarantees optimum positioning and alignment of the flow cell (Z shape and on-column). It minimizes the distance between the flow cell and the photodiode [10] and allows for easy capillary column replacement.

A d.c. power supply capable of delivering up to 30 kV (Alpha III, Model 3807; Brandenburg, Surrey, U.K.) was used to provide the high voltage. Sample introduction was accomplished manually by hydrostatic injections with a height of 10 cm for 5 s. All data were collected with a Kontron Datasystem 450, using MT-2 chromatography software (Kontron Instruments).

THEORY

UV detection

In UV detection, flow cells of longer path length (l_c) exhibit increased sensitivities. If, however, the volume of the flow cell has to be minimized, the I.D. of the flow cell must be reduced, which results in a smaller aperture width (d_c). As a consequence, the optical transmittance of the flow cell decreases rapidly, resulting in poor linearity and increased noise levels. For UV detectors with common cylindrical flow cells, the ideal optics have numbers for the optical aperture (d_c/l_c) within the range 1/10 to 1/5 [11]. Fig. 2 illustrates qualitatively this optimum aperture range for micro flow cells with volumes ranging from 2 to 20 nl.

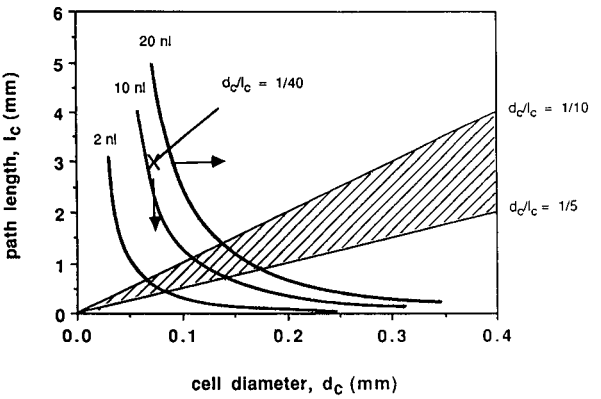

Fig. 2. Aperture ratios (d_c/l_c) for cylindrical flow cells. Optimum (shaded area), 3-mm Z-shaped (×); arrows indicate directions for aperture optimization.

For values below 1/10 the utilizable light energy rapidly decreases, resulting in increased noise and poor linearity. For values above 1/5 the path length becomes too short, resulting in poor sensitivity. Optimum values for d_c/l_c are in the shaded area. In principle, longitudinal (Z-shaped) capillary flow cells have the same cylindrical geometry as common flow cells used in UV detection. Assuming that the same aperture ratios (d_c/l_c) are valid for the capillary flow cells, values far beyond the optimum of 1/10 result, *e.g.*, 1/40 for a 3 mm × 75 μm I.D. capillary flow cell. However, the substantial gain in sensitivity with Z-shaped flow cells counterbalances the drawbacks of increased noise and loss in linearity. Nevertheless, ideal optical d_c/l_c ratios can only be accomplished with capillaries of larger I.D. and/or shorter path lengths.

Dispersion in CE

In CE, the dispersion of a zone can be expressed by its total variance [12,13]. Assuming an ideal Gaussian distribution of the zone, the total variance can then be summed in terms of its individual variances according to the well known relationship

$$\sigma^2_{tot} = \sigma^2_{col} + \sigma^2_{inj} + \sigma^2_{det} \quad (1)$$

where σ^2_{col} is the variance generated during the migration of the zone in the capillary column and σ^2_{inj} and σ^2_{det} are variances originating from the injection and detection system, respectively.

The spreading of the zone in the capillary (σ^2_{col}), which includes the longitudinal molecular diffusion, dispersion by Joule heating and deviation from the ideal electroosmotic plug flow, is usually the major contributor to σ^2_{tot}. For longitudinal flow cells with a path length longer than 3 mm, the detection system starts to exhibit a sizable contribution to the total peak distortion and therefore should be considered.

For an ideal rectangular zone, the dispersion of the detector cell (σ^2_{det}) can be expressed as

$$\sigma^2_{det} = l^2_c/12 \quad (2)$$

where l_c is the path length of the detector cell [14]. Hence the dispersion of a zone in a flow cell is determined mainly by the path length. Since in CE the separation is still in progress in the flow cell, it is advisable to define the influence of the path length as zone distortion, rather than dispersion.

Assuming that the injection and other factors that contribute to the total dispersion of the zone are relatively small in comparison with σ^2_{col} and σ^2_{det}, and by replacing σ^2_{tot} by l_c^2/N in eqn. 1, the following equation can be derived for the maximum tolerable path length ($l_{c\ max}$) of the flow cell [5]:

$$l_{c\ max} = [(12/N)^{1/2}]\ \{[f/(1 - f)]^{1/2}\}\ L \tag{3}$$

where f is the fraction of theoretical plates lost that is tolerated, N the number of theoretical plates and L the length of the capillary column (from column inlet to detector).

If a moderate loss in efficiency can be tolerated, path lengths of up to 3 mm are possible (see Fig. 3). For example, if a loss of 30% in plate numbers ($f = 0.3$) can be tolerated, we can calculate for a 1-m column and an efficiency of 600 000 theoretical plates a maximum path length of almost 3 mm. In agreement with the Beer–Lambert law, the gain in sensitivity would be substantial.

RESULTS AND DISCUSSION

Influence of the bends (Z shape)

To examine the influence of the 3-mm Z-shaped flow cell on the electrophoretic process, without interfering with the UV detection, two similar capillary columns with on-column detection were used (see Table I). One of the capillaries had an additional Z-shaped flow cell (bends) in the separation part of the column. The two capillary columns were tested under identical conditions. Both capillaries showed identical electropherograms. The resulting efficiencies and asymmetries for the nucleoside–nucleotide test mixture are summarized in Table I.

As expected, the bending of a small portion of the capillary column into a Z

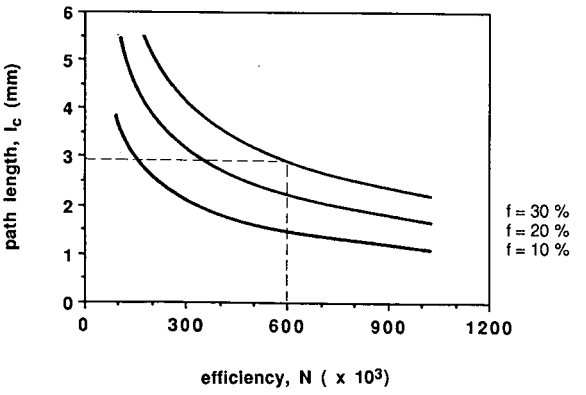

Fig. 3. Maximum tolerable path length *vs.* column efficiency for different fractional losses (f), in efficiency for a capillary column of 1 m length.

TABLE I

INFLUENCE OF BENDS (Z SHAPE) ON EFFICIENCY (N) AND ASYMMETRY (s)

Compound	On-column		On-column + bends	
	N ($\times 10^3$)	s	N ($\times 10^3$)	s
2'-Deoxycytidine	142	0.93	119	0.90
2'-Deoxyguanosine	166	1.09	155	1.07
2'-Deoxyguanosine-5'-MP	173	0.82	180	0.79
2'-Deoxycytidine-5'-MP	162	0.78	166	0.74

shape has virtually no influence on the electrophoretic process. The data for both types of capillary column are fairly similar with respect to our instrumentation (manual injection, no thermostating). No difference in the resulting current could be observed.

Noise

The Z-shaped flow cell is more susceptible to detection of impurities and contamination (so-called "chemical noise") than less sensitive on-column detection. Capillary washing and pretreatments that have been described for improving the reproducibility of the electrophoretic process [15,16] become important for stabilizing the baseline. The effect of capillary washing using a highly sensitive 5-mm Z-shaped flow cell is depicted in Fig. 4. In general, extended washing of the capillary with water (to

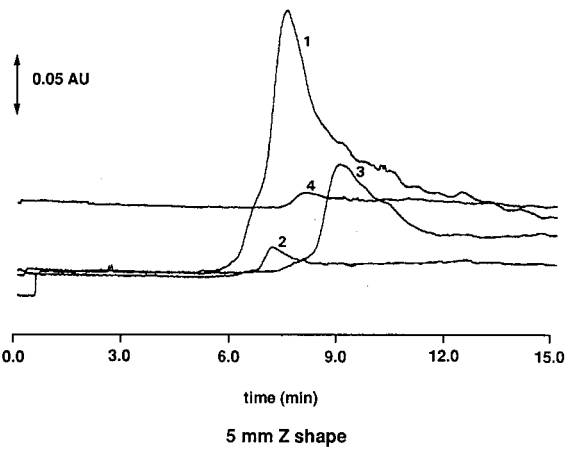

Fig. 4. Influence of capillary washing on baseline stability in MEC: 60 cm (40 cm to detector) × 75 μm I.D. fused-silica capillary; 6 mM borate–10 mM phosphate–75 mM SDS (pH 8.5) buffer; 11 kV, 30 μA; detection at 254 nm, rise time 2 s. All flushing steps are *ca.* 5 column volumes in 1 min. 1 = Flushing with 0.1 M NaOH and buffer; 2 = flushing with 0.1 M NaOH, water and buffer; 3 = flushing with 0.1 M HCl and buffer; 4 = flushing with 0.1 M HCl, water and buffer.

remove the acid or base) before flushing with buffer solution improves the baseline considerably. When no water was used after the acid or base treatment, variations in the baseline appeared.

Under static conditions (no voltage applied) both type of flow cell showed similar noise levels with values ranging from 0.040 to 0.062 mAU at 254 nm (see Table II). As soon as a high voltage is applied the noise increases in proportion to the voltage, as reported by Walbroehl and Jorgenson [17]. This increase in noise is even more pronounced with Z-shaped flow cells. At a moderate voltage of 11 kV the noise level is nearly twice that for on-column detection (0.125 *vs.* 0.067 mAU) utilizing a 50 μm I.D. capillary column. The results of the noise measurements for capillaries of 50 and 75 μm I.D. are given in Table II. Further, Table II lists data obtained using 75 μm I.D. capillaries at different wavelengths. At lower wavelengths, such as 210 nm, a considerable increase in noise was observed for the Z-shaped flow cell (0.40 *vs.* 0.15 mAU), caused by the larger, less UV-transparent volume segment of buffer solution captured in the longitudinal flow cell.

Signal and signal-to-noise ratio (S/N)

Figs. 5 and 6 show the micellar electrokinetic chromatography (MEC) [18–20] of nucleosides–nucleotides and peptides, respectively, using the two types of flow cell.

TABLE II

SIGNAL AND NOISE VALUES FOR Z-SHAPED AND ON-COLUMN FLOW CELLS

Parameter	λ = 254 nm			
	On-column flow cell		Z-shaped flow cell	
	50 μm I.D.	75 μm I.D.	50 μm I.D.	75 μm I.D.
Static noise (mAU)	0.047	0.040	0.057	0.062
Dynamic noise[a] (mAU)	0.067	0.062	0.125	0.105
Signal, S[b] (mAU)	4.1	6.6	29.0	67.0
$S/S_{on\text{-}column}$	1	1	7.1	10.2
S/N	62	106	232	638
$(S/N)/(S/N)_{on\text{-}column}$	1	1	3.7	6.0
	λ = 210 nm			
	On-column flow cell (75 μm I.D.)		Z-shaped flow cell (75 μm I.D.)	
Dynamic noise[a] (mAU)	0.15		0.40	
Signal, S[c] (mAU)	2.3		32.5	
$S/S_{on\text{-}column}$	1		14.1	
S/N	15		81	
$(S/N)/(S/N)_{on\text{-}column}$	1		5.4	

[a] At 11 kV.

[b] Measured with 2′-deoxyguanosine, peak No. 2, Fig. 5.

[c] Measured with val-5-angiotensin II, peak No. 3, Fig. 6.

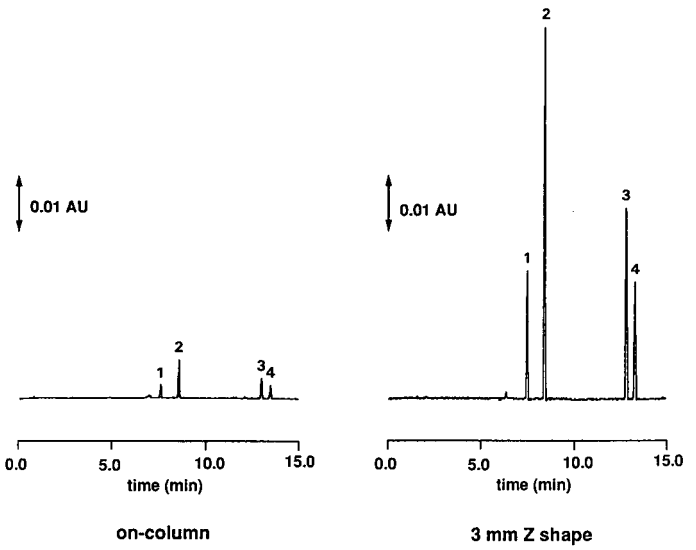

Fig. 5. Separation of nucleosides and nucleotides by MEC: 60 cm (40 cm to detector) × 75 μm I.D. fused-silica capillary; 6 m*M* borate–10 m*M* phosphate–75 m*M* SDS (pH 8.5) buffer; 11 kV, 30 μA; hydrostatic injection 10 cm, 5 s; detection at 254 nm, rise time 2 s; 50 μg/ml (0.35 ng absolute) each, in water. Peaks: 1 = 2′-deoxycytidine; 2 = 2′-deoxyguanosine; 3 = 2′-deoxyguanosine-5′-monophosphate; 4 = 2′-deoxycytidine-5′-monophosphate.

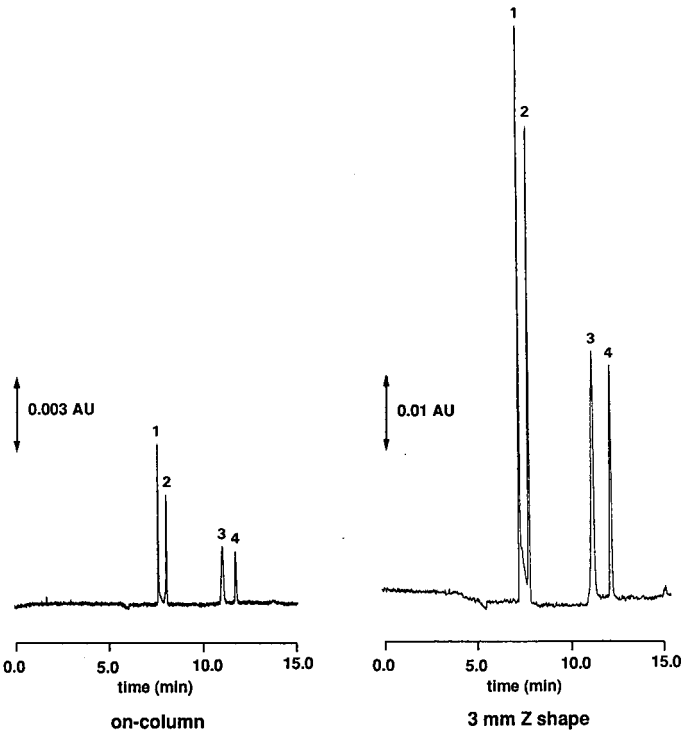

Fig. 6. Separation of peptides by MEC: 60 cm (40 cm to detector) × 75 μm I.D. fused-silica capillary; 10 m*M* borate–50 m*M* SDS (pH 8.5) buffer; 11 kV, 20 μA; hydrostatic injection 10 cm, 5 s; detection at 210 nm, rise time 2 s; 50 μg/ml (0.35 ng absolute) each, in water. Peaks: 1 = met-enkephalin; 2 = leu-enkephalin; 3 = val-5-angiotensin II; 4 = angiotensin II.

At 254 nm enhancements in signal of up to 10.2-fold could be realized (see Table II). At a wavelength of 210 nm, a 14.1-fold improvement in the signal could be measured for val-5-angiotensin II.

Considering the noise levels listed above, an overall improvement in S/N of 6.0-fold at 254 nm and of 5.4-fold at 210 nm result when using the 3-mm Z-shaped flow cell.

Using a Z-shaped flow cell of *ca.* 4 mm path length, enhancements of more than 10-fold in S/N could be realised (see Fig. 7). Capillary columns of smaller I.D. (*e.g.*, 50 μm) yields lower S/N. For 2'-deoxyguanosine an S/N of 3.7 was measured, in contrast to 6.0 with the 75 μm I.D. capillary column. Reducing the I.D. of the capillary column while maintaining the O.D. constant (280 μm) results in a thicker glass wall of the tubing, which reduces the proportion of light passing through the sample.

Maximum tolerable path length and observed column efficiency

Several workers [21,22] have shown that for on-column detection with a slit aperture, the maximum aperture length should not exceed 0.8 mm. Thus, for an optimum longitudinal flow cell the maximum acceptable path length should be $\leqslant 0.8$ mm to prevent distortion of the zone. In practice, however, a compromise must be made between maximum achievable sensitivity and minimum peak distortion. In Table III the loss in efficiency is given for the electropherograms shown in Fig. 5. With a decrease of more than 30% for the 60-cm capillary column (40 cm to the detector), a considerable loss in efficiency results when using the 3-mm longitudinal flow cell. On the other hand, the loss in resolution is less pronounced, owing to its square root dependence on the efficiency. This is illustrated by comparing the resolution of the two electropherograms in Fig. 5. Alternatively, Z-shaped flow cells can be used in longer capillary columns (*e.g.*, 120 cm, 100 cm to the detector) to minimize the loss in efficiency to an acceptable value (see Table III). The observed loss in efficiency shows good agreement with the theoretical values calculated with eqn. 3, and confirms its validity.

Despite the observed loss in efficiency of *ca.* 32% on average for the 60-cm

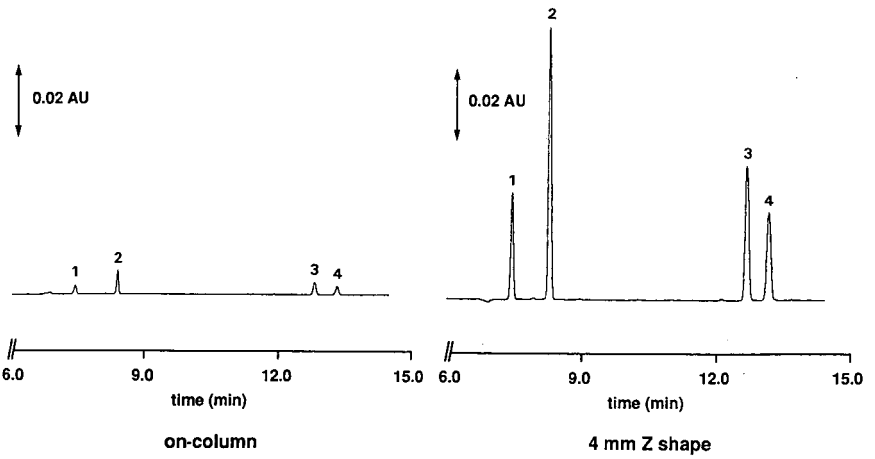

Fig. 7. Separation of nucleosides and nucleotides by MEC. Conditions and peaks as in Fig. 5.

TABLE III

CALCULATED AND OBSERVED LOSS IN EFFICIENCY (N)

Compound	60-cm capillary column (40 cm to detector)			
	On-column ($N \times 10^3$)	Z-shaped ($N \times 10^3$)	Loss (%)	
			Calc.[a]	Obs.
2′-Deoxycytidine	100	68.5	32	32
2′-Deoxyguanosine	145	98.2	40	32
2′-Deoxyguanosine-5′-MP	202	136	49	33
2′-Deoxycytidine-5′-MP	190	133	47	30
	120-cm capillary column (100 cm to detector)			
	On-column ($N \times 10^3$)	Z-shaped ($N \times 10^3$)	Loss (%)	
			Calc.[a]	Obs.
2′-Deoxycytidine	391	293	23	25
2′-Deoxyguanosine	382	322	22	16
2′-Deoxyguanosine-5′-MP	351	314	21	11
2′-Deoxycytidine-5′-MP	317	267	19	16

[a] Calculated with eqn. 3, assuming $N = N_{\text{on-column}}$.

column and of *ca.* 17% on average for the 120-cm column, the resolution is not greatly affected, demonstrating the usefulness of Z-shaped flow cells even for columns as short as 40 cm.

Linearity, detection limits and reproducibility

To evaluate the linearity of the Z-shaped flow cell independent of the electrophoretic process (*i.e.*, injection, temperature, column, etc.), the static linearity test was used [16]. For the solutes tested the linearity ranged from 2.5 to 3 orders of magnitude at both 210 and 254 nm, with response indices of 0.93 and 0.96, respectively.

At the high concentration end the calibration graphs flatten owing to stray light caused by the small aperture ratio. The limits of detection (S/N = 2) for the nucleosides were 0.31–0.47 and 0.51–0.63 μg/ml for the enkephalins, respectively.

In comparison with on-column detection, the detectability was up to six times lower when the 3-mm Z-shaped flow cell was used.

The reproducibility between flow cells was measured with a series of eight capillary columns. The entire series showed identical performance within the limits of our test system. Similar results in flow-cell reproducibility and enhanced detectability have been found for other type of detectors using 3-mm Z-shaped flow cells.

CONCLUSIONS

Capillary columns with Z-shaped flow cells provide higher sensitivities than conventional on-column detection. With a 6-fold improvement in S/N under CE conditions, the gain is less than one would expect just considering the increase in path

length (theoretically up to 80-fold). This is due to the fact that a considerable part of the light is probably guided by the glass wall of the capillary, the presence of scattered light and the increase in noise with the applied voltage. On the other hand, the substantial gain in the signal of up 14.1-fold confirms that Z-shaped flow-cell detection has significant potential when using common UV detectors. The observed loss in efficiency of 17–32% shows good agreement with the theoretical values. Most capillary electroseparations, in particular free solution, semi-preparative and MEC with typical efficiencies of (3–4) · 10^5 plates/m, can be accomplished utilizing the Z-shaped flow cell without sacrificing much of the resolution.

To benefit fully from the advantages of the Z-shaped flow cell, however, further improvements are required. This would include synergy between the detector and flow cell. On the detector side, optimization of the light beam (parallel light rather than divergent or convergent) and adaptation of the photodiode (miniaturization) should reduce the noise considerably. On the flow cell side, the influence of the wall thickness, grounding of the flow cell, possible use of refractive index matching fluids, etc., should be further investigated.

ACKNOWLEDGEMENTS

The authors thank Kontron Instruments (Milan, Italy) and the StiPT, Executive Organization for Technology Policy of the Ministry of Economic Affairs, The Netherlands, for providing support for this work.

REFERENCES

1 A. G. Ewing, R. A. Wallingford and T. M. Olefirowicz, *Anal. Chem.*, 61 (1989) 292A.
2 W. G. Kuhr, *Anal. Chem.*, 62 (1990) 403R.
3 D. M. Goodall, D. K. Lloyd and S. J. Williams, *LC · GC Int.*, 3 (1990) 28.
4 T. Tsuda, J. V. Sweedler and R. Zare, *Anal. Chem.*, 62 (1990) 2149.
5 I. H. Grant and W. Steuer, *J. Microcolumn Sep.*, 2 (1990) 74.
6 J. P. Chervet, M. Ursem, J. P. Salzmann and R. W. Vannoort, *J. High Resolut. Chromatogr.*, 12 (1989) 278.
7 J. P. Chervet, LC Packings, patent pending.
8 J. W. Jorgenson and K. D. Lukacs, *Anal. Chem.*, 53 (1981) 1298.
9 J. W. Jorgenson and K. D. Lukacs, *Science* (Washington, D.C.), 222 (1983) 266.
10 J. Vindevogel, G. Schuddinck, C. Dewaele and M. Verzele, *J. High Resolut. Chromatogr. Chromatogr. Commun.*, 11 (1988) 317.
11 D. Ishii, *Introduction to Microscale High-Performance Liquid Chromatography*, VCH, Weinheim, 1988, p. 22
12 X. Huang, W. F. Coleman and R. N. Zare, *J. Chromatogr.*, 480 (1989) 95.
13 H. K. Jones, N. T. Nguyen and R. D. Smith, *J. Chromatogr.*, 504 (1990) 1.
14 J. C. Sternberg, *Adv. Chromatogr.*, 2 (1966) 205.
15 H. H. Lauer and D. McManigill, *Anal. Chem.*, 58 (1986) 166.
16 W. J. Lambert and D. L. Middleton, *Anal. Chem.*, 62 (1990) 1585.
17 Y. Walbroehl and J. W. Jorgenson, *J. Chromatogr.*, 315 (1984) 135.
18 S. Terabe, K. Otsuka, K. Ichikawa, A. Tsuchiya and T. Ando, *Anal. Chem.*, 56 (1984) 111.
19 J. Liu, F. Banks, Jr., and M. Novotny, *J. Microcolumn Sep.*, 1 (1989) 136.
20 M. J. Sepaniack, D. F. Swaile and A. C. Powell, *J. Chromatogr.*, 480 (1989) 185.
21 T. Wang, R. A. Hartwick and P. B. Champlin, *J. Chromatogr.*, 462 (1989) 147.
22 S. Terabe, K. Otsuka and T. Ando, *Anal. Chem.*, 61 (1989) 251.

Journal of Chromatography, 543 (1991) 451–461
Elsevier Science Publishers B.V., Amsterdam

CHROM. 23 119

Analysis of endoproteinase Arg C action on adrenocorticotrophic hormone by capillary electrophoresis and reversed-phase high-performance liquid chromatography[a]

RICK J. KRUEGER

Department of Biochemistry and School of Biological Sciences, 314 BcH, University of Nebraska, Lincoln, NE 68583-0718 (U.S.A.)

T. R. HOBBS

Isco Inc., P.O. Box 5347, Lincoln, NE 68505 (U.S.A.)

KEVIN A. MIHAL[b]

Department of Biochemistry and School of Biological Sciences, 314 BcH, University of Nebraska, Lincoln, NE 68583-0718 (U.S.A.)

J. TEHRANI

Isco Inc., P.O. Box 5347, Lincoln, NE 68505 (U.S.A.)

and

M. G. ZEECE

Department of Food Science and Technology, 354 FIC, University of Nebraska, Lincoln, NE 68583-0919 (U.S.A.)

(First received September 26th, 1990; revised manuscript received January 7th, 1991)

ABSTRACT

The specificity and rate of cleavage of adrenocorticotrophic hormone (ACTH) peptide bonds by endoproteinase Arg C were analyzed using capillary electrophoresis (CE) and reversed-phase (C_{18}) high-performance liquid chromatography (HPLC). Acidic cleavage products were readily resolved by CE in uncoated capillaries using low ionic strength electrolytes. However, products predicted to have a net positive charge greater than 2 or more than 4 positively charged groups per peptide did not migrate out from the capillary at low ionic strength. Addition of salts and zwitterions to the electrolyte decreased capillary–peptide interactions such that all of the ACTH peptides examined were eluted with high efficiency separation by CE. Commercially obtained endoproteinase Arg C preparations exhibited peptidase activity at Lys^{15}–Lys^{16} and at Lys^{16}–Arg^{17} in addition to the expected cleavage at Arg–X bonds. ACTH peptide bond cleavage rates for Arg^{8}–Trp^{9}, Arg^{17}–Arg^{18}, Lys^{15}–Lys^{16}, and Lys^{16}–Arg^{17} were 1.46, 0.096, 0.057, and 0.029 μmol min^{-1} mg^{-1} respectively. CE separations generally exhibited better resolution and were accomplished in shorter times than C_{18} HPLC separations. These properties make CE a particularly appropriate method for kinetic analysis of proteolytic enzyme action on peptide substrates.

INTRODUCTION

Development of high efficiency peptide separation methods has stimulated progress in areas as diverse as purification of prohormone processing proteinases [1]

[a] Journal series No. 9360, Agricultural Research Division, University of Nebraska-Lincoln.

[b] Present address: Department of Biochemistry, Boston University School of Medicine, Boston, MA 02118, U.S.A.

0021-9673/91/$03.50

and the study of protein structure using tryptic digestion [2]. Peptide separations are often achieved with reversed-phase (C_{18}) high-performance liquid chromatographic (HPLC) methods. However, resolution of complex or structurally similar mixtures of peptides by C_{18} HPLC may require relatively long analysis times and elaborate gradient solvent programming.

Application of capillary electrophoresis (CE) to protein and peptide separations has demonstrated that extremely high separation efficiency and resolution can be obtained by this method [3–5]. A potential obstacle in CE separations is adsorption of peptides and proteins to the wall of the capillary, resulting in low separation efficiency or irreversible binding of analyte to the capillary. Such interactions are generally strongest for basic peptides and proteins [3].

Three approaches have been used to reduce these interactions. One strategy is to derivatize the inner wall of the capillary with functional groups that chemically block silanol groups or sterically shield them from interaction with analytes [6,7]. A second method is to alter the pH of the electrolyte such that silanol groups of the capillary are protonated [8] (low pH) or basic groups of the analyte are deprotonated [9] (high pH). These changes can reduce capillary–analyte interactions, but the pH extremes required may alter the structure of biological analytes. The third approach is to decrease binding interactions by increasing the ionic strength of the electrolyte. Jorgenson and co-workers [3,10] have employed this tactic to achieve high efficiency separation of relatively basic proteins at pH values near neutrality.

In this report we compare CE and C_{18} HPLC separation methods for kinetic analysis of the action of a proteolytic enzyme, endoproteinase Arg C, on a peptide substrate, adrenocorticotrophic hormone (ACTH). Endoproteinase Arg C hydrolyzes most Arg–X peptide bonds [11]. However, additional cleavage at Lys–Lys and Lys–Arg bonds was observed for ACTH (see Fig. 1). We also demonstrate the application of CE for measurement of rates of peptide bond cleavage. The influence of net charge and total positive charges on peptide adsorption to the capillary wall during CE separation is discussed.

EXPERIMENTAL

Materials

Tyr^3ACTH(3–9), ACTH(1–10), and ACTH(1–16) were obtained from Bachem Bioscience (Philadelphia, PA, U.S.A.). ACTH(7–24) was prepared by solid phase methods using *tert.*-butyloxycarbonyl protected amino acids. Porcine ACTH(1–39) was purchased from Sigma (St. Louis, MO, U.S.A.) and purified by chromatography on Whatman CM-52 cellulose (Hillsboro, OR, U.S.A.) and preparative C_{18} HPLC. Acetyl-L-methionine-1-naphthyl ester was from Serva (Garden City Park, NY, U.S.A.). CE electrolyte components were obtained from Sigma.

Endoproteinase Arg C was obtained from Boehringer Mannheim (Indianapolis, IN, U.S.A.) and Sigma. Similar results were obtained with both preparations. The heterogeneity of these enzyme preparations was examined by non-denaturing polyacrylamide gel electrophoresis (PAGE) [12]. Three major and six minor protein bands were observed when the gel was silver-stained. Four activity bands were observed when a comparable gel was stained for esterase activity using acetyl-L-methionine-1-naphthyl ester as the substrate [12], one corresponding to each of the

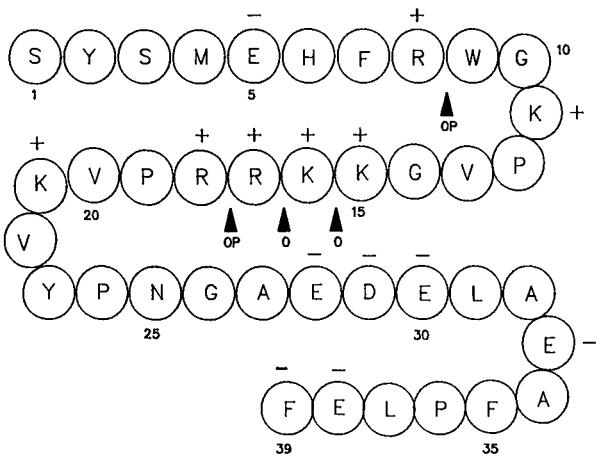

Fig. 1. ACTH sequence and points of cleavage by endoproteinase Arg C. The amino acid sequence of porcine ACTH and the sites of predicted (P) and observed (O) cleavage by endoproteinase Arg C preparations are shown. Residues denoted by + or − signs are predicted to be charged at pH 8.0, as calculated using the constants of Noszal and Osztas [18].

major silver-stained bands, and one to a minor silver-stained band. This indicates that these enzyme preparations probably contain more than one proteolytic activity. Non-endoproteinase Arg C activities may account for the cleavage observed at Lys–Lys and Lys–Arg bonds (see Discussion).

Peptide bond cleavage measurements

Enzymatic cleavages were carried out with endoproteinase Arg C in 0.12 *M* $NaHCO_3 \cdot NH_4OH$, pH 8.5 or 40 m*M* Tris–40 m*M* Tricine, pH 8.2 at 37°C. Peptide bond cleavage rates measured in these two buffers were the same. For HPLC analysis proteinase action was stopped by addition of 0.05 volumes of 6 *M* HCl. Samples were centrifuged at 14 000 *g* for 5 min and stored at −20°C until the supernatant was analyzed by C_{18} HPLC. Samples analyzed by CE were injected directly into the capillary without a quench step.

The identity of reaction products was established by amino acid analysis of fractions collected from HPLC separations. Peptides were hydrolyzed in 6 *M* HCl, converted to their phenylthiocarbamyl forms, and resolved by C_{18} HPLC [13].

High-performance liquid chromatography

Products from proteolytic cleavage reactions were resolved by C_{18} HPLC using a BakerBond wide pore (J. T. Baker) 5 μm, 250 × 4.6 mm I.D. column. Separations were achieved with linear gradients of 0.05% trifluoroacetic acid (TFA) in water (solvent A) and 0.05% TFA, 50% aq. acetonitrile (solvent B); using 80% solvent A to 30% Solvent A over 25 min (except where noted), followed by a 2-min wash cycle with 100% solvent B, at a flow-rate of 1 ml/min. The absorbance of the eluate was monitored at 210 nm. Peak areas were calculated using a Waters Maxima 820 data analysis system.

Capillary electrophoresis

An Isco (Lincoln, NE, U.S.A.) prototype electrophoresis system was used for these studies. The system includes an Isco CV [4] variable-wavelength UV monitor with cassette-mounted capillary cell, a Spellman Model EPM30PNX1696 ± 30 kV power supply, and a split flow sample injection system [14]. CE separations were carried out with 50 cm long uncoated capillaries, 50 μm I.D. (Polymicron, Phoenix, AZ, U.S.A.). Temperature was controlled by forced ambient air stabilization of the capillary compartment. Data were recorded and analyzed with an Isco ChemResearch data management system using an IBM PC computer. In addition to the electrolytes noted in figure legends, a range of electrolytes was used for CE analysis of ACTH peptides. The systems tested, with ACTH(1–39) theoretical plate values and migration times, respectively, shown in parentheses were: 40 m*M* Tris–40 m*M* Tricine–0.1 *M* NaCl, pH 8.3 (16 050, 9.2 min); 40 m*M* phosphate–2 *M* betaine pH 7.5 (44 000, 9.7 min); 40 m*M* phosphate–0.1 *M* K_2SO_4, pH 7.0 (107 600, 19.7 min); 40 m*M* phosphate–2 *M* betaine–0.1 *M* K_2SO_4, pH 7.6 (201 000, 28.2 min); 0.1 *M* 2-(N-cyclohexylamino)ethanesulfonic acid (CHES)–0.25 *M* K_2SO_4–1 m*M* EDTA, pH 9.0 (84 500, 49.4 min); 20 m*M* 3-(cyclohexylamino)-1-propenesulfonic acid (CAPS)–10 m*M* KCl, pH 10.5 (7100, 4.9 min); 40 m*M* 2-(N-morpholino)ethanesulfonic acid (MES)–2 *M* betaine–40 m*M* K_2SO_4, pH 5.5 (221 700, 48.5 min); and 0.1 *M* sodium phosphate, pH 2.5 (109 000, 5.9 min).

Analysis of peptide bond cleavage rates

Peptide quantities in cleavage reactions were determined from peak areas, which were converted to molar quantities by reference to peak areas obtained from injections of standard peptide solutions. The peptide concentration of standard solutions was determined by ultraviolet absorbance measurements [15]. Rates of peptide cleavage were determined from plots of peptide concentration *vs.* reaction time. The slopes of linear portions of these plots gave the rate of peptide bond cleavage. Rates were usually determined with reactions that had gone to less than 10% of completion. However, no product inhibition was observed even in reactions carried to 50% of completion. For determination of K_M values, the rate of peptide bond cleavage was measured as a function of substrate concentration. K_M values were then obtained from plots of $1/V$ *vs.* 1/[s].

RESULTS

Identification of cleavage products resolved by C_{18} HPLC

The peptides derived from endoproteinase Arg C hydrolysis of porcine ACTH(1–39) were initially examined by monitoring the reaction products as a function of time using C_{18} HPLC (Fig. 2). Incubation for 0.5 h (upper trace, Fig. 2) resulted in two peptide products. Peaks 4 (retention time, t_R = 12.8 min) and 5 (t_R = 26.5 min) were identified as ACTH(1–8) and ACTH(9–39), respectively, by amino acid analysis, which indicated that the Arg^8–Trp^9 bond was the most rapidly cleaved by endoproteinase Arg C action. After a 3-h incubation, ACTH(9–39) was largely cleaved to other products (Fig. 2, lower trace). The peaks were identified as: peak 1, ACTH(9–16) (t_R = 5.6 min); peak 3, ACTH(9–15) (t_R = 7.4 min); peak 7, ACTH(17–39) (t_R = 27.4 min); and peak 8, ACTH(18–39) (t_R = 28.1 min). Peaks

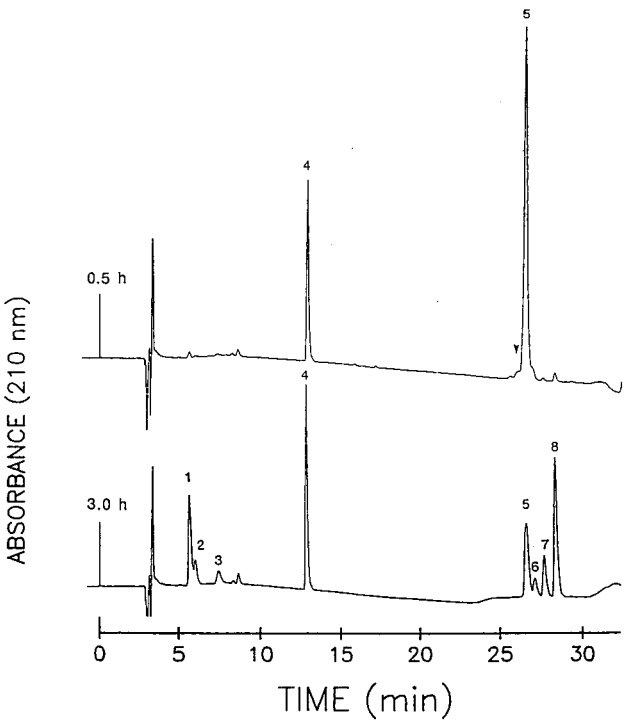

Fig. 2. Resolution of ACTH(1–39) cleavage products by C_{18} HPLC. ACTH(1–39) (80 μM) and endoproteinase Arg C (14 μg/ml) were incubated in a volume of 33 μl at 37°C as described under Experimental. The reactions were quenched after 0.5 (upper) and 3.0 h (lower), and the products resolved by C_{18} HPLC. The elution time of the substrate, ACTH(1–39), is indicated by the arrow (t_R = 26.0 min). The vertical bar at time $t = 0$ represents 0.05 absorbance units. Peaks were identified as ACTH peptides: 1 = 9–16; 3 = 9–15; 4 = 1–8; 5 = 9–39; 7 = 17–39; and 8 = 18–39. Peaks 2 and 6 appeared transiently and were not obtained in sufficient quantity to permit identification.

2 and 6 appeared transiently, and were not obtained in sufficient quantity to permit identification. These results indicated that cleavage occurred at Lys^{15} and Lys^{16}, in addition to the expected cleavage at Arg^{17}. ACTH peptides (1–8), (9–15), (17–39), and (18–39) were resistant to further cleavage when incubated with endoproteinase Arg C for up to 24 h.

CE separation of peptides

CE separations of endoproteinase Arg C treated ACTH were initially performed in 80 m*M* Tris, 80 m*M* Tricine, pH 8.2, and a typical electropherogram is shown in Fig. 3. The electrolyte employed for this separation was similar in pH and ionic strength to that previously reported for analysis of tryptic digests of proteins [16]. Under these conditions, neither the starting material, ACTH(1–39), nor the cleavage products (9–39) and (9–16) were observed in the electropherogram. Injection of standard solutions of these three peptides, as well as ACTH(1–16), confirmed that these peptides did not elute from the capillary. However, ACTH fragments (9–15), (1–8), (17–39),

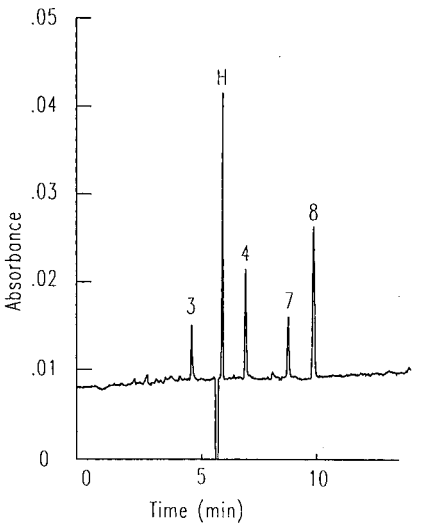

Fig. 3. Analysis of ACTH(1–39) cleavage products in low ionic strength electrolyte. ACTH(1–39) (6 nmol, 27.4 μg) was incubated with endoproteinase Arg C (1 μg) as indicated in the Experimental section. The reaction products were then subjected to CE, which was carried out at 25 kV, 12 μA in 80 m*M* Tris–80 m*M* Tricine, pH 8.2. The elution profile was monitored at 200 nm (0.10 AUFS). Peaks were identified as: 3 = 9–15; 4 = 1–8; 7 = 17–39; 8 = 18–39; H = histidine standard.

and (18–39) did elute and were well resolved in a relatively short analysis time under these conditions.

Effect of pH and ionic strength on CE separation of ACTH peptides

The peptides that did not elute from the capillary were those predicted to have a higher number of positively charged groups, and/or net charge (Table I). It seemed likely that interactions between these positively charged groups of the peptide and

TABLE I

PREDICTED CHARGE PROPERTIES FOR ACTH DERIVED PEPTIDES AT pH 8.0

Predicted charges present at pH 8.0 on the residue side chains and α-amino and α-carboxyl groups were calculated using the microconstants determined by Noszal and Osztas [18].

Peptide	Positive	Negative	Net
(1–39)	7.1	7	+0.1
(1–8)	1.1	2	−0.9
(1–16)	4.1	2	+2.1
(9–16)	3.1	1	+2.1
(9–15)	2.1	1	+1.1
(17–39)	3.1	6	−2.9
(18–39)	2.1	6	−3.9

silanol groups of the capillary were responsible for adsorption of peptides to the capillary. Therefore the influence of ionic strength on CE separation was examined for two of the peptides that were predicted to have a large number of positively charged groups, *i.e.*, ACTH(1–39) and (1–16).

Addition of NaCl to the electrolyte (80 m*M* Tris–80 m*M* Tricine, pH 8.2) decreased adsorption and increased the separation efficiency for both ACTH(1–16) and (1–39) (Fig. 4). The theoretical plate values observed for ACTH(1–16) at 20, 40, and 60 m*M* NaCl were 570, 6160, and 9190, respectively. ACTH(1–39) appeared to interact most strongly with the capillary and was not observed until the NaCl concentration in the electrolyte was raised to 60 m*M*. Increasing the NaCl concentration to 90 m*M* improved theoretical plate values from 5060 (60 m*M*) to 17 020. These results strongly suggest that the cause of low efficiency in these separations was electrostatic in nature.

The efficiency of ACTH(1–39) separation was examined in a number of electrolyte systems (see Methods). In general, increased electrolyte ionic strength or relatively acidic conditions resulted in higher theoretical plate values. The combined phosphate–betaine–K_2SO_4, pH 7.6 electrolyte was among the most efficient, yielding 201 000 theoretical plates. Electrophoresis conducted at pH 10.5 resulted in relatively

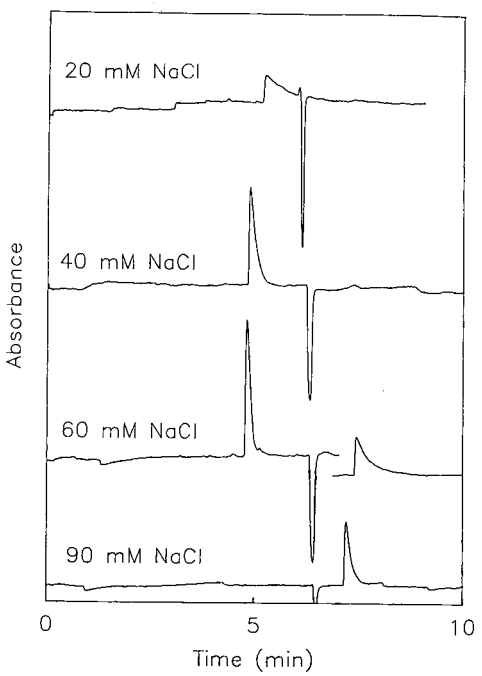

Fig. 4. Effect of NaCl concentration on CE mobility of ACTH(1–39) and (1–16). ACTH(1–39) or ACTH(1–16) was introduced into the capillary, and peptides were analyzed using 80 m*M* Tris–80 m*M* Tricine, pH 8.2 as the electrolyte, to which NaCl was added: 20 m*M*, (1–16) only; 40 m*M*, (1–16) only; 60 m*M* (1–16) and (1–39); 90 m*M* (1–39) only. The separation was carried out at 25 kV, and the elution profile was monitored at 200 nm. The negative pen deflection corresponds to the migration of the neutral zone.

low separation efficiencies. However, migration times were extremely short, and this can be advantageous for kinetic measurements (see Discussion). Conversely, the highest separation efficiency was obtained at pH 5.5 in the presence of betaine and K_2SO_4.

Comparison of CE and C_{18} HPLC separation of peptides derived from endoproteinase Arg C cleavage of ACTH(1–39)

Comparison of CE and C_{18} HPLC separation of ACTH(1–39) cleavage products resulting from endoproteinase Arg C action is shown in Fig. 5. CE separation was performed using a Tris–Tricine electrolyte system that provided moderate resolution and relatively short analysis times. Under these conditions, CE generally provided better separation of peptide pairs [except ACTH(1–39) and (9–39)]. The total time required for analysis is substantially less with CE, particularly as a wash cycle and column re-equilibration time were not required, as they were for the C_{18} separation.

Kinetic analysis of endoproteinase Arg C hydrolysis of ACTH peptide bonds

Kinetic measurements of peptide bond hydrolysis can be performed if either product can be resolved from the substrate peptide. We therefore used CE separations for rate measurements that provided moderate separation efficiency and relatively short migration times.

ACTH(1–39) was incubated with endoproteinase Arg C and samples analyzed at various times to determine the rates of hydrolysis of the Arg^8–Trp^9, Lys^{16}–Arg^{17}, and Arg^{17}–Arg^{18} bonds. These values determined by C_{18} HPLC separations were 1.46, 0.029, and 0.096 μmol min^{-1} mg^{-1}. The hydrolysis rate of the Lys^{15}–Lys^{16} bond of

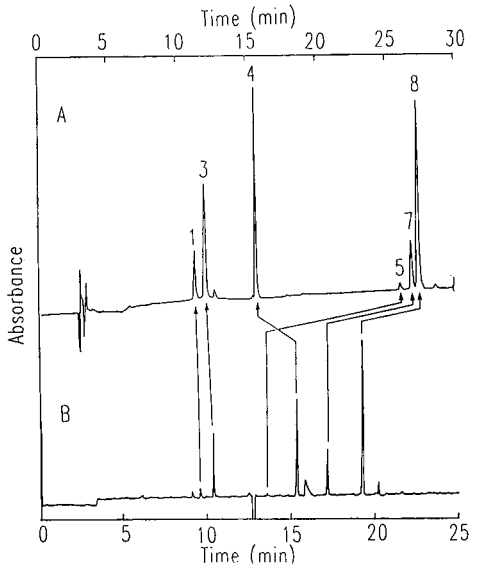

Fig. 5. Separation of cleavage products derived from endoproteinase Arg C treatment of ACTH(1–39). ACTH(1–39) was subjected to proteolytic cleavage as described in the Experimental section. The components of the reaction mixture were then analyzed by C_{18} HPLC (upper panel) using a linear gradient from 10 to 80% solvent B over 28 min or CE (lower panel) using 200 m*M* Tris–200 m*M* Tricine, pH 8.2 as the electrolyte at 25 kV. Peak identities are as noted in Fig. 2.

TABLE II

RATES OF Arg–Trp BOND CLEAVAGE OF ACTH PEPTIDES BY ENDOPROTEINASE Arg C

Substrate	Separation method[a]	
	C_{18} HPLC	CE
ACTH(1–39)	1.46[b]	1.49
ACTH(1–16)	1.28[b]	1.25
ACTH(1–10)	0.095	0.136
Tyr^3ACTH(3–9)	0.007[b]	N.D.[c]
ACTH(7–24)	0.55	N.D.

[a] Units are μmol min^{-1} mg^{-1} endoproteinase Arg C.

[b] V_{max} determined from plot of $1/V$ *vs.* 1/[s]. All other values were initial rates determined at 100 μM peptide substrate.

[c] N.D. = Not determined.

ACTH(11–16), measured by C_{18} HPLC analysis of an ACTH(1–16) cleavage reaction, was 0.057 μmol min^{-1} mg^{-1}.

The hydrolysis observed at the Lys^{15}–Lys^{16} and Lys^{16}–Arg^{17} bonds was unexpected both because of the known specificity of endoproteinase Arg C action on the carboxyl side of arginine residues and for the Lys^{15}–Lys^{16} bond because of the exoproteolytic nature of the cleavage. The rate of Arg^8–Trp^9 bond cleavage was therefore examined in a number of truncated ACTH peptides to determine the influence of the proximity of the amino and carboxyl termini on peptide bond hydrolysis rate. The results in Table II show that relatively rapid cleavage rates are maintained when the Arg^8–Trp^9 bond is only one residue away from the amino terminus, 0.55 μmol min^{-1} mg^{-1} in ACTH(7–24) *vs.* 1.46 μmol min^{-1} mg^{-1} in ACTH(1–39), a factor of 2.7 difference. Close proximity to the carboxyl terminus has a larger effect, as the cleavage rate decreased by a factor of 15 [1.46 μmol min^{-1} mg^{-1} *vs.* 0.095 μmol min^{-1} mg^{-1} for ACTH(1–10)] when Trp was one residue removed from the carboxyl terminus. The hydrolytic rate was decreased by a factor of 200 when Trp was the C terminal residue [0.007 μmol min^{-1} mg^{-1} for Tyr^3ACTH(3–9)]. These effects are due to alterations in k_{cat}, not K_M, because the K_M values for cleavage of the Arg^8–Trp^9 bond are quite similar for ACTH(1–39) (6.9 μM), ACTH(1–16) (6.2 μM), and Tyr^3ACTH(3–9) (6.1 μM). Peptide bond cleavage rates measured by CE analysis were quite similar to those measured by C_{18} HPLC. K_M values could not be determined by CE analysis however, because of detector sensitivity limitations.

DISCUSSION

Kinetic analysis of ACTH cleavage by endoproteinase Arg C was conducted using CE and C_{18} HPLC to resolve peptide products. Resolution and measurement of the more basic ACTH peptides by CE required the presence of moderate levels of ionic or zwitterionic components in the electrolyte. Commercially obtained preparations of endoproteinase Arg C were found to cleave ACTH at some Arg–X bonds, as expected, and also at Lys–Lys and Lys–Arg bonds, but not at Arg–Pro, Lys–Pro, or Lys–Val.

The resistance of the Arg–Pro bond to cleavage is consistent with the observation that a mammalian endopeptidase activity that cleaves X–Pro bonds has not been observed to date [17].

Our initial attempts to resolve peptides from proteolytic reaction mixtures using CE showed that some ACTH peptides were adsorbed to the capillary. ACTH(1–39), (1–16), and (9–16) were not eluted from the capillary in CE separations carried out with low ionic strength electrolytes (Fig. 3). Similar low ionic strength CE electrolytes (pH 8) provided excellent separation of peptides derived from complete tryptic digests [19]. However, these systems are not useful for analysis of peptides containing a higher content of basic residues. Using similar electrolytes, we observed substantial adsorption of peptides containing as few as three basic residues. Higher concentrations of NaCl were required to achieve efficient elution for ACTH(1–39) than for ACTH(1–16) (Fig. 4), and this suggests that the number of positively charged groups may be as important as net charge in determining the strength of peptide–capillary interactions. Note that ACTH(1–16) is predicted to have a more positive net charge than ACTH(1–39) at pH 7–9. Net charge also appears to be a factor however, as ACTH(17–39) and ACTH(9–16) are predicted to have the same number of positively charged groups, yet ACTH(17–39), which has a negative net charge, showed no indication of adsorption, even at low ionic strength, whereas ACTH(9–16) did. These results are in agreement with previous studies of basic proteins that also demonstrated low separation efficiencies caused by adsorption to the capillary wall, which can be overcome by addition of salt or zwitterions to the electrolyte [3,10]. Our examination of the electrophoretic properties of ACTH(1–39) using the electrolyte systems developed by Bushey and Jorgenson [3] showed that the behavior of this peptide was generally similar to that of lysozyme and α-chymotrypsinogen with respect to theoretical plate values obtained in these systems. Their high efficiency phosphate–betaine–K_2SO_4 system also gave high (200 000) theoretical plate values with ACTH-(1–39).

CE resolved ACTH cleavage products with different net charge efficiently, and generally in shorter analysis times than C_{18} HPLC. CE separations also have the distinct advantage with respect to kinetic measurements of proteolytic enzyme action that analyses can be made in relatively short times. With some electrolytes these times may be 5 min or less in some analyte combinations (see Methods), which is less than the time required to wash the HPLC column with 100% solvent B and re-establish starting solvent conditions in our C_{18} analyses. Separations by C_{18} HPLC, however, are capable of analyzing much larger sample volumes. This is particularly useful for analysis of low concentrations of peptides, which is often required when making K_M measurements.

Endoproteinase Arg C preparations obtained from two commercial sources gave essentially identical ACTH cleavage patterns. The relative bond cleavage rates were Arg^8–Trp^9, 50; Arg^{17}–Arg^{18}, 3.3; Lys^{15}–Lys^{16} [measured in hydrolysis of ACTH(1–16)], 2.0; and Lys^{16}–Arg^{17}, 1.0. Cleavage at Arg^8–Trp^9 and Arg^{17}–Arg^{18} was expected from previous work of Schenkein *et al.* [11]. It is likely that the unexpected hydrolyses occurring at Lys^{15}–Lys^{16} and Lys^{16}–Arg^{17} were catalyzed by another proteolytic enzyme present in the endoproteinase Arg C preparations. This putative non-endoproteinase Arg C activity appears to display significant cleavage specificity, as the Lys^{21}–Val^{22} bond was not hydrolyzed at a measurable rate.

As anticipated from the studies of Schenkein *et al.* [11], proximity of the cleavage site to the peptide termini influenced the rate of bond cleavage. Kinetic analyses indicated that this was a result of lower k_{cat} values, and not due to changes in K_M. Cleavage of the Arg^8–Trp^9 bond was much more rapid when Trp^9 was more than two residues removed from the C terminal, but still occurred at measurable rates even when Trp was the C terminal residue. Close proximity of Arg^8 to the N terminal had a smaller effect on the rate of bond hydrolysis. The rate of Arg^{17}–Arg^{18} bond cleavage was also influenced by the position of the bond relative to the N terminal. This bond was hydrolysed fairly rapidly when ACTH(1–39) was the substrate. The same bond appeared to be completely resistant to hydrolysis in ACTH(17–39).

Our results demonstrate that CE separations employing low ionic strength electrolytes that provide excellent separation of peptides derived from tryptic digests can result in significant adsorption of peptides by the capillary for molecules containing as few as three positively charged groups. However, extremely high efficiency separations can be achieved using high ionic strength electrolytes such as those developed by Jorgenson and co-workers or relatively acidic low ionic strength electrolytes. In addition, very short analysis times of peptide mixtures make CE a particularly attractive method for kinetic analysis of proteinase action on peptide substrates.

ACKNOWLEDGEMENTS

The authors wish to thank Chaomei Lin for assistance with amino acid analysis, Tracy Doane for preparation of figures, and Dr. Gautam Sarath for assistance with proteinase activity staining. This work was supported by grants from the UNL Research Council (R.J.K.) and the UNL Center for Biotechnology (M.G.Z.).

REFERENCES

1 G. E. Maret and J.-L. Fauchere, *Anal. Biochem.*, 172 (1988) 248.
2 J. H. Frenz, S. L. Wu and W. S. Hancock, *J. Chromatogr.*, 480 (1989) 379.
3 M. M. Bushey and J. W. Jorgenson, *J. Chromatogr.*, 480 (1989) 301.
4 F. Kilar and S. Hjertén, *J. Chromatogr.*, 480 (1989) 351.
5 Z. Deyl, V. Rohlicek and R. Struzinsky, *J. Liq. Chromatogr.*, 12 (1989) 2515.
6 S. Hjertén, *J. Chromatogr.*, 347 (1985) 191.
7 G. J. M. Bruin, R. Huisden, J. C. Kraak and H. Poppe, *J. Chromatogr.*, 480 (1989) 339.
8 R. M. McCormick, *Anal. Chem.*, 60 (1988) 2322.
9 H. H. Lauer and D. McManigill, *Anal. Chem.*, 58 (1986) 166.
10 J. S. Green and J. W. Jorgenson, *J. Chromatogr.*, 478 (1989) 63.
11 I. Schenkein, M. Levy, E. C. Franklin and B. Frangione, *Arch. Biochem. Biophys.*, 182 (1977) 64.
12 E. Schaller and O. von Deimling, *Anal. Biochem.*, 93 (1979) 251.
13 R. A. Ebert, *Anal. Biochem.*, 154 (1986) 431.
14 J. Tehrani and L. Day, *Am. Biotech. Lab.*, 7 (1989) 32.
15 G. Allen, *Sequencing of Proteins and Peptides*, Elsevier, Amsterdam, 1981, pp. 26–27.
16 R. G. Nielsen, R. M. Riggin and E. C. Rickard, *J. Chromatogr.*, 480 (1989) 393.
17 N. A. Roberts, J. A. Martin, D. Kinchington, A. V. Broadhurst, J. C. Craig, I. B. Duncan, S. A. Galpin, B. K. Handa, J. Kay, A. Krohn, R. W. Lambert, J. H. Merrit, J. S. Mills, K. E. B. Parks, S. Redshaw, A. J. Ritchie, D. L. Taylor, G. J. Thomas and P. J. Machin, *Science (Washington D.C.)*, 248 (1990) 358.
18 B. Noszal and E. Osztas, *Int. J. Peptide Protein Res.*, 33 (1989) 162.
19 R. G. Nielsen and E. C. Rickard, *J. Chromatogr.*, 516 (1990) 99.

Journal of Chromatography, 543 (1991) 463–470
Elsevier Science Publishers B.V., Amsterdam

CHROM. 23 125

Separation and microanalysis of growth factors by Phast system gel electrophoresis and by DNA synthesis in cell culture

KOU-WHA KUO*

Department of Biochemistry, Kaohsiung Medical College, 100 Shih-Chuan 1st Road, Kaohsiung 80708 (Taiwan)

HSING-WU YEH

Department of Biochemistry and Molecular Biology, University of Arkansas for Medical Sciences, 4301 W. Markham, Little Rock, AR 72205 (U.S.A.)

DAVID Z. J. CHU

Department of Surgery, University of Arkansas for Medical Sciences, 4301 W. Markham, Little Rock, AR 72205 (U.S.A.)

and

YUN-CHI YEH

Department of Biochemistry and Molecular Biology, University of Arkansas for Medical Sciences, 4301 W. Markham, Little Rock, AR 72205 (U.S.A.)

(First received December 12th, 1990; revised manuscript received January 24th, 1991)

ABSTRACT

A simple, micro-scale method was established for the characterization of growth factors at picogram levels using Phast system gel electrophoresis followed by monitoring the mitogenic activity by DNA synthesis in cell culture instead of staining methods. The separations and bioassays were carried out with a procedure involving Phast polyacrylamide gel electrophoresis or isoelectric focusing, gel slicing along the template, elution of growth factors through Transwell membranes and measurement of [^{3}H]thymidine incorporation into DNA of normal rat kidney (NRK) fibroblasts. Transwell cell culture chamber inserts separated sliced gel pieces from culture cells and also permitted the direct elution of growth factors into the culture medium. The lower limit of sensitivity for human epidermal growth factor (hEGF) and transforming growth factor type alpha (TGF-α) were about 50 and 200 pg, respectively. At these concentrations, they were not detectable by the current most sensitive silver staining technique. Iodinated hEGF and TGF-α were also used to demonstrate the feasibility of determining the isoelectric point and molecular weight of peptides at picogram levels. This method is reliable, reproducible and can improve current methods for the characterization of growth factors.

INTRODUCTION

Polypeptide growth factors and growth inhibitors are regulatory agents that act to control cell proliferation and differentiation *in vitro* and *in vivo* [1–5]. The isolation of growth factors in homogeneous form, such as epidermal growth factor (EGF), transforming growth factor type alpha (TGF-α), fibroblast growth factor (FGF) and

0021-9673/91/$03.50

platelet-derived growth factor (PDGF), made structural and functional characterization possible and allowed studies of the molecular mechanisms of their actions and genetic analysis [6–12]. However, many biologically important polypeptide growth factors or inhibitors remain to be isolated and characterized.

During the isolation process for peptide growth regulators, the identification of any specific factor in a complex mixture of growth factors is difficult. Moreover, only a small amount of the purified peptide factors will be available at the final stage of purification for identification and characterization. In addition, other complicated problems are that at very low concentrations, in the nanogram range, peptide factors are easily washed away from the gel matrix by the standard staining procedure after polyacrylamide gel electrophoresis (PAGE), and some growth regulators cannot be detected with Coomassie blue or silver nitrate, even if retained in the gel matrix in sufficient amounts.

To circumvent these problems, a simple microanalytical method is desirable. In this paper, we describe an effective method combining Phast gel electrophoresis and the Transwell cell culture system to measure growth factor mitogenic activity. This technique does not require staining procedures and provides a significant improvement over current identification methods.

EXPERIMENTAL

Materials

Phast gel, silver staining kit and standard proteins for measuring p*I* and molecular weight were purchased from Pharmacia (Piscataway, NJ, U.S.A.). Transwell cell culture chamber inserts were obtained from Costar (Cambridge, MA, U.S.A.) and recombinant human EGF (hEGF) was purchased from Amgen Biologicals (Thousand Oaks, CA, U.S.A.). Recombinant human TGF-α was obtained from Triton Biosciences (Alameda, CA, U.S.A.). Carrier-free ^{125}I and [^{3}H]thymidine were purchased from ICN Biomedicals (Irvine, CA, U.S.A.). Other chemicals were of analytical reagent grade.

Cell line and cell culture

Normal rat kidney (NRK) fibroblast cells, clone 49F, were purchased from American Type Culture Collection (Rockville, MD, U.S.A.). The cells were cultured at 37°C in a humidified atmosphere of carbon dioxide–air (5:95). The culture medium consisted of Dulbecco's modified Eagle's medium (DMEM) (GIBCO, Grand Island, NY, U.S.A.) supplemented with 10% (v/v) newborn calf serum (Hazelton Product, Denver, PA, U.S.A.), 50 μg/ml gentamicin and 30 m*M* tricine. The cells (1×10^4 cells/ml) were seeded in each 1-ml well of 24-well multi-dishes with DMEM–10% calf serum for 24 h and then the medium was replaced with DMEM–0.1% calf serum for at least 24 h prior to use.

Iodination of hEGF and TGF-α

Growth factors were labeled with carrier-free ^{125}I according to the chloramine method using published procedures [13,14]. Carrier-free ^{125}I (0.2 mCi) was added to 1 μg of growth factor in 12.5 μl of 1 *M* phosphate buffer (pH 7.4). Iodination was initiated by the addition of 2.5 μl of chloramine-T (2 mg/ml in 0.05 *M* phosphate

buffer, pH 7.4). The reaction was carried out for 1 min at room temperature with gentle shaking, then 10 μl of sodium metabisulfite (5 mg/ml) and 30 μl of sodium iodide (10 mg/ml) were added to stop the reaction. Bovine serum albumin (30 μl, 5%) was added and the labeled growth factor was separated from unreacted iodine by passage through a Sephadex G-25 column (20 cm × 0.5 cm I.D.). The labeled growth factors were stored at −20°C.

Bioanalysis of growth factors

Phast system PAGE. Samples were separated on Phast gel media (50 × 43 × 0.45 mm) or Phast gel isoelectric focusing (IEF) media (50 × 43 × 0.35 mm) with a Phast system gel electrophoresis apparatus (Pharmacia, Uppsala, Sweden). For sodium dodecyl sulfate (SDS) PAGE, the growth factors were dissolved in 10 m*M* Tris–HCl buffer (pH 6.8) containing 2.5% (v/v) of SDS and heated at 100°C for 5 min. It was carried out for 20–50 min depending on the kind of electrophoresis.

Elution of growth factors. After completion of electrophoresis, the slab gel was sliced along the template (Fig. 1A) with a razor blade into equal pieces of 4 × 3 mm, scraped and each piece transferred into an indivual Transwell (Fig. 1B), that had been prewashed with sterilized water and phosphate-buffered saline solution. The wells were then placed in a 24-well plate containing quiescent NRK cells and incubated for 18 h at 37°C. The gels in the Transwells were rinsed with the original medium in the wells and then the gels and the Transwells were removed before adding [^{3}H]thymidine to measure the rate of DNA synthesis.

DNA synthesis. A 20-μl volume of [^{3}H]thymidine (0.5 μCi) was added to each well and incubated at 37°C for 4 h. The incorporation was terminated by diluting with 1 ml of cold thymidine (100 μg/ml). DNA was precipitated with cold 10% trichloroacetic acid (TCA) and washed once with 5% TCA, then 95% ethanol. [^{3}H]DNA was dissolved in 0.5 ml of 0.2 *M* sodium hydroxide solution and transferred to vials containing 2.5 ml of Ecolume scintillation fluid (ICN Biomedicals). [^{3}H]DNA was measured using a Beckman Model LS 6800 scintillation counter.

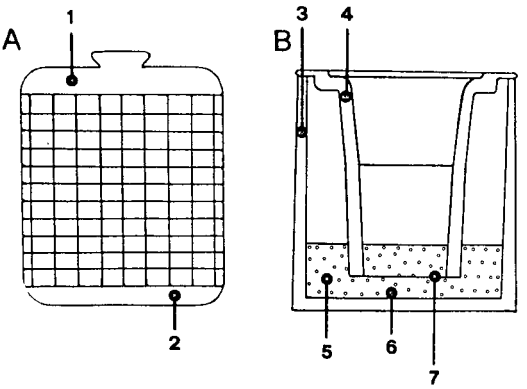

Fig. 1. Illustration of microanalysis of growth factors. After electrophoresis, the gel was sliced along the designed template (A) and transferred into a Transwell (B). The measurement of [^{3}H]thymidine incorporation is described under Experimental. 1 = Cathode; 2 = anode; 3 = 24-well cell culture plate; 4 = Transwell; 5 = culture medium; 6 = monolayer of cell; 7 = porous membrane.

RESULTS

Determination of biological activity of growth factor by direct elution from gels through Transwell membranes

We have successfully determined the biological activity of hEGF at the picogram level by eluting the growth factor from small, ultra-thin pieces of acrylamide gels (4 × 3 × 0.45 mm). After placing the gels on Transwell membranes and inserting the Transwell chamber into the cell culture medium, we were able to eliminate inhibition to the cells caused by direct contact of the gels. To determined the sensitivity, hEGF and TGF-α in amounts ranging from 2 to 400 pg were separated by 20% Phast gel native PAGE. The sliced gels were then transferred into the Transwells and the mitogenic activities were measured (Fig. 2). The sensitivity for hEGF and TGF-α were 50 and 200 pg, respectively.

Recovery of growth factors from acrylamide gels through Transwell membranes.

The kinetics of the elution profile of a growth factor after PAGE was examined. A 1-ng amount of hEGF was separated by 20% Phast gel native PAGE and then transferred into Transwells. The gel pieces were removed from the culture medium at different time intervals between 15 min and 20 h. Mitogenic activity was tested by [^{3}H]thymidine incorporation. As shown in Fig. 3, more than 95% of hEGF was eluted into the medium within 1 h of incubation. There was no need for shaking or a special extraction procedure for eluting the growth factor from gel slices under these conditions.

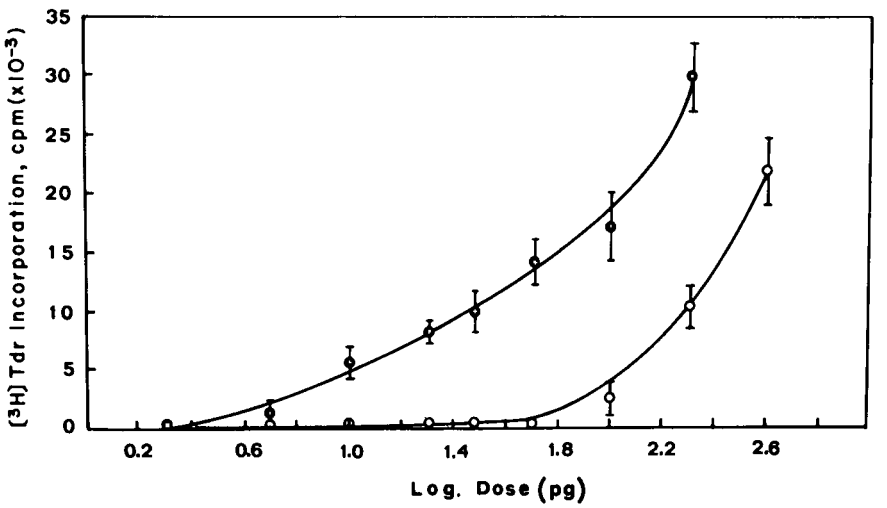

Fig. 2. Concentrations of hEGF and TGF-α that affect DNA synthesis of NRK cells. Different concentrations of (●) hEGF and (○) TGF-α, as indicated, were separated by 20% Phast gel native PAGE. [^{3}H]Thymidine incorporation into DNA was determined after incubation of the sliced gels for 18 h. Data points represent means ± standard errors of the difference between the presence and absence of the growth factors from triplicate experiments.

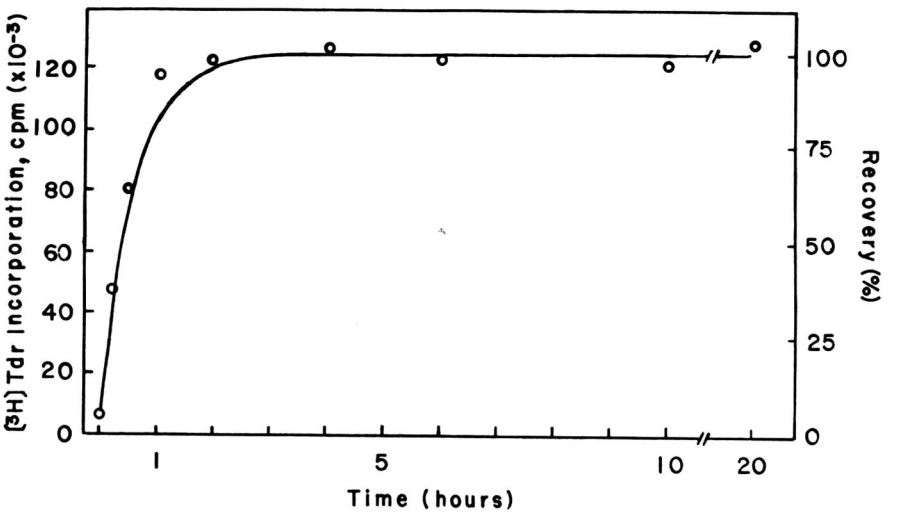

Fig. 3. Recovery of hEGF activities from Phast polyacrylamide gels. An equal concentration of hEGF (1 ng) was separated by 20% Phast gel native PAGE. At various time intervals, the gels were removed from the Transwells. [^{3}H]Thymidine incorporation was initiated after 20 h. The percentage recoveries were calculated based on the maximum activity of hEGF eluted from the gels. The efficiency was more than 75% of that obtained from hEGF (1 ng) added directly to culture medium for 20 h under the same conditions.

Determination of isoelectric points by monitoring mitogenic activity after isoelectric focusing

A 2-ng amount of hEGF or TGF-α was used to determine its isoelectric point. Neither hEGF nor TGF-α could be detected by silver staining at this low concentration. A 1-μl volume of the samples (2 ng/μl) was separated on Phast gel IEF 3–9 by IEF, followed by slicing of the gel into 4 × 3 mm pieces. The sliced gels were added to Transwell without washing. As shown in Fig. 4, the profiles of mitogenic activity after isoelectric focusing revealed that hEGF and TGF-α were well separated and their p*I* values were calculated to be 4.4 and 6.8, which were consistent with published data [15,16]. The above results illustrate that one can determine isoelectric points of mitogens at nanogram levels or less by IEF. This is much lower than the range detectable by the most sensitive silver staining technique [17].

Determination of isoelectric points, molecular weight and purity of iodinated growth factors.

[^{125}I]hEGF and [^{125}I]TGF-α were used to determine isoelectric points and molecular weights by the proposed microanalytical methods. As shown in Fig. 5, [^{125}I]hEGF and [^{125}I]TGF-α were separated with isoelectric points of 4.4 and 6.8. respectively, confirming the observation in Fig. 4 using mitogenic activity as a marker. The iodinated growth factors were also used as examples to determine molecular weights by SDS-PAGE. [^{125}I]hEGF and [^{125}I]TGF-α were separated and their molecular weights were calculated to be 6000 and 5000 dalton, respectively (Fig. 6), compared with standard molecular weight markers. These results demonstrate that

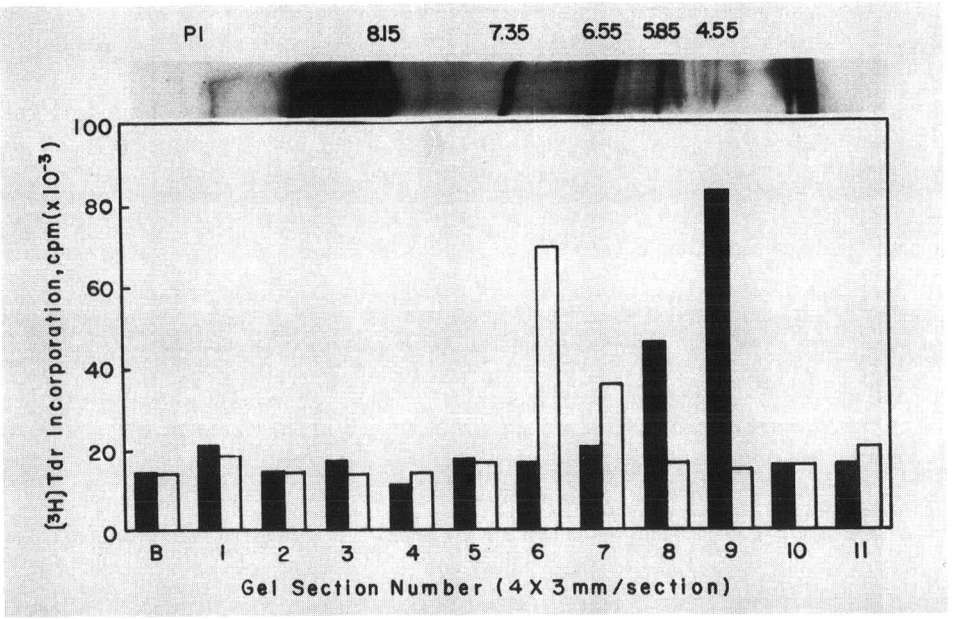

Fig. 4. Microanalysis of hEGF and TGF-α by isoelectric focusing. (■) hEGF (2 ng) and (□) TGF-α (2 ng) were separated on Phast gel IEF 3–9 by IEF and determined by monitoring DNA synthesis, as described under Experimental. Standard proteins stained by silver staining were used as markers. B = background; Nos. 1–11 = gel section numbers from cathode to anode.

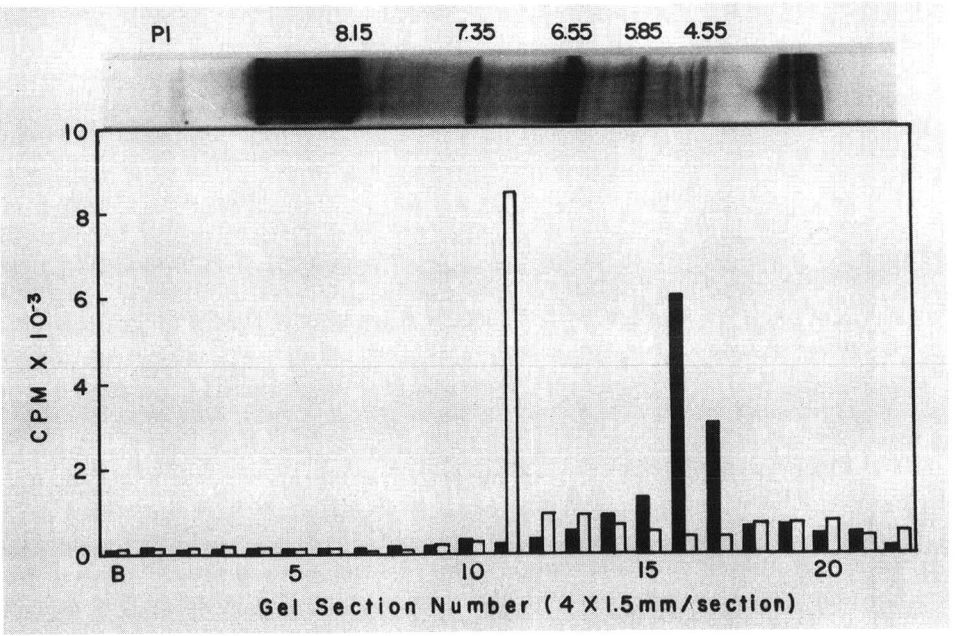

Fig. 5. Separation of [^{125}I]hEGF and [^{125}I]TGF-α by isoelectric focusing. A 1-μl volume (■) [^{125}I]hEGF ($1.4 \cdot 10^4$ cpm/μl) and (□) [^{125}I]TGF-α ($1.7 \cdot 10^4$ cpm/μl) were used for separation on Phast gel IEF 3–9 by IEF and determined by measuring radioactivity in a γ counter. Standard proteins stained by silver staining were used as markers. B = background; Nos. 1–22 = gel section numbers from cathode to anode.

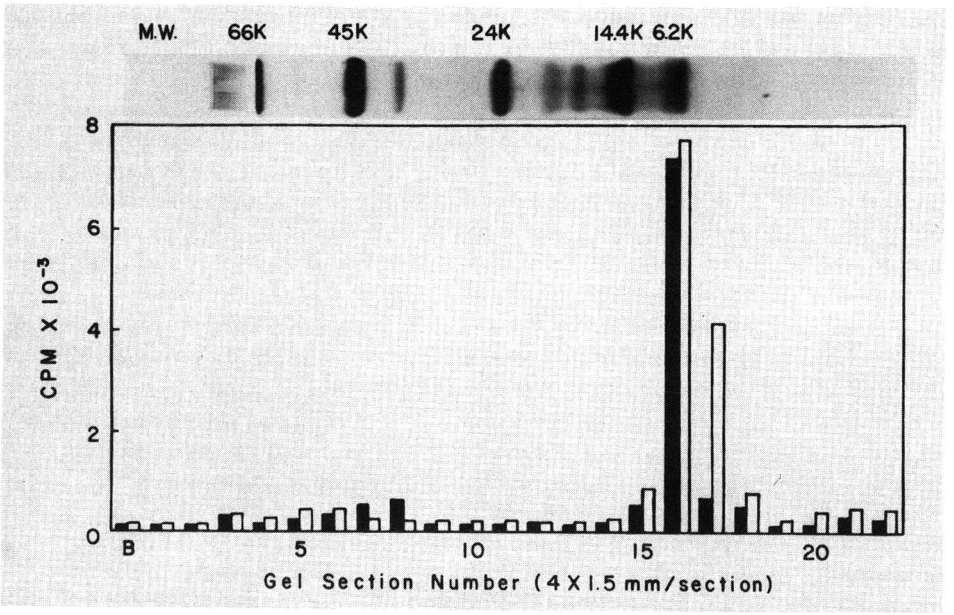

Fig. 6. Determination of molecular weight of [^{125}I]hEGF and [^{125}I]TGF-α by 20% Phast gel SDS-PAGE. (■) [^{125}I]hEGF ($1.8 \cdot 10^4$ cpm/μl) and (□) [^{125}I]TGF-α ($2.0 \cdot 10^4$ cpm/μl) were used for separation by Phast gel SDS-PAGE (20% polyacrylamide gel) and determined by measuring radioactivity in a γ counter. Other details as in Fig. 5.

isoelectric points and molecular weights of growth factors and purity of preparation can be determined by this technique with much higher sensitivity than using standard staining procedures.

DISCUSSION

Electrophoresis is widely employed for determining the properties of purified proteins. In general, the sensitivity of protein detection in the gel has been improved significantly by utilizing the silver staining method [17]. However, some proteins do not stain well with silver nitrate. Low concentrations of growth factors, e.g., IGF-I (50 ng), hEGF (30 ng) and TGF-α (100 ng), cannot be detected in gels by existing staining methods. In this paper, we have shown that as little as 50 pg of hEGF can be separated by electrophoresis and shown an increase in DNA synthesis in NRK cells. Hence picogram amounts of growth factors, which cannot be detected by conventional staining techniques, can now be detected and characterized. We have also shown that the isoelectric point of growth factors can be determined by their biological activity with better sensitivity than using the silver nitrate staining method.

Picogram amounts of growth factors were successfully transferred into a cell culture system by cutting ultra-thin layer of gel into slices (4 × 3 × 0.45 mm) and placing them in Transwells. It was shown that 95% of the growth factor was eluted within 1 h by examining mitogenic activity for NRK cells. Further, the content of

ampholytes and free acrylamide, in a total volume of only 5.4 mm^3 of the gel slice, was also low, which minimized the possible toxicity to the cells. Therefore, we were able to determine the biological activity of growth factors at extremely low concentrations.

The effective performance of this method was due to the fact that Phast gel was fixed on a hard film with a uniform size. During electrophoresis, the separations were controlled by the apparatus under the same conditions. In addition, Transwell chamber inserts, originally desgined for cell culture, were used to support sliced gels to prevent any physical interference with the cells. After electrophoresis, the sliced gels were directly transferred into the Transwells to minimize the loss of growth factors. The Transwells are durable and can be used repeatedly. The sensitivity of this analysis can be increased by iodinating the samples, followed by SDS-PAGE, native PAGE and IEF to estimate molecular weight, p*I*, electrical properties and purity (Figs. 5 and 6). The highly improved detection and identification technique described here should have wide applications and be useful for the isolation and characterization of many peptide growth regulators, mitogens or inhibitors.

ACKNOWLEDGEMENTS

We express our gratitude to Mr. Steven Nelson for his assistance. This work was supported in part by NIH grant CA44818.

REFERENCES

1 G. J. Graham, E. G. Wright, R. Hewick, S. D. Wolpe, N. M. Wilkie, D. Donaldson, S. Lorimore and I. B. Pragnell, *Nature (London)*, 344 (1990) 442.
2 R. James and R. A. Bradshaw, *Annu. Rev. Biochem.*, 53 (1984) 259.
3 Y. C. Yeh, L. A. Scheving, T. H. Tsai and L. E. Scheving, *Endocrinology*, 109 (1981) 644.
4 D. Barnes and G. Sato, *Cell*, 22 (1980) 649.
5 R. A. Bradshaw and S. Prentis, *Oncogenes and Growth Factors*, Elsevier, New York, 1987.
6 J. Scott, M. Urdea, M. Quiroga, R. Sanchez-Pescados, N. Fong, M. Selby, W. J. Rutter and G. I. Bell, *Science*, 221 (1983) 236.
7 D. Gospodarowicz, S. Massoglia, J. Cheng, G. M. Lui and P. Bölhen, *J. Cell Phys.*, 122 (1985) 323.
8 P. Bölhen, A. Baird, F. Esch, N. Ling and D. Gospodarowicz, *Proc. Natl. Acad. Sci. U.S.A.*, 81 (1984) 5364.
9 E. W. Raines and R. Ross, *J. Biol. Chem.*, 257 (1982) 5154.
10 M. D. Waterfield, G. T. Scrace, N. Whittle, P. Stroobant, A. Johnsson, A. Wateson, B. Westermark, C. H. Heldin, J. San Huang and T. F. Deuel, *Nature (London)*, 304 (1983) 35.
11 R. F. Doolittle, M. W. Hunkapiller, L. E. Hood, S. G. Devare, K. C. Robbins, S. A. Aaronson and H. N. Antoniades, *Science (Washington, D.C.)*, 221 (1983) 275.
12 T. K. Alexandrides and R. J. Smith, *J. Biol Chem.*, 264 (1989) 12922.
13 W. M. Hunter and F. C. Greenwood, *Nature (London)*, 194 (1962) 495.
14 P. J. McConahey and F. J. Dixon, *Methods Enzymol.*, 70 (1980) 210.
15 S. Cohen, *J. Biol. Chem.*, 237 (1962) 1555.
16 J. E. De Larco and G. J. Todaro, *Proc. Natl. Acad. Sci. U.S.A.*, 75 (1978) 4001.
17 J. Heukeshoven and R. Dernick, *Electrophoresis*, 6 (1985) 103.

Journal of Chromatography, 543 (1991) 471–474
Elsevier Science Publishers B.V., Amsterdam

CHROM. 23 210

Short Communication

Gradient C_{18} high-performance liquid chromatography of gibberellins

JIANN-TSYH LIN* and ALLAN E. STAFFORD
Western Regional Research Center, Agricultural Research Service, U.S. Department of Agriculture, Albany, CA 94710 (U.S.A.)
GEORGE L. STEFFENS
Beltsville Agricultural Research Center, Agricultural Research Service, U.S. Department of Agriculture, Beltsville, MD 20705 (U.S.A.)
and
NOBORU MUROFUSHI
Department of Agricultural Chemistry, University of Tokyo, Bunkyoku, Tokyo (Japan)
(First received October 30th, 1990; revised manuscript received February 14th, 1991)

ABSTRACT

Retention times of 66 gibberellins (GAs) in gradient C_{18} high-performance liquid chromatography (HPLC) are reported. These include the retention times of 21 new GAs added to our previously reported 24 GAs. Retention times of the other 21 GAs are the ranges estimated from previously reported C_{18} HPLC. The polarity order (elution order) of GAs with hydroxyl groups at different locations and orientations is $12\alpha > 13 > 11\beta > 16\alpha > 1\alpha > 2\alpha > 15\beta > 1\beta > 2\beta > 3\alpha > 3\beta$.

INTRODUCTION

High-performance liquid chromatography (HPLC) is now a routine procedure for the purification and separation of gibberellins (GAs), a group of plant hormones. We have previously reported both the reversed-phase C_{18} HPLC and the normal-phase silica HPLC of GAs and their methyl esters [1]. These four HPLC systems can be sequentially used for purification and identification of radioactive GAs in metabolism studies using a radioactive flow detector. Reversed-phase C_{18} HPLC of free GAs has been the most frequently used and reported HPLC system [1–6]. For the positive identification of endogenous GAs in plants, gradient C_{18} HPLC of free GAs is usually used before bioassay and gas chromatography (GC)–mass spectrometry (MS) or GC–selected ion monitoring (SIM). We reported previously the retention times of 24 GAs in a gradient C_{18} HPLC system. Jensen *et al.* [2] reported the retention times of 42

GAs in isocratic C_{18} HPLC systems. Since gradient C_{18} HPLC can separate all the free GAs in one HPLC run, and isocratic C_{18} HPLC cannot, gradient C_{18} HPLC is the method of choice for the analysis of endogenous GAs in plants. We report here the retention times of additional GAs in our gradient C_{18} HPLC system, and incorporate some data of Jensen *et al.* [2] and Koshioka *et al.* [3] into this HPLC system to assist the analysis of GAs of plant origin.

EXPERIMENTAL

A Waters Assoc. liquid chromatograph was used which consisted of two pumps (M510), a multiwavelength detector (M490) and a data and chromatography control station (M840). The injector was a Rheodyne Model 7125. The column was a reversed-phase C_{18} column (25 cm × 4.6 mm I.D., 5 μm, Ultrasphere ODS; Beckman, San Ramon, CA, U.S.A.). The GA standards (about 1–5 μg each) dissolved in less than 25 μl of methanol were chromatographed on the column. Eluent, linear gradient from 35% methanol in water (containing 0.05% acetic acid) to 100% methanol (containing 0.05% acetic acid) in 40 min; flow-rate, 1 ml/min; initial pressure, 120 bar; final pressure, 55 bar. *ent*-Kaurenoic acid and *ent*-kaurene (dissolved in ethanol) were eluted by the gradient followed by 100% methanol (containing 0.05% acetic acid) isocratically.

RESULTS AND DISCUSSION

Retention times of GAs in the gradient C_{18} HPLC are given in Table I in the order of elution. We have previously reported the retention times of 24 GAs in this gradient C_{18} HPLC system [1]. Since that report we can add to this list the retention times of 16 GA standard and 5 endogenous GAs from immature apple seeds [7] which were identified by GC–SIM in HPLC fractions. The retention times of 21 other GAs in Table I were estimated as ranges based on previous publications by Jensen *et al.* [2] and Koshioka *et al.* [3]. The HPLC columns and eluents used by Jensen *et al.* [2] and Koshioka *et al.* [3] were different from those of this work. However, the orders of elutions of GAs shown were the same in general. When listing the retention ranges estimated in Table I we assumed that the elution orders of GAs including the GAs not available to us were the same. There are in total 66 GAs listed in Table I. Some GAs such as GA_{48}, GA_{58}, GA_{69} and GA_{71} not listed in Table I have been purified previously by gradient C_{18} HPLC [8.9], however, several HPLC fractions were combined for the identification by GC–MS and the ranges of the estimated retention times are too large to be listed here.

Retention times [2,4] and HPLC fractions [3,5] of GAs in isocratic [2,4,6] and gradient [3,5,6] C_{18} HPLC have been reported. The GAs for which new retention data were measured in this work are as follows with references of previous works: GA_8 [2,3,5], GA_{29} [2,5], GA_{39} [2], GA_{33} [2], gibberellenic acid [3], GA_{30} [2], GA_{23} [2,5], GA_{28} [2], GA_{38} [2], GA_{41} [2], GA_{26} [2], GA_3 [2–6], 3-epi-GA_1 [3], GA_1 [2–6], GA_{29} catabolite [3], $\Delta^{1(10)}GA_1$ counterpart [3], GA_6 [2], GA_{18} [2,3,5], GA_{35} [2], GA_1 methyl ester [3], $\Delta^{1(10)}GA_1$ counterpart methyl half ester [3], GA_{22} [2], GA_{21} [2], GA_{31} [2], GA_{43} [3], GA_5 [2–6], GA_{10} [2], GA_{16} [2], GA_{20} [2–6], GA_{27} [2], GA_{47} [2], GA_{36} [2,5], GA_{13} [2–5], GA_{40} [2], allogibberic acid [3], GA_{44} [2,5], GA_{19} [2,3,5], GA_{34} [2,3], GA_{17}

TABLE I

RETENTION TIMES OF GIBBERELLINS IN GRADIENT C_{18} HPLC

For HPLC conditions, see Experimental.

Gibberellins[a]	Retention times (min)	Gibberellins	Retention times (min)
GA_{55}	5.03	GA_{27}	19.61
GA_8	5.08	GA_{47}	19.6–20.4[b]
GA_{29}	6.0–6.5[b]	GA_{36}	20.44
GA_{39}	6.0–6.5[b]	GA_{13}	20.47
iso-GA_3	6.36	GA_{68}	20.5[c]
GA_{32}	6.50	GA_{40}	20.5–22.0[b]
GA_{33}	6.98	Allogibberic acid	20.5–22.5[b]
Gibberellenic acid	7.42	GA_{44}	21.4[c]
GA_{30}	7.46	GA_{63}	21.5[c]
GA_{23}	7.7–8.2[b]	GA_{19}	22.41
GA_{28}	8.0–8.4[b]	GA_{54}	22.58
GA_{38}	8.2–8.6[b]	GA_{34}	22.83
GA_{41}	9.1–9.3[b]	GA_{62}	23.5[c]
GA_{26}	9.1–9.3[b]	GA_{17}	23.74
GA_3	9.38	epi-Allogibberic acid	23.5–24.0[b]
3-epi-GA_1	9.41	GA_{37}	24.07
GA_1	10.51	GA_{61}	24.5[c]
GA_{29} catabolite	10.5–11.0[b]	GA_{51}	24.5[c]
$\Delta^{1(10)}GA_1$ counterpart	11.32	3-epi-GA_4	24.42
GA_6	11.5–12.3[b]	GA_7	24.92
GA_{18}	12.0–12.5[b]	iso-GA_7	25.0–26.0[b]
GA_{35}	12.89	GA_4	26.07
GA_1 methyl ester	13.40	GA_{53}	27.81
$\Delta^{1(10)}GA_1$ counterpart methyl half ester	13.2–13.6[b]	GA_{14}	28.17
GA_{22}	13.61	GA_{24}	28.86
GA_{21}	14.25	GA_9	29.36
GA_2	14.96	GA_{25}	29.54
GA_{31}	16.07	GA_{15}	29.76
GA_{43}	14.5–17.5[b]	GA_4 methyl ester	29.0–31.0[b]
GA_5	17.86	GA_{12}	32.0–38.0[b]
GA_{10}	17.8–18.4[b]	GA_{12}-ald	38.0–44.0[b]
GA_{16}	18.42	*ent*-Kaurenoic acid	44.82
GA_{20}	18.97	*ent*-Kaurene	60.72

[a] For structures of GAs, see refs. 3 and 10.

[b] The ranges of elution times were estimated from the data of Jensen *et al.* [2] and Koshioka *et al.* [3] (fraction/min).

[c] Detected by GC–SIM in HPLC fractions (fraction/min) from immature apple seeds [7]. The ranges are ± 0.5 min.

[2,5], epi-allogibberic acid [3], GA_{37} [2,5], GA_{51} [2], 3-epi-GA_4[3], GA_7 [2–6], iso-GA_7 [3], GA_4 [2–6], GA_{53} [2,3], GA_{14} [2–5], GA_{24} [2], GA_9 [2–6], GA_{25} [3–5], GA_{15} [2], GA_4 methyl ester [3], GA_{12} [2,3,5], GA_{12}-ald [2,3], *ent*-kaurenoic acid [3] and *ent*-kaurene [3].

The more polar compounds elute sooner from reversed-phase C_{18} HPLC. We have previously given the polarity order (elution order) of GAs with hydroxyl groups at different locations and orientations as $12\alpha > 16\alpha > 13 > 11\beta > 1\alpha > 2\alpha > 1\beta >$

$2\beta > 3\alpha > 3\beta$. Based on the retention times of additional GAs reported in Table I, 15β-hydroxyl GAs can be included in this order and the location of 16α-hydroxyl GAs in this polarity order is modified. The new polarity order is $12\alpha > 13 > 11\beta > 16\alpha > 1\alpha > 2\alpha > 15\beta > 1\beta > 2\beta > 3\alpha > 3\beta$. All of the examples we can find in Table I are as follows: $12\alpha > 13$; $GA_{31} > GA_5$, $GA_{30} > GA_3$. $GA_{39} > GA_{28}$. $13 > 11\beta$; $GA_1 > GA_{35}$. $11\beta > 16\alpha$; $GA_{35} > GA_2$. $16\alpha > 1\alpha$; $GA_2 > GA_{16}$. $1\alpha > 2\alpha$; $GA_{16} > GA_{47}$. $2\alpha > 15\beta$; $GA_{47} > GA_{63}$. $15\beta > 1\beta$; $GA_{63} > GA_{54}$. $1\beta > 2\beta$; $GA_{55} > GA_8$, $GA_{54} > GA_{34}$. $2\beta > 3\alpha$; $GA_{29} >$ 3-epi-GA_1. $3\alpha > 3\beta$; 3-epi-$GA_1 >$ GA_1, 3-epi-$GA_4 > GA_4$. All of the examples given here are without any exception in the polarity order, while the examples in the polarity order we gave previously [1] had one exception. Gibberellins with a double bond are more polar than those without the double bond in the C_{18} HPLC system and examples are as follows: $GA_3 > GA_1$, $GA_7 > GA_4$, $GA_5 > GA_{20}$, $GA_{62} > GA_{61}$, $GA_{68} > GA_{63}$.

The approximate retention times of GAs not listed in Table I can be predicted using the retention times in Table I and the retention properties given here. The HPLC of $GA_{51,61,62,63,68}$ have not been previously reported and the standards are not presently available to us. We successfully predicted the retention times of these GAs in immature apple seeds [7] as demonstrated by GC–SIM of the correct HPLC fractions using the retention times in Table I and retention properties given here. Since 1-min fractions were collected, the retention times given in Table I are in the range of ± 0.5 min. The retention time of GA_{60} is not given in Table I, but it is eluted between GA_8 and GA_1 [11], which agrees with the retention properties presented.

REFERENCES

1 J.-T. Lin and A. E. Stafford, *J. Chromatogr.*, 452 (1988) 519.
2 E. Jensen, A. Crozier and A. M. Monteiro, *J. Chromatogr.*, 367 (1986) 377.
3 M. Koshioka, J. Harada, K. Takeno, M. Noma, T. Sassa, K. Ogiyama, J. S. Taylor, S. B. Rood, R. L. Legge and R. P. Pharis, *J. Chromatogr.*, 256 (1983) 101.
4 J.-T. Lin and E. Heftmann, *J. Chromatogr.*, 213 (1981) 507.
5 M. G. Jones, J. D. Metzger and J. A. D. Zeevaart, *Plant Physiol.*, 65 (1980) 218.
6 G. W. M. Barendse, P. H. van de Werken and N. Takahashi, *J. Chromatogr.*, 198 (1980) 449.
7 J.-T. Lin, A. E. Stafford and G. L. Steffens, personal communication.
8 P. Gaskin, S. J. Gilmour, J. R. Lenton, J. MacMillan and V. M. Sponsel, *J. Plant Growth Regul.*, 2 (1984) 229.
9 H. Yamane, S. Fujioka, C. R. Spray, B. O. Phinney, J. MacMillan, P. Gaskin and N. Takahashi, *Plant Physiol.*, 86 (1988) 857.
10 P. Hedden, in L. Rivier and A. Crozier (Editors), *Principles and Practice of Plant Hormone Analysis*, Vol. 1, Academic Press, San Diego, CA, 1987, p. 9.
11 P. Hedden, personal communication.

Journal of Chromatography, 543 (1991) 475–478
Elsevier Science Publishers B.V., Amsterdam

CHROM. 23 137

Short Communication

Elimination of the temperature-induced loss of the enantioselectivity of chemically bonded albumin

ZDENĚK ŠIMEK[a] and RADIM VESPALEC*
Institute of Analytical Chemistry, Czechoslovak Academy of Sciences, Kounicova 42, 611 42 Brno (Czechoslovakia)
and
JAN ŠUBERT
Drug Control Laboratory, Institute of National Health, Jilemnického 2–4, 614 00 Brno (Czechoslovakia)
(First received November 2nd, 1990; revised manuscript received January 25th, 1991)

ABSTRACT

The enantioselectivity of bonded bovine serum albumin (BSA) which has been destroyed by high temperatures can be restored by exposure to methanol, common water-based mobile phases are inefficacious. The effectiveness of methanol demonstrates that BSA enantioselectivity, though conformationally dependent, is not conditioned by native conformation of BSA. Therefore, a systematic study is advised of the influence of denaturing factors on BSA enantioselectivity.

INTRODUCTION

The idea of using bovine serum albumin (BSA) as a chiral selector in liquid chromatography arose from the fact that albumin is capable of selectively binding compounds that differ only in their steric structures. Biological functions of albumin in living organisms are ascribed to, among other factors, the existence of a particular steric conformation of the albumin molecule, called the native form. In view of the sensitivity of BSA conformation to medium effects such as pH, ionic strength and chemical composition [1,2], it is improbable that the conformation of albumin in the separation system is identical with its conformation in living organisms. This applies in particular to albumin bonded to a solid matrix. In spite of this, bonded albumin retains the ability to distinguish steric conformations of solutes [3,4].

[a] Present address: Department of Chemistry, Technical University, Gorkého 7, 662 38 Brno (Czechoslovakia).

0021-9673/91/$03.50

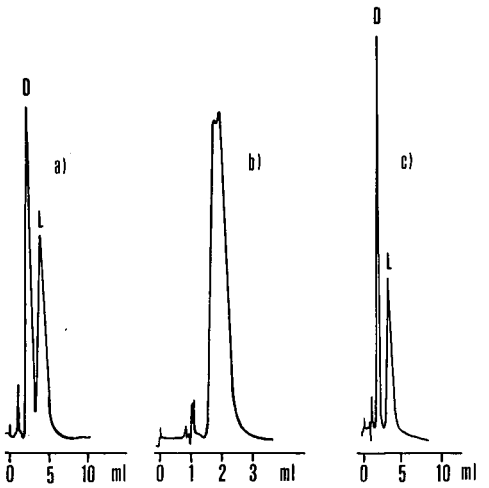

Fig. 1. Separation of D,L-tryptophan on Separon HEMA 1000–BSA sorbent (a) prior to heating, (b) after heating to 96°C and (c) after heating and washing with methanol. Separation conditions: CGC column (150 × 3.3 mm I.D.) packed with Separon HEMA 1000–BSA; temperature, ambient; mobile phase, 50 m*M* phosphate buffer in water (pH 7.5); flow-rate, 0.5 ml/min; injection, 2 μl of 0.46 m*M* D,L-tryptophan; detection, UV (254 nm). Quantitative characteristics of separations: (a) $k_1 = 1.42$, $\alpha = 2.21$, $R_s = 1.60$; (b) $k_1 = 0.87$, $\alpha = 2.61$, $R_s = 3.42$.

The chromatographic properties of the separation system can be controlled effectively by temperature. However, heating results in changes in albumin conformation and leads to its denaturation [1,2].

EXPERIMENTAL AND RESULTS

To test the effect of heating BSA on the enantioselectivity of the separation, we used BSA chemically bonded to a hydroxyethylmethacrylate matrix (Separon HEMA 1000–BSA sorbent; Tessek, Prague, Czechoslovakia). D,L-Tryptophan, whose L-form is transported by albumin in living organisms, was selected as a model solute. Fig. 1a shows the selectivity of the separation of D,L-tryptophan on a column filled with Separon HEMA 1000–BSA stored for *ca.* 1 year at 5°C in phosphate buffer (pH 7.5) containing 0.1% sodium azide. After being equilibrated with 50 m*M* phosphate buffer (pH 5.93), the column was heated in a stream of this mobile phase in a thermostat up to 96 ± 1°C within 40 min and allowed to stand at 96 ± 1°C for the following 30 min. The heated column almost lost its ability to separate tryptophan (Fig. 1b). Conditioning of the heated column with 50 m*M* phosphate buffer (pH 7.45) at ambient temperature for 40 h did not change the selectivity of the separation and conditioning with 50 m*M* buffer (pH 2.53) (at ambient temperature for 24 h) improved it only negligibly. The enantioselectivity of the separation of D,L-tryptophan was re-established by washing the column with methanol (Fig. 1c). The separation selectivity in Fig. 1c agrees with that on the same sorbent immediately after BSA bonding ($k_1 = 1.80$, $\alpha = 2.64$) [5].

DISCUSSION

The finding that methanol, which also has a denaturing effect [1,2], re-established the enantioselectivity of bonded BSA is remarkable. First it reveals the reversibility of the loss of BSA enantioselectivity caused by thermal treatment. It confirms that the ability of BSA to bind solutes enantioselectively is conditioned neither by the native conformation nor by any other conformation close to it. Chemically bonded albumin, having been heated and subsequently washed with methanol, could not acquire any structure analogous to the native one in the mobile phase of pH 7.45. The native form exists only in aqueous medium in the pH range 4.8–7.0 [6,7]. The results of the experiment do not cast doubt on the likely link between the selectivity of the separation of D,L-tryptophan and the steric conformation of bonded BSA. The experiment also shows that neither an identical nor an unambiguously negative effect of denaturating factors on the enantioselectivity of BSA as a chiral selector can be expected in advance. The reason can be found in different mechanisms of the actions of the various denaturating factors.

The possibility of restoring the selectivity of tryptophan separation reduced by heating by exposure to methanol has immediate practical importance. Provided that BSA in free solution and BSA bonded to a solid carrier are influenced similarly by the environment and temperature, speculations leading to important conclusions for practical applications can be based on the influence of temperature and methanol on the enantioselectivity of tryptophan separation.

Conformational changes of albumin are caused not only by temperature and methanol but also by other factors, *e.g.*, the pH of the environment [1,2]. Therefore, it cannot be discounted that a decrease in the selectivity of tryptophan separation on Separon HEMA 1000–BSA stored for almost 1 year at pH 7.5 (with respect to the selectivity on the freshly prepared sorbent) may be connected with changes in albumin conformation at pH >7.

Each enantiomer is sorbed at particular points of the BSA chain. Its retention depends on the accesibility of appropriate sorption centres and, as a consequence, also on the BSA conformation [6,7]. Therefore, changes in BSA conformation manifested by a decrease in tryptophan retention need not necessarily lead to a decrease in retention of any enantiomeric solute. If this expectation is proved, the management of BSA conformation can serve as a new method for the regulation of the enantioselectivity of bonded BSA.

Systematic studies on the enantioselectivity of bonded BSA are a prerequisite for a decision on the correctness of these two and other possible speculations. The information that BSA enantioselectivity is conditioned neither by the native form nor a conformation close to it should be one of principal starting points.

REFERENCES

1 H. D. Jakubke and H. Jescheit, *Aminosauren, Peptide, Proteine*, Akademie-Verlag, Berlin, 1969, p. 263.
2 M. Joly, *A Physico-Chemical Approach to the Denaturation of Proteins*, Academic Press, London, 1965; Russian translation, *Fizicheskaya Khimiya Denaturatsia Zelkov*, Mir, Moscow, 1968, p. 212.
3 S. Allenmark and S. Anderson, *Chirality*, 1 (1989) 154.
4 S. Allenmark, *J. Liq. Chromatogr.*, 9 (1986) 425.
5 Z. Šimek and R. Vespalec, *J. High Resolut. Chromatogr.*, 12 (1989) 61.

6 S. Tormod, *Acta Univ. Ups.*, No. 21 (1985) 58.
7 T. Peters, in F. W. Putnam (Editor), *The Plasma Proteins— Structure, Function and Genetic Control*, Vol. I, Academic Press, New York, 2nd ed., 1975, p. 133.

Journal of Chromatography, 543 (1991) 479–482
Elsevier Science Publishers B.V., Amsterdam

CHROM. 23 111

Short Communication

Separation of 18α- and 18β-glycyrrhetinic acid by high-performance thin-layer chromatographic densitometry

G. VAMPA* and S. BENVENUTI
Dipartimento di Scienze Farmaceutiche, Università degli Studi di Modena, Via Campi 183, 41100 Modena (Italy)

(First received October 3rd, 1990; revised manuscript received December 20th, 1990)

ABSTRACT

A high-performance thin-layer chromatographic method with scanning densitometry was developed for the simultaneous separation and determination of 18α- and 18β-glycyrrhetinic acid.

INTRODUCTION

Glycyrrhetinic acid (GA), the aglycone of glycyrrhizin (GL), the main component of the root of *Glycyrrhiza glabra* L., has anti-inflammatory [1–3], antiulcerous [4], antihepatotoxic [5–7], antiallergic [8], anticarcinogenic [9] and hypertensive activity [7].

Glycyrrhetinic acid exists as two stereoisomers, 18α-GA (*trans*) and 18β-GA (cis) (Fig.1). Their specific activities have not yet been ascertained: the anti-inflamma-

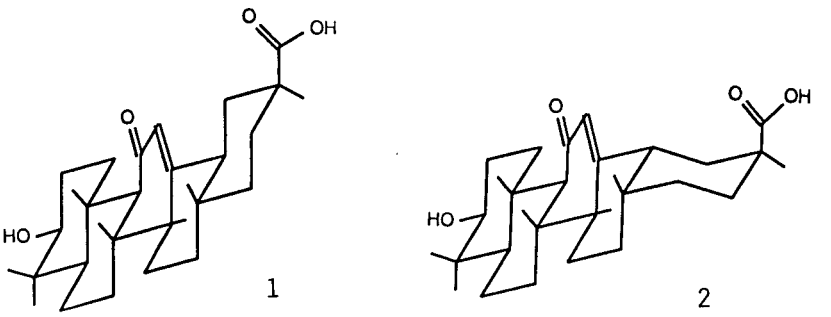

Fig. 1. Structures of (1) 18α-GA and (2) 18β-GA.

0021-9673/91/$03.50

tory action, one of the most important properties of glycyrrhetinic acid, has been attributed, for example, either to the 18β-form [2] or to the 18α-form, or to a combination of the two [10].

Qualitative and quantitative analyses of 18β-GA have been conducted by means of various chromatographic techniques, such as high-performance liquid chromatography (HPLC) [11–15] and, as the silyl ether [16] or methyl derivative [17], by gas chromatography (GC). Only Amagaya *et al.* [18] have determined both isomers simultaneously by GC, after derivatization with diazomethane.

As the two stereoisomers seem to have different pharmacological properties, it is clearly important to test each isomer separately, and therefore the aim of this study was to establish a method to separate 18α-GA and 18β-GA using a high-performance thin-layer chromatographic (HPTLC) approach.

EXPERIMENTAL

18α- and 18β-GA were purchased from Sigma (St. Louis, MO, U.S.A.). All solvents were of analytical-reagent grade and were obtained from BDH (Milan, Italy).

Pure samples of 18α- and 18β-GA (10^{-4} *M*) were dissolved in chloroform–methanol (1:1, v/v) and spotted, separately and in combination, on 10 × 20 cm precoated silica gel F_{254} plates (Merck, Darmstadt, Germany) using a Linomat IV instrument (Camag, Muttenz, Switzerland).

The solvent used for development was butanol–ethanol–2 *M* ammonia solution (6:2:1, v/v/v). All chromatograms were developed at room temperature using the ascending technique in a chromatographic tank previously saturated with eluent mixture. The layers were dried in a forced current of air, then analysed at 254 nm by the fluorescence quenching method using a Camag TLC Scanner II (Camag) equipped with an M 280 Olivetti PC operating the Cats 3.04 scanning program. The scanner was set up as follows: band with, 10 nm; span, 25; slit, 5 × 0.2 mm; and scanning speed, 5 mm/s.

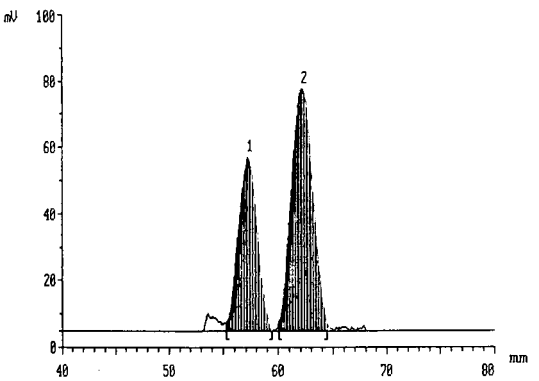

Fig. 2. Separation of (1) 18α-GA (157 ng) and (2) 18β-GA (302 ng) by HPTLC with the solvent system butanol–ethanol–2 *M* ammonia solution (6:2:1, v/v/v).

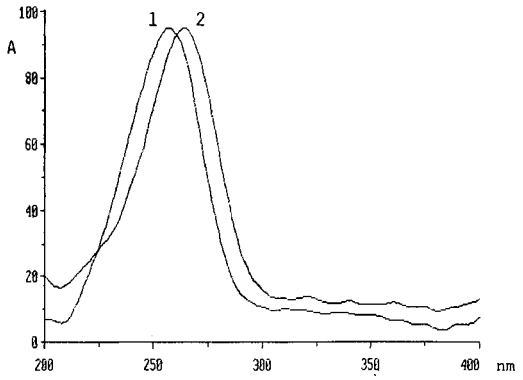

Fig. 3. UV absorption spectra of (1) 18α-GA and (2) 18β-GA determined by scanning the HPTLC plate in the reflectance mode.

RESULTS AND DISCUSSION

Fig. 2 shows the chromatographic resolution of the mixture of the two isomers; the spots were baseline separated with this development system. Fig. 3 shows the UV absorption spectrum of 18α- and 18β-GA obtained by scanning the HPTLC plate in the reflectance mode; 18α-GA shows maximum absorption at 258 nm and 18β-GA at 264 nm.

Table I shows the experimental analyses of a series of isomer mixtures containing various amounts of the two components. The experimental values were calculated by comparing the areas under the peaks with a calibration graph. The summarized data represent the means of six determinations.

The detection limit (at a signal-to-noise ratio of 2) was 1.93 ng for 18α-GA and 2.09 ng for 18β-GA. Although the determination of the α-isomer is the more accurate and reproducible of the two, the HPTLC method may be said to be accurate, reproducible and selective and to allow the rapid, simultaneous determination of the two isomers.

TABLE I

ANALYTICAL RECOVERY OF A MIXTURE OF 18α- AND 18β-GLYCYRRHETINIC ACID

18α-GA				18β-GA			
Amount applied (ng)	Amount found (ng)	Recovery (%) (mean, n = 6)	S.D. (ng)	Amount applied (ng)	Amount found (ng)	Recovery (%) (mean, n = 6)	S.D. (ng)
117.10	113.62	97.02	1.39	171.45	172.77	100.70	5.78
175.65	177.93	101.30	5.23	228.60	225.22	98.52	8.50
234.20	233.27	99.60	9.71	171.45	171.75	100.30	8.72
292.75	299.75	102.33	6.14	114.30	107.30	93.90	5.40
117.10	116.89	99.80	2.95	285.75	284.25	99.47	10.21
292.75	293.46	100.20	6.46	228.60	226.51	99.08	7.95

REFERENCES

1 R. S. H. Finney and G. F. Somers, *J. Pharm. Pharmacol.*, 10 (1958) 613.
2 K. Takahashi, S. Shibata, S. Yano, M. Harada, H. Saito, Y. Tamura and A. Kumagai, *Chem. Pharm. Bull.*, 28 (1980) 3449.
3 K. K. Tangri, P. K. Seth, S. S. Parmar and K. P. Bhargava, *Biochem. Pharmacol.*, 14 (1965) 1277.
4 K. Takagi, S. Okabe and R. Saziki, *Jpn. J. Pharmacol.*, 19 (1969) 418.
5 Y. Kiso, M. Tohkin and H. Hikino, *Planta Med.*, 49 (1983) 222.
6 Y. Kiso, M. Tohkin, H. Hikino, M. Hattori, T. Sakamoto and T. Namba, *Planta Med.*, 50 (1984) 298.
7 S. Ishida, Y. Sakiya, T. Ichikawa and S. Awazu, *Chem. Pharm. Bull.*, 37 (1989) 2509.
8 H. Inoue, T. Mori, S. Shibata and H. Saito, *Chem. Pharm. Bull.*, 35 (1987) 3888.
9 H. Nishino, K. Kitagawa and A. Iwashima, *Carcinogenesis*, 5 (1984) 1529.
10 S. Amagaya, E. Sugishita, Y. Ogihara, S. Ogawa, K. Okada and T. Aizawa, *J. Pharm. Dyn.*, 7 (1984) 923.
11 Y. Sakiya, Y. Akada, S. Kawano and Y. Miyauchi, *Chem. Pharm. Bull.*, 27 (1979) 1125.
12 J. Killachy, M. S. F. Ross and T. D. Turner, *Planta Med.*, 30 (1976) 310.
13 T. Ichikawa, S. Ishida, Y. Sakiya and Y. Akada, *Chem. Pharm. Bull.*, 32 (1984) 3734.
14 T. H. Beasley, Sr., H. W. Ziegler and A. D. Bell, *J. Chromatogr.*, 175 (1979) 350.
15 N. Sadley-Sosnowska, *J. Pharm. Biomed. Anal.*, 5 (1987) 289.
16 D. Larry, *J. Assoc. Off. Anal. Chem.*, 55 (1972) 275.
17 Th. Vondenhof, K. W. Glombitza and M. Steiner, *Sci. Pharm.*, 41 (1973) 155.
18 S. Amagaya, E. Sugishita, Y. Ogihara, S. Ogawa, K. Okada and T. Aizawa, *J. Chromatogr.*, 320 (1985) 430.

Journal of Chromatography, 543 (1991) 483
Elsevier Science Publishers B.V., Amsterdam

CHROM. 23 183

Book Review

HPLC of biological macromolecules —Methods and applications (*Chromatographic Science Series*, Vol. 51), edited by K. M. Gooding and F. Regnier, Marcel Dekker, New York, 1990, XIII + 676 pp., price US$ 150.00 (U.S.A. and Canada), US$ 180.00 (other countries), ISBN 0-8247-7879-0.

Interest in biomacromolecules has been growing very rapidly in the last two decades. Among the various aspects involved in the analysis of biomacromolecules the separation process is an important analytical challenge and various groups have worked in this area. High-performance liquid chromatography (HPLC) is one of the separation methods being studied extensively and it has become a valuable analytical tool in this area. The complexity of biomacromolecules enables various analytical approaches to be used based on different chemical interaction models, but from the scattered literature it is difficult to obtain a clear overview, allowing a strategy to be developed.

This book is a useful guide for those starting in this field but is also of interest for more experienced workers, giving rapid access to more detailed information. The book is organized in three parts. The first part focuses on the basic techniques used in the HPLC of biomacromolecules. Extensive attention is paid to support materials. The overview given for this aspect is extremely useful and gives clear guidelines for tailoring the physical structure of silicas and criteria important for selecting silica- or organic polymer-based materials. Several chromatographic approaches are discussed, namely size-exclusion, ion-exchange, hydrophobic interaction, metal interaction and reversed-phase chromatography. These various techniques are well described with sufficient emphasis on practical aspects. Separation based on gradient elution is highlighted and a systematic approach for optimizing this method is outlined in a very clear way. In addition to the separation process, some attention is also paid to sample pretreatment, while detection, including among others pre-/post-column derivatization, is discussed in a scattered way throughout all the different papers.

Parts two and three focus on the application of the techniques to the separation of mainly polypeptides, but polynucleotides are also discussed. The broad range of polypeptides covered includes amino acids/peptides, (iso)enzymes, membrane and ribosomal proteins, haemoglobin variants, histones, antibodies and glycoproteins. The change in conformation of various macromolecules depending on the chemical environment is, of course, an important parameter and attention is paid to this aspect.

The book, written by many specialists in macromolecular research, is a valuable source of information for a wide range of scientists, from interested researchers to those active in the field. It is a practical guide containing also fundamental concepts and a good update of current research.

Leiden (The Netherlands) JAN VAN DER GREEF

Author Index

PUBLICATION SCHEDULE FOR 1991

Journal of Chromatography and Journal of Chromatography, Biomedical Applications

MONTH	D 1990	J	F	M	A	M	
Journal of Chromatography	535/1 + 2	536/1 + 2 537/1 + 2 538/1	538/2 539/1 539/2	540/1 + 2 541/1 + 2 542/1	542/2 543/1	543/2 544/1 + 2 545/1	The publication schedule for further issues will be published later
Cumulative Indexes, Vols. 501–550							
Bibliography Section				560/1			
Biomedical Applications		562/1 + 2 563/1	563/2	564/1	564/2 565/1 + 2	566/1 566/2	

INFORMATION FOR AUTHORS

(Detailed *Instructions to Authors* were published in Vol. 522, pp. 351–354. A free reprint can be obtained by application to the publisher, Elsevier Science Publishers B.V., P.O. Box 330, 1000 AH Amsterdam, The Netherlands.)

Types of Contributions. The following types of papers are published in the *Journal of Chromatography* and the section on *Biomedical Applications:* Regular research papers (Full-length papers), Review articles and Short Communications. Short Communmications are usually descriptions of short investigations, or they can report minor technical improvements of previously published procedures; they reflect the same quality of research as Full-length papers, but should preferably not exceed six printed pages. For Review articles, see inside front cover under Submission of Papers.

Submission. Every paper must be accompanied by a letter from the senior author, stating that he/she is submitting the paper for publication in the *Journal of Chromatography*.

Manuscripts. Manuscripts should be typed in double spacing on consecutively numbered pages of uniform size. The manuscript should be preceded by a sheet of manuscript paper carrying the title of the paper and the name and full postal address of the person to whom the proofs are to be sent. As a rule, papers should be divided into sections, headed by a caption (*e.g.*, Abstract, Introduction, Experimental, Results, Discussion, etc.). All illustrations, photographs, tables, etc., should be on separate sheets.

Introduction. Every paper must have a concise introduction mentioning what has been done before on the topic described, and stating clearly what is new in the paper now submitted.

Abstract. All articles should have an abstract of 50–100 words which clearly and briefly indicates what is new, different and significant.

Illustrations. The figures should be submitted in a form suitable for reproduction, drawn in Indian ink on drawing or tracing paper. Each illustration should have a legend, all the *legends* being typed (with double spacing) together on a *separate sheet*. If structures are given in the text, the original drawings should be supplied. Coloured illustrations are reproduced at the author's expense, the cost being determined by the number of pages and by the number of colours needed. The written permission of the author and publisher must be obtained for the use of any figure already published. Its source must be indicated in the legend.

References. References should be numbered in the order in which they are cited in the text, and listed in numerical sequence on a separate sheet at the end of the article. Please check a recent issue for the layout of the reference list. Abbreviations for the titles of journals should follow the system used by *Chemical Abstracts*. Articles not yet published should be given as "in press" (journal should be specified), "submitted for publication" (journal should be specified), "in preparation" or "personal communication".

Dispatch. Before sending the manuscript to the Editor please check that the envelope contains four copies of the paper complete with references, legends and figures. One of the sets of figures must be the originals suitable for direct reproduction. Please also ensure that permission to publish has been obtained from your institute.

Proofs. One set of proofs will be sent to the author to be carefully checked for printer's errors. Corrections must be restricted to instances in which the proof is at variance with the manuscript. "Extra corrections" will be inserted at the author's expense.

Reprints. Fifty reprints of Full-length papers and Short Communications will be supplied free of charge. Additional reprints can be ordered by the authors. An order form containing price quotations will be sent to the authors together with the proofs of their article.

Advertisements. Advertisement rates are available from the publisher on request. The Editors of the journal accept no responsibility for the contents of the advertisements.